PAPER 89-8

CONTRIBUTIONS TO CANADIAN COAL GEOSCIENCE

Canada

1989

Agencies and companies that have directly assisted the research reported in this volume include the following:

Acadia University, Department of Geology
Alberta Research Council, Alberta Geological Survey
Bergbauforschung GmbH, Germany
BP Exploration Canada Ltd.
British Columbia Ministry of Energy, Mines and Petroleum Resources, Geological Survey Branch
Bullmoose Mine (Teck Corporation)
Canadian Hunter Exploration Ltd.
Cape Breton Development Corporation (DEVCO)
Cardinal River Coals Ltd.
Crows Nest Resources Ltd.
Esso Resources Canada Ltd.
Government of Yukon, Department of Economic Development, Energy and Mines Branch
Gregg River Resources Ltd.
Gulf Canada Resources Ltd.
Luscar Ltd.
Manalta Coal Ltd.
Nova Scotia Department of Mines and Energy
Petro-Canada
Quintette Coal Ltd.
Smoky River Coal Ltd.
The University of Newcastle-upon-Tyne, Organic Geochemistry Unit
Tyrrell Museum of Palaeontology
Universite Laval, Department of Chemical Engineering
University of British Columbia, Department of Geological Sciences
Utah Mines Ltd.
Whitehorse Coal Corporation

Thanks to all of these and the many others who have provided valuable support for recent coal-related activities of the Geological Survey of Canada. It is hoped that results from these activities will contribute significantly to efficient and responsible exploration, development and use of Canada's coal resources.

GEOLOGICAL SURVEY OF CANADA
PAPER 89-8

CONTRIBUTIONS TO CANADIAN COAL GEOSCIENCE

1989

Energy, Mines and Resources Canada

Énergie, Mines et Ressources Canada

Available in Canada through

authorized bookstore agents and other bookstores

or by mail from

Canadian Government Publishing Centre
Supply and Services Canada
Ottawa, Canada K1A 0S9

and from

Geological Survey of Canada offices:

601 Booth Street
Ottawa, Canada K1A 0E8

3303-33rd Street N.W.,
Calgary, Alberta T2L 2A7

100 West Pender Street
Vancouver, B.C. V6B 1R8

A deposit copy of this publication is also available for reference
in public libraries across Canada

Cat. No. M44-89/8E
ISBN 0-660-13142-0

CONTENTS

COAL GEOSCIENCE AND INFORMATION/DATA PROCESSING TECHIQUES

INTRODUCTION

Canada is one of the world's nations that are particularly well endowed with coal, and Canadian coal production, consumption and exports are undergoing unprecedented expansion. The Geological Survey of Canada (GSC) conducts a program of coal geoscience research directed to assessing the nation's coal resources in terms relevant to their exploration, evaluation, development, utilization and management. This program is based at the Institute of Sedimentary and Petroleum Geology in Calgary. The research provides information enabling Government and industry to respond effectively to future Canadian coal development opportunities. The ability of Canadian coal producers to provide a competitive product at a competitive price in the future will depend, to a large degree, on geological factors that affect the location, mineability and character of Canadian coals.

This volume includes 21 papers that provide significant interim results from some current coal geoscience research that is being supported by the Geological Survey of Canada. The diversity of topics provides some indication of the scope of the GSC's Coal Program. Co-authorship of several contributions, by geoscientists in the GSC, provincial agencies, universities, and/or private companies, reflects the collaborative approach that is generally taken to achieve national coal geoscience objectives.

The various agencies and companies that have directly assisted the coal studies reported in this volume are acknowledged on the inside back cover. The Federal Inter-departmental Panel on Energy Research and Development provides substantial funding for the coal geoscience research through its program on "Coal Supply". An Independent Review Committee comprising representatives of Canadian coal producers and users, coal producing provinces, universities, Federal Government agencies and The Coal Association of Canada, periodically reviews the GSC's current and planned coal geoscience activities. It provides recommendations on preferred focus and direction of these activities, helping to ensure that the geoscience needs of those involved in Canadian coal exploration and development are being addressed effectively.

G. Grant Smith
Head, Coal Geology Subdivision
Institute of Sedimentary and
Petroleum Geology
Calgary, Alberta

INTRODUCTION

Au niveau mondial, le Canada est l'un des pays aux ressources en charbon les plus abondantes. De ce fait, la production, la consommation et les exportations charbonnières connaissent une croissance sans précédent. La Commission géologique du Canada (CGC) dirige un programme de recherche sur le charbon qui a pour but l'estimation du potentiel canadien en ressources charbonnières, en tenant compte de l'exploration, l'évaluation, la mise en valeur, l'utilisation et la gestion des dites ressources. Le programme est centralisé à l'Institut de géologie sédimentaire et pétrolière, à Calgary. La recherche fournit les informations nécessaires au gouvernement et à l'industrie, afin de bien orienter les décisions éventuelles relatives à la mise en valeur de ce combustible. Dans l'avenir, la capacité des producteurs canadiens à livrer un produit de qualité à un prix compétitif dépendra en grande partie des paramètres géologiques qui influencent l'emplacement, l'exploitabilité et la qualité des ressources canadiennes en charbon.

Le présent document comprend 21 études qui donnent les résultats provisoires de quelques recherches en cours dans le domaine du charbon, subventionnées par la Commission géologique du Canada. La diversité des sujets d'étude donne une idée de l'envergure du programme sur le charbon de la CGC. La participation de plus d'un auteur à la rédaction de nombreux documents, notamment de géoscientifiques de la CGC, d'organismes provinciaux, du milieu universitaire ou de sociétés privées, reflète la démarche collaborative qui est généralement suivie, afin d'atteindre les objectifs fixés dans le domaine du charbon à l'échelle nationale.

Les différents organismes et sociétés qui ont donné leur appui aux études sur le charbon présentées ici sont remerciés en troisième de couverture. Le Groupe interministériel de recherche et d'exploitation énergétiques du gouvernement fédéral fournit des sommes importantes à la recherche sur le charbon, par le biais de son programme concernant l' "offre en charbon". Les activités menées par la CGC dans le domaine du charbon, tant celles en cours que prévues, sont périodiquement analysées par un comité indépendant de révision, auquel participent des représentants des producteurs et des utilisateurs de charbon canadien, des provinces productrices de charbon, des universités, d'organismes du gouvernement fédéral et de l'Association charbonnière canadienne. Ce comité formule des recommandations sur l'orientation que devraient prendre les travaux de la CGC, permettant ainsi de s'assurer de bien répondre aux besoins des agents responsables de l'exploration et de la mise en valeur du charbon.

G. Grant Smith
Chef de la Subdivision de la géologie du charbon
Institut de géologie sédimentaire et pétrolière
Calgary, Alberta

Stratigraphy, sedimentology and depositional environments of the coal-bearing Stellarton Formation, Nova Scotia

R.D. Naylor[1], W. Kalkreuth, W.D. Smith[1], and G.M. Yeo[2]
Institute of Sedimentary and Petroleum Geology, Calgary

Naylor, R.D., Kalkreuth, W., Smith, W.D., and Yeo, G.M., Stratigraphy, sedimentology and depositional environments of the coal-bearing Stellarton Formation, Nova Scotia. In Contributions to Canadian Coal Geoscience, Geological Survey of Canada, Paper 89-8, p. 2-13, 1989.

Abstract

The 6 by 18 km Stellarton Basin of Northern Nova Scotia is a rhomb graben formed in response to dextral movement along the Hollow and Cobequid faults. From the Westphalian B through D over 2.6 km of grey and red coal-bearing strata (the Stellarton Formation) were deposited as the graben opened. Basin-fill patterns were controlled primarily by changes in the rate of tectonic subsidence. When subsidence rates and water levels within the basin were low, thick peat swamps and shallow lakes formed near the basin center and red beds were deposited near basin margins. When subsidence rates and water levels were high, deep lakes formed at the basin center and were subsequently partly infilled by grey lacustrine delta deposits. Peat swamps occasionally developed on delta plains, during abandonment phases, and gradually drowned when a central basin lake expanded.

Résumé

Le bassin Stellarton, situé dans le nord de la Nouvelle-Écosse et mesurant 6 km de large sur 18 km de long, est un fossé rhomboédrique d'effondrement tectonique, formé à la suite d'un mouvement dextre le long des failles de Hollow et de Cobequid. Dans les niveaux westphaliens B à D, plus de 2,6 km de couches houillères grises et rouges (la formation de Stellarton) ont été mises en place lorsque le fossé s'est ouvert. Les structures de remplissage de la dépression ont été contrôlées surtout par les changements survenus au niveau du taux de progression de l'effondrement tectonique. Quand les taux de subsidence et les niveaux d'eau dans le bassin étaient bas, des marais tourbeux épais et des lacs peu profonds se sont formés près du centre du bassin et des couches rouges ont été mises en place près des rives du bassin. Quand les taux de subsidence et les niveaux d'eau étaient élevés, des lacs profonds se sont formés au centre du bassin et ont été subséquemment partiellement remplis par des sédiments deltaïques gris de nature lacustre. Des marais tourbeux se sont quelquefois développés dans des plaines deltaïques, pendant des phases d'abandon, pour être graduellement inondés quand un lac se développait dans le centre du bassin.

INTRODUCTION

The Stellarton Basin, located in central northern Nova Scotia (Fig. 1), has also been referred to as the Pictou Coalfield (e.g. Bell, 1940; Hacquebard and Donaldson, 1969) and the Stellarton Graben (e.g. Yeo and Ruixiang, 1987). The basin is small, measuring only 6 by 18 km, but contains in excess of 35 coal seams, 0.05 to 13.41 m thick.

Early workers, including Dawson (1868), Logan and Hartley (1869), Poole (1904), Bell (1940) and Haites (1956), outlined the major structural and stratigraphic elements of the basin. Dawson (1868), Poole (1904) and Bell (1940) described and classified its fossil flora and fauna. The sedimentology of the rocks of the Stellarton Basin was not considered in detail by early workers, although Bell (1940, 1958) recognized that much of the coal-bearing stratigraphic succession within the basin is of lacustrine origin.

Investigation of the organic petrography and detailed stratigraphic study of the coals was initiated by Hacquebard and Donaldson (1969). They suggested that the coals of the Stellarton Basin originated as hypautochthonous peat deposits in a completely enclosed and slowly subsiding lacustrine basin.

A significant increase in coal exploration from the mid 1970s to the present day has paralleled renewed interest in geological research within the Stellarton Basin. This paper summarizes the results of some of the most recent stratigraphic and sedimentological research and presents some new ideas on the factors which controlled formation of coals within the basin.

[1]Nova Scotia Department of Mines and Energy
1701 Hollis Street, P.O. Box 1087
Halifax, Nova Scotia B3J 2X1

[2]Acadia University
Department of Geology
Wolfville, Nova Scotia B0P 1X0

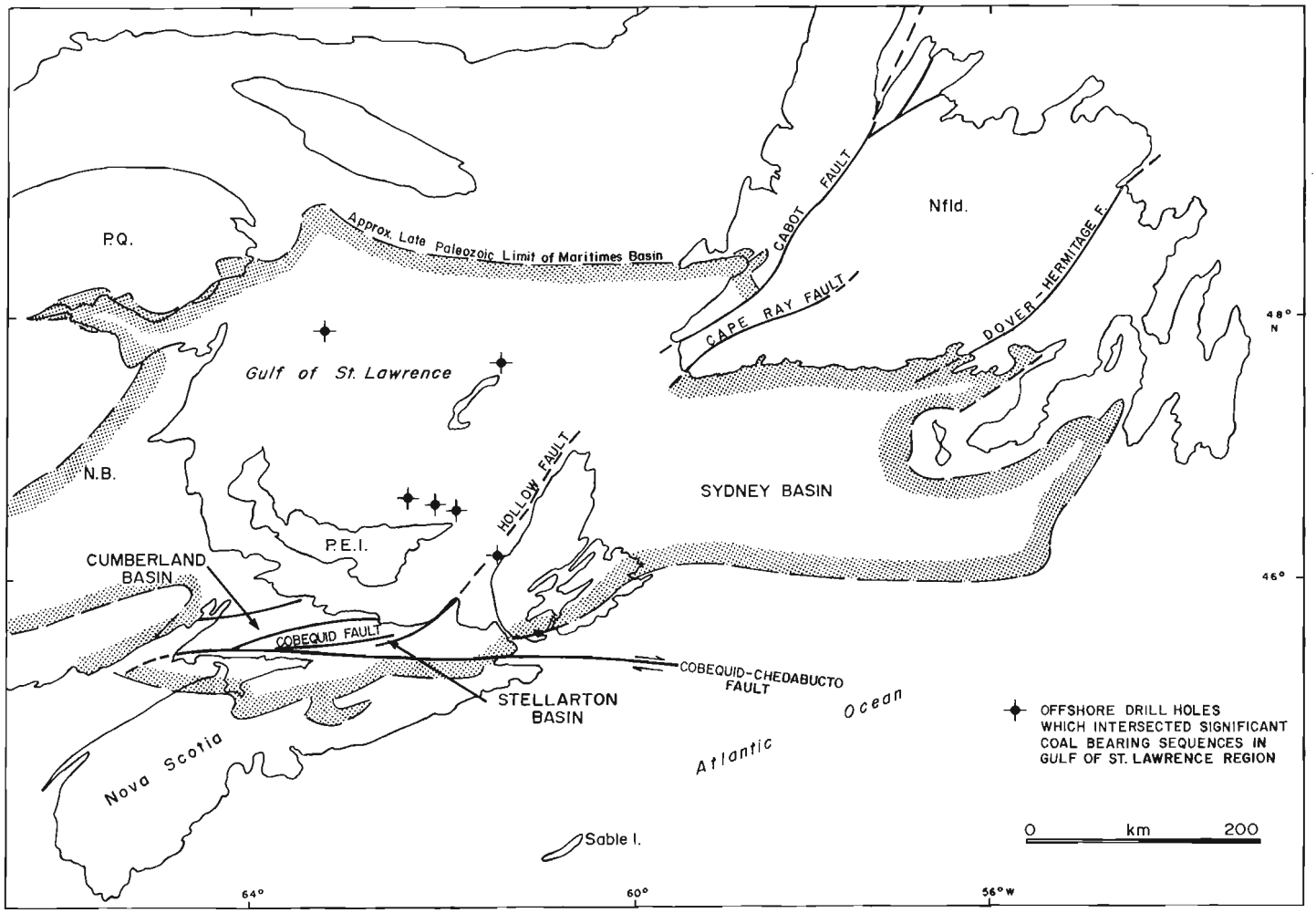

Figure 1. *Location of the Stellarton Basin and other major coal-bearing regions of the Maritimes Basin: the Cumberland Basin, the offshore Gulf of St. Lawrence region (drill holes) and the Sydney Basin.*

STRUCTURAL DEVELOPMENT OF THE BASIN

The Stellarton Basin is positioned between the terminal ends of two of Nova Scotia's major fault systems, the Hollow and Cobequid faults. In response to Late Carboniferous dextral movement along both of these faults, the Stellarton Basin developed as a rhomb graben. Further details of the structural development of the basin are found elsewhere (Gao, 1987; Yeo and Ruixiang, 1987).

STRATIGRAPHY AND SEDIMENTOLOGY

The 2.6 km thick coal-bearing stratigraphic succession within the Stellarton Basin has been variously referred to as the Stellarton Series (Bell, 1926, 1940), Stellarton Group (Bell, 1958) and Stellarton Formation (Fralick and Schenk, 1981). Stellarton Formation is used here in accordance with the most frequent usage of recent workers. Figure 2 illustrates the stratigraphy of the Stellarton Basin relative to the Late Carboniferous stratigraphy of the other major coal-bearing regions of the Maritimes Basin: the Cumberland Basin, the Sydney Basin and the offshore Gulf of St. Lawrence region.

The Stellarton Formation was subdivided by Bell (1940) into six members, in ascending order: Skinner Brook, Westville, Plymouth, Albion, Coal Brook and Thorburn. The member boundaries and stratigraphic position of the coals (named) and oil shales (numbered) are illustrated by Figure 3.

Basinwide correlation of 60 oil shale units (Naylor et al., 1987, 1988; Smith et al., 1988) and refinements to coal seam correlations, provide a detailed stratigraphic framework for structural, sedimentological, and petrographical studies. To date, however, no formal refinements to the stratigraphic subdivision of Bell (1940) have been proposed.

Bell (1940), on the basis of macroflora, assigned a late Westphalian B to early Westphalian C age to the Stellarton Formation. Regional palynological studies by Barss and Hacquebard (1967) suggested a late Westphalian B to Westphalian C age for the formation. This work has been refined by recent palynological studies (Dolby, 1986; Dolby in Yeo et al., 1988), which indicate a probable Westphalian B age for the lower Skinner Brook Member, an early Westphalian C age for the Westville Member, a mid Westphalian C age for the Albion Member, a late Westphalian C age for the Coal Brook Member, and a late Westphalian C to early D age for the Thorburn Member.

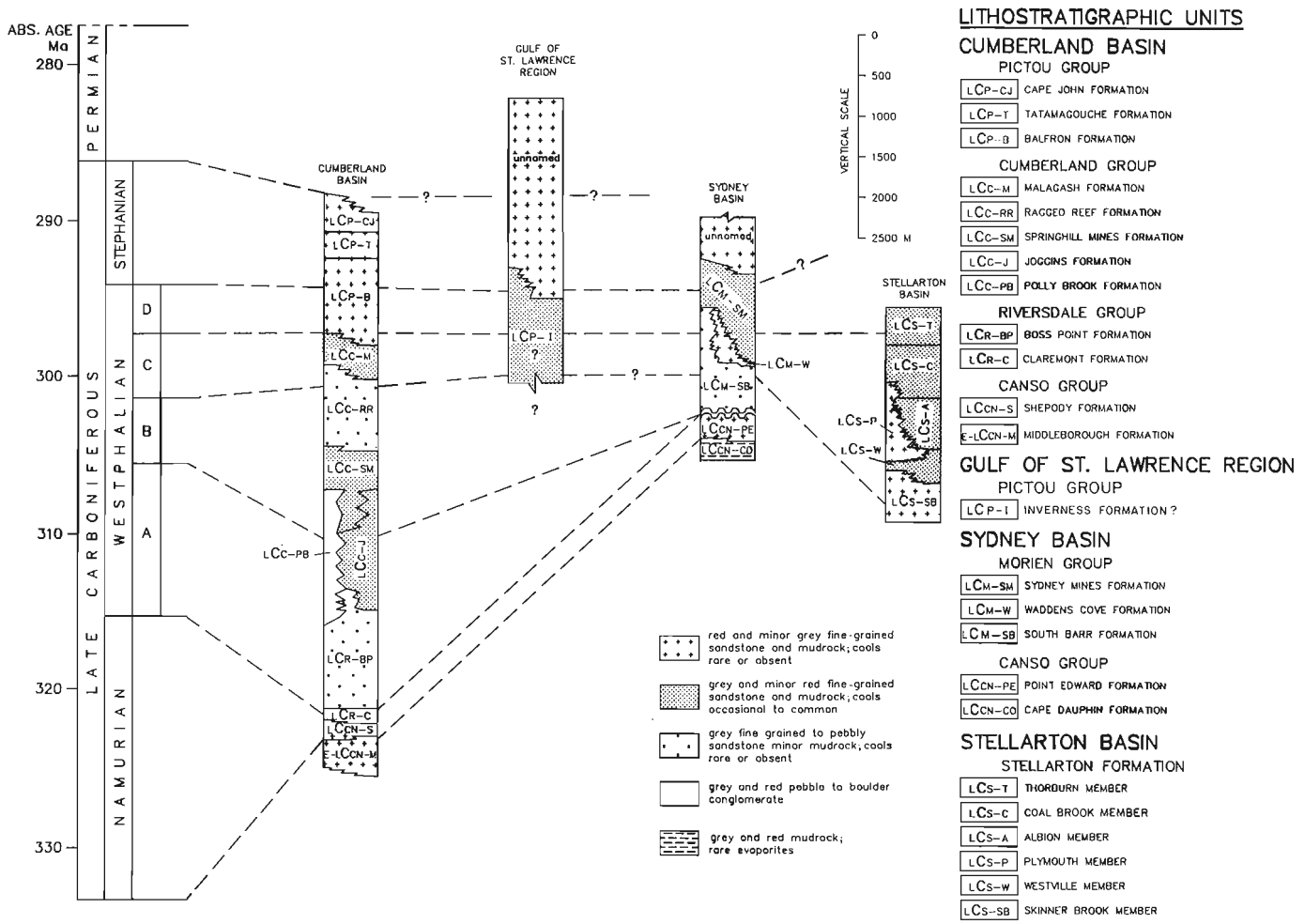

Figure 2. *Stratigraphy of the Stellarton Basin relative to other major coal-bearing regions of the Maritimes Basin: the Cumberland Basin, the offshore Gulf of St. Lawrence region and the Sydney Basin (see locations Fig. 1). Stratigraphic nomenclature and boundaries for the Cumberland Basin from Ryan et al. (1988); biostratigraphy of the offshore Gulf of St. Lawrence region modified after Hacquebard (1986); lithostratigraphy of the Sydney Basin from Boehner and Giles (1986), biostratigraphy of the Sydney Basin from Gibling et al. (1987) and Dolby (1988).*

Skinner Brook Member

The Skinner Brook Member, the lowermost member of the Stellarton Formation, outcrops at the western end of the Stellarton Basin (Fig. 4). It comprises red and mottled red and green mudrocks, sandstones and rare pebble conglomerates. The sedimentology of these rocks has received little study. The Skinner Brook Member is in diachronous contact with the coal-bearing Westville Member toward the basin centre.

Westville Member

The Westville Member occurs primarily in the subsurface and outcrops only locally on the west side of the Stellarton Basin (Fig. 4). It may also form part of a small fault block at the eastern basin margin. In the central area of the basin, an abrupt lithological change exists within the member. The upper half of the member (above the Acadia Seam) consists of oil shale interbedded with variably laminated grey mudrock. The lower half of the member (below the Acadia Seam) is a sequence of interbedded coal, grey fine grained sandstone, and mudrock. Near the western basin margin this lithological change is less apparent due to the deterioration of coal seams and interfingering of sandstones with the oil shales and mudrock of the upper half of the member.

The coals of the Westville Member are 2.43 to 4.40 m thick and are best developed upsection and toward the basin centre (Hacquebard and Donaldson, 1969). Toward the basin margins the coals generally pass into impure coal without seam splitting, a feature termed lithification by Hacquebard and Donaldson (1969).

The mudrock and sandstone underlying the coal seams commonly have disrupted laminae, rhizoconcretions and poorly preserved stigmarian rootlets. Sandstone and mudrock in the lower half of the member, which are not directly below coals, commonly have distinct laminae which are not bioturbated by roots.

Toward the centre of the basin, the oil shale and mudrock sequences of the upper half of the member lack beds with roots. The oil shales are dark grey to black, faintly laminated and clay-rich. The mudrocks have either rhythmic "varve-like" laminae or lenticular sandstone laminae. Both

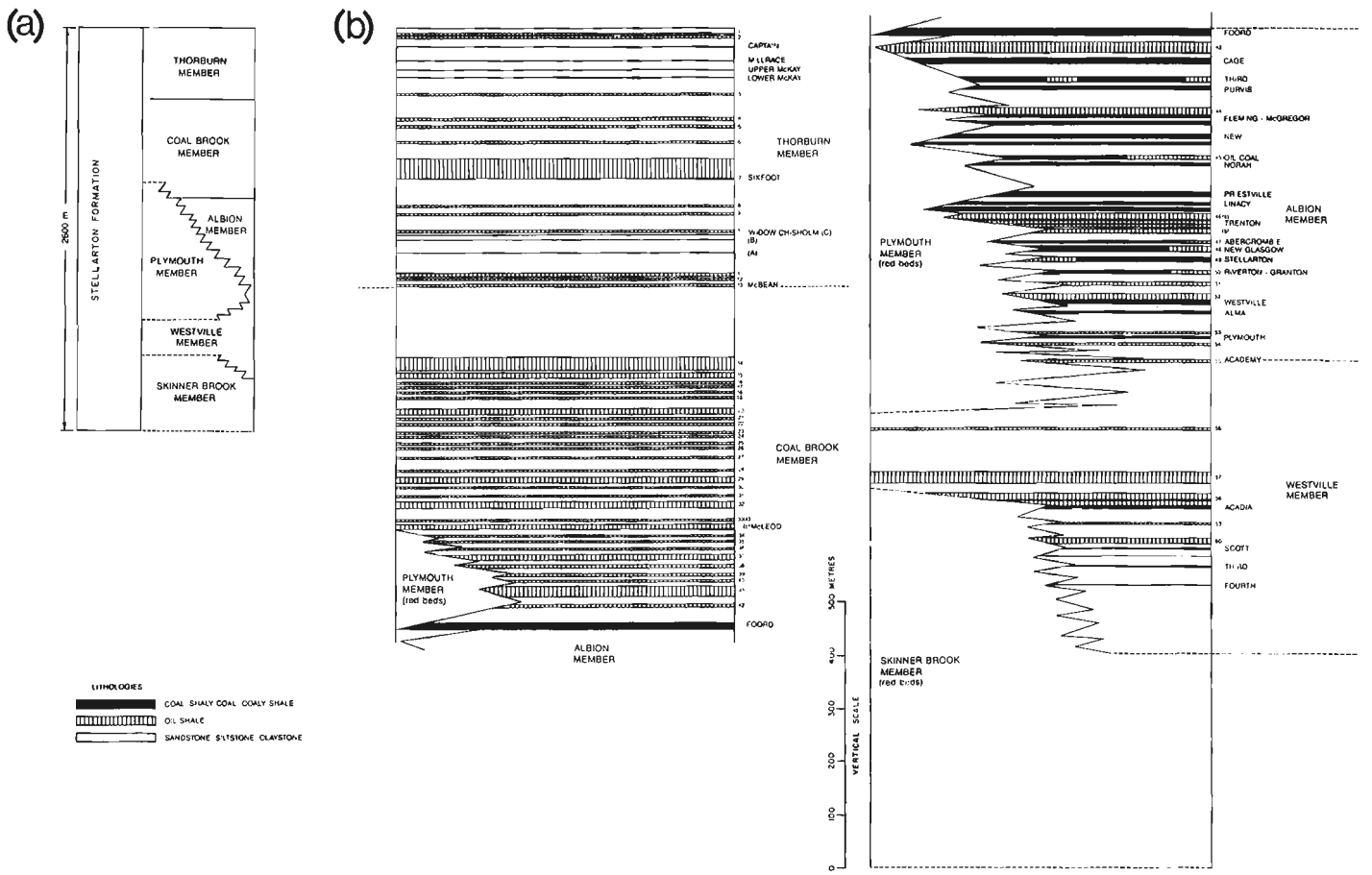

Figure 3. *Stratigraphy of the Stellarton Formation. (a) member boundaries (b) position of coal seams (named) and oil shales (numbered).*

the oil shales and the mudrocks frequently contain ostracodes, branchiopods (*Cyzicus* sp.), fish scales and plant fragments.

Near the western basin margin, the sandstones interbedded with oil shale and mudrock in the section above the Acadia Seam are commonly horizontally stratified with bed thickness and grain size increasing upsection. Mudrocks at the base of these coarsening upward sequences commonly contain ostracodes and plant fragments. Toward the basin margins the upper portion of the Westville Member interfingers with the red beds of the Plymouth Member.

Plymouth Member

The Plymouth Member is best developed near the southern basin margin (Fig. 4) and interfingers basinward with both the coal-bearing Westville and Albion Members. The Plymouth Member, like the Skinner Brook Member, comprises thickly interbedded red or mottled red-green mudrock, sandstone, and minor conglomerate. Bioturbation (roots) and reddening of Plymouth Member strata makes description of small scale sedimentary structures difficult. Reduction zones around poorly preserved stigmarian rootlets and calcareous or sideritic rhizoconcretions are common in the mudrocks. Sandstones are commonly trough cross-stratified or horizontally-stratified and contain rhizoconcretions and silicified zones (duricrusts) locally. Rare poorly preserved plant impressions are observed within the Plymouth Member. No faunal remains have been recovered.

Albion Member

The Albion Member outcrops in the western and south-central areas of the basin (Fig. 4). Coals of this member have been the target of exploration drilling since the turn of the century. Hence, the member has been cored over much of the basin.

The Albion Member contains 20 coal seams which range in thickness from 1 to 13.4 m and are interbedded with oil shale, organic-rich mudrock, organic-poor mudrock and very fine to medium grained sandstone. The coals are best developed in the basin centre and decrease in quality, through lithification, toward all but the northern basin margin (Haquebard and Donaldson, 1969). The coals, like those of the Westville Member, generally increase in areal extent upsection (Bell, 1940; Hacquebard and Donaldson, 1969).

Oil shales of the Albion Member are typically black, clay-rich and non-laminated with occasional plant fragments and rare ostracodes. They are inferred to be more canneloid than the oil shales of the Coal Brook Member and are typically found as partings within coal seams (Fig. 3). In rare instances, roots have been observed in those oil shales that underlie coals. The oil shales grade laterally, as well as vertically, into coals and organic-rich mudrocks.

The organic-rich mudrocks are dark grey to black, faintly colour banded to massive, and locally contain coaly laminae. Plant remains and bioturbation by roots are common; pelecypod impressions are very rare. These mudrocks grade into either coal or organic-poor mudrock.

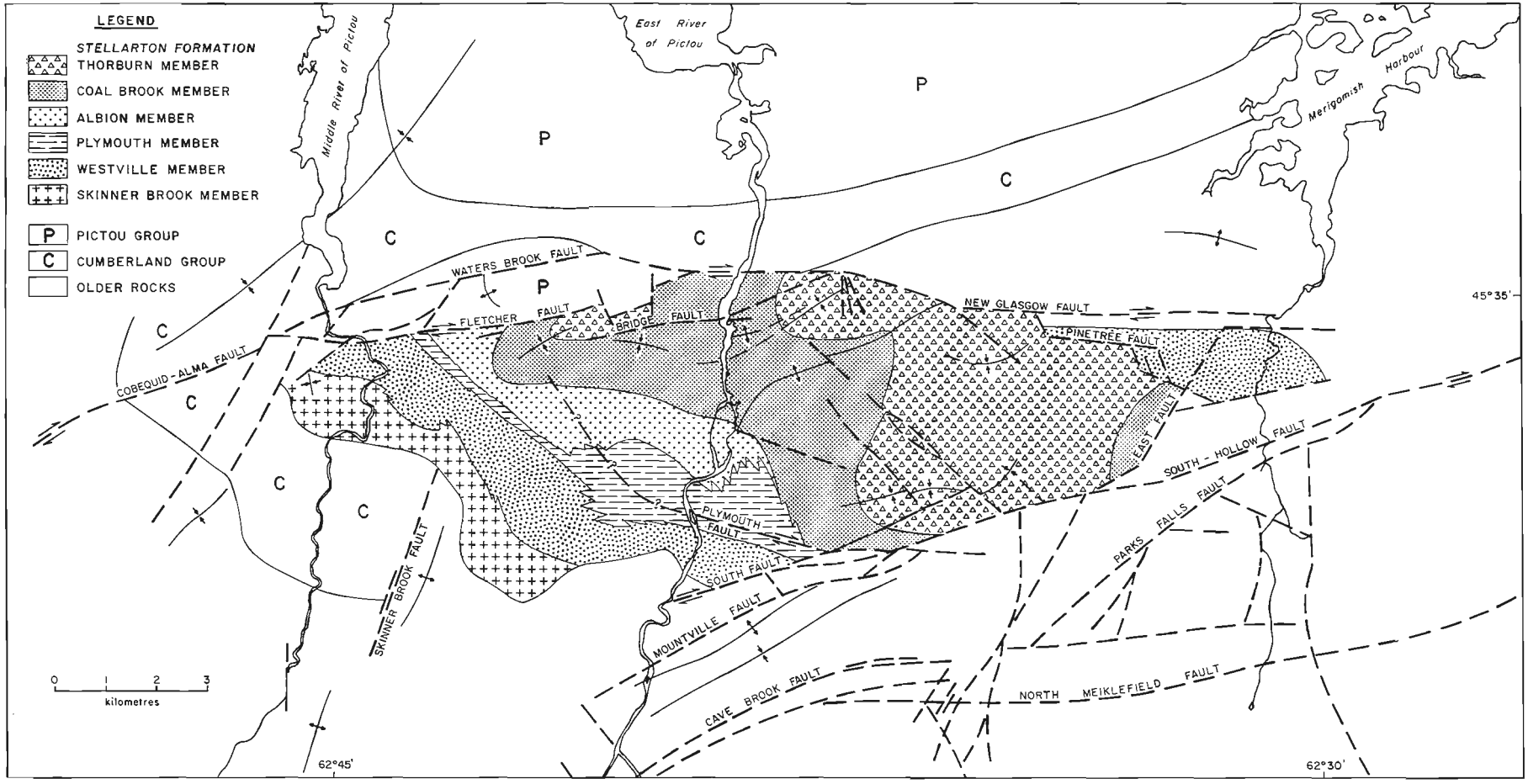

Figure 4. *Geological sketch map of the Stellarton Basin; modified after Yeo and Ruixiang (1987).*

The organic-poor mudrocks are grey, massive or faintly laminated, with rare to abundant siderite bands. Organic material is not well preserved but plant impressions are locally common. Bioturbation by roots may be observed locally but generally it is not as pervasive as in the organic-rich mudrocks. These mudrocks grade upward or are sharply overlain by sandstones. The sandstones are grey, fine to medium grained, rooted, and commonly contain rhizoconcretions. Small-scale sedimentary structures are poorly preserved. Lack of suitable exposure has hindered study of large bedforms.

Coal Brook Member

The Coal Brook Member, like the Albion Member, is known from outcrop and drillcore throughout much of the basin (Fig. 4). The boundary between the Albion and Coal Brook Members is the top of the Foord Seam (Fig. 3b).

In the central part of the basin, the Coal Brook Member consists of a 500 m thick sequence of interbedded oil shale (1-35 m thick) and grey rhythmically layered mudrock (5-20 m thick). Toward basin margins, the member thickens locally to more than 900 m and comprises thin coals, oil shales, mudrocks and thick sequences of grey sandstone. Grey pebble to cobble conglomerates are found locally at the southeastern and northwestern basin margins.

The only significant coal seam known within the member is the McLeod Seam (Fig. 3b) which is best developed toward basin margins. The seam undergoes a lateral facies change basinward from humic coal through cannel shale to oil shale (Naylor et al., 1987; Paul, 1988). Rooted zones are generally found below the seam.

The oil shales of the member are dark grey to black, clay-rich, generally non-laminated, and contain pelecypods (*Anthraconauta* sp.), ostracodes, disarticulated fish remains and plant fragments. The oil shales grade into rhythmically layered mudrocks and, in rare instances, coal.

The rhymically layered mudrocks contain varve-like laminae up to 2 cm thick. Each varve has a grey silty, massive or normal-graded lower half in gradational or sharp contact with a dark grey, clay-rich, normal-graded upper half. Rare poorly preserved carbonaceous plant fragments and very rare ostracode and pelecypod (*Anthraconauta* sp.) impressions are the only fossils observed.

Toward basin margins, the rhythmically layered mudrocks interfinger with coarsening-upward sequences that grade from mudrocks with lenticular, or even parallel sandstone laminae, through rippled sandstones to horizontally stratified sandstones with parting lineations. All of the sandstones have distinct carbonaceous laminae consisting of macerated plant fragments. The rippled sandstones exhibit both small ripple bedding and climbing ripple lamination, which are occasionally disrupted by pelecypod escape burrows.

The pebble to cobble conglomerates at the basin margin are generally horizontally stratified to low angle cross-stratified. They commonly overlie coarsening-upward sequences of grey horizontally stratified sandstones.

Thorburn Member

The Thorburn Member (average 490 m thick) is the uppermost member of the Stellarton Formation and is preserved only at the eastern end of the basin (Fig. 4). The member has many similarities with the Coal Brook Member including coarsening of strata toward basin margins and coal seams that grade basinward into oil shales.

Toward the basin centre, oil shales and rhythmically layered mudrocks are the predominant lithofacies. Coarsening-upward sandstone sequences commonly interfinger with the mudrocks closer to basin margins. Thick fining-upward sequences of grey sandstones, which do not thin basinward, occur below some of the thin coal seams (e.g. Widow Chisholm B Seam, Fig. 3b). Thicker coals, such as the McKay Seams, are interbedded with organic-rich and organic-poor mudrocks and relatively thin sequences of sandstone and lenticular bedded mudrocks. At the southeastern basin margin, grey conglomerates, horizontally stratified sandstones, and trough cross-bedded sandstones are common.

The coals of the Thorburn Member are 0.10 to 2.75 m thick. Underclays or extensively rooted sandstones underlie most of the coals even where they pass laterally into oil shales. Some thin coals can also be traced laterally to organic-rich mudrocks. The coals are generally overlain by organic-poor mudrocks with distinct siderite bands and no obvious bioturbation.

Two distinct types of oil shales are found in the Thorburn Member. The first type is identical to those of the Coal Brook Member. The second, locally known as stellarite, has pale grey and dark grey even, parallel, laminae which are 1 to 2 cm thick. The pale grey laminae fluoresce bright yellow when subjected to long wavelength ultraviolet light. Stellarite samples commonly contain abundant ostrocodes, pelecypods and fish remains. A stellarite interval is also found in the Albion Member underlying the Oil Coal Seam (Fig. 3b). Contortion of the pale grey and grey laminae throughout this interval is probably a result of bioturbation by roots.

The mudrocks, with varve-like laminae and intercalated with coarsening-upward sequences, are like those of the Coal Brook Member. The fining-upward sequences of grey sandstone are 10 to 35 m thick, coarse to fine grained, trough cross-stratified, and continuous laterally for 3 to 5 km. Bedset thickness and grain size both decrease upsection. These sequences have erosional bases and are generally overlain by trough cross-laminated fine grained sandstones.

The organic-rich and organic-poor mudrocks associated with the thicker coals are like those of the Albion Member. The organic-rich mudrocks are generally 1 to 10 cm thick and usually have rooted zones below them. The organic-poor mudrocks commonly have distinct siderite bands. The grey, thinly interbedded sandstones and even, parallel, and lenticular laminated mudrock sequences associated with the organic-rich and organic-poor mudrocks are generally penetrated by roots and are 1 to 9 m thick. The sandstones are variably laminated, but ripple laminae are common. The mudrocks are similar to those previously described. These sequences are traceable laterally for 1 to 3 km but the percentage of sandstone and even, parallel, and lenticular laminated mudrock within a sequence is highly variable between sections. Thicker sandstones (1-3 m) within these sequences appear to have very high length to width ratios and erosional bases.

The grey, pebble to cobble conglomerates at the southeastern basin margin exhibit both trough and low angle cross-stratification. The grey, low angle cross-stratified sandstones, cap coarsening-upward sequences of horizontally stratified sandstone like those of the Coal Brook Member. The high angle trough cross-stratified conglomerates are generally thick and in erosional contact with rooted, trough cross-stratified fine grained sandstones similar to those described above.

LITHOFACIES OR LITHOFACIES SEQUENCE	DIAGNOSTIC SEDIMENTARY STRUCTURES, FOSSILS	DEPOSITIONAL PROCESS AND ENVIRONMENT	SKINNER	BOK	WESTVILLE	ALBION	PLYMOUTH	COAL BROOK	THORBURN
Coal	-Microbanded -Oil shale interbeds	-Accumulation and peatification of organic matter. -Peat swamp with high water level	-		O¢	A¢	-	Rm	Om
Oil Shale	-Non-laminated or even parallel laminae which fluoresce (Stellarite) -Bivalves, fish remains, plants	-Algae, clays, humic matter from suspension -Lacustrine	-		O¢	R¢	-	A¢	C¢
Rhythmically Layered Mudrock	-Varve-like laminae	-Turbidite flows and suspension -Lacustrine (Pro-Delta)	-		O¢	R¢	-	A¢ Om	C¢ Om
Organic-Rich Mudrock	-High organic content -Disrupted coaly laminae and fragments -Roots, plants	-Clays and humic matter from suspension -Poorly drained swamp	-		O¢	A¢	-	Rm	Rm
Organic-Poor Mudrock	-Low organic content -Roots, plants -Siderite bands	-Clays from suspension -Well drained swamp-shallow lacustrine	-		C¢	A¢	-	-	Om
Even Parallel or Lenticular Laminated Mudrock	-Even parallel or lenticular sandstone laminae -Rare pelecypod burrows, bivalves and plant fragments	-Parallel laminae from suspension -Lenticular laminae, starved ripples -Subaqueous delta and delta plain	-		C¢	R¢	-	Cm	Cm
Red Mudrock	-Massive -Rhizoconcretions -Poorly preserved plants	-Suspension -Delta plain, distal alluvial fan (soil)	Am		-	-	Am	-	Rm
Mudrocks Coarsening to Horizontally Stratified Sandstone	-Coarsening-upward sequence: mudrocks to rippled sandstone to horizontally stratified sandstone	-Suspension to upper flow regime -Lacustrine-distributary mouth bar delta	-		-	-	-	Am-¢	Om-¢
Horizontally Stratified, Coarsening-Upward Sandstone	-Horizontal stratification -Rare roots at top of sequence	-Suspension -Deep water lacustrine delta	-		Om	-	-	Om	Om
Thinly Interbedded Sandstone and Mudrock	-Rippled, parallel laminated and massive sandstone interbedded with even parallel to lenticular laminated mudrock	-Predominantly lower flow regime -Delta plain	-		-	-	-	Rm	Om
Thick Trough Cross-Stratified Sandstone	-Trough cross-beds -10-35 m thick -Laterally extensive	-Traction -Sandy braided or meandering river (Upper delta plain)	-		-	-	-	Rm	Om R¢
Grey Trough Cross-Stratified Conglomerate	-Trough cross-stratification -Associated with trough cross-stratified sandstones	-Traction -Briaded river (Upper delta plain)	-		-	-	-	-	O¢
Red Sandstone and Conglomerate	?	-Traction -Alluvial fan or fluvial	Om		-	-	Rm	-	-

R = Rare; O = Occasional; C = Common; A = Abundant; m = Basin Margin; ¢ = Basin Centre; m-¢ = Between Basin Margin and Basin Centre

DEPOSITIONAL PROCESS AND ENVIRONMENTS

Table 1 lists the various lithofacies and lithofacies sequences outlined in the member descriptions. It also summarizes the sedimentology, depositional process and environment, abundance and stratigraphic location of each lithofacies and lithofacies sequence. More detailed descriptions of the lithofacies of the Stellarton Formation and interpretation of their depositional process and environment are given elsewhere (Naylor, 1981; Naylor et al., 1987; Snow 1988; Smith et al., in prep). An expanded description of the depositional process and environment of each of the lithofacies and the lithofacies sequences is listed in Table 1.

Coal

Hacquebard and Donaldson (1969), Kalkreuth and Macauley (1987), Yeo et al. (1988), Paul (1988) and Yeo (in press) have all used organic petrography to interpret the conditions of formation of the basin's coals. The discussion here is confined to the macroscopic and stratigraphic features of the coals.

The Stellarton coals are very finely banded (microbands) suggesting that the swamps in which they formed were commonly subjected to flooding (Hacquebard and Donaldson, 1969; Calder, 1979; Teichmüller and Teichmüller, 1982). These floods gently rearranged organic material within their general site of deposition, a process referred to as hypautochthony, hence hypautochthonous coals (Hacquebard and Donaldson, 1969). High water levels in the swamps are also indicated by the tendency of the coals to pass laterally and vertically into oil shales.

A hypautochthonous origin as opposed to an allochthonous origin, is supported by evidence of rooting under most coals. The occurrence of oil shales (lacustrine origin) or organic-rich mudrocks (poorly drained swamp deposits) over many of the seams suggests that peat accumulation was terminated by drowning of the swamps.

Oil shales

Both the non-laminated and stellarite oil shales originated through the accumulation of clays, algae and humic matter from suspension at the bottom of lakes with a restricted sediment supply. The lake bottom sediment conditions must have been anaerobic to allow preservation of organic matter. The overlying lake waters, however, were at least periodically oxygenated as they supported algal growth, ostracodes and a fish population.

Rhythmically layered ("varved") mudrocks

During periods of high sediment discharge into a lake, turbid underflows deposited the coarse grained lower half of each "varve". When sediment supply to the lake was more restricted the clay-rich upper half was deposited by differential settling of clays and silt from suspension. Formation of varve-like laminae in a similar manner has been reported in modern lakes by a number of authors including Ludlam (1967), Gustavson (1975) and Strum and Matter (1978).

Organic-rich mudrocks

Ubiquitous bioturbation by roots, and a relatively high organic content, suggests that the water levels were low enough to allow plant growth while these mudrocks were deposited. Thin coaly layers and fragments within these mudrocks indicate that peats occasionally formed, but sediment influx restricted their development. These mudrocks are interpreted as poorly-drained swamp deposits similar to the modern examples described by Coleman (1966).

Organic-poor mudrocks

A general decrease in bioturbation by roots, relative to the organic-rich mudrocks, suggests that water levels were high enough to restrict plant growth. The poor preservation of organic matter indicates that the waters in which these mudrocks were deposited were relatively well oxygenated. This lithofacies is interpreted as well drained swamp and shallow lacustrine deposits, similar to those described by Coleman (1966).

Even parallel and lenticular laminated mudrocks

These mudrocks are most commonly found within the Thorburn, Coal Brook and Westville members. The even parallel laminae were deposited from suspension. The lenticular laminae were formed by the migration of current ripples with deficient sand supply. Similar mudrocks have also been interpreted as wave reworked by de Raff et al. (1977). These mudrocks are interpreted as both lacustrine and delta plain deposits.

Red mudrocks

Extensive bioturbation by roots and the presence of poorly preserved plant remains indicates that these deposits were vegetated. They are probably oxidized soils developed on delta plains and alluvial fan aprons.

Mudrocks coarsening to horizontally stratified sandstones

The upward transition from even, parallel, and lenticular laminated mudrocks through fine grained rippled sandstones to fine- to medium grained horizontally stratified sandstones indicate that sediment supply and flow regime increased upsection. The even, parallel, and lenticular laminae of mudrocks at the base of these sequences were deposited in an identical manner to those described above. The common occurrence of climbing ripples and pelecypod escape burrows within the rippled sandstones suggests that they were formed when sediment supply rates were high and the flow regime was still relatively low. The parting lineations on bedding planes of the horizontally stratified sandstones indicate that they were deposited under upper flow regime conditions.

The features described above and the general lack of rooting suggests that these sequences are mouth bar deposits of a prograding lacustrine delta.

Coarsening upward, horizontally stratified sandstone

These sequences generally occur closer to the basin margin on average than the coarsening upward sequences described above. Their coarsening upward nature, the confinement of roots to near sequence tops, and the close association with oil shales, suggests that these sequences are also deposits of prograding lacustrine deltas. The general lack of current-produced structures, such as ripples and parting lineations, suggests that these sandstones may be suspension deposits.

Deposition of sand-sized sediment at river mouths without significant bed friction requires 1) high outflow velocities; 2) small density contrasts between river and lake waters; and 3) a high ratio of depth of lake waters in front of the distributary mouth to distributary channel depths (Axelsson, 1967; Wright, 1977). These conditions probably existed near the Stellarton Basin margin where steep gradient streams entered deep lakes during periods of high water level within the basin.

The grey pebble to cobble conglomerate sequences which cap these coarsening-upward sequences are probably proximal distributary channel deposits that progressed over the delta as it infilled the lake.

Thinly interbedded sandstone and mudrock (even, parallel, or lenticular laminated)

The elongate shape of the thick (1-3 m) sandstones of these sequences indicate that they were deposited in river channels which had limited lateral migration. The sandstone and mudrock sequences, which these channels eroded, are commonly rooted suggesting that channels were confined laterally by vegetation. These sandstones have been interpreted by Naylor (1981) and Snow (1988) as distributary channel deposits. The more thinly interbedded sequences of sandstone and mudrock found gradationally overlying, or lateral to, these sandstones were deposited in interdistributary areas, probably as crevasse splays and overbank deposits (Naylor, 1981; Snow, 1988).

Thick trough cross-stratified sandstones

The vertical arrangement of bed forms and lateral continuity of these sandstone sequences is consistent with deposition by sandy braided rivers (Walker and Cant, 1984). Alternatively, multistoried, multilateral sandstones such as these can be meandering river deposits formed during periods of slow tectonic subsidence (Allen, 1979).

Grey trough cross-stratified conglomerate

These grey conglomerates are inferred to be deposits of gravelly braided rivers. The rooted trough cross-stratified sandstones closely associated with them are interpreted as deposits of sandy bars which migrated over the channel gravels. Penetration of the sandstones by roots indicates that these deposits became vegetated as the active channel migrated elsewhere on the delta plain. Similar deposits have been described by Miall (1978) and Rust (1978).

Red conglomerates, sandstones and duricrusts

The red sandstone and conglomerates of the Plymouth and Skinner Brook members are inferred to be, in part, alluvial fan and fan apron deposits derived from erosion of basin margins. The sandstones are probably, also in large part, fluvial deposits sourced by more regional drainage basins.

The occurrence of rhizoconcretions and poorly preserved plant impressions in the sandstones suggests these deposits were vegetated. Duricrusts from the coal-bearing Morien Group similar to those found in the Plymouth Member have been described by Gibling (1987). Their formation was attributed to weathering of vegetated soils in humid climates with seasonal fluctuations in ground water level. These deposits require further study.

DEPOSITIONAL HISTORY

Three phases of subsidence and sedimentation within the Stellarton Basin were recognized by Yeo and Ruixiang (1987). Deposition of the Skinner Brook and Westville members occurred during the first phase, the Plymouth and Albion members during the second phase, and the Coal Brook and Thorburn members during the third phase.

During the first two phases, coal-bearing central basin grey beds gradually replaced basin margin red beds upsection (see Fig. 3). The transgression of grey beds toward basin margins was interpreted to indicate a gradual slowing in basin subsidence and sedimentation rates.

During the third phase, rapid subsidence during Coal Brook time was considered responsible for higher water levels and deposition of sediments in "deep lakes". Slowing of subsidence rates during Thorburn time was thought to have resulted in the final infilling of the basin.

An alternate depositional history for the Stellarton Formation is presented below. It is in part based on the observation by Blair (1986) that lacustrine and regionally sourced fluvial deposits respond quickly to increased basin subsidence by migrating over locally derived basin margin deposits (e.g. alluvial fans).

During the initial phase of basin infill, subsidence rates and water levels within the basin were low, basin margins were rapidly eroded, and the red beds of the Skinner Brook Member were deposited basinward. As subsidence rates and water levels gradually increased, the grey coal-bearing shallow lacustrine deposits of the Westville Member expanded toward basin margins.

After deposition of the Acadia Seam, subsidence rates increased dramatically resulting in accumulation of thick sequences of non-rooted lacustrine deposits (oil shales, "varved" mudrocks, lenticular bedded mudrocks) at the basin centre. Near basin margins, "deep water" delta deposits (coarsening-upward, horizontally stratified sandstones) predominated.

Abundant rooting, thick central basin coals, and basin margin red beds indicate that, on average, low water levels and slow subsidence rates existed throughout Plymouth-Albion time. In response to slow rates of subsidence, basin margins were more actively eroded and alluvial fan and fan apron deposits (red sandstones and conglomerates) prograded basinward.

During intervals of increased subsidence, shallow lakes formed at the basin centre and expanded rapidly toward the basin margin. These lakes were gradually infilled, plant communities became more common, and poorly drained swamps formed. These swamps became increasingly restricted in areal extent, possibly in response to more luxurient plant growth, and peat swamps developed.

The thick nature of many of the Albion coals indicate that peat swamps were generally protected for long periods from permanent flooding and significant sediment contamination. This suggests that subsidence rates remained close to peat accumulation rates and most of the sediment being carried into the peat swamps was filtered out along its margin. This would explain why the Albion coals lithify toward basin margins.

Upsection the Albion Member gradually expands toward the basin margin. This suggests that subsidence rates increased and lake and swamp deposits (organic-poor and

organic-rich mudrocks and peat) developed increasingly closer to basin margins as the lake area expanded. As peat swamps became larger, they were less susceptible to sediment contamination and flooding. This may explain why coals of the Albion Member improve in quality and thickness upsection.

During deposition of the Thorburn and Coal Brook members, water levels and subsidence rates were high. A lake, which existed continuously at the basin centre, was partially infilled by lacustrine delta deposits ("varved" mudrocks, coarsening upward sequences). When sediment supply to the basin was cut off or restricted, delta abandonment occurred and algal-rich muds, the precursors of oil shales, accumulated on the lake floor.

In rare instances, when the lake did not transgress too quickly, peat swamps developed on abandoned delta plains. These swamps were gradually drowned through lake expansion resulting in the transgression of algal-rich muds over peat deposits. This explains why coals of the Thorburn and Coal Brook members thicken toward basin margins and thin basinward through a lateral facies change to oil shales.

During deposition of the Thorburn Member, periodic slowing of tectonic subsidence and/or an increase in regionally sourced sediment supply occasionally occurred. This resulted in the deposition of thick sandy fluvial deposits (trough cross-stratified sandstones).

CONCLUSIONS

Basin-fill patterns within the Stellarton Basin varied largely in response to several interrelated factors, specifically: changes in the rate of tectonic subsidence, water levels, and the influence of regional, versus local, sediment supply. The thickest coals of the formation, those of the Albion and Westville members, were formed when subsidence rates were low. During these intervals, lakes at the basin centre were completely infilled allowing thick peat swamps to develop. When subsidence rates were too low, the areal extents of these peat swamps were limited by low water levels toward basin margins. As subsidence rates increased, the swamps expanded toward basin margins. Because of their increased size, these swamps remained protected for longer periods from sediment contamination and drowning.

During intervals when subsidence rates were high, a lake covered much of the basin floor. These lakes were partly infilled by regionally sourced lacustrine delta deposits allowing peat swamps to occasionally form on abandoned delta plains. As a result, the coals of the Thorburn and Coal Brook members, which formed during periods of rapid subsidence, are only developed toward basin margins.

REFERENCES

Allen, J.R.
1979: Studies in fluviatile sedimentation: an elementary geometrical model for the connectedness of avulsion-related channel sand bodies. Sedimentary Geology, v. 24, p. 253-267.

Axelsson, V.
1956: The Laitaure Delta: a study of deltaic morphology and process. Geografiska Annaler, v. 29, p. 1-127.

Barss, M.S. and Hacquebard, P.A.
1967: Age and stratigraphy of the Pictou Group in the Maritime Provinces as revealed by fossil spores. In Geology of the Atlantic Region, E.R.W. Neale and H. Williams (eds.); Geological Association of Canada, Special Paper 4, p. 267-282.

Bell, W.A.
1926: Carboniferous formations of Northumberland Strait, Nova Scotia. Geological Survey of Canada, Summary Report, 1924, Part C, p. 142-180.

1940: The Pictou Coalfield, Nova Scotia. Geological Survey of Canada, Memoir 225, 160 p.

1958: Possibilities for occurrence of petroleum reservoirs in Nova Scotia. Nova Scotia Department of Mines, 177 p.

Blair, T.C.
1986: Tectonic and hydrologic controls on cyclic alluvial fan, fluvial, and lacustrine rift-basin sedimentation; Jurassic-Lowermost Cretaceous TODOS Santos Formation, Chiapas, Mexico. Journal of Sedimentary Petrology, v. 57, p. 845-865.

Boehner, R.C. and Giles, P.S.
1986: Geological map of the Sydney Basin. Nova Scotia Department of Mines and Energy, Map 86-1 (1:50,000).

Calder, J.H.
1979: Effects of subsidence and depositional environment on the formation of lithotypes in a hypautochthonous coal of the Pictou Coalfield. Nova Scotia Department of Mines and Energy, Paper 79-6, 23 p.

Coleman, J.M.
1966: Ecological changes in a massive freshwater clay sequence. Gulf Coast Association of Geological Societies, Transactions, v. 16, p. 159-174.

Dawson, J.W.
1868: Acadian Geology. Second edition, MacMillan and Company, London, p. 421-468.

Dolby, G.
1986: Palynological analysis of samples from the AP-83-0372 corehole, Stellarton Basin, Nova Scotia. Unpublished report prepared for the Nova Scotia Department of Mines and Energy, 6 p.

1988: Palynology of the Morien Group, Sydney Basin, Cape Breton Island, Nova Scotia. Unpublished report prepared for Nova Scotia Department of Mines and Energy, 10 p.

Fralick, P.W. and Schenk, P.E.
1981: Molasse deposition and basin evolution in a wrench tectonic setting: The late Paleozoic eastern Cumberland Basin: Maritime Canada. In Sedimentation and Tectonics in Alluvial Basins. A.D. Miall (ed.); Geological Association of Canada Special Paper 23, p. 77-98.

Gao, R.
1987: Deformation characteristics of the eastern Cobequid and Hollow Fault Zones and Stellarton Basin, Nova Scotia. University of New Brunswick, unpublished M.Sc. thesis, 227 p.

Gibling, M.R.
1987: Carboniferous channels confined by duricrusts in the Sydney Basin of Nova Scotia. In Geological Association of Canada - Mineralogical Association of Canada, Joint Annual Meeting 1987, Program with Abstracts, v. 12, p. 46.

Gibling, M.R., Boehner, R.C., and Rust B.R.
1987: The Sydney Basin of Atlantic Canada: an Upper Paleozoic strike-slip basin in a collisional setting. In Basins and Basin Forming Mechanisms, C. Beaumont and T. Tankard (eds.); Canadian Society of Petroleum Geologists, Memoir 12, p. 299-309.

Gustavson, T.C.
1975: Sedimentation and physical limnology in proglacial Malaspina Lake, Southern Alaska. In Glaciofluvial and Glaciolacustrine sedimentation, A. Jopling and B. McDonald (eds.); Society of Economic Paleontologists and Mineralogists, Special Publication 23, p. 249-263.

Hacquebard, P.A.
1986: The Gulf of St. Lawrence Carboniferous Basin: the largest coalfield of eastern Canada. Canadian Mining and Metallurgical Bulletin, v. 29, p. 67-78.

Hacquebard, P.A. and Donaldson, J.R.
1969: Carboniferous coal deposition associated with flood-plain and limnic environments in Nova Scotia. Geological Society of America, Special Paper 114, p. 143-190.

Haites, T.B.
1956: Some geological aspects of the Pictou coalfield with reference to their influence on mining operations. In Third Conference on the Origin and Constitution of Coal, Crystal Cliffs, Nova Scotia; Nova Scotia Department of Mines and Energy and Nova Scotia Research Foundation, Halifax, Nova Scotia, p. 39-74.

Kalkreuth, W.D. and Macauley, G.
1987: Organic petrology and geochemical (Rock-Eval) studies on oil shales and coals from the Pictou and Antigonish areas, Nova Scotia, Canada. Bulletin of Canadian Petroleum Geology, v. 35, p. 263-295.

Logan, W.E., and Hartley, E.
1869: Reports on a part of the Pictou Coalfield, Nova Scotia. Geological Survey of Canada, Report of Progress 1866-69, p. 3-53.

Ludlam, S.D.
1967: Sedimentation in Cayuga Lake, New York. Limnology and Oceanography, v. 12, p. 618-632.

Miall, A.D.
1978: Lithofacies types and vertical profile models in braided river deposits: a summary. In Fluvial Sedimentology, A.D. Miall (ed.); Canadian Society of Petroleum Geologists, Memoir 5, p. 597-604.

Naylor, R.D.
1981: Geological evaluation of the McKay seams of the Thorburn coal district, Pictou County, Nova Scotia. Nova Scotia Department of Mines and Energy, Unpublished report, 36 p.

Naylor, R.D., Smith, W.D., and Black, M.C.
1987: The use of oil shales as a guide to coal exploration at the eastern end of the Stellarton Basin. In Program and Summaries, Tenth Annual Open House and Review of Activities, Nova Scotia Department of Mines and Energy, Information Series No. 12, p. 15-19.

Naylor, R.D., Smith, W.D., Prime, G.A., Black, M.C., and Conrod, D.J.
1988: Geology - Stellarton Basin (East Half), Pictou County, Nova Scotia. Nova Scotia Department of Mines and Energy, Open File Report 86-052, 107 p.

Paul, J.
1988: Kohlenpetrographische Und geochemische Untersuchungen an Kohlen und Olschiefern des McLeod-horizontes, Pictou coalfield, Nova Scotia, Canada. Diplomarbeit (Unpublished Master Thesis), University of Köln, West Germany, 137 p.

Poole, H.S.
1904: Report on the Pictou coalfield. Geological Survey of Canada, Annual Report, v. 14, part M, p. 1-38.

Raaf, J.F.M, De Boersma, J.R., and Gelder, A. Van
1977: Wave-generated structures and sequences from a shallow marine succession, Lower Carboniferous, County Cork, Ireland. Sedimentology, v. 24, p. 451-483.

Rust, B.R.
1978: Depositional models for braided alluvium. In Fluvial Sedimentology, A.D. Miall (ed.); Canadian Society of Petroleum Geologists, Memoir 5, p. 605-625.

Ryan, R.J., Deal, A., Calder, J.H., and Boehner, R.C.
1988: Preliminary geological field maps of Springhill and Apple River. Nova Scotia Department of Mines and Energy, Open File Map 88-42.

Smith, W.D., Gillis, K.S., and Montgomery, S.A.
1988: Stellarton Basin Project. In Report of Activities, Part A, Mines and Mineral Branch, D.R. MacDonald and Y. Brown (eds.); Nova Scotia Department of Mines and Energy Report 88-3, p. 21-29.

in prep: Geological map of the Stellarton Basin (west half), Pictou County, Nova Scotia (1:5000). Nova Scotia Department of Mines and Energy.

Snow, R.J.
1988: Stratigraphy of the upper Thorburn Member, Stellarton Group, Nova Scotia. Acadia University, unpublished M.Sc. thesis, Wolfville, Nova Scotia, 257 p.

Strum, M. and Matter, A.
1978: Turbidites and varves in Lake Brienz (Switzerland): deposition of clastic deposits by density currents. In Modern and Ancient Lake Sediments, A. Matter and M.E. Tucker (eds.); International Association of Sedimentologists, Special Publication 2, p. 147-168.

Teichmüller M. and Teichmüller R.
1982: Fundamentals of coal petrology. In Stach's textbook of coal petrology; Gebruder Borntrager, Berlin, p. 5-218.

Walker, R.G. and Cant D.J.
1984: Sandy fluvial systems. In Facies models, R.G. Walker (ed.); Geoscience Canada, Reprint Series 1, p. 71-89.

Wright, D.
1977: Sediment transport and deposition of river mouths: a synthesis. Geological Society of America, Bulletin, v. 88, p. 857-868.

Yeo, G.M.
in press: Petrology and depositional environment of the Foord Seam, Pictou Coalfield, Nova Scotia. Maritime Sediments and Atlantic Geology.

Yeo, G.M., Kalkreuth, W.D., Dolby, G., and White, J.C.
1988: Preliminary report on petrographic, palynological, and geochemical studies of coals from the Pictou Coalfield, Nova Scotia. In Current Research, Part B, Geological Survey of Canada, Paper 88-1B, p. 29-40.

Yeo, G.M. and Ruixiang, G.
1987: Stellarton Graben: A late Carboniferous pull apart basin in northern Nova Scotia. In Basins and basin forming mechanisms, C. Beaumont and T. Tankard (eds.); Canadian Society of Petroleum Geologists, Memoir 12, p. 299-309.

Gates Formation (Lower Cretaceous) coals in Western Canada: a sedimentological and petrographical study

W. Kalkreuth, D.A. Leckie, and M. Labonté
Institute of Sedimentary and Petroleum Geology, Calgary

Kalkreuth, W., Leckie, D.A., and Labonté, M., Gates Formation (Lower Cretaceous) coals in Western Canada: a sedimentological and petrographical study. In Contributions to Canadian Coal Geoscience, Geological Survey of Canada, Paper 89-8, p. 14-25, 1989.

Abstract

Coal seams formed on Lower Cretaceous wave-dominated strandplain sediments in Western Canada are characterized by great lateral continuity, substantial thicknesses, relatively low ash, and low sulphur contents. The coals formed behind an active shoreline in areas undergoing subsidence due to shale compaction and dewatering. The zone of peat accumulation was generally protected from fluvial flooding and storm/tidal inundations. Statistical evaluation of petrographic properties, by correspondence analysis, of the Lower Cretaceous Gates Formation coals shows that the strandplain coals form distinctive petrographic groups characterized by relatively low vitrinite contents and high inertinite contents. Liptinite contents are negligible. Tissue preservation indices and gelification indices indicate a forest-type depositional environment in which a relatively low water table allowed the accumulation of oxidized and partly oxidized components. Significant amounts of detrital components indicate that some transportation of the organic material took place prior to deposition.

Résumé

Des filons houillers, du Crétacé inférieur, formés dans l'Ouest canadien au sein de sédiments de plaines littorales sous l'action des vagues, sont caractérisés par une grande continuité latérale, des épaisseurs importantes, de faibles teneurs en cendres et en soufre. Ces charbons se sont formés à l'arrière des zones littorales actives, dans des endroits subissant des abaissements de terrain causés par la compaction et l'assèchement des schistes argileux. La zone où s'accumulait la tourbe était généralement protégée des inondations riveraines ainsi que de celles causées par les tempêtes ou les marées. Une évaluation statistique des propriétés pétrographiques, par l'analyse des correspondances sur des données provenant de charbons inclus dans la formation de Gates qui date du Crétacé inférieur, montre que les charbons provenant de zones de plaine littorale sont caractérisés par de faibles teneurs en vitrinite et de hautes teneurs en inertinite. Les teneurs en liptinite sont négligeables. Les indices de préservation des fibres ainsi que les indices de gélification établissent l'existence d'un milieu de sédimentation de type forestier dans lequel le niveau phréatique était relativement bas, ce qui a favorisé l'accumulation de composants oxydés ou partiellement oxydés. La présence de quantités importantes de composants détritiques indique que des matières organiques ont été transportées avant que la sédimentation ne se produise.

INTRODUCTION

Although many models have been proposed for the formation of coal (e.g., Stach et al., 1982; McCabe, 1984), there is no satisfactory explanation for thick and widespread coal deposits resting directly on regionally extensive sheets of sandstone and conglomerate which were deposited along wave-dominated coastlines. Yet coals formed in this depositional setting are economically significant, being thick and having relatively low ash and sulphur contents.

Laterally continuous, extensive sheets of coal up to 12 m thick, sitting directly on littoral sandstones have long been recognized as generally having formed on broad coastal plain deposits (Spieker and Reeside, 1925). Interpretations for deposition of the coal have varied from coastal plain swamps (Spieker and Reeside, 1925), barrier island lagoons (Young, 1955; Doelling, 1972), delta plains (Cotter, 1976) and delta-front foreshore deposits (Levy, 1985). More recently, many of these coastal deposits have been interpreted as deposits of progradational wave-dominated deltas and associated strandplains (Balsely and Parker, 1983; Levy, 1985; Leckie, 1986).

Petrographic composition of low rank coals has been used extensively to describe the environments of deposition in ancient peat swamps (e.g., Teichmüller, 1962; Schneider, 1978, 1980; von der Brelie and Wolf, 1981; Hagemann and Wolf, 1987). For bituminous coals, such as the Lower Cretaceous coals of the Rocky Mountain Foothills, comprehensive data and interpretations as to the relationship between petrographic composition and paleoenvironments of peat formation are found less frequently (Hacquebard and Donaldson, 1969; Cameron, 1972; Allshouse and Davis, 1984; Diessel, 1982, 1986; Hunt et al., 1986). The methods which have been used to relate coal petrographic characteristics to environments of deposition include lithotype, microlithotype and maceral analyses.

In the present study, maceral analyses have been used to relate petrographic composition of the coals to environments of deposition. Diessel (1982), in a study on Australian coals, discussed the diagnostic values of individual coal macerals. In the vitrinite group, the occurrence of vitrinite A (telenite, telocollinite) indicates an origin from wood-producing plants. Vitrinite B (desmocollinite), although commonly representing a major proportion of the total vitrinite component, is less diagnostic because this maceral

may have been derived from a variety of organic sources. Liptinite macerals such as sporinite, resinite, cutinite and alginite all refer to specific sources and some, like alginite, are also indicators of the relative position of the water table during peat accumulation. In the inertinite group, macerals such as semifusinite and fusinite refer to an origin from woody sources, but also indicate slightly drier to very dry conditions in the peat swamp where these components were exposed to oxidation processes and/or fungal attacks. There is also a possibility of forest fires contributing a substantial amount of fusinite (pyrofusinite) to the overall coal composition. The other facies-diagnostic maceral of the inertinite group appears to be inertodetrinite which represents broken-up pieces of fusinite and semifusinite, thus indicating an origin from woody precursors. The association of inertodetrinite with degraded vitrinite (vitrinite B) and sporinite in Carboniferous and Permian coals has previously been interpreted to represent a reed-type moor environment characterized by substantial degradation of the organic matter (Teichmüller, 1962; Diessel, 1982). In a more recent study, Diessel (1986) defined a Tissue Preservation Index (TPI) and a Gelification Index (GI) for a number of Australian coals and was able, in comparison with sedimentologically well-characterized associated strata, to assign specific depositional environments (dry forest swamp, wet forest swamp, fen, marsh).

The objectives of this paper are to relate coal characteristics to depositional environments of the coals in the Lower Cretaceous Gates Formation in Western Canada. A north-south cross section along the Lower Cretaceous interval in the Rocky Mountain Foothills is shown in Figure 1. Locations of outcrop sections analyzed for a larger, more regional study (Kalkreuth and Leckie, in press) are shown. The present study provides a detailed example of coal characteristics and depositional environments of Gates Formation coals from the Luscar coalfield of the southern study area (Fig. 1, location 3) and a more general description for regional occurrences of Gates Formation coals.

CHARACTERISTICS OF WAVE-DOMINATED DELTAS AND STRANDPLAINS

Characteristics of wave-dominated deltas and strandplains are shown in Figure 2. The coals formed on regionally extensive sheets of shoreface sand and/or gravel that were deposited along the coast of wave-dominated deltas and associated strandplains (Fig. 2). Sediment brought to the shoreline by the distributaries was reworked and redistributed by wave action and longshore drift. Riverine flow, transporting sediment to the coast, is concentrated in one or two major distributary channels (Coleman, 1981) that generally remained fixed over long periods of time. Representative vertical sequences which resulted from shoreline progradation are shown in Figure 3.

LOWER CRETACEOUS GATES FORMATION, WESTERN CANADA

The Albian Gates Formation consists of several upward-coarsening sequences (Fig. 1), formed on the western margin of the North American Cretaceous epeiric seaway. Gates shorelines prograded northwards as a series of sand and gravel-rich, wave-dominated deltas and strandplains (Leckie and Walker, 1982; Leckie, 1986) that extended as a sheet sand laterally along strike for at least 230 km and downdip for up to 90 km. The lowermost shoreline sediments of the Gates Formation are underlain by 206 m of marine shales of the Moosebar Formation at Bullmoose Mountain and 42 m at Mt. Torrens (Fig. 1).

The shoreface sandstones are directly overlain by a coal-bearing unit with coals in excess of 12 m thick, which can be traced laterally for 230 km, directly above the underlying sheet sandstone. The upper Gates Formation in the south and central portion of the study area (Fig. 1, Locations 1 to 8) can generally be considered as having been deposited in an upper delta-plain to fluvial environment.

The marine to nonmarine cycles of the upper part of the Gates Formation at its northern limit (Fig. 1, Locations 9 to 12) also contain sheet sandstones and conglomerates 30 to 40 km wide and greater than 150 km long. They are capped by thin coals or carbonaceous shales a few centimetres to decimetres thick (Cant, 1984; Leckie, 1986).

PETROGRAPHIC CHARACTERISTICS OF LOWER CRETACEOUS COALS

In the context of the present study 357 whole seam samples were analysed petrographically. Coals were collected in the Rocky Mountain Foothills over a distance of approximately 600 km from Mountain Park in the southeast to Pink Mountain in the northwest (Fig. 1). The samples represent a number of depositional environments, ranging from the alluvial fan deposits of the Cadomin Formation and the deltaic-fluviatile/coastal plain successions of the Gething Formation to the alluvial to coastal plain sequences of the Gates Formation (Mountain Park Member and Grande Cache Member, respectively).

Sampling and petrographic analysis

The samples were collected as channel samples from outcrop and mine sites. In cases where a number of successive samples had been taken from a seam, a composite sample was prepared according to the thickness of the individual layers. The samples were then processed according to standard procedures (Bustin et al., 1985). Petrographic composition was determined by maceral analyses based on 500 counts/sample using a slightly modified Stopes-Heerlen system (ICCP, 1963) for the classification of coal macerals. Maceral contents are expressed in volume per cent on a mineral matter free basis (m.m.f.).

Correspondence analyses

In order to facilitate a comparison and interpretation of the large number of samples, the petrographic data and a number of additional variables such as the vitrinite/inertinite ratio obtained from the maceral analyses were first evaluated for similarity levels and significance using correspondence analysis. For details of calculations and applications in geology see Lebart et al. (1984) and David et al. (1977). In general, in this type of statistical analysis, groups of sample points can be interpreted as a result of the same processes or belonging to a specific family. Similarly, nearby variable points will indicate high similarity levels between the variables. A group of sample points will be characterized by the variable points close to that group. Points plotting near the centre of gravity represent undifferentiated distributions and are considered to be of low significance. In general the greater the distance from the centre of gravity the greater the significance of variables and samples. However, loadings (proportional to frequencies) and absolute contributions to the principal axis must be checked before final judgement is made (Tables 1 and 2). For further details, see Kalkreuth and Leckie (in press). The strandplain coals form distinct groups in the correspondence diagram (Fig. 4).

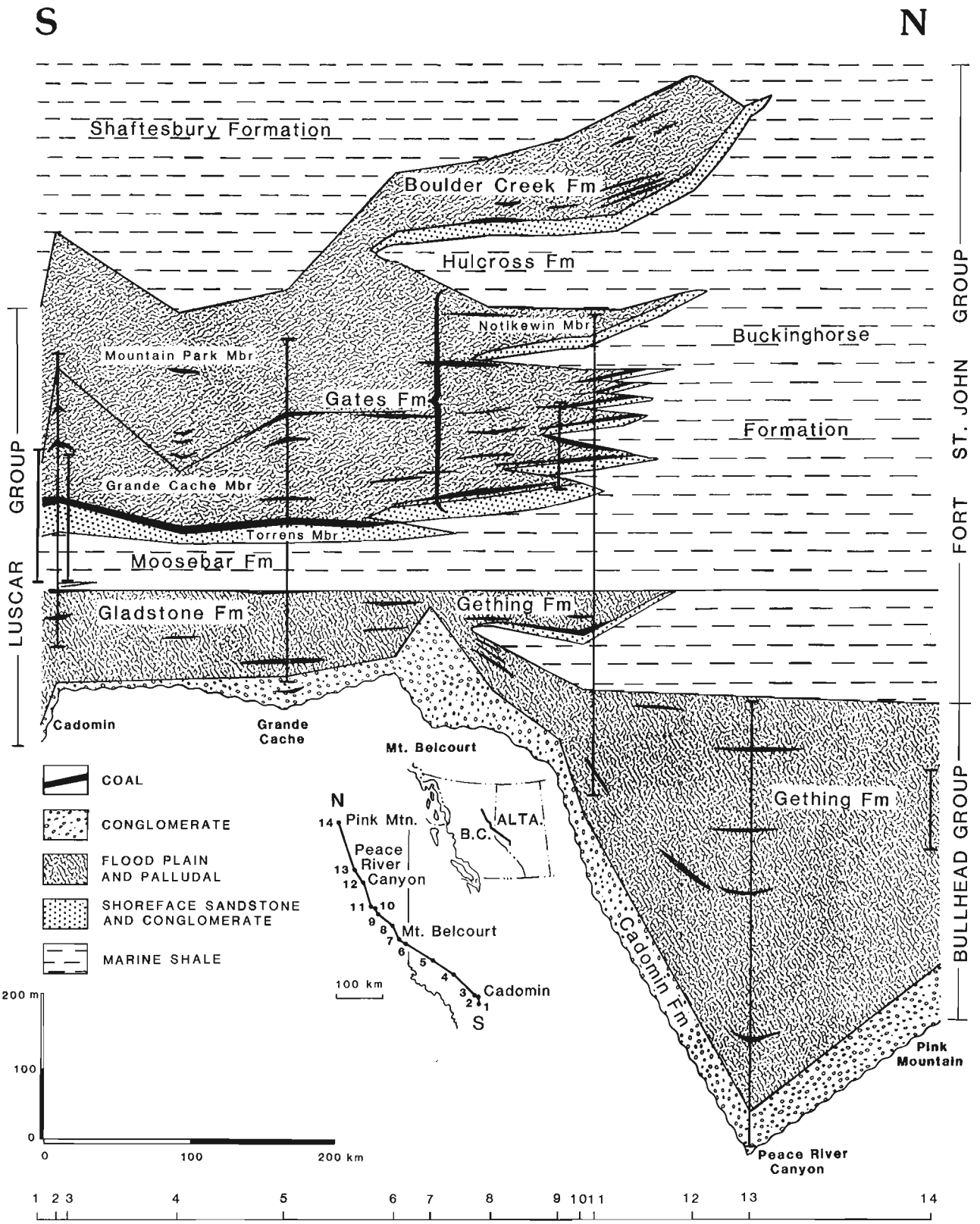

Figure 1. *North-south cross section along the Foothills of western Alberta and northeastern British Columbia. Vertical bars in section represent locations used for detailed coal petrographic analyses. Location of sections used for control are 1 = Mountain Park; 2 = Cadomin; 3 = Luscar; 4 = Little Berland and South Berland Rivers; 5 = Grande Cache; 6 = Mt. Torrens and Torrens Ridge; 7 = Mt. Belcourt; 8 = Duke Mountain; 9 = Mesa, Shikano and Wolverine Pits, Tumbler Ridge; 10 = Mt. Spieker; 11 = Bullmoose Mountain; 12 = Dokie Ridge; 13 = Peace River Canyon; and 14 = Pink Mountain. Data from Stott (1968, 1984), Carmichael (1983), Leckie (1983) and Gibson (pers. comm., 1987).*

Absolute contribution levels of macerals and mineral matter show that the first principal axis (F1; Fig. 4) is composed of vitrinite contents on the one side and inertinite contents on the other (Table 1). The second principal axis (F2; Fig. 4) has the highest contribution from mineral matter contents with only minor contributions from liptinite macerals (Table 1). Close similarity levels are indicated for many of the Gates coals by proximity and overlapping areas that are characterized by large amounts of inertinite macerals. The contributions of mineral matter and liptinite macerals to these inertinite-rich coals is generally small. A few subgroups also exist. One subgroup has greater contributions of mineral matter whereas maceral distribution (inertinite vs vitrinite) stays more or less constant. Another subgroup has significantly increased vitrinite contents commonly associated with higher amounts of mineral matter.

Coal seams collected from the underlying Torrens Member and some examples from coals developed within the upper part of the Grande Cache Member in the south are generally characterized by increased vitrinite contents and substantial amounts of mineral matter. Regionally there appears to be more similarity between the coals of the Grande Cache Member in the south than in the north, where lower similarity levels are indicated by the formation of subgroups as illustrated in the correspondence analysis graph (Fig. 4).

In a second correspondence analysis, a number of petrographic indices (Fig. 5) were tested for similarities and significance levels among themselves and in their relation to the original variables (macerals and mineral matter). The correspondence analyses graph (Fig. 5) shows that the absolute contributions to the first two principal axes are highest for parameters such as V/I ratio, T/F ratio and Gelification Index (G.I.) which describe the variations in vitrinite and inertinite contents (Table 2). These parameters have the highest significance in the context of this study. Less significant, with only minor contributions to the first two principal axes, are the parameters SF/F ratio, W/D ratio and Tissue Preservation Index (T.P.I.; Table 2); the latter two describe variations in preserved tissue versus detrital components. Negligible contributions come from parameters such as IR ratio, VA/VB ratio and S/D ratio which means that these parameters are highly insignificant in the interpretation of the coals investigated (Fig. 5, Table 2).

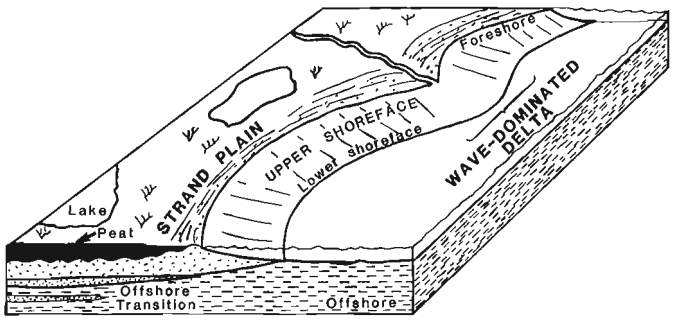

Figure 2. General characteristics of wave-dominated deltas and strandplains which form a laterally continuous sheet of sandstone and/or conglomerate.

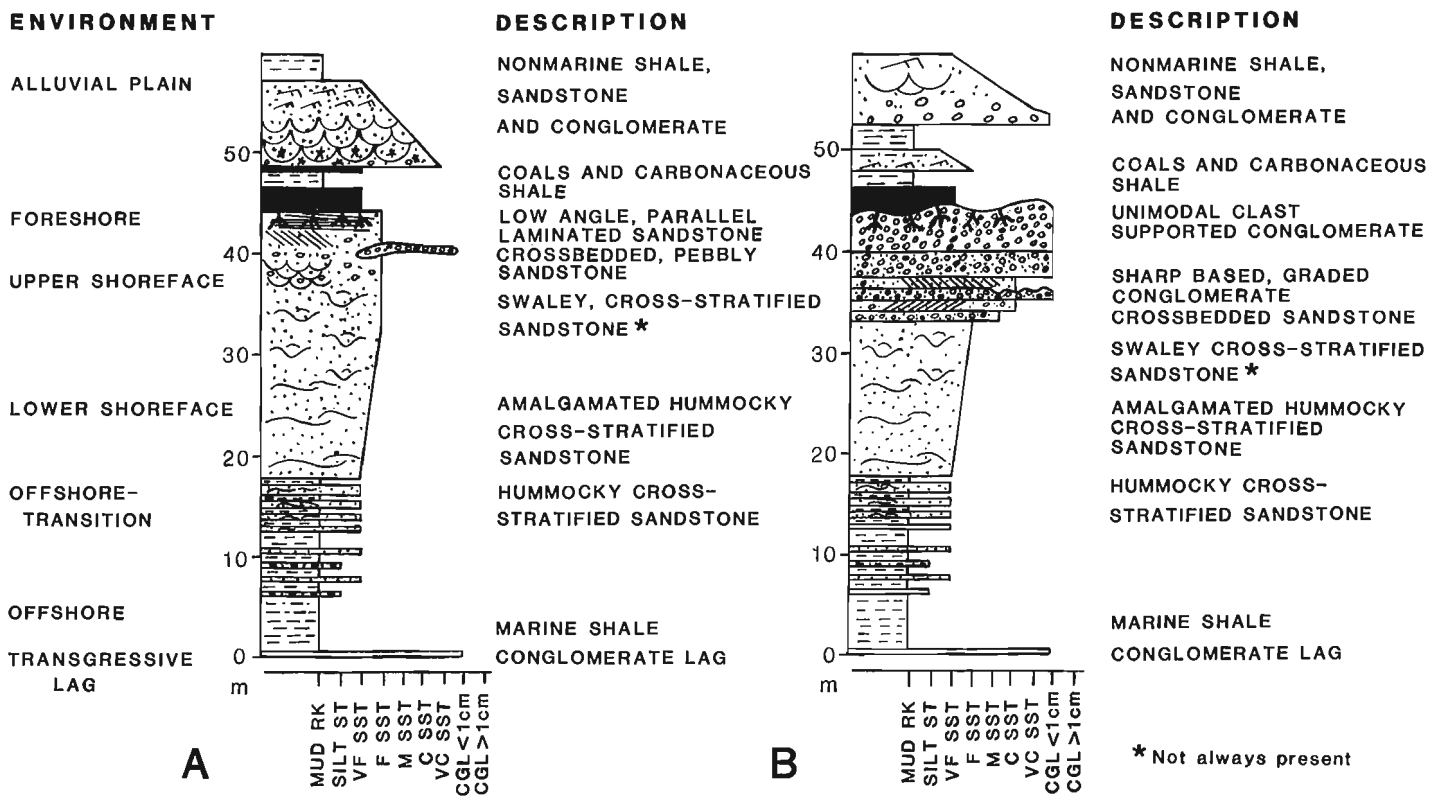

Figure 3. Generalized vertical sections resulting from the progradation of wave-dominated coastlines.

TABLE 1

Masses and absolute contributions from macerals and mineral matter to the first six principal axes (correspondence analysis, 1st run)

Variables	Masses	Distribution	Absolute Contributions					
			F1	F2	F3	F4	F5	F6
VITA	.158	.29	25.1	1.5	11.8	10.3	9.7	.2
VITB	.154	.10	.1	4.6	24.2	22.8	8.5	.0
VDET	.003	12.54	1.6	19.4	38.3	28.6	11.0	.2
VTOT	.314	.07	11.8	3.8	.2	2.2	.0	.3
SF	.072	.38	16.0	.0	3.1	.0	1.5	14.3
FUS	.021	.44	1.9	.0	.1	1.6	5.7	18.1
IDET	.051	.41	8.9	2.6	.0	4.0	.7	49.5
MAC	.008	.84	2.3	.3	1.2	.6	.1	.0
MIC	.003	1.74	.3	.0	.0	.3	.0	4.5
ITOT	.156	.28	28.7	.5	2.6	.8	1.3	.0
SPOR	.004	1.33	.0	.4	.5	5.4	14.1	.7
CUT	.000	1.00	.0	.0	.0	.0	.0	.0
RES	.000	8.59	.3	.3	.0	5.0	11.8	1.6
OTH	.000	12.43	.0	.2	.4	2.1	4.9	3.6
LTOT	.006	1.56	.0	.7	.4	11.7	30.7	3.4
MIN	.049	1.10	3.0	65.6	17.2	4.5	.1	3.4

TABLE 2

Masses and absolute contributions from macerals, mineral matter contents and petrographic indices to the first six six principal axes (correspondence analyses, 2nd run)

Variables	Masses	Distribution	Absolute Contributions					
			F1	F2	F3	F4	F5	F6
VITA	.128	.16	5.4	.3	10.4	.6	1.6	18.9
VITB	.137	.09	.5	3.7	1.7	12.9	.8	17.1
VDET	.002	11.20	.5	15.2	2.2	.0	54.8	6.2
VTOT	.267	.04	1.4	.4	9.0	9.4	.9	.0
SF	.068	.35	9.5	.8	1.7	8.7	.0	2.0
FUS	.020	.41	1.2	.0	1.9	.3	.0	2.8
IDET	.048	.40	5.9	.4	8.0	.1	.5	2.6
MAC	.008	.80	1.3	.9	.3	1.4	.0	.5
MIC	.002	1.76	.3	.1	.0	.0	.0	1.2
ITOT	.146	.26	17.9	.4	4.7	5.3	.0	.1
SPOR	.004	1.32	.0	1.0	1.4	.0	.5	11.0
CUT	.000	1.00	.0	.0	.0	.0	.0	.0
RES	.000	8.88	.1	.5	.4	.3	.0	6.0
OTH	.000	15.05	.0	.3	.3	.0	.3	3.1
LTOT	.005	1.55	.0	1.7	2.4	.0	.5	18.6
MIN	.043	1.03	.7	58.7	7.8	4.2	15.3	.1
A/B	.004	.45	.3	.2	.4	.4	.0	2.9
SF/F	.017	.79	2.1	.0	3.6	1.0	1.0	1.2
V/I	.016	1.63	10.7	2.0	5.3	.0	.2	.6
T/F	.017	3.31	21.1	5.6	18.7	1.0	.0	1.5
I-RATIO	.008	.39	.0	.0	1.9	2.1	.0	1.4
W/D	.030	1.24	7.6	3.1	9.7	48.4	5.6	.3
TPI	.007	1.79	.5	1.0	.0	2.7	17.2	.0
GI	.017	1.83	13.0	3.5	7.9	.0	.4	1.3
S/D	.005	.17	.0	.0	.4	1.0	.0	.7

Coal characteristics and depositional environments of the Gates coals

Gregg River Mine, Luscar

The section sampled (Fig. 1, location 3) is shown in Figure 6 and represents a composite separated by 650 m. Samples were collected from a thin coal seam developed in the shoreface sandstone of the Torrens Member, the Jewel seam directly on the shoreface sandstones, and the Ruff seam from the upper delta plain deposits. Within this sequence, systematic trends in maceral contents, mineral matter content and in the petrographic indices are apparent (Fig. 6). The seam from the Torrens Member has a very high vitrinite content (93%) whereas inertinite content is low (7%). Liptinite macerals were found only in traces. The mineral matter content is very high (47%). In contrast, the samples collected from the Jewel seam show a drastic decrease in vitrinite contents (46 to 58%) whereas inertinite macerals account for 40 to 52%. Macerals of the liptinite group (in the form of sporinite) are still rare (up to 2%). Mineral matter contents in the Jewel seam range from 2 to 23%. Higher vitrinite content is indicated for the Ruff seam (96%) that contains only minor contributions of inertinite (3%) and liptinite (1%). The Ruff seam at this location has a mineral matter content of 21%. Many of the petrographic indices show distinct changes with respect to the stratigraphic position of the coal seams. Related to the overall contents of vitrinite and inertinite macerals, the Jewel seam has a very low V/I ratio, whereas the Torrens seam and the Ruff seam have high ratios. Preservation of the organic matter appears to be best in the Ruff seam, which is characterized by a high VA/VB ratio, a high W/D ratio, a high S/D ratio and a very high Tissue Preservation Index. In contrast, the Jewel seam appears to have a lesser degree of plant preservation, mainly because of substantial amounts of inertodetrinite (low W/D and S/D ratios) and vitrinite B (low VA/VB ratio). Within the inertinite group, semifusinite is the predominant maceral (22 to 24%, high SF/F ratios, Fig. 6), whereas the total amount of structured inertinite (fusinite and semifusinite) is always greater than inertodetrinite (IR ratios = 1.35 to 2.02, Fig. 6).

To assess the type of prevailing moor during accumulation of the organic matter, the Gelification and Tissue Preservation Indices for the five coals were plotted in a facies diagram (Fig. 7) as proposed by Diessel (1986). The three samples of the Jewel seam plot very close to each other, which indicates a similar type of depositional environment for these strandplain coals. They must have been formed under relatively dry conditions as indicated by the high amounts of inertinite macerals (semifusinite, inertodetrinite, to a lesser extent fusinite). The major split of the seam as illustrated in Figure 6 might be a result of local flooding adjacent to distributary channels, or a result of lacustrine conditions caused by temporarily and locally increased subsidence rates. The Torrens seam has a much higher Gelification Index (Fig. 7) due to a very high vitrinite content and low amounts of inertinite. The formation of the Torrens seam most likely reflects slight sea level fluctuations during deposition of the Torrens Member in which peat accumulated while a relatively high water table level was maintained, as indicated by the large amounts of gelified plant remains. The Ruff seam in the Gregg River Mine area is highly variable in thickness, ash content and lateral

continuity. Very high Gelification and Tissue Preservation Indices (Fig. 7) are the result of the Ruff seam being made up almost entirely of vitrinite. As such, the Ruff seam might represent a locally flooded moor of the upper delta plain which had a significant influx of mineral matter associated with a relatively high water table.

CORRESPONDENCE ANALYSIS (68.94% of total variance)

INPUT: 357 samples, 16 variables (macerals and mineral matter content)

HISTOGRAMS OF THE FIRST EIGENVALUES

	EIGENVALUE	%	% CUM.	
1	.14722440	47.55	47.55	**********
2	.06619453	21.38	68.94	**********
3	.02458061	7.94	76.88	**********
4	.02217416	7.16	84.04	**********
5	.01848809	5.97	90.01	**********
6	.00880679	2.84	92.85	**********
7	.00620995	2.01	94.86	**********
8	.00458683	1.48	96.34	**********
9	.00421238	1.36	97.70	**********
10	.00387766	1.25	98.96	**********
11	.00284707	.92	99.87	**********
12	.00029741	.10	99.97	**********
13	.00004946	.02	99.99	**********
14	.00004036	.01	100.00	**********
15	.00000011	.00	100.00	**********

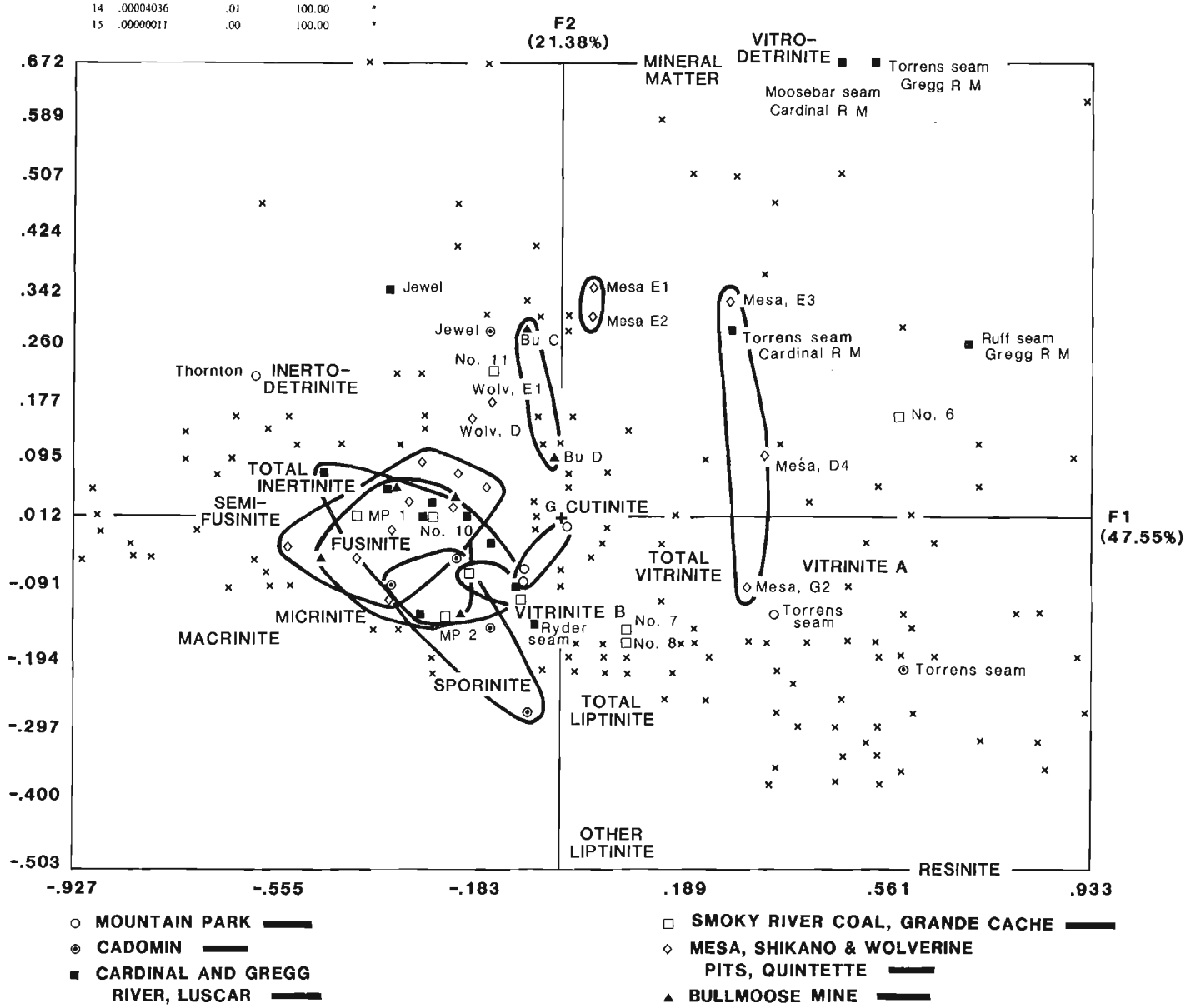

Figure 4. *Diagram illustrating similarity levels of Lower Cretaceous coals with respect to maceral contents and mineral matter content. The encircled areas indicate ranges for Lower Cretaceous Gates coals from locations 1, 2, 3, 5, 9 and 11, Figure 1. "x" = point of undefined sample.*

CORRESPONDENCE ANALYSIS (59.15% of total variance)

INPUT: 334 samples, 25 variables (macerals, mineral matter, ratios)

HISTOGRAMS OF THE FIRST EIGENVALUES

	EIGENVALUE	%	% CUM.	
1	.18711610	45.01	45.01	**********
2	.05877273	14.14	59.15	**********
3	.04273815	10.28	69.43	**********
4	.02895065	6.96	76.39	**********
5	.02148402	5.17	81.56	**********
6	.01628027	3.92	85.48	*******
7	.01320793	3.18	88.65	*****
8	.01115207	2.68	91.34	*****
9	.00711949	1.71	93.05	***
10	.00672826	1.62	94.67	***
11	.00447071	1.08	95.74	**
12	.00376298	.91	96.65	**
13	.00357801	.86	97.51	**
14	.00335086	.83	98.34	**
15	.00289114	.70	99.04	**

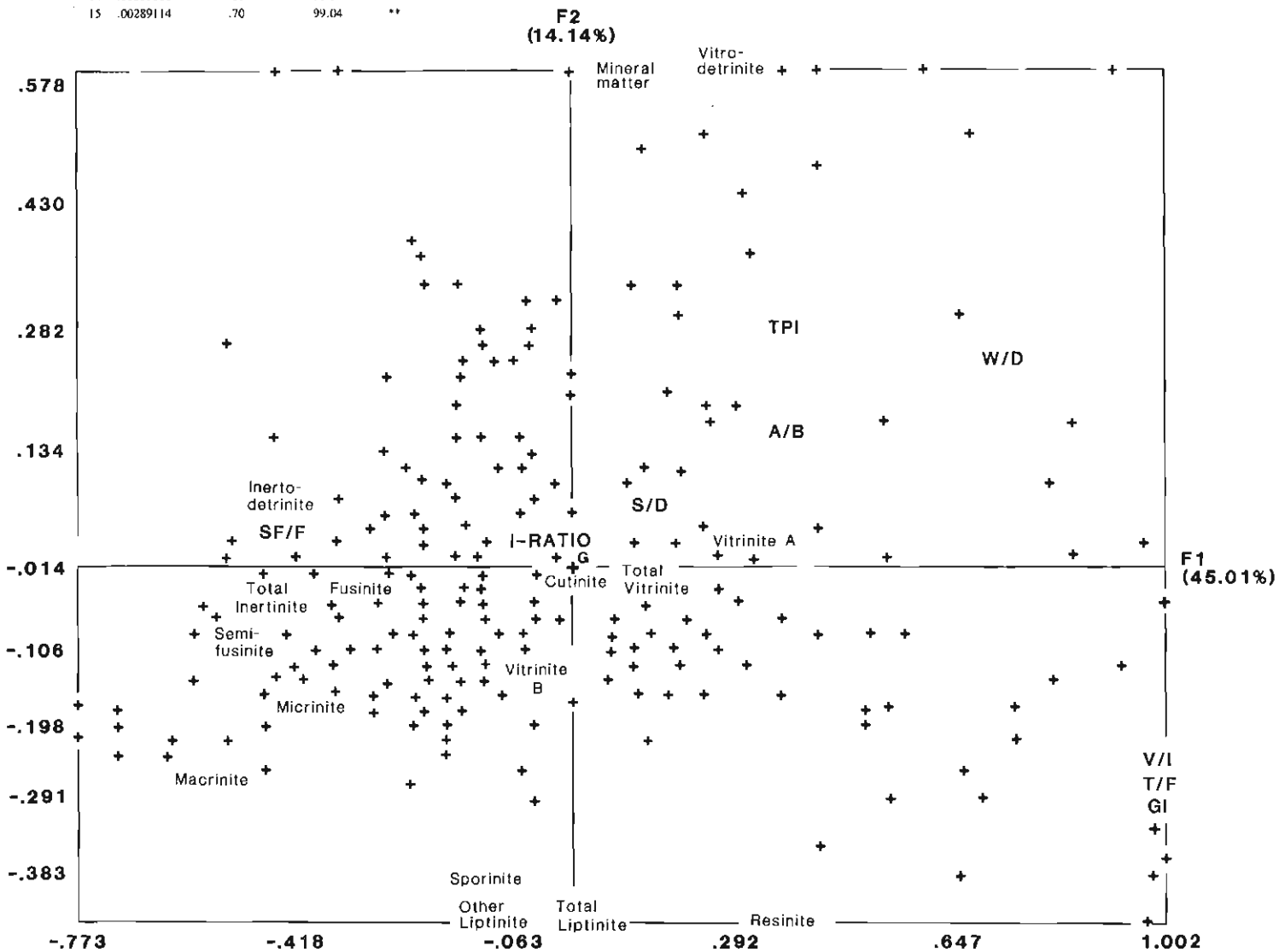

Figure 5. *Diagram illustrating similarity levels for petrographic indices with respect to samples and maceral data. "x" = point of undefined sample. Petrographic Indices are: Gelification Index = (Total Vitrinite + Macrinite)/(Semifusinite + Fusinite + Inertodetrinite); IR ratio = (Semifusinite + Fusinite)/(Inertodetrinite + Macrinite + Micrinite); S/D ratio = (Vitrinite A + Fusinite + Semifusinite)/(Alginite + Sporinite + Inertodetrinite + Vitrinite B + Vitrodetrinite); SF/F ratio = Semifusinite/Fusinite; T/F ratio = Total Vitrinite/(Fusinite + Semifusinite); Tissue Preservation Index = (Vitrinite A + Fusinite + Semifusinite)/(Vitrinite B + Macrinite + Inertodetrinite); V/I ratio = Total Vitrinite/Total Inertinite; VA/VB ratio = Vitrinite A/Vitrinite B and W/D ratio = (Vitrinite A + Fusinite + Semifusinite)/(Alginite + Sporinite + Inertodetrinite).*

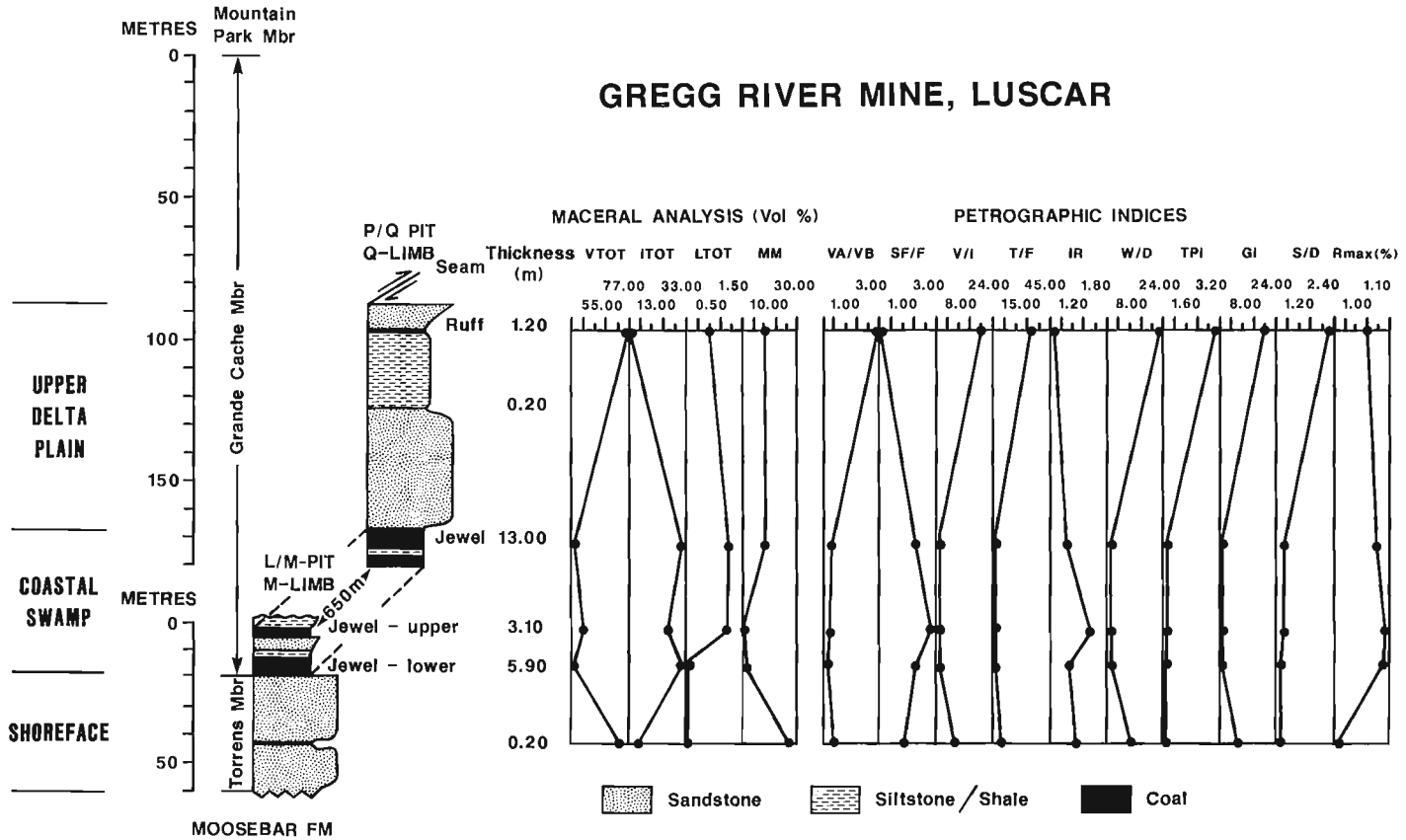

Figure 6. Maceral data, mineral matter contents and petrographic indices for Lower Cretaceous Gates coals, Gregg River Mine, Luscar (stratigraphic section from Langenberg, Macdonald and Strobl, Alberta Geological Survey, unpublished). Rmax % = mean maximum vitrinite reflectance. For abbreviations of petrographic indices, see Figure 5.

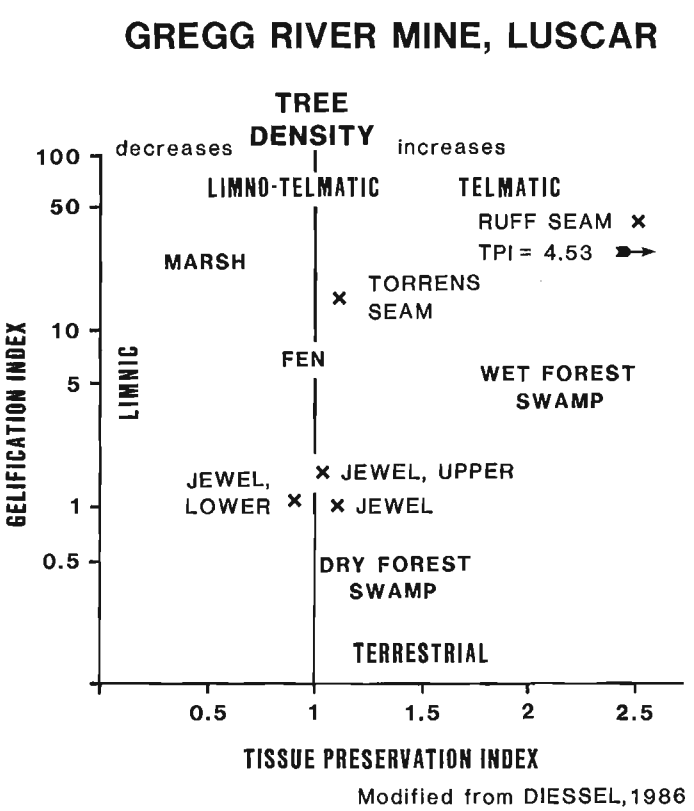

Figure 7. Facies diagram for Lower Cretaceous Gates coals at Gregg River Mine, Luscar.

General petrographic characteristics of Gates coals

In addition to the detailed examination of the coals from the Gregg River Mine, three other sections of the Gates Formation (Fig. 1, locations 5, 9 and 11) were examined by Kalkreuth and Leckie (in press). The results indicate that the coals which accumulated on the strandplain above the marine sandstones of the Torrens Member form distinct groups (Fig. 4). However, considerable petrographic variation occurs among these groups and there is also some overlapping of petrographic characteristics for the overlying coals from the upper and lower delta plains.

The coals are generally characterized by relatively low vitrinite contents from 45 to 66% with a mean of 57%. In contrast, inertinite contents are relatively high (31-53% mean = 42%). Within the inertinite group, major components are semifusinite (14-24%, mean = 20%), inertodetrinite (8-19%, mean = 13%) and fusinite (3-10%, mean = 5%). Liptinite content is low, (nil to 9%, mean = 2%). The relatively low vitrinite contents and high amounts of inertinite macerals, in particular semifusinite, indicate rather low water tables during peat accumulation in which a substantial part of the organic matter was oxidized prior to final burial.

Mineral matter in most of the coals is low, ranging from 2 to 11% with a mean of 6%. Three seams form a separate group for which increasing amounts of mineral matter were determined (23-29%). The high mineral matter content in these seams may be related to local flooding adjacent to fluvial channels.

Overall, petrographic indices vary from one sample to the other. The V/I ratios range from 0.85 to 2.00 (mean = 1.40) which indicates for most of the coals the predominance of gelified components (vitrinite) over non-gelified (inertinite macerals). Within the vitrinite group, the VA/VB ratio indicates a slight dominance of vitrinite B over vitrinite A (mean = 0.86), which suggests that substantial amounts of woody materials were decomposed prior to burial. The same holds true for the relatively high proportion of inertodetrinite which is derived from mechanical breakdown of fusinite and semifusinite precursors. The IR ratios ([semifusinite + fusinite]/inertodetrinite) range for the strandplain coals from 1.16 to 2.64 with a mean of 1.58. That means that in all of these coals the sum of semifusinite + fusinite macerals is greater than inertodetrinite. IR ratios <2 were considered by Diessel (1982) to reflect hypauthochtonous and allochthonous conditions in the ancient peat swamps where dominantly semifusinite, fusinite and inertodetrinite were deposited. This indicates that some transportation took place during the accumulation of the Gates Formation shoreface/strandplain peats. Tissue preservation indices are low to intermediate (T/F: 0.22 - 2.01, mean = 1.02; TPI Index: 0.64 - 1.54, mean = 1.14). These values indicate for the strandplain coals a forest-swamp type of depositional environment with periods of low water tables during which substantial amounts of oxidized and partly oxidized materials were formed. The relatively high contents of the non-gelified macerals semifusinite, fusinite and inertodetrinite relative to the amounts of gelified components (i.e., vitrinite) leads to relatively low gelification indices (1.00 - 2.27, mean = 1.59). Applying a coal facies diagram, as proposed by Diessel (1986), for many of the shoreface/strandplain coals of the Lower Cretaceous, a forest-moor type of depositional environment is envisioned (Fig. 8). Some coals are characterized by somewhat higher gelification indices but similar TPI indices, which indicates a shift to a less forested, fen-like depositional environment characterized by a larger input of aquatic plants such as reeds and sedges.

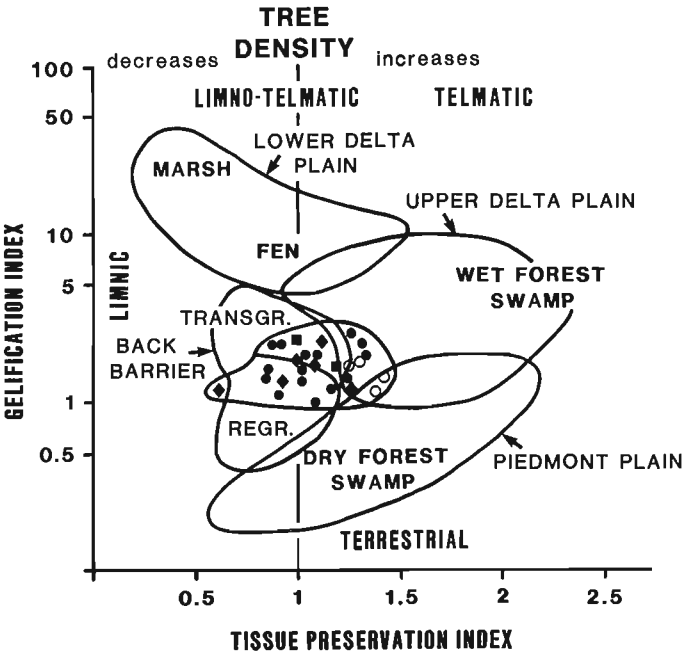

- MOUNTAIN PARK, CARDINAL AND GREGG RIVER MINES, LUSCAR
- SMOKY RIVER COAL, GRANDE CACHE
- MESA AND WOLVERINE PITS, QUINTETTE COAL, TUMBLER RIDGE
- BULLMOOSE MINE, TUMBLER RIDGE

Figure 8. Coal facies and depositional environments for the Lower Cretaceous Gates Formation strandplain coals (modified from Diessel, 1986).

PROPOSED MODEL FOR FORMATION OF STRANDPLAIN COALS

A model for coal formation on progradational wave-dominated deltas and strandplains is shown in Figure 9. For this model, the shoreline deposits of the prograding deltaic/strandplain system are considered to be similar to a tea saucer (Fig. 9). The zone of active sediment supply and high wave energy was represented by the high energy beaches which acted as the saucer rim. Sediment brought to the shoreline by distributaries was redistributed along the coast by longshore drift. Even though the coastlines were high energy ones, with high rates of sediment supply, all the wave energy was expended on the foreshore and shoreface and none was transmitted landward of the beach except when large storms, perhaps combined with high tides, occurred. Many of the coals show large amounts of components such as inertodetrinite and vitrinite B, which are probably related to occasional flooding and storm events, at which time mechanical breakdown of original source materials took place during transport. Although mineral matter content is generally low (averaging Vol. 6%), some seams have mineral matter contents up to 30 Vol. %, perhaps due to flooding and storm events.

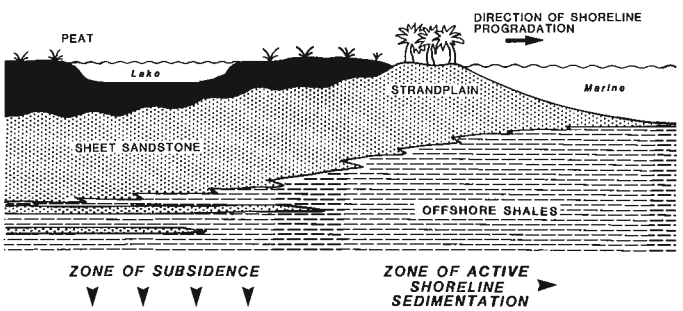

Figure 9. Depositional model to illustrate the formation of laterally continuous coals above regionally extensive strandplain deposits.

The shoreface sandstones formed a platform on which the coal and peat accumulated. The platform was relatively flat with gentle undulations due to paleobeach ridge topography (e.g., Leckie and Walker, 1982; Young, 1976; Curray et al., 1969). This relief would have affected the water table, which in turn played a major role in the preservation of source materials (gelified organic materials such as vitrinite versus nongelified materials such as fusinite and semifusinite). Although the coals formed directly on coastal deposits, they would not have formed at the shoreline. The presence of brackish or salt marshes having a high H_2S content would have generated sulphur-rich, pyritic coal (Postma, 1982; Cohen, 1984). Instead, the coals are characterized by low sulphur contents, and thus were probably not affected by aqueous sulphate from marine

waters which would produce high sulfur coals (Cohen, 1984). The low sulphur content indicates that the peats were removed from the active shoreline and there was minimal brackish or no marine influence.

The shoreface sandstones of the strandplain began to subside almost immediately after their deposition and, as a result, it is only the immediate coastal sands which are at sea level. The marine muds in front of the wave-dominated delta were initially deposited with a high porosity, typically exceeding 50% (Hamilton, 1976). Compaction of the muds was rapid during the initial stages of burial, there typically being a porosity reduction of 15 to 17% in the first 200 m (Hamilton, 1976). Mechanical compaction squeezed out interstitial water and the increased temperature and confining pressure also released chemically bound water from clays and other hydrated minerals. The expelled waters flowed updip and landwards and may have contributed to recharging the strandplain water table (Galloway and Hobday, 1983). The subsidence was largely the result of compaction of the underlying shales by dewatering and clay particle rearrangement with a lesser tectonic contribution. The shoreline zone of active sedimentation was, in effect, a hingeline which migrated seawards.

This model satisfies the two major requirements for peat accumulation: 1) protection from active sedimentation; and 2) a high water table for the formation and preservation of organic matter (McCabe, 1984). The petrographic characteristics of the coals indicate fluctuating water tables that led to high amounts of oxidized to partially oxidized components (semifusinite and fusinite contents, averaging 20 and 5 Vol. %, respectively) which were formed during periods of relative dryness. Protection from active sedimentation landward from the shoreline is inherent in the wave-dominated coastline model (Fig. 9). The wave dominated delta had only one or two active distributaries (Coleman, 1981) and consequently large areas were removed from active clastic sedimentation. Thus, this reduced the detrital influx and produced low-ash peats. Furthermore, the rapidly subsiding strandplain sands were the platform (i.e. inner, lower portion of the tea saucer) on which the peats accumulated.

It is critical to the model that the rate of subsidence matches the rate of peat accumulation. If the rate of upward growth of the peat swamp is matched by subsidence due to shale compaction, then substantial thicknesses of peat can accumulate. If the rate of subsidence exceeds the rate of peat formation then the area will be submerged and a large, probably shallow lake will form instead of a peat forming swamp.

A reasonably high groundwater table is a prerequisite for high organic productivity and preservation of peat. Wave-dominated deltas and strandplains have a shallow water table and contain one of the most highly transmissive and laterally uniform aquifers (Galloway and Hobday, 1983). Upper shoreface sands have a low mud content due to persistent wave agitation above fair weather wave base. As such, they form an isotropic and homogeneous medium bounded above and below by the less permeable lower shoreface sands and shales of the offshore zone. Porosities through the nonindurated shoreface sands are typically 30 to 50% (Freeze and Cherry, 1979). The climate during deposition of Gates Formation sediments was generally humid to subhumid, providing an ample meteoric source for groundwater recharge. Discharge of meteoric-derived groundwater dominates water table circulation, and a meteoric recharged groundwater system can maintain a very large area having a shallow to emergent water table that is ideal for plant growth and peat preservation. Preliminary investigations on lithotype variations within the Gates Formation seams suggest that the coals are characterized by great variations in vertical succession, indicative of fluctuating water tables. The groundwater rises or maintains its position as compaction of the peat mat takes place and the strandplain subsides. The peat essentially develops and maintains its own water table. In the examples described above, the coals formed over progradational shoreface sediments at a time when relative sea level would have been at a standstill or beginning to fall. Thus, the high water tables were not the result of sea level rise.

CONCLUSIONS

Coal seams formed on the wave-dominated, strandplain sediments of the Gates Formation are characterized by great lateral continuity (tens to hundreds of kilometres), substantial thicknesses (up to 12 m), relatively low ash and low sulphur contents. The coals formed behind an active shoreline in areas undergoing subsidence due to shale compaction and dewatering. The zone of peat accumulation was removed from the shoreline and generally protected from fluvial flooding and storm/tidal inundations. Statistical evaluation, by correspondence analysis, of the Gates Formation showed that strandplain coals formed distinctive statistical groups that are characterized by relatively low vitrinite contents and high inertinite contents. In the inertinite group, semifusinite and inertodetrinite dominate. Liptinite contents are negligible. Tissue preservation and gelification indices for the strandplain coals indicate a forest-type depositional environment in which relatively low water tables allowed the accumulation of oxidized and partly oxidized components (fusinite and semifusinite). Fair amounts of detrital components such as inertodetrinite and vitrinite B are diagnostic that some transportation of the organic material took place prior to burial.

ACKNOWLEDGMENTS

We would like to thank management and mine geologists of Luscar Mine, Gregg River Mine, Smoky River Coal Ltd., Quintette Mine and Bullmoose Mine for allowing access to, and sampling from, the mine sites. Most of the coals were analyzed petrographically by D. Marchioni of Petro-Logic Services, Calgary. The section at Gregg River Mine was provided by W. Langenberg, D. Macdonald and R. Strobl of the Alberta Geological Survey. The paper benefited from the critical reviews by I. Banerjee and D. Marchioni.

REFERENCES

Allshouse, S.D. and Davis, A.
1984: Petrographic variation due to depositional setting of the Lower Kittanning seam, western Pennsylvania. In A Database for the Analysis of Compositional Characteristics of Coal Seams and Macerals, Final Report, Part 7, Coal Research Section, Pennsylvania State University, 95 p.

Balsely, J.K. and Parker, L.R.
1983: Cretaceous wave-dominated delta, barrier island, and submarine fan depositional systems: Book Cliffs, east-central Utah. Unpublished Field Guide, 163 p.

Bustin, R., Cameron, A., Grieve, D., and Kalkreuth, W.
1985: Coal Petrology - Its Principles, Methods and Applications. Geological Association of Canada, Short Course Notes, v. 3, Victoria, B.C., 2nd ed., 273 p.

Cameron, A.R.
1972: Petrography of Kootenay coals in the Upper Elk and Crowsnest areas, British Columbia and Alberta. In Proceedings of the First Geological Conference on Western Canada Coal, G.B. Mellon, J.W. Kramers, and E.J. Seagel (eds.); Research Council of Alberta Information Series no. 60, p. 31-42.

Cant, D.J.
1984: Development of shoreline-shelf bodies in a Cretaceous epeiric sea deposit. Journal of Sedimentary Petrology, v. 54, p. 541-556.

Carmichael, S.M.M.
1983: Sedimentology of the Lower Cretaceous Gates and Moosebar formations, northeast coalfields, British Columbia. University of British Columbia, unpublished Ph.D. thesis, 285 p.

Cohen, A.
1984: The Okefenokee Swamp: a low sulphur end-member of a shoreline-related depositional model for coastal plain coals. International Association of Sedimentologists, Special Publication no. 7, p. 321-240.

Coleman, J.M.
1981: Deltas: Processes of Deposition and Models for Exploration. Burgess Publishing, Minneapolis, 124 p.

Cotter, E.
1976: The role of deltas in the evolution of the Ferron Sandstones and its coals, Castle Valley, Utah. Brigham Young University Geology Studies, v. 22, p. 15-42.

Curray, J.R., Emmel, F.J., and Crampton, P.J.S.
1969: Holocene history of a strand-plain, lagoonal coast, Nayarit, Mexico. In Coastal Lagoons - A Symposium, A.A. Castanares and F.B. Phleger (eds.); Universidad Nacional Autônoma, Mexico, p. 63-100.

David, M., Dagbert, M., and Beauchemin, Y.
1977: Statistical analysis in geology: correspondence analysis method. Colorado School of Mines, Quarterly, v. 72, no. 1, p. 1-60.

Diessel, C.F.K.
1982: An appraisal of coal facies based on maceral characteristics. Australian Coal Geology, Part 2, v. 4, p. 474-484.

1986: The correlation between coal facies and depositional environments. In Advances in the Study of the Sydney Basin; Proceedings of 20th Symposium, The University of Newcastle, p. 19-22.

Doelling, H.H.
1972: Central Utah coal fields: Sevier-Sanpete, Wasatch Plateau, Book Cliffs and Emery. Utah Geology and Minerals Survey, Bulletin no. 793, p. 1-102.

Freeze, R.A. and Cherry, J.A.
1979: Groundwater. Englewood Cliffs, Prentice Hall, 604 p.

Galloway, W.E. and Hobday, D.K.
1983: Terrigenous clastic depositional systems. Springer-Verlag, New York, 423 p.

Hacquebard, P.A. and Donaldson, J.R.
1969: Carboniferous coal deposition associated with flood-plain and limnic environments in Nova Scotia. In Environments of Coal Deposition, E.C. Dapples and M.E. Hopkins (eds.); Geological Society of America, Special Paper no. 114, p. 143-191.

Hagemann, H. and Wolf, M.
1987: New interpretations of the facies of the Rhenish brown coal of West Germany. International Journal of Coal Geology, v. 7, p. 335-348.

Hamilton, E.L.
1976: Variations of density and porosity with depth in deep-sea sediments. Journal of Sedimentary Petrology, v. 46, p. 280-300.

Hunt, J., Brakel, A., and Smyth, M.
1986: Origin and distribution of Bayswater Seam and its correlatives in the Permian Sydney and Gunnedah Basins, Australia. Australian Coal Geology, v. 6, p. 59-75.

ICCP (International Committee for Coal Petrology)
1963: International Handbook of Coal Petrography, 2nd ed. Centre National de la Recherche Scientifique, Paris, France, variously paged.

Kalkreuth, W. and Leckie, D.A.
in press: Sedimentological and petrographical characteristics of Cretaceous strandplain coals: a model for coal accumulation from the North American Western Interior Seaway. International Journal of Coal Geology.

Lebart, L., Morineau, A., and Warwick, K.
1984: Multivariate Descriptive Statistical Analysis. John Wiley and Sons, New York, 231 p.

Leckie, D.A.
1983: Sedimentology of the Moosebar and Gates Formations (Lower Cretaceous). McMaster University, Hamilton, Ontario, unpublished Ph.D. thesis, 515 p.

1986: Rates, controls, and sand-body geometries of transgressive-regressive cycles: Cretaceous Moosebar and Gates formations, British Columbia. American Association of Petroleum Geologists, Bulletin, v. 70, p. 516-535.

Leckie, D.A. and Walker, R.G.
1982: Storm and tide dominated shorelines in Cretaceous Moosebar-Gates interval - outcrop equivalents of deep basin gas trap in western Canada. American Association of Petroleum Geologists, Bulletin, v. 66, p. 138-157.

Levy, R.A.
1985: Depositional model for understanding geometry of Cretaceous coals: major coal seams, Rock Springs Formation, Green River Basin, Wyoming. American Association of Petroleum Geologists, Bulletin, v. 69, p. 1359-1380.

McCabe, P.J.
1984: Depositional environment of coal and coal-bearing strata. Special Publication of the International Association of Sedimentologists, v. 7, p. 13-42.

Postma, D.
1982: Pyrite and siderite formation in brackish and freshwater swamp sediments. American Journal of Science, v. 282, p. 1151-1183.

Schneider, W.
1978: Zu einigen Gesetzmässigkeiten der faziellen Entwicklung im 2. Lausitzer Flöz. Zeitschrift für Angewandte Geologie, v. 24, p. 125-130.

1980: Mikropaläobotanische Faziesanalyse in der Braunkohle. Neue Bergbautechnik, v. 10, p. 670-675.

Spieker, E.M. and Reeside, J.B. Jr.
1925: Cretaceous and Tertiary formations of the Wasatch Plateau, Utah. Geological Society of America, Bulletin, v. 6, p. 435-454.

Stach, E, Mackowsky, M. Th, Teichmüller, M., Taylor, G.H., Chandra, D., and Teichmüller, R.
1982: Coal Petrology, 3rd ed. Gebrüder Borntraeger, Berlin-Stuttgart, 535 p.

Stott, D.F.
1968: Lower Cretaceous Bullhead and Fort St. John Groups, between Smoky and Peace Rivers, Rocky Mountain Foothills, Alberta and British Columbia. Geological Survey of Canada, Bulletin 152, 279 p.

1984: Cretaceous sequences of the foothills of the Canadian Rocky Mountains. In The Mesozoic of Middle North America, D.F. Stott and D.J. Glass (eds.); Canadian Society of Petroleum Geologists, Memoir 9, p. 85-107.

Teichmüller, M.
1962 Die Genese der Kohle. Compte Rendu, Quatrième Congrès de Stratigraphie et de Géologie du Carbonifère, p. 699-722.

von der Brelie, G. and Wolf, M.
1981 Zur Petrographie und Palynologie heller und dunkler Schichten im Rheinischen Hauptbraunkohlenflöz. Fortschritte in der Geologie von Rheinland und Westfalen, v. 29, p. 95-163.

Young, R.G.
1955: Sedimentary facies and intertonguing in the Upper Cretaceous of the Book Cliffs, Utah-Colorado. Geological Society of America, Bulletin, v. 66, p. 177-201.

1976: Genesis of Western Book Cliff coals. Brigham Young University Geology Studies, no. 22, p. 3-14.

Coal geology and resource potential of the Lower Cretaceous Luscar Group in west-central Alberta

F.M. Dawson
Institute of Sedimentary and Petroleum Geology, Calgary

Dawson, F.M., Coal geology and resource potential of the Lower Cretaceous Luscar Group in west-central Alberta. In Contributions to Canadian Coal Geoscience, Geological Survey of Canada, Paper 89-8, p. 26-31, 1989.

Abstract

Current knowledge of the coal resource potential of the Luscar Group is concentrated in the regions north of the Blackstone River in the Alberta Foothills. The Luscar project was initiated to compile and synthesize existing geological data and gather new data where required, in order to assess the coal resource potential within the regions to the south. Preliminary results of this project indicate that the main coal-bearing sequence lies within the Grande Cache Member of the Gates Formation of the Luscar Group. Up to six zones are present, of which two appear to be of potentially mineable thickness. The rocks have been highly folded and faulted, giving rise to a series of linear trends of coal-bearing strata parallel to the Front Ranges of the Rocky Mountains. This paper presents the geological framework upon which the coal resource potential of the Luscar Group will be determined. A series of 1:50 000 maps (to be published at a later date) and an accompanying report have been compiled to illustrate the distribution and structural complexity of the coal measure, as well as the developmental constraints that exist within the region.

Résumé

Les connaissances actuelles se rapportant à l'évaluation des ressources charbonnières du groupe de Luscar concernent surtout les régions situées au nord de la rivière Blackstone, dans les contreforts des Rocheuses, en Alberta. Le projet Luscar a été entrepris dans le but de compiler et de synthétiser les données géologiques disponibles et d'acquérir de nouvelles données, là ou le besoin existe, afin d'évaluer les ressources charbonnières possibles des régions plus au sud. Les résultats préliminaires indiquent que la séquence charbonnière la plus importante se trouve à l'intérieur du membre de Grande Cache, de la formation de Gates, du groupe de Luscar. Il est possible d'y distinguer jusqu'à six zones parmi lesquelles deux semblent être d'une épaisseur suffisante pour en rendre l'exploitation rentable. De nombreux plis et failles ont agi sur ces roches, suscitant la formation d'une série de directions linéaires dans les couches charbonnières, orientées d'une manière parallèle au chaînon frontal des Rocheuses. Cet article présente les grandes lignes géologiques à partie desquelles le potentiel en ressources charbonnières du groupe de Luscar sera déterminé. Une série de cartes à 1/50 000 (à paraitre à une date ultérieure) ainsi qu'un rapport ont été compilés afin d'illustrer la répartition et la complexité structurale des unités charbonnières et d'indiquer les obstacles au développement qui existent dans cette région.

PREVIOUS WORK

Coal has long been known to occur in the Foothills of western Alberta. G.M. Dawson (1886) was the first to assign geological names to the coal-bearing sequences in this region. It was not until the early 1900's (Malloch, 1911), that the coal resource potential of the region from Nordegg south to the Clearwater River was examined. In the 1940's, the Geological Survey of Canada undertook a regional mapping program in the region. Maps produced by MacKay (1941a, 1941b, 1943), Erdman (1945, 1946, 1950), Henderson (1945), and Crombie and Erdman (1946) displaying surface distribution of rock units, have been the basis for considering the geology of the area. From the 1950's to the present, much of the geological work conducted in the Foothills of Alberta has been concentrated in the regions north of Nordegg, toward Hinton and Grande Cache. Geologists such as Douglas (1956), Mellon (1967), McLean and Wall (1981), McLean (1982) and Langenberg and McMechan (1985) have examined in detail the Lower Cretaceous strata in these regions north of Nordegg, perhaps due to better outcrop exposure, or to the significant coal resources that are known in these regions. Few publications examining the Lower Cretaceous strata within the Foothills region from the North Saskatchewan River southward to the Clearwater River have been produced during the past 40 years.

INTRODUCTION

Coal resources of Early Cretaceous age outcrop within the disturbed belt of the Foothills of western Alberta. The main coal-bearing strata are within the Gates Formation of the Luscar Group, which extends within the Inner foothills from the Bow River northward into British Columbia. The Luscar project was initiated in 1988 to examine the coal potential of the Luscar Group, from the Clearwater River in the south, to the North Saskatchewan River in the north (Fig. 1). The rocks have been highly faulted and folded as a result of the Laramide Orogeny, producing near surface coal resources that are restricted to narrow bands of outcropping Luscar strata that parallel the Front Ranges of the Rocky Mountains.

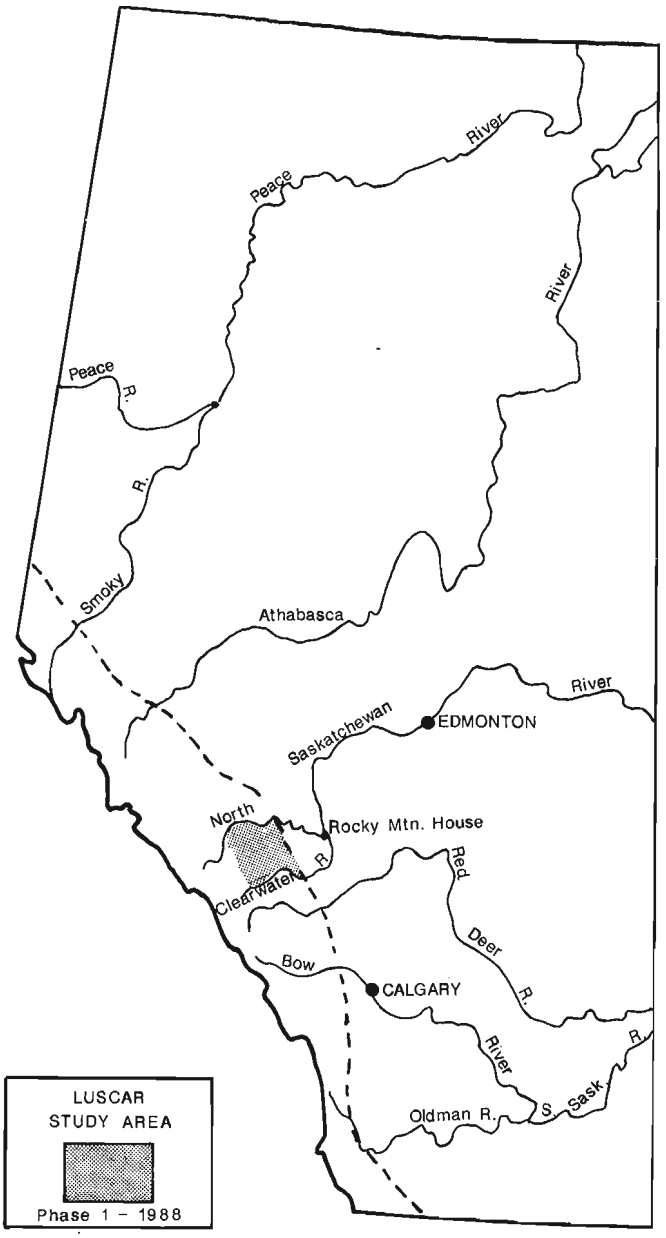

Figure 1. *General location map.*

The Luscar project entails the compilation and synthesis of subsurface and surface exploration data, coupled with gathering of new data where required, to provide the basis upon which an assessment of the resource potential and characteristics of the coal can be made. Existing subsurface information is very limited, and the lithostratigraphic interpretations made during the 1940's are outdated. Geological mapping was undertaken during the summer of 1988 to upgrade the existing geological information and to provide greater data control within the coal-bearing areas.

The final results of the Luscar project will comprise a report of the coal resource potential for the region, and a series of geological maps (1:50 000 scale) and cross sections. Four map sheets based upon the National Topographic Surveys system have been created. These maps (Fig. 2), 83 B/3, 83 B/4, 83 B/5 and 83 C/8, display regional geology and coal distribution and features such as coal leases, drillhole locations, and Provincial regulatory land use categories that constrain coal exploitation possibilities. This paper presents the stratigraphic framework of the Luscar Group in the project region upon which the examination of the coal potential is based.

Coal exploration by private industry was undertaken in the 1970's. However, the results of these programs are not publicly available. Consolidation Coal Company and Hudbay Coal Company were the major firms involved in this effort, with smaller programs conducted by Clearwater Coal Company and Brascan Resources Limited. Most of the exploration consisted of geological mapping, followed by the drilling of numerous coal exploration boreholes.

Recently Rosenthal (1988a) examined the Luscar Group stratigraphy in the region. This study was directed toward a better understanding of the hydrocarbon potential east of the Foothills belt.

STRATIGRAPHIC NOMENCLATURE

The Lower Cretaceous Luscar Group contains marginal marine to nonmarine strata derived from the Columbian Orogen during the Early Cretaceous. In west-central Alberta, the Luscar Group is approximately 400 m thick and can be divided into several distinctive, mappable formations, as defined by Langenberg and McMechan (1985) (Fig. 3).

The base of the Luscar Group is represented by the Cadomin Formation. This unit consists of interbedded, coarse grained, quartzitic sandstone and chert and quartz-rich pebble conglomerate. The Cadomin Formation varies from 5 to 15 m in thickness in the project area, and forms a distinctive resistant unit in outcrop. The base is sharp and lies unconformably on the interbedded sandstones and mudstones of the Nikanassin Formation.

Lying conformably above the Cadomin Formation are interbedded sandstones and mudstones of the Gladstone Formation (Fig. 4). This formation is approximately 75 m thick and consists of dark grey, quartzitic, fine grained sandstones, and dark grey mudstones. Thin, carbonaceous shale or coal beds are present throughout. The sandstone beds are resistant in outcrop and are distinctive by the quartz sheen of weathering. The top of the Gladstone Formation is gradational with the overlying Moosebar Member of the Gates Formation (Fig. 3).

The strata that overlie the Gladstone Formation consist of dark grey to black mudstones and siltstones of marine to marginal marine origin. Pelecypods, gastropods and ostracodes are abundant throughout the sequence. In northeastern British Columbia and northwestern Alberta, this interval has been defined as the Moosebar Formation (Langenberg and McMechan, 1985), and is greater than 200 m thick. Within the study area, strata that are correlative to the Moosebar Member are less than 65 m thick and represent a gradational marine to continental sequence with the overlying sediments. For this paper, in the Foothills of west-central Alberta, the Moosebar interval has been defined as a member of the overlying Gates Formation, and is interpreted as representing the marginal marine facies of the sequence. The Moosebar Member is correlative with the Ostracode zone of the Mannville Group in the subsurface of the Alberta Plains (Rosenthal, 1988b). The top of the Moosebar Member is represented by a thin mudstone unit lying immediately above a conglomeratic sequence approximately 15 to 20 m in thickness (Fig. 4).

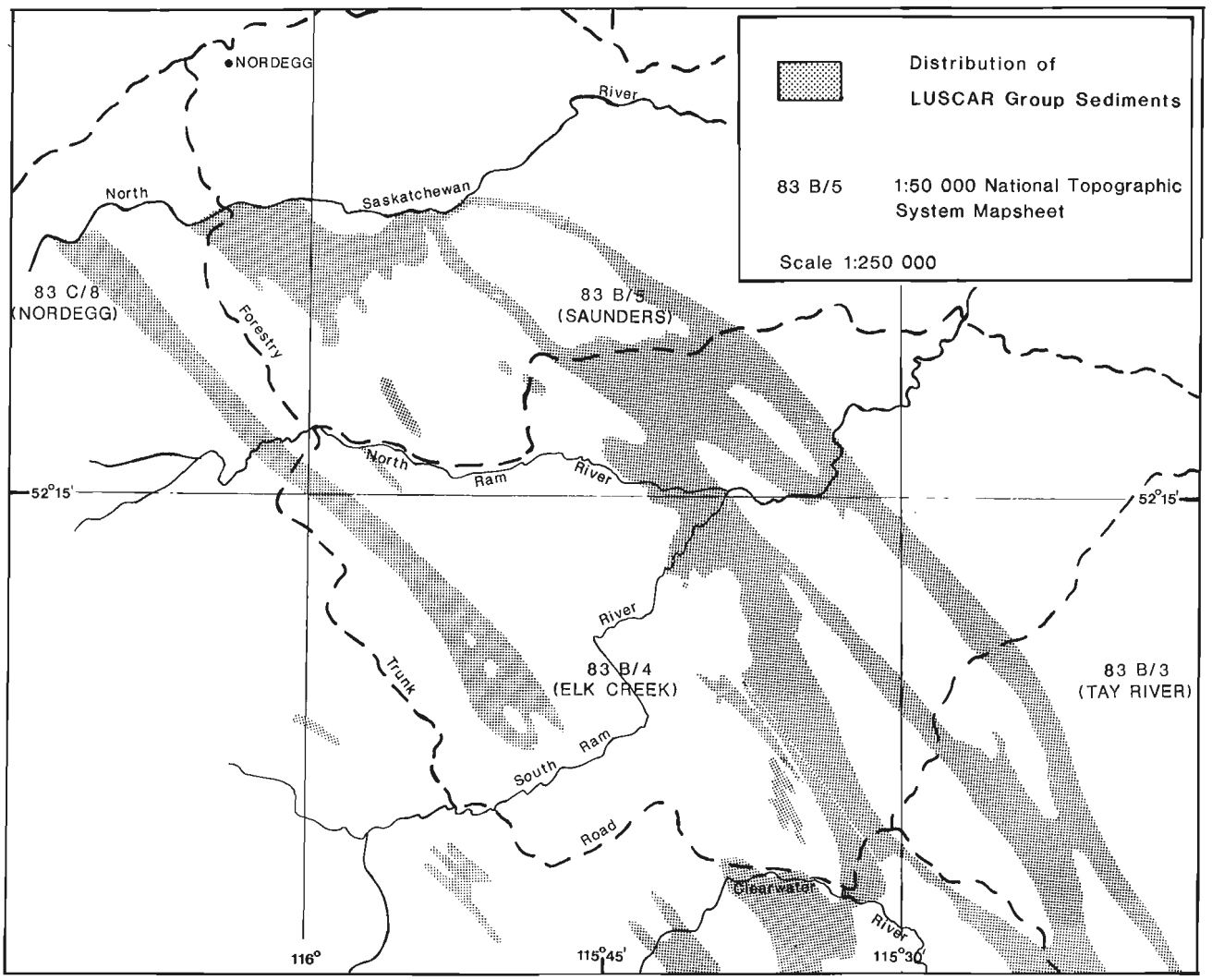

Figure 2. *Distribution of Luscar Group strata illustrating 1:50 000 mapsheets.*

This conglomerate is correlative to the subsurface Hoadley complex (Rosenthal, 1988a) of the Alberta Plains, a series of beach deposits associated with the progradation of the clastic sediments of the Mannville Group into the Moosebar sea during Early Cretaceous time. The Hoadley complex, where present, signifies, for mapping purposes, the base of the overlying coal-bearing sequence. The base of the Hoadley complex consists of quartzitic sandstone, approximately 3 to 5 m thick, overlain by a thin (1-2 m), recessive mudstone unit. Immediately above is a predominantly coarsening-upward sequence of fine to medium grained, light grey sandstone and clast supported pebble conglomerate (Rosenthal, 1988a). The Hoadley conglomerate is very similar lithologically to the Cadomin Formation. The unit is usually capped by a mudstone or thin coal zone (seam No. 6). The conglomeratic beach facies of the Hoadley complex appears to be limited laterally to a predominantly east-west trend, and pinches out rapidly to the north and south, whereas the underlying quartzite unit is more widely distributed.

Lying conformably above the Moosebar Member are the main coal-bearing rocks, defined as the Grande Cache Member of the Gates Formation (Langenberg and McMechan, 1985). Strata consist of interbedded, fine grained, orange to brown weathering sandstone and orange to dark brown mudstone and siltstone. The rocks are highly feldspathic, significantly different from the siliceous pre-Moosebar strata. This difference can be utilized in the mapping of isolated outcrops. The Grande Cache Member is approximately 110 m thick and contains up to six coal zones, of which two, (zones 1 and 3), appear to be of potentially mineable thickness. Zone 3 lies approximately 35 m above the Hoadley complex, and zone 1 a further 40 m above. Both coal zones are widely variable, with thicknesses up to 4.5 m being reported.

Above the Grande Cache Member is a thick sequence of interbedded, fine grained sandstone and mudstone, with minor carbonaceous beds, defined as the Mountain Park Member of the Gates Formation. These rocks usually display a distinctive greenish grey colour, which can be attributed to their high feldspar content. The Mountain Park Member is predominantly barren of coal, with only minor carbonaceous beds near the top. Occasionally, channel deposits up to 40 m thick downcut into the underlying Grande Cache Member. The Mountain Park Member is approximately 150 to 200 m thick, and the base is usually represented by a thick, massive, greenish grey, cliff forming sandstone. The top of the Mountain Park Member is sharp and unconformable with the overlying marine strata of the Blackstone Formation. This contact is frequently represented by a pebble conglomerate varying in thickness from 10 cm up to 6 m. The matrix of the conglomerate is predominantly mudstone and is easily distinguishable from the conglomeratic units of the Moosebar Member and the Cadomin Formation.

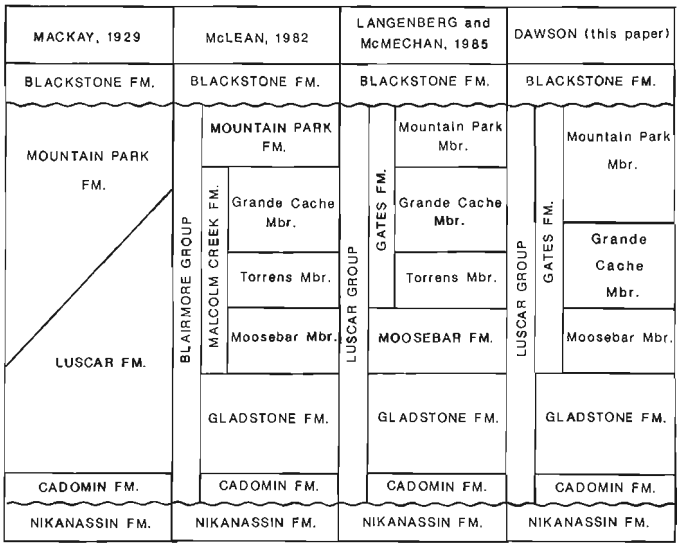

Figure 3. *Stratigraphic nomenclature of central Alberta Foothills.*

The overlying marine Blackstone Formation comprises up to 530 m of dark grey, fissile mudstone and siltstone with occasional bright orange weathering concretionary beds (Stott, 1963). The Blackstone Formation is usually recessive; the only complete exposures occur along the South Ram River.

Middle to Upper Cretaceous strata exposed within the study area belong to the Cardium, Wapiabi and Brazeau formations. Thin coal zones of the middle Brazeau Formation have been exploited in the Alexo-Saunders region along the North Saskatchewan River.

COAL STRATIGRAPHY

The major coal development within the Lower Cretaceous Luscar Group is restricted to the Grande Cache Member of the Gates Formation. Minor carbonaceous beds have been observed within the Gladstone Formation and the upper section of the Mountain Park Member of the Gates Formation. However, these beds are very thin and poorly developed. Six separate coal zones within the Grande Cache Member are present over an interval of approximately 80 to 110 m. Of these, zones 1 and 3 appear to have the greatest thickness and widest distribution. Zone 3 may be correlative with the Medicine River coal in the subsurface to the east of the study area (Rosenthal, 1988a). Thicknesses vary from 0.5 to 4.0 m. Zone 1 lies approximately 30 to 40 m above zone 3 and ranges in thickness from 1.0 to 4.0 m. The other coal zones, 2, 4, 5 and 6, appear to be less than 1.0 m thick and are much more discontinuous.

Regionally, the coal beds of the Grande Cache Member appear to thin to the west. Coal exposures along Cripple Creek are generally less than 1.0 m thick. Coal beds exposed farther to the west appear to be less than 0.6 m thick. Conversely, to the east, along the Fall Creek trend, coal zones up to 4.5 m have been observed in outcrop and drill-core. Parallel to the Rocky Mountains, the development of coal zones tends to thicken from south to north. This may be related to the progradation of nonmarine sediments into the retreating Moosebar sea to the north, during Early Cretaceous time.

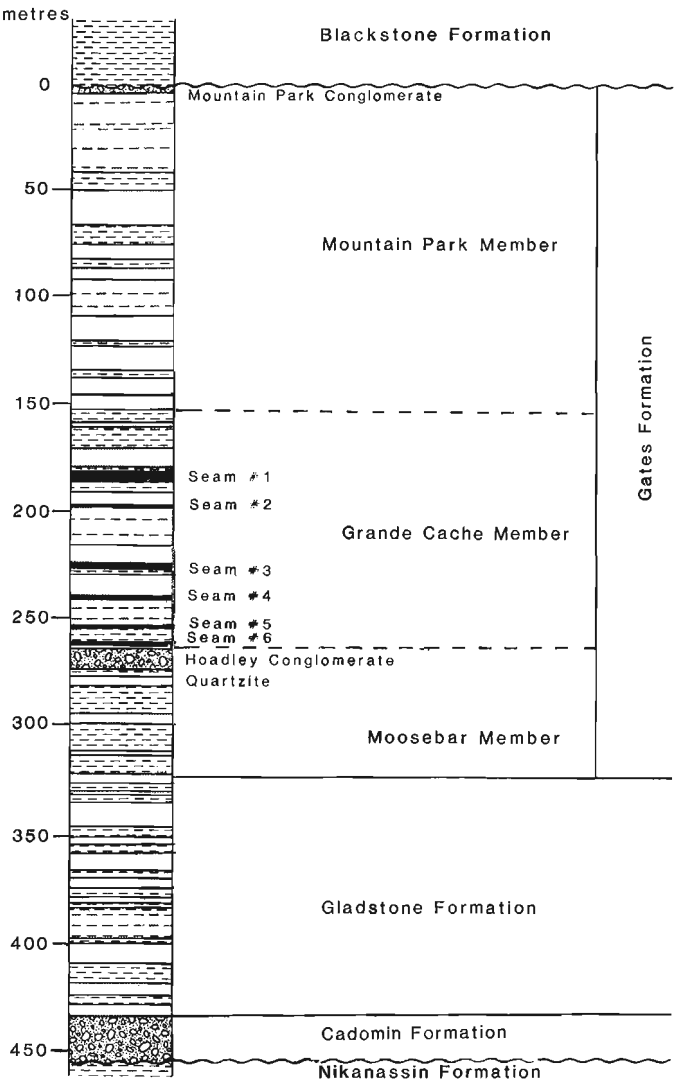

Figure 4. *Type section of the Luscar Group, Fall Creek area, central Alberta Foothills.*

STRUCTURE

The Luscar project area lies within the structurally deformed belt of the Inner Foothills of west-central Alberta. Strata of Early to Late Cretaceous age have been highly folded and faulted as a result of the Laramide Orogeny. The axes of the main structural features trend northwest, parallel to the Rocky Mountain Front Ranges to the west. Tectonic deformation appears to increase from east to west. In the east, anticlinal and synclinal structures form open folds with gentle dips. The number of reverse faults associated with the folding is decreased. To the west, folding is more intense and many of the anticlinal and synclinal structures contain vertical to overturned limbs. Reverse faults associated with these tight folds are more common with numerous splays and frequent repetition of stratigraphic sequences. The high degree of folding and faulting has also led to considerable small-scale deformation associated with the major structures. Along the South Ram River, west of the Forestry Trunk Road (Highway 40), folding of Luscar and Nikanassin formations is very intense, and the deformation appears to be almost ptygmatic in nature (Plate 1).

The structural complexity of the strata within the project area has resulted in the coal-bearing sequence being restricted to linear strike trends along the flanks of major folds or faults. There are relatively few areas where the strata are flat lying. Smaller-scale structural features, such as bedding plane fault splays and drag folds, have further complicated these trends. The intense deformation associated with the major structures has resulted in the coal, in most cases, being highly sheared. Along Cripple Creek, some structural thickening of the coal zones has been observed. It is possible that localized, structurally thickened pods of coal may exist within the project region.

RESOURCE POTENTIAL

Potential coal resources within the Luscar project area appear to be contained almost totally in the coal zones of the Grande Cache Member of the Gates Formation. Of the six coal zones recognized, only zones 1 and 3 appear to attain sufficient thickness to be potentially mineable. Ranging in thickness from 0.5 m to greater than 4.0 m, these two main coal zones appear to be widely distributed. Preliminary results indicate that the coals thin toward the west, and may be too thin to be mineable along the farthest west strike trend of Gates Formation strata. Coal exposures in the eastern region of the project area indicate that the main coal zones are up to 4.5 m thick and favourable mining situations may exist.

Tight folding and low angle reverse faults are common throughout the project area, increasing in frequency toward the west. Individual coal zones have the potential to be structurally thickened, producing localized thickened pods of coal that may enhance mining possibilities. Laramide tectonism has commonly resulted in intense shearing of the coal, with resulting coal size degradation (i.e. relative high proportion of fine coal). The coal is medium to low volatile bituminous in rank, similar to the metallurgical coal being mined near Hinton and Grande Cache.

The exploitation of the coal resources of the eastern slopes region of Alberta is still regulated according to land categories established by the Provincial coal policy of 1976. This policy is currently being reconsidered, and a new, updated version should be presented within the next few years. Recently, the Department of Forestry of Alberta has produced a series of Integrated Resource Plans for the Alberta Foothills. The Nordegg-Red Deer River Sub-Regional Integrated Resource Plan (1986) covers the Luscar project area. This Integrated Resource Plan categorizes the lands within the study area by land usage. The 1:50 000 scale map sheets produced for the Luscar project illustrate the coal policy and land usage categories for the area, and relates these to the distribution of the coal-bearing strata, thus allowing potentially favorable coal exploration targets to be delineated.

FUTURE WORK

Compilation of existing data supplemented by limited field studies pertinent to assessing coal potential of the Luscar Group between the North Saskatchewan and Clearwater rivers provides the basis for considering coal exploration and development possibilities in the region. Successful completion of this present study should be followed by similar cursory studies of coal potential in the Luscar Group in the region between the Clearwater and Bow rivers, and in the region between the North Saskatchewan and Blackstone rivers. Ultimately, available information pertinent to the coal potential of the Luscar Group throughout the Foothills of Alberta can be integrated for coherent presentation in support of public and commercial planning.

ACKNOWLEDGMENTS

G.G. Smith and T. Jerzykiewicz provided technical review of this paper. Their written comments are greatly appreciated. Manuscript preparation was provided by Donna Smith and edited by J.M. MacGillivray.

Plate 1. *Ptygmatic folding of Nikanassin strata along the Ram River.*

REFERENCES

Alberta Forestry Resource Evaluation and Planning Division
1986: Nordegg-Red Deer Sub-Regional Integrated Resource Plan. ENR Technical Report T/1-No. 10.

Crombie, G.P. and Erdman, O.A.
1946: Alexo, Alberta, second preliminary map. Geological Survey of Canada, Paper 45-23.

Dawson, G.M.
1886: Preliminary report on the physical and geological features of that portion of the Rocky Mountains between the latitude 49° and 51°30'. Geological Survey of Canada, Annual Report (new series) 1885, v.1, p. 1-169b.

Douglas, R.J.W.
1956: Nordegg, Alberta. Geological Survey of Canada, Paper 55-34.

Erdman, O.A.
1945: Saunders map area, Alberta. Geological Survey of Canada, Paper 45-25.

1946: Cripple Creek map-area, Alberta. Geological Survey of Canada, Preliminary map 46-22A.

1950: Alexo and Saunders map-areas, Alberta. Geological Survey of Canada, Memoir 254.

Henderson, J.E.
1945: Fall Creek map-area, Alberta. Geological Survey of Canada, Paper 45-19.

Langenberg, C.W. and McMechan, M.E.
1985: Lower Cretaceous Luscar Group (revised) of the northern and north-central Foothills of Alberta. Bulletin of Canadian Petroleum Geology, v. 33, p. 1-11.

MacKay, B.R.
1941a: Bighorn River map-area, Alberta. Geological Survey of Canada, Preliminary map 41-9.

1941b: Brazeau map-area, Alberta. Geological Survey of Canada, Preliminary map 41-4.

1943: Foothills belt of central Alberta, (preliminary map). Geological Survey of Canada, Paper 43-3.

Malloch, G.S.
1911: Bighorn Coal Basin, Alberta. Geological Survey of Canada, Memoir 9E.

McLean, J.R.
1982: Lithostratigraphy of the Lower Cretaceous coal-bearing sequence, Foothills of Alberta. Geological Survey of Canada, Paper 80-29.

McLean, J.R. and Wall, J.H.
1981: The Early Cretaceous Moosebar Sea in Alberta. Bulletin of Canadian Petroleum Geology, v. 29, p. 334-377.

Mellon, G.B.
1967: Stratigraphy and petrology of the Lower Cretaceous Blairmore and Mannville Groups, Alberta Foothills and Plains. Research Council of Alberta, Bulletin 21.

Rosenthal, L.R.P.
1988a: Stratigraphy and depositional facies, Lower Cretaceous Blairmore-Luscar-Mannville groups, west-central Alberta. University of Manitoba, Unpublished Ph.D. thesis, 600 p.

1988b: Wave dominate shorelines and incised channel trends: Lower Cretaceous Glauconite Formation, west-central Alberta. In Proceedings of a Canadian Society of Petroleum Geologists Technical Meeting, Calgary, Alberta, September 14-16, 1988, Sequences, Stratigraphy, Sedimentology: Surface and Subsurface, D.P. James and D.A. Leckie (eds.); Canadian Society of Petroleum Geologists, Memoir 15, p. 207-220.

Stott, D.F.
1963: The Cretaceous Alberta Group and equivalent rocks, Rocky Mountain Foothills, Alberta. Geological Survey of Canada, Memoir 317.

A distinctive terrestrial palynofloral assemblage from the lower Campanian Chungo Member, Wapiabi Formation, southwestern Alberta: a key to regional correlations

A.R. Sweet and D.R. Braman[1]
Institute of Sedimentary and Petroleum Geology, Calgary

Sweet, A.R. and Braman, D.R., A distinctive terrestrial palynofloral assemblage from the lower Campanian Chungo Member, Wapiabi Formation, southwestern Alberta: a key to regional correlations. In Contributions to Canadian Coal Geoscience, Geological Survey of Canada, Paper 89-8, p. 32-40, 1989.

Abstract

An earliest early Campanian palynoflora is described from the Wapiabi Formation, Chungo Member from foothill localities along the Highwood River and Trap Creek, southwestern Alberta. The assemblage is characterized by the presence of ***Aquilapollenites*** *sp.,* ***Azonia parva*** *Wiggins, 1976,* ***Foveotetradites*** *sp.,* ***Proteacidites thalmanni*** *Anderson, 1960,* ***P.*** *sp.,* ***Pseudoplicapollis newmanii*** *Nichols & Jacobson, 1982 and* ***Pseudointegricorpus*** *spp. This combination of species allies the assemblage with the* ***Pseudoplicapollis newmanii*** *and* ***Aquilapollenites senonicus*** *interval zones of Nichols et al. (1983) and to the "early triporate" suite of Norris et al. (1975). It is distinguished from assemblages present in the Chungo Member of more northern localities by the low diversity of triprojectate pollen and the conspicuous presence of triporate pollen of the genera* ***Proteacidites*** *and* ***Pseudoplicapollis****. These differences imply a substantially older age for the Chungo in the vicinity of the Highwood River compared to that of more northern localities.*

Résumé

Le présent article décrit une flore palynologique du début du Campanien inférieur, observée dans le Membre de Chungo de la Formation de Wapiabi. Les échantillons analysés proviennent des contreforts, plus précisément du bord de la rivière Highwood et du ruisseau Trap, dans le sud-ouest de l'Alberta. L'assemblage présente les espèces suivantes : ***Aquilapollenites*** *sp.,* ***Azonia parva*** *Wiggins, 1976,* ***Foveotetradites*** *sp.,* ***Proteacidites thalmanni*** *Anderson, 1960,* ***P.*** *sp.,* ***Pseudoplicapollis newmanii*** *Nichols et Jacobson, 1982 et* ***Pseudointegricorpus*** *spp. Cet assemblage d'espèces permet d'établir une corrélation avec les zones comprenant des intervalles à* ***Pseudoplicapollis newmanii*** *et* ***Aquilapollenites senonicus*** *de Nichols et al. (1983), de même qu'avec la série évolutive des "premiers triporés" de Norris et al. (1975). La différence entre cet assemblage pollinique et d'autres assemblages du même membre observés plus au nord est la faible diversité du pollen de type triprojeté et la présence de triporés du genre* ***Proteacidites*** *et* ***Pseudoplicapollis****. Ces différences permettent d'assigner un âge beaucoup plus ancien au Membre de Chungo des environs de la rivière Highwood qu'à celui situé plus au nord.*

INTRODUCTION

The correlation of lithological units within the upper part of the Wapiabi Formation and the lower part of the Belly River and Brazeau formations along the extent of the foothills of southern and central Alberta is enigmatic. Stott (1963, Figs. 10 and 11) used the top of the Thistle Member and the base of the Nomad Member as datums in his correlation of columnar sections along the extent of the foothills. In his study, he treated the contacts between lithological units as time lines (Stott, 1963, Table IV) with the exception of the intertonguing relationship he recognized as occurring between the Chungo and Hanson members in the southern foothills. In contrast, Wall and Germundson (1963, Fig. 3) and Wall (1967), using the first occurrence of their upper pelagic microfauna as a datum, considered lithological units within the Wapiabi Formation to be diachronous along the extent of the foothills. Rosenthal and Walker (1987) have subsequently published a summary of a detailed sedimentological study by Rosenthal (1984) in which they propose a north to south (and east to west) intertonguing relationship between the Chungo and Nomad members in addition to the Chungo-Hanson intertonguing accepted by Stott. The former intertonguing relationship is a result of their correlating the Chungo of the more northern (Barrier Lake and Ghost Dam) and eastern (Longview) sections with only the lower part of the Chungo exposed in the Highwood, Trap Creek and Sheep River sections. Most recently Wasser (1988) used the top of the 'Eagle Formation' (Chungo) as a datum during his study of the 'Judith River Formation' in the Pembina region.

This study is based on samples of grey and dark grey mudstones, carbonaceous shale and coal from exposures of the Chungo sandstone along Trap Creek near its junction with the Highwood River and at the first two localities along Highwood River downstream from the mouth of Trap Creek (Fig. 1). The sedimentology of these localities has been extensively studied (Nelson and Glaister, 1975; Glaister and Nelson, 1978; Walker and Hunter in Walker, 1982; Nadon, 1984; Rosenthal, 1984; Rosenthal and Walker, 1987). The Trap Creek and Highwood River No. 2 localities are lithologically similar whereas the more downstream Highwood River No. 1 locality (note reversal in the sequence of sections in Walker, 1982, Fig. 26) contains a higher proportion of sandstone (Fig. 2).

[1]Tyrrell Museum of Palaeontology, Drumheller, Alberta T0J 0Y0

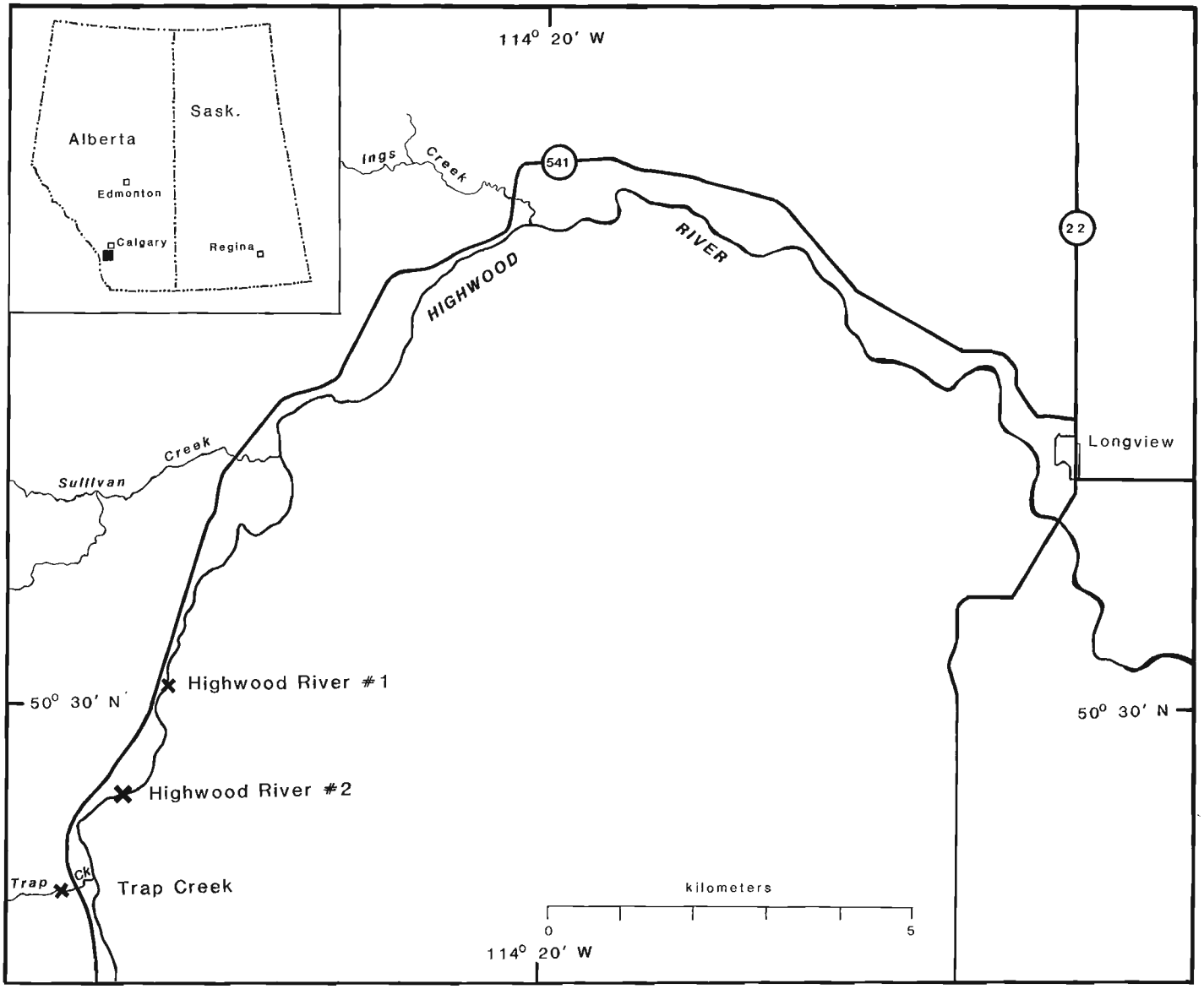

Figure 1. *Locality map. Trap Creek Section: centered in Sec. 36, Twp. 17, Rge. 4, W5. Highwood River No 2 Section: NE1/4, Sec. 1, Twp. 18, Rge. 4, W5. Highwood River No. 1 Section: SW1/4, Sec. 7, Twp. 18, Rge. 3, W5.*

The intent of this paper is to provide the beginnings of a palynological database to test the various correlation schemes that have been proposed for the upper members within the Wapiabi Formation. Additionally, as most of these correlation schemes involve the use of regressive and transgressive surfaces as datums and as the transgressive surfaces can be related to sequence boundaries (Haq et al., 1987), this and follow-up studies will test the reliability of such surfaces as datums within the context of the Western Interior Basin and globally. Such tests are critical to advancing our understanding of the lateral relationships in the succeeding terrestrial and sometimes coal-bearing Belly River and Brazeau formations. Time relationships are equally important in formulating depositional models directed towards exploiting the proven (Wasser, 1988) oil and gas potential of these formations.

Palynological assemblages recovered from 12 samples of the terrestrial facies exposed in the three sections illustrated in Figure 2 are presented. Relative abundances are based on counts of about 200 specimens from unsieved residues. A brief comparison is made to assemblages from the Chungo and contiguous strata from localities directly west of Calgary (Bateman Ridge, Lsd. 3, Sec. 2, Twp. 25, Rge. 5, W5th; Noble Ridge, Lsd. 5, Sec. 9, Twp. 25, Rge. 5, W5th), a subject of a detailed ongoing study and from along the Little Berland River (Lsd. 5, Sec. 5, Twp. 54, Rge. 2, W5th). Future studies will be directed towards providing additional comparative data from the Crowsnest area of southern Alberta and northern sections of the Chungo and Chinook sandstones.

Stratigraphy

Major lithostratigraphic studies related to the upper portion of the mostly marine Wapiabi Formation and the lower part of the continental Brazeau Formation interval include Stott (1963), Rosenthal (1984) and Rosenthal and Walker (1987).

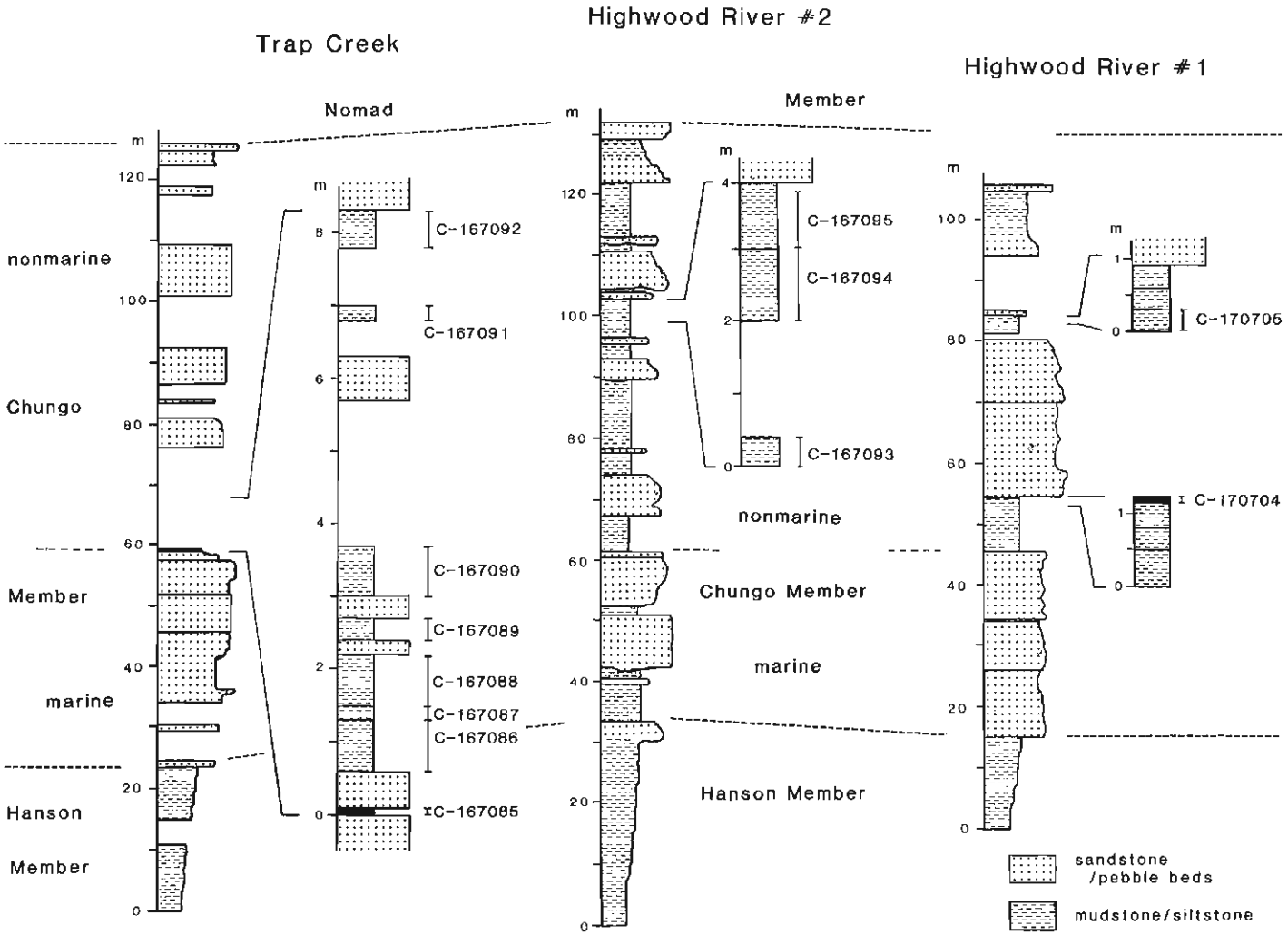

Figure 2. *Generalized lithological sections modified after Walker and Hunter in Walker (1982, Fig. 26) with expanded intervals showing the location of samples used in this study.*

Only the upper four of the seven members described by Stott (1963) as subdivisions of the Wapiabi Formation are relevant to this study. The most laterally extensive and lowest of these, the Thistle Member, represents the maximum transgressive event during Wapiabi deposition as it contains a pelagic microfauna, albeit in numbers lower than in equivalent strata in the plains region (Wall and Germundson, 1963). The initial phase in the final regression of the midcontinental seaway (Stott, 1963, p. 127; Wall, 1967, p. 32) from the central foothills region starts with the overlying Hanson Member. No definite break marks the contact between the Hanson and the overlying siltstones and sandstones of the Chungo Member. Stott (1963) drew the contact between these members at the base of the first massive siltstone in sections north of the Sheep River. From the Sheep River southward the contact was drawn at the base of a massive sandstone with the underlying interbedded sandstone, shale and siltstone units being included in the Hanson Member. The Hanson Member was not recognized by Stott (1963) along the Oldman River. Rosenthal (1984), like Stott (1963), considers the Hanson to be absent in the south, being replaced by a thickened, sandier and, in part, more continental Chungo Member. However, Rosenthal differs from Stott in placing the Hanson - Chungo boundary at the base of the first occurrence of interbedded sandstone, shale and siltstone units in the south-central foothills.

The dominantly sandstone Chungo Member is interpreted as representing continuation of the regressive phase initiated during the time of Hanson deposition (Stott, 1963; Rosenthal, 1984). The boundary between the sandstones of the Chungo Member and the overlying marine shales of the Nomad Member is marked by a chert pebble bed up to slightly more than one metre thick in north-central Alberta, whereas farther south it is marked by a concretionary bed with scattered chert pebbles (Stott, 1963, p. 117-118). This sometimes conglomeratic unit can be interpreted as representing the first phase of the transgression succeeding the Chungo Member (Rosenthal, 1984, p. 167).

Rosenthal (1984, p. 23) treats the Chungo interval as part of the Wapiabi Formation throughout southern and south-central Alberta. Notwithstanding this, Wall and Germundson (1963), Stott (1963) and Rosenthal and Walker (1987) all express the idea that the so called Chungo of the Highwood-Sheep River region differs substantially from the Chungo closer to the more northern type area. Webb and Hertlein (1934) introduced the term 'Highwood sandstone' for a sandstone and sandy shale unit occurring within the uppermost part of the 'Upper Concretionary Shale zone' (in part the Hanson Member of the Wapiabi Formation in Stott, 1963) along the Highwood River in a section close to Longview. Stott (1963) placed the Highwood sandstone within

the lower part of the Chungo Member. Stott's nomenclature has been subsequently followed by Rosenthal et al. (1984) and Rosenthal and Walker (1987). The contact between the Chungo and Nomad members has been taken as a time horizon which approximates the lower-upper Campanian boundary (Stott, 1963).

The dark grey shales of the Nomad Member contain some sandstone and siltstone interbeds that increase in abundance upwards. Its base is marked by a persistent chert-pebble bed as noted before and its upper contact is placed at the base of the first massive, trough cross-stratified sandstones marking the next regressive phase (Rosenthal, 1984, p. 87, 97; Stott, 1963, p. 119). The Nomad Member is the last transgressive phase of the Wapiabi Sea. Regressive continental rocks overlie the Nomad: the Belly River Formation south of the Sheep River and the Brazeau Formation north of the Sheep River.

A latest Santonian age is the oldest that can be inferred for the section under study based on records of the index species *Desmoscaphites bassleri* Reeside from unspecified sections of the Hanson Member (upper concretionary zone) presumably from the central Alberta foothills (Webb and Hertlein, 1934, p. 1413; Jeletzky, 1968; p. 42). The Santonian-Campanian boundary is placed by Jeletzky (1968, p. 42) between the top of the *Desmoscaphites bassleri* zone and the overlying *Scaphites hippocrepis* zone. Jeletzky (1968, p. 42) states that 'the *Scaphites* (*Desmoscaphites*) fauna occurs throughout the upper concretionary shale and the transition members of the Wapiabi Formation' in the southern and central foothills and that the *Scaphites hippocrepis* fauna is completely absent throughout the foothills. However, he also comments that the rarity of the diagnostic elements leaves uncertain the exact position of the Santonian-Campanian boundary relative to the top of the Wapiabi Formation.

An upper age limit can be established utilizing arguments derived from the foraminifera present in the Chungo and Nomad members. Wall and Sweet (1982) reported arenaceous foraminifera from the Wapiabi Formation (Chungo and Nomad Members) at Bateman Ridge comparable to those of the *Lenticulina* sp. Zone of Wall (1967). Caldwell et al. (1978) also considered the *Lenticulina* sp. Zone assemblage to be present in beds transitional from the Wapiabi Formation to those of the overlying continental sequences throughout the foothills of Alberta. To the east the *Lenticulina* sp. Zone corresponds to the *Quinqueloculina sphaera* Subzone of the *Glomospira* Zone and the lower part of the *Eoeponidella linki* Zone or alternatively spans the ranges of the *Baculites asperiformis* and the overlying *B. gregoryensis* zones (Caldwell et al., 1978). The position of the early - late Campanian boundary accepted by Caldwell et al. (1978) is between the *Baculites asperiformis* Zone and the underlying *Baculites obtusus* Zone. Based on the above relationships an early late Campanian age is the upper age limit for the Chungo and Nomad members. It is therefore apparent that the assemblages reported herein fall within the time span of latest Santonian to possibly late Campanian.

Palynological Setting

Zonations based on terrestrial palynomorphs spanning the Santonian-Campanian interval of the Western Interior basin have been developed by Norris et al. (1975), Nichols et al. (1982) and Nichols and Sweet (in press). As discussed in Nichols and Sweet (in press) the earliest Campanian, in the region of the study area, is the time of the initial radiation in the triprojectate complex. This aspect of the terrestrial flora during the early Campanian is complemented by the presence of species of *Azonia* and triporate pollen of the Normapolles and *Proteacidites* complexes. Together these, and associated species, provide an as yet under utilized, high resolution biostratigraphic tool capable of establishing lines of correlation within the upper part of the Wapiabi Formation.

RESULTS

Plate 1, figures 1 to 52, illustrates many of the species in the assemblage and Table 1 gives the relative abundances of major groups of palynomorphs and occurrences of some of the more biostratigraphically important species. Monolete miospores, *Laevigatosporites* and *Hazaria*, average 10% of the assemblage. *Hazaria* is usually infrequent, but is sometimes abundant as in the 12 cm-thick coal near the base of the Highwood River No. 1 section. This coal also differs from most samples in containing abundant *Gleicheniidites*, a characteristic shared by the stratigraphically highest sample collected in the Trap Creek section. Both of these samples are at the top of the first recessive interval overlying the basal sandstone units identified as marine and shoreface by Rosenthal and Walker (1987).

The relative abundance of trilete miospores averages about 20% but, as seen in Table 1, varies considerably between samples. Most belong to either the genus *Cyathidites* or *Deltoidospora*, with, as mentioned above, *Gleicheniidites* sometimes being abundant. Miospores commonly present include *Foveosporites pantostiktos* Phillips & Felix, 1971, *Microreticulatisporites uniformis* Singh, 1971 and *Osmundacidites* sp. and more rarely *Plicatella undosa* (Hedlund) Davies, 1985, *Cicatricosisporites* spp., *Foraminisporis* spp., *Interulobites* sp. and *Klukisporites foveolatus* Pocock, 1964.

The Taxodiaceae-Cupressaceae complex averages 45% of the total assemblage compared to 2.5% for all other types of gymnosperm pollen. Less common types of gymnosperm pollen include *Quadripollis krempii* Drugg, 1967, bisaccate pollen, *Equisetosporites* spp. and *Eucommiidites minor* Groot & Penny, 1960.

The most biostratigraphically significant portion of the total assemblage is angiosperm pollen with an average abundance of 20%. Slightly over one half (11.5%) of the angiosperm pollen is relatively simple, tricolpate and tricolporate pollen. Monocolpate pollen referrable to *Arecipites, Liliacidites* and rarely *Weylandipollis* (C-167085 and C-167095) averages about 2% of the assemblage. Several types of triporate pollen are present including: *Proteacidites thalmanni* and *P.* sp. which together average 2%; *Pseudoplicapollis newmanii* Nichols & Jacobson, 1982 which occurs less consistently but still averages 1%; and *Paliurus triplicatus* Anderson, 1960 (*Scabratriporites*) which also averages 1% in relative abundance. A restricted number of species of triprojectate pollen are present. The most frequent form is a new, relatively small species of *Pseudointegricorpus* which occurs in several samples but usually does not show up in the counts (Table 1). In addition, several specimens of a finely spinous, heteropolar species of *Aquilapollenites* were observed in C-167089 and C-167090. Other species possibly allied to triprojectate pollen include: common cf. *Cranwellia* sp. in C-167090; common *Loranthacites* sp. in C-167089, C-167092, C-167095 and C-170704; and rare *Pleurospermaepollenites* sp. (*Tricolporopollenites* sp.) 1 in C-167090 and *T.* sp. 2 (both of Norris et al., 1975) in C-167087. Two specimens of *Azonia* sp. cf. *A. parva* Wiggins, 1976 were observed in C-170704 and a small sized species of *Foveotetradites* was observed in C-167085 and C-167092.

PLATE 1

Selected biostratigraphically significant species. All figures X 750.

Figure 1. *Klukisporites foveolatus* Pocock, 1964; GSC 93666, P3260-3e, 139.1 x 12.3, GSC locality C-167087.

Figure 2. *Plicatella undosa* (Hedlund) Davies, 1985; GSC 93667, P3365-4c, 109.6 x 9.3, GSC locality C-170704.

Figure 3. *Cicatricosisporites annulatus* Archangelsky & Gamerro, 1966 in Singh, 1971, Pl. 6, figs. 13-15; GSC 93668, P3260-7c, 129.8 x 14.3, GSC locality C-167091.

Figure 4. *C. aralicus* (Bolkhovitina) Brenner, 1963; GSC 93669, P3261-3c, 119.8 x 8.3, GSC locality C-167095.

Figure 5. *C. ornatus* Srivastava, 1972; GSC 93670, P3261-3c, 113.2 x 11.3, GSC locality C-167095.

Figure 6. *Distaltriangulisporites* sp.; GSC 93671, P3260-8c, 133.9 x 17.2, GSC locality C-167092.

Figure 7. *Interulobites* sp.; GSC 93672, P3260-8c, 128.6 x 15.4, GSC locality C-167092.

Figure 8. *Foraminisporis* sp.; GSC 93673, P3260-8c, 135.4 x 16.4, GSC locality C-167092.

Figure 9. *Heliosporites kemensis* (Chlonova) Srivastava, 1972; GSC 93674, P3260-7c, 132.2 x 18.3, GSC locality C-167091.

Figure 10. *Quadripollis krempii* Drugg, 1967; GSC 93675, P3260-3e, 116.0 x 7.2, GSC locality C 167087.

Figure 11. *Peromonolites* sp.; GSC 93676, P3261-3c, 109.8 x 15.1, GSC locality C-167095.

Figures 12, 13. *Equisetosporites* spp.

12. GSC 93677, P3260-1a, 115.3 x 10.7, GSC locality C-167085.

13. GSC 93678, P3260-7d, 140.3 x 5.8, GSC locality C-167091.

Figure 14. *Eucommiidites minor* Groot & Penny, 1960; GSC 93679, P3261-2d, 134.0 x 6.4, GSC locality C-167094.

Figure 15. *Schizosporis* sp.; GSC 93680, P3260-8d, 115.9 x 13.3, GSC locality C-167092.

Figure 16. *Ginkgocycadophytus* sp.; GSC 93681, P3260-7d, 140.6 x 6.3, GSC locality C-167091.

Figures 17, 18. *Aquilapollenites* sp.

17. GSC 93682, P3260-8d, 116.0 x 13.4, GSC locality C-167092.

18. GSC 93683, P3260-5c, 112.8 x 14.7, GSC locality C-167089.

Figure 19. *Azonia* sp. cf. *A. parva* Wiggins, 1976; GSC 93684, P3365-4d, 129.8 x 14.6, GSC locality C-170704.

Figure 20. cf. *Cranwellia* sp.; GSC 93685, P3260-6c, 109.3 x 16.2, GSC locality C-167090.

Figure 21. *Liliacidites* sp.; GSC 93686, P3260-7d, 139.8 x 9.2, GSC locality C-167091.

Figure 22. *Weylandipollis* sp.; GSC 93687, P3260-1d, 120.7 x 4.7, GSC locality C-167085.

Figure 23. *Virgo amiantopollis* (Srivastava) Ward, 1986; GSC 93688, P3261-2d, 138.4 x 4.7, GSC locality C-167094.

Figure 24. *Foveotetradites* sp.; GSC 93689, P3260-8d, 136.3 x 5.4, GSC locality C-167092.

Figures 25, 26. *Loranthacites* sp.

25. GSC 93690, P3365-4d, 122.6 x 20.3, GSC locality C-170704.

26. GSC 93691, P3260-8d, 135.6 x 11.6, GSC locality C-167092.

Figure 27. *Fraxinoipollenites variabilis* Stanley, 1965; GSC 93692, P3260-8d, 136.8 x 14.3, GSC locality C-167092.

Figure 28. *Tricolpites* sp. A; in Nichols and Jacobson, 1982, Pl. 4, fig. 1.; GSC 93693, P3260-6c, 120.3 x 8.3, GSC locality C-167090.

Figure 29. *Tricolpites* sp.; GSC 93694, P3260-8d, 137.6 x 7.8, GSC locality C-167092.

Figure 30. *Nyssapollenites* sp.; GSC 93695, P3260-6c, 135.2 x 19.1, GSC locality C-167090.

Figures 31, 32. Tricolporate angiosperm pollen.

31. GSC 93696 (equatorial view), P3260-5d, 116.9 x 20.3, GSC locality C-167089.

32. GSC 93697 (polar view), P3260-7d, 140.2 x 18.2, GSC locality C-167091.

Figures 33-35. Oblate?, tricolpate angiosperm pollen.

33. GSC 93698, P3260-7d, 140.6 x 7.8, GSC locality C-167091.

34. GSC 93699, P3260-7d, 117.2 x 11.7, GSC locality C-167091.

35. GSC 93700, P3260-7c, 133.6 x 21.7, GSC locality C-167091.

Figure 36. Tetraporate; GSC 93701, P3260-5d, 116.2 x 13.3, GSC locality C-167089.

Figures 37, 38. *Pseudoplicapollis newmannii* Nichols & Jacobson, 1982.

37. GSC 93702, P3260-5d, 125.7 x 14.3, GSC locality C-167089.

38. GSC 93703, P3260-5d, 124.8 x 23.6, GSC locality C-167089.

Figures 39, 40. *Proteacidites* sp.

39. GSC 93704, P3260-6c, 127.6 x 7.1, GSC locality C-167090.

40. GSC 93705, P3260-6c, 133.3 x 6.7, GSC locality C-167090.

Figures 41-45. *Proteacidites thalmanni* Anderson, 1960.

41. GSC 93706, P3260-7c, 137.6 x 18.4, GSC locality C-167091.

42. GSC 93707, P3260-7c, 133.7 x 16.6, GSC locality C-167091.

43. GSC 93708, P3260-7d, 127.2 x 16.6, GSC locality C-167091.

44. GSC 93709, P3260-8d, 107.3 x 14.3, GSC locality C-167092.

45. GSC 93710, P3260-8d, 138.4 x 12.7, GSC locality C-167092.

Figures 46, 47. *Paliurus triplicatus* Anderson, 1960 (*Scabratriporites*).

46. GSC 93711, P3260-2d, 134.5 x 5.8, GSC locality C-167086.

47. GSC 93712, P3261-2d, 135.0 x 13.4, GSC locality C-167094.

Figures 48, 49. *Pseudointegricorpus* sp.

48. GSC 93713, P3260-1d, 124.6 x 20.7, GSC locality C-167085.

49. GSC 93714, P3260-8d, 139.0 x 2.1, GSC locality C-167092.

Figures 50, 51. *Pleurospermaepollenites* sp. (*Tricolporopollenites* sp. 1 in Norris et al., 1975).

50. GSC 93715, P3260-2d, 133.6 x 5.6, GSC locality C-167086.

51. GSC 93716, P3260-3d, 123.3 x 17.7, GSC locality C-167087.

Figure 52. *Pleurospermaepollenites* sp.; GSC 93717, P3260-6c, 124.6 x 13.3, GSC locality C-167090.

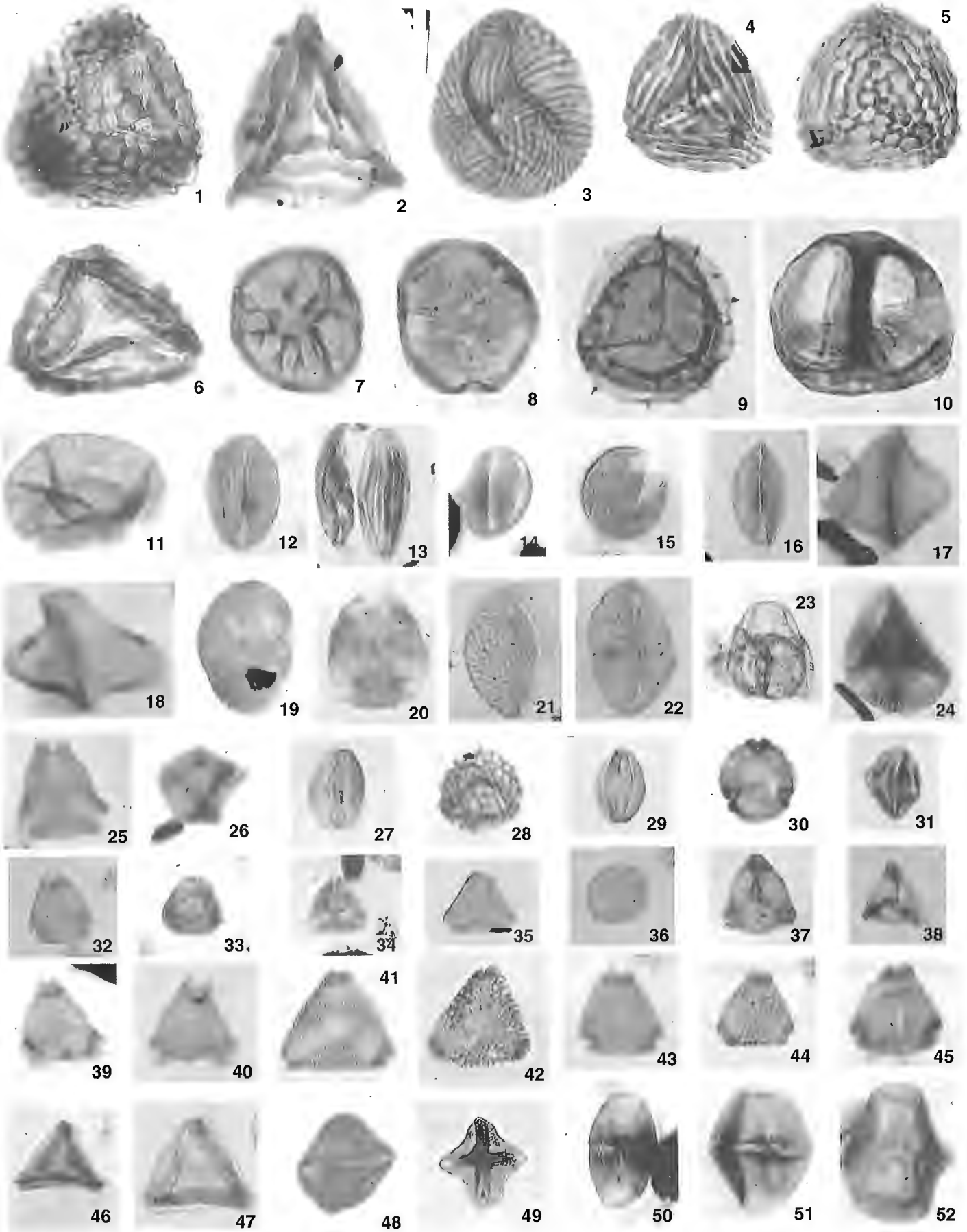
1
2
3
4
5
6
7
8
9
10
11
12
13
14
15
16
17
18
19
20
21
22
23
24
25
26
27
28
29
30
31
32
33
34
35
36
37
38
39
40
41
42
43
44
45
46
47
48
49
50
51
52

TABLE 1

The relative abundances of major groups of terrestrial palynomorphs and the occurrences of some of the biostratigrahically significant species in individual samples

GSC Locality Number	RELATIVE ABUNDANCE: Groups: Monolete spores	Trilete spores	Taxodiaceae–Cupressaceae	Other gymnosperm pollen	Angiosperm pollen	Breakdown of Angiosperm Pollen: Triclpate and tricolporate pollen	Monocolpate pollen	*Proteacidites* spp.	*Pseudoplicapollis newmanii*	*Paliurus triplicatus* (*Scabratriporites*)	*Pseudointegricorpus* sp.	Other	Lithology
Trap Creek													
C–167085	21	9	54	3	14	6	3	<1	2		1	2	coal
C–167086	13	12	53	5	17	7	5	1	1	2		<1	grey mudstone
C–167087	7	33	32	3	26	13	1	1	6	1		4	coaly shale
C–167088	17	14	51	3	8	3	2	1		1		1	grey mudstone
C–167089	9	22	41	3	25	17	3	2		1	p	2	grey mudstone/coaly shale
C–167090	11	20	53	3	13	5	2	1	2	1	p	2	grey mudstone/coaly shale
C–167091	2	7	66	<1	24	17	1	4		<1		2	dark grey mudstone
C–167092	5	30	36	5	24	19	4	1	<1	<1	p	<1	dark grey mudstone
Highwood River #2													
C–166093	very sparse recovery												dark brown shale
C–167094	6	22	40	2	29	18	2		1	<1		5	dark brown shale
C–167095	1	12	60	2	25	8	2	9	<1	2		4	coaly shale/coal
Highwood River #1													
C–170704	11	32	34	<1	23	14	2	4		2			coal
C–170705	15	53	18	<1	14	12	<1						black shale

DISCUSSION AND CONCLUSIONS

The assemblage from the Highwood River and Trap Creek exposures is similar, in the prominence of the triporate genera *Proteacidites* and *Pseudoplicapollis*, to the earliest Campanian *Pseudoplicapollis newmanii* interval zone of Nichols et al., 1982. It is reminiscent of the "early triporate suite" of Norris et al. (1975) given the common presence of *Proteacidites* and *Pleurospermaepollenites* sp. (*Tricolporopollenites* sp. 1) and the rare occurrences of *Aquilapollenites*. This "early triporate suite" was reinterpreted as Coniacian to perhaps early Campanian in age by Nichols and Sweet (in press). The reported Chungo assemblage differs from that of the *P. newmanii* interval zone in containing rare specimens of *Aquilapollenites* and a second genus of triprojectate pollen, *Pseudointegricorpus*. These species suggest an affinity to the younger (early but not earliest Campanian) *Aquilapollenites senonicus* interval zone of Nichols et al. (1982). In Norris et al. (1975), the next younger "early loranthaceous suite" (reinterpreted as early Campanian in age by Nichols and Sweet, in press) has a significantly greater diversity of triprojectate pollen. Together these comparisons suggest that the reported palynoflora is earliest Campanian in age – just subsequent to the *Aquilapollenites* datum of Nichols and Sweet (in press) which approximates the Santonian-Campanian boundary.

The presence of *Quadripollis krempii* and *Foveotetradites* in this flora extends the range of these genera upward from the late Turonian records made by Sweet and McIntyre (1988).

More critical to understanding the time relationships of sands encompassed within the present definition of the Chungo Member, is the conspicuous difference between the palynofloras described in this paper and those of the Chungo Member in the region of the Bow Valley and further north. In the Bateman Ridge section (Wall and Sweet, 1982; Braman and Sweet, 1988) a more diverse array of triprojectate species occurs in the Chungo Member and underlying strata including *Aquilapollenites trialatus* var. *variabilis* Tschudy & Leopold 1971, *A. turbidus* Tschudy & Leopold, 1971, *A.* sp. (heteropolar, finely spinous), *Mancicorpus unicus* (Chlonova) Stanley, 1970 and a larger species of *Pseudointegricorpus* than seen in this study. The Chungo yields a flora comparable to that of the Bateman Ridge section in a more northern section on the Little Berland River (unpublished palynological data based on samples from Section 5 to 19 of Stott, 1963). These more diverse assemblages suggest a significant age difference exists between sections along the Highwood River and vicinity and those within the region of the Bow Valley and northward. Indeed, it can be argued that the Chungo palynoflora at Bateman Ridge and farther north belongs to the *Aquilapollenites senonicus* interval zone of Nichols et al. (1982) or alternatively the "early loranthaceous suite" of Norris et al. 1975. These biostratigraphic units are considered correlative by Nichols and Sweet (in press) and to be of early but not earliest Campanian age. The respective overlying zones are either of late or middle Campanian age (Nichols and Sweet, in press). Hence, the implied difference in the age of the Chungo of the Highwood area and that of the Bow Valley and farther north is between earliest early Campanian and late if not latest early Campanian. Therefore, the Chungo of the Bow Valley area and north does not correlate with any older horizon than the Chungo-Nomad disconformity of the Highwood area.

These age differences refute the correlation diagram given in Rosenthal and Walker (1987). Additionally, it is unlikely that any significant amount of time can be accounted for in the disconformity which Rosenthal and Walker (1987) place within the nonmarine facies of the Chungo as the palynofloras from above and below the position of the disconformity appear to be closely comparable. Our results suggest a pattern of correlation more similar to that of Wall and Germundsen (1963) in that their use of the "upper pelagic zone" as a datum forced an offset in the alignment of the Chungo (Chinook and Highwood sandstones) interval with an implied younger age for the sands in the north.

REFERENCES

Braman, D.R. and Sweet, A.R.
1988: Palynology and micropaleontology of strata contiguous with the Campanian, marine Wapiabi to continental Brazeau Formation transition, south-central Alberta foothills, Canada. Seventh International Palynological Congress, Brisbane, Abstracts, p. 16.

Caldwell, W.G.E., North, B.R., Stelck, C.R., and Wall, J.H.
1978: A foraminiferal zonal scheme for the Cretaceous System in the interior plains of Canada. In Western and Arctic Canadian Biostratigraphy, C.R. Stelck and B.D.E. Chatterton (eds.); Geological Association of Canada, Special Paper 18, p. 495-575.

Glaister, R.P. and Nelson, H.W.
1978: Trap Creek (Upper Cretaceous). In Field Guide to Rock Formations of Southern Alberta, N.C. Ollerenshaw and L.V. Hills (eds.); Canadian Society of Petroleum Geologists, Calgary, p. 83-89.

Haq, B.U., Hardenbol, J., and Vail, P.R.
1987: Chronology of fluctuating sea levels since the Triassic. Science, v. 235, p. 156-1166.

Jeletzky, J.A.
1968: Macrofossil zones of the marine Cretaceous of the western interior of Canada and their correlation with the zones and stages of Europe and the western interior of the United States. Geological Survey of Canada, Paper 67-72, 66 p.

Nadon, G.C.
1984: Part D. Highwood River section: an Upper Cretaceous delta/barrier island complex. In Depositional Cycles and Facies Within the Upper Cretaceous Wapiabi and Belly River Formations of West-Central Alberta, L. Rosenthal, D. Leckie, and G. Nadon (eds.); Canadian Society of Petroleum Geologists, Field Trip Guidebook, p. 29-54.

Nelson, H.W. and Glaister, R.P.
1975: Trap Creek basal Belly River section, a deltaic progradational sequence. In Guidebook to Selected Sedimentary Environments in Southwestern Alberta, Canada, M.S. Shawa (ed.); Canadian Society of Petroleum Geologists, Calgary, p. 41-56.

Nichols, D.J., Jacobson, S.R., and Tschudy, R.H.
1982: Cretaceous palynomorph biozones for the central and northern Rocky Mountain region of the United States. In Geologic Studies of the Cordilleran Thrust Belt, R.B. Powers (ed.); Rocky Mountain Association of Geologists, Denver, Colorado 1982 Symposium (1983), p. 721-733.

Nichols, D.J. and Sweet, A.R.
in press: Biostratigraphy of Upper Cretaceous nonmarine palynofloras in a north-south transect of the Western Interior Basin. In W.G.E. Caldwell and E.G. Kauffman (eds.); Geological Association of Canada, Special Paper.

Norris, G., Jarzen, D.M., and Awai-Thorne, B.V.
1975: Evolution of the Cretaceous terrestrial palynoflora in Western Canada. In The Cretaceous System of the Western Interior of North America, W.G.E. Caldwell (ed.); Geological Association of Canada, Special Paper 13, p. 31-54.

Rosenthal, L.R.P.
1984: The stratigraphy, sedimentology and petrography of the Upper Cretaceous Wapiabi and Belly River Formations in southwestern Alberta. M.Sc. thesis, McMaster University, Hamilton, Ontario.

Rosenthal, L., Leckie, D., and Nadon, G.
1984: Depositional cycles and facies relationships within the Upper Cretaceous Wapiabi and Belly River formations of west-central Alberta. Canadian Society of Petroleum Geologists, Field Guide, 54 p.

Rosenthal, L.R.P. and Walker, R.G.
1987: Lateral and vertical facies sequences in the Upper Cretaceous Chungo Member, Wapiabi Formation, southern Alberta. Canadian Journal of Earth Sciences, v. 24, p. 771-783.

Stott, D.F.
1963: The Cretaceous Alberta Group and equivalent rocks, Rocky Mountain Foothills, Alberta. Geological Survey of Canada, Memoir 317, 306 p.

Sweet, A.R. and McIntyre, D.J.
1988: Late Turonian marine and nonmarine palynomorphs from the Cardium Formation, north-central Alberta foothills, Canada. In Sequences, Stratigraphy, Sedimentology: Surface and Subsurface, D.P. James and D.A. Leckie (eds.); Canadian Society of Petroleum Geologists, Memoir 15, p. 499-516.

Walker, R.G.
1982: Clastic units of the Front Ranges, Foothills and Plains between Field, B.C. and Drumheller, Alberta. International Association of Sedimentologists field excursion guidebook 21A, p. 61-71.

Wall, J.H.
1967: Cretaceous foraminifera of the Rocky Mountain Foothills, Alberta. Research Council of Alberta, Bulletin 20, 185 p.

Wall, J.H. and Germundson, R.K.
1963: Microfaunas, megafaunas, and rock-stratigraphic units in the Alberta Group (Cretaceous) of the Rocky Mountain Foothills. Bulletin of Canadian Petroleum Geology, v. 11, p. 327-349.

Wall, J.H. and Sweet, A.R.
1982: Upper Cretaceous-Paleocene stratigraphy, micropaleontology and palynology of the Bow Valley area, Alberta; 1982 AAPG-CSPG Field Trip 10, Canadian Society of Petroleum Geologists, Calgary, 47 p. and Appendix 1, 7 p.

Wasser, G.G.M.
1988: A geological evaluation of the Judith River Formation (Belly River Formation) in the Pembina region. In Sequences, Stratigraphy, Sedimentology: Surface and Subsurface, D.P. James and D.A. Leckie (eds.); Canadian Society of Petroleum Geologists, Memoir 15, p. 563-570.

Webb, J.B. and Hertlein, L.G.
1934: Zones in Alberta Shale ("Benton" Group) in foothills of southwestern Alberta. American Association of Petroleum Geologists, Bulletin, v. 18, p. 1387-1416.

Synopsis: "Controls on the distribution of coal in the Campanian to Paleocene post-Wapiabi strata of the Rocky Mountain Foothills (Canada)"

T. Jerzykiewicz
Institute of Sedimentary and Petroleum Geology, Calgary

Jerzykiewicz, T., Synopsis: "Controls on the distribution of coal in the Campanian to Paleocene post-Wapiabi strata of the Rocky Mountain Foothills (Canada)". In Contributions to Canadian Coal Geoscience, Geological Survey of Canada, Paper 89-8, p. 41-42, 1989.

Abstract

Coals in the post-Wapiabi strata of the Rocky Mountain Foothills are found in the upper Campanian, lower Maastrichtian and lower Paleocene stratigraphic sequences. Large-scale facies relationships and detailed sedimentological data indicate that the coal-forming swamps originated in marginal marine, marginal lacustrine and floodplain environments. The coal-forming swamps developed only when there was a combination of appropriate diastrophic and favourable climatic conditions. This happened twice during the depositional history of the Rocky Mountain Foothills in periods of tectonic quiescence (early Maastrichtian and early Paleocene) in the northern, humid part of the basin. At those times the semiarid conditions in the southern part of the basin precluded the formation of coal-forming swamps. The semiarid conditions in this part of the basin were overridden in the late Campanian by the influence of the Bearpaw Sea, which led to the formation of thin coals in the back barrier environment.

Résumé

Les charbons des couches "post-Wapiabi" dans les contreforts des Rocheuses se trouvent dans des séquences stratigraphiques du Campanien supérieur, du Maastrichtien inférieur et du Paléocène inférieur. Les relations de faciès sur une grande échelle et les données sédimentologiques détaillées indiquent que les marais propices à la formation du charbon provenaient de milieux marins paraliques, de milieux lacustres paraliques, et de plaines d'inondation. Ces marais se développaient seulement quand il y avait une combinaison appropriée de conditions diastrophiques et un climat favorable. Tel a été le cas, deux fois, au cours de l'histoire sédimentaire des contreforts des Rocheuses, durant des périodes de repos tectonique (début du Maastrichtien et début du Paléocène) dans la partie humide située au nord du bassin. Pendant ces périodes, les conditions semi-arides de la partie sud du bassin empêchaient la formation de marais propices à la formation du charbon. Ces conditions semi-arides ont disparu durant le Campanien supérieur sous l'influence de la mer de Bearpaw, phénomène qui a entraîné la formation de charbons finement stratifiés dans les milieux d'arrière-barrière.

Of the many controlling factors in the development of coal-forming swamps, three operate on a large regional scale: tectonism, climate and sea level changes. Therefore, a large regional approach is needed in order to assess the impact of these controls. Such an approach requires considerable knowledge about syndepositional tectonics, climate and position of the shoreline. Large-scale stratigraphic correlation of coal-bearing strata with barren facies is necessary. Such a correlation for the post-Wapiabi coal-bearing strata in the Rocky Mountain Foothills was published recently (Jerzykiewicz and Sweet, 1988). This correlation, in combination with a study of the provenance of post-Wapiabi sandstone (Mack and Jerzykiewicz, in press) and of the sedimentology, enabled the recognition of five stages in the sedimentary history of the basin in the late Campanian to early Paleocene (Fig. 1). Stages III and V, dominated by coarse grained fluvial facies, reflect major thrusting events in the Rocky Mountains (Mack and Jerzykiewicz, in press). The intervening stage IV and stage II, represented largely by fine grained sediments and coal-bearing facies, coincide with periods of relative tectonic quiescence. Lateral distribution of coal-bearing strata within sequences II and IV indicate, however, that the development of coal-forming swamps required a combination of favourable tectonic and climatic conditions. These were met only in the northern, humid part of the basin.

Paleoclimatic differences between the humid northern part of the basin and the southern semiarid part are marked by the distribution of climatically sensitive facies, i.e. coal and caliche (Jerzykiewicz and Sweet, 1988). Although the caliche paleosols were better developed in the strata deposited in periods of thrusting, and the coal-bearing facies developed during tectonic quiescence, the relative regional climatic difference across the basin was maintained throughout its entire post-Wapiabi depositional history.

Tectonically generated physiographic changes in the source area may produce climatic differences reflected in facies variations of the basin. In the case discussed here, however, the orographic influence on the climate was combined with the impact of high altitude atmospheric circulation. This assumption is based on the comparison between the distribution of the semiarid and humid paleosols in the Campanian to the Paleocene and the present distribution of the soil moisture regimes in Alberta (Fremlin, 1974, p. 43).

The semiarid climatic conditions in the southern part of the basin were overridden by the influence of the Bearpaw Sea. Thin coals, formed in back barrier swamps associated with the Bearpaw shoreline, occur above the semiarid paleosols. The mature semiarid paleosols were developed in

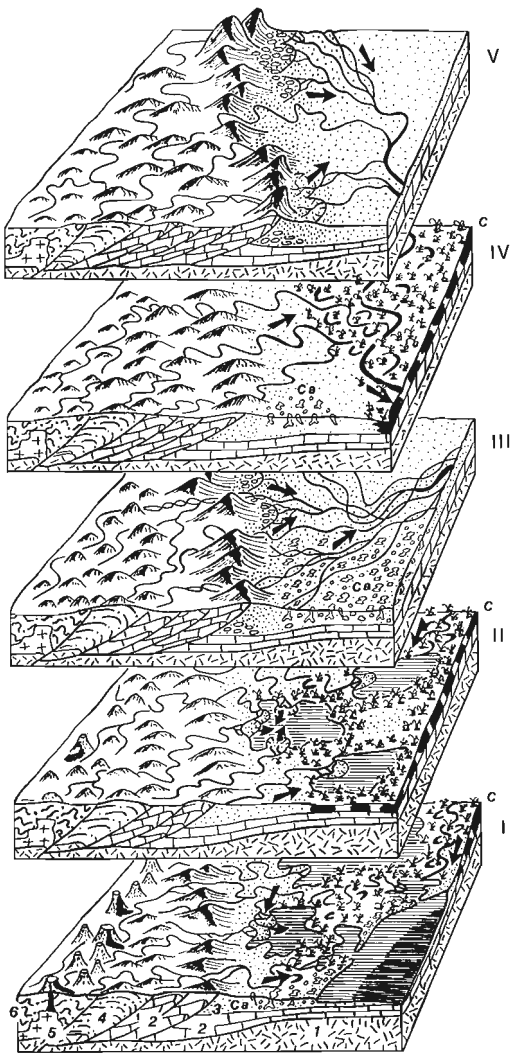

Figure 1. *Coal-forming swamps in the Rocky Mountain Foothills in the late Campanian to early Paleocene. Numbers I - V correspond to the following stratigraphic sequences: (I) Belly River - lowermost St. Mary River, lower Brazeau (Upper Campanian), (II) Upper St. Mary River, upper Brazeau (lower Maastrichtian), (III) Lower Willow Creek, lower Coalspur (upper Maastrichtian), (IV) Upper Willow Creek, upper Coalspur (lower Paleocene), (V) Porcupine Hills - Paskapoo (Paleocene). Numbers 1 - 6 stand for the following: (1) Precambrian crystalline basement of the Canadian Shield; (2) Paleozoic carbonate-rich rocks and Mesozoic siliciclastic rocks of the Front Range and eastern Main Ranges; (3) Cretaceous to Paleocene siliciclastic rocks of the Western Canada Foreland Basin; (4) Precambrian and lower Paleozoic of the western Main Ranges; (5) Mesozoic intrusive igneous rocks and associated volcanics; (6) Precambrian metasedimentary rocks of the Omineca belt. Ca, caliche paleosols; C, coal.*

Note that the coal-forming swamps developed in stages I, II and III.

marginal marine settings indicating transgression of the sea in the arid part of the basin of the southern Foothills. Coals associated with the marginal marine facies below and above the Bearpaw shale have much better developed correlatives in the Judith River Formation (McLean, 1971) and in the lower part of the Horseshoe Canyon Formation (Hughes, 1984; Dawson et al., this volume) farther northeast in the humid part of the basin.

By demonstrating that the distribution of coal in the Foothills is closely related to changes in tectonism, climate and sea level, a framework is provided for future discussions of the post-Wapiabi coal-bearing strata in the remaining part of the Western Canada Foreland Basin.

REFERENCES

Dawson, F.M., Cameron, A.R., and Jerzykiewicz, T.
1989: Distribution and character of coal in the Battle River Coalfield, east-central Alberta. (This volume.)

Fremlin, G. (ed.)
1974: Soil climate. In The National Atlas of Canada, 4th edition; The Macmillan Company of Canada Ltd., Toronto, Ontario, p. 43.

Hughes, J.D.
1984: Geology and depositional setting of the late Cretaceous, upper Bearpaw and lower Horseshoe Canyon formations in the Dodds-Round Hill coalfield of central Alberta - a computer-based study of closely-spaced exploration data. Geological Survey of Canada, Bulletin 361, p. 1-81.

Jerzykiewicz, T. and Sweet, A.R.
1988: Sedimentological and palynological evidence of regional climatic changes in the Campanian to Paleocene sediments of the Rocky Mountain Foothills, Canada. Sedimentary Geology, v. 59, p. 29-76.

Mack, G.H. and Jerzykiewicz, T.
in press: Provenance of post-Wapiabi sandstones and its implications for Campanian to Paleocene tectonic history of the southern Canadian Cordillera. Canadian Journal of Earth Sciences.

McLean, J.R.
1971: Stratigraphy of the Upper Cretaceous Judith River Formation in the Canadian Great Plains. Saskatchewan Research Council, Geology Division Report No. 11, p. 1-96.

Preliminary results of a continuing study of the stratigraphic context, distribution and characteristics of coals in the Upper Cretaceous to Paleocene Wapiti Group, northwestern Alberta

F.M. Dawson and W. Kalkreuth
Institute of Sedimentary and Petroleum Geology, Calgary

Dawson, F.M. and Kalkreuth, W., Preliminary results of a continuing study of the stratigraphic context, distribution and characteristics of coals in the Upper Cretaceous to Paleocene Wapiti Group, northwestern Alberta. In Contributions to Canadian Coal Geoscience, Geological Survey of Canada, Paper 89-8, p. 43-48, 1989.

Abstract

The Upper Cretaceous to Paleocene Wapiti Group outcrops in northwestern Alberta and northeastern British Columbia. The general lack of understanding of the stratigraphy, coupled with the potential coal resources of region have led to the implementation of the Wapiti Project. This undertaking will examine the regional aspects of stratigraphy and sedimentology of the Wapiti Group for assessing distribution and character of contained coals. Two major coal-bearing sequences within the upper third of the 1700 m thick Wapiti Group have been identified. Each of these intervals is approximately 100 m thick and contains numerous coal seams up to 6 m thick. Thin discontinuous coal horizons, up to 2 m thick, are occasionally present in the lower interval of the Wapiti Group. It appears that a correlation between the Wapiti Group strata and the Saunders Group to the south will be possible with further work. Future work for the Wapiti Project will encompass regions south and east of the Smoky River, and north into northeastern British Columbia.

Résumé

Le groupe de Wapiti, dont la mise en place date du Crétacé supérieur au Paléocène, affleure dans le nord-ouest de l'Alberta et le nord-est de la Colombie-Britannique. Le manque de compréhension qui existe généralement concernant la stratigraphie de cette région conjugé à la possibilité d'y trouver des ressources charbonnières intéressantes sont les deux raisons qui ont mené à la mise en oeuvre du projet Wapiti. Les aspects régionaux de la stratigraphie et de la sédimentologie du groupe de Wapiti seront examinés afin d'évaluer la répartition et les caractéristiques des charbons qui s'y trouvent. Il existe deux séquences charbonnières principales à l'intérieur du tiers supérieur des 1700 m d'épaisseur de groupe de Wapiti. Chacune de ces deux séquences est d'une épaisseur d'environ 100 m et contient plusieurs filons houillers dont l'épaisseur peut atteindre 6 m. Des horizons houillers discontinus, mesurant jusqu'à 2 m d'épaisseur, sont occasionnellement présents dans l'intervalle inférieur du groupe de Wapiti. Il semble qu'une corrélation pourrait être établie entre les couches du groupe de Wapiti et le groupe de Saunders situé plus au sud, cependant, de plus amples travaux s'avèrent nécessaires dans ce domaine. Des travaux futurs dans le cadre du projet Wapiti engloberont les régions situées au sud et à l'est de la rivière Smoky, ainsi que les régions plus a nord s'étendant vers le nord-est de la Colombie-Britannique.

INTRODUCTION

The Wapiti study area extends from northeastern British Columbia to the Berland River in north-central Alberta, paralleling the Rocky Mountains to the west. Although the study is interprovincial, only the region bounded by the sixth meridian to the east and the British Columbia border to the west has been examined to date. This initial phase of the study (1988-89), extends from the Smoky River in the south to north of Grande Prairie, encompassing an area of approximately 600 km^2 (Fig. 1).

Wapiti Group coal occurrences in northwestern Alberta were first reported by Dawson in 1878. Allan and Carr (1946), conducted a reconnaisance study of the coal potential of the Wapiti River - Cutbank River region in 1946. In 1972, Kramers and Mellon (1972), documented the existing knowledge of coal resources for the region. Since then, numerous exploration programs have been conducted throughout the region. However, none of these data has been synthesized, or compiled into a regional study. The Geological Survey of Canada's present project was undertaken to examine all available data for the Wapiti Group and to establish a geological framework upon which coal distribution and character of contained coals can be assessed. This paper presents preliminary results of the investigations conducted during the summer of 1988. It outlines a stratigraphic framework upon which future studies can be based.

SCOPE OF PROJECT

The Wapiti Project was initiated in 1988 to improve understanding of the regional stratigraphy and coal potential of the Upper Cretaceous to Paleocene strata in the geographic region extending from northwestern Alberta into northeastern British Columbia and Yukon Territory. The purpose of the project is to establish a regional stratigraphic framework for the Wapiti Group based upon lithostratigraphy and biostratigraphy. The development of this framework will provide the base upon which the distribution and character of the contained coals can be defined. The initial stage of the project examines the area bounded by the sixth meridian to the east and the British Columbia border to the west. This area was chosen because of the availability of primary geological data, both outcrop and subsurface, and the high level of coal exploration activity currently being undertaken in the region. Preliminary results, as presented in this paper,

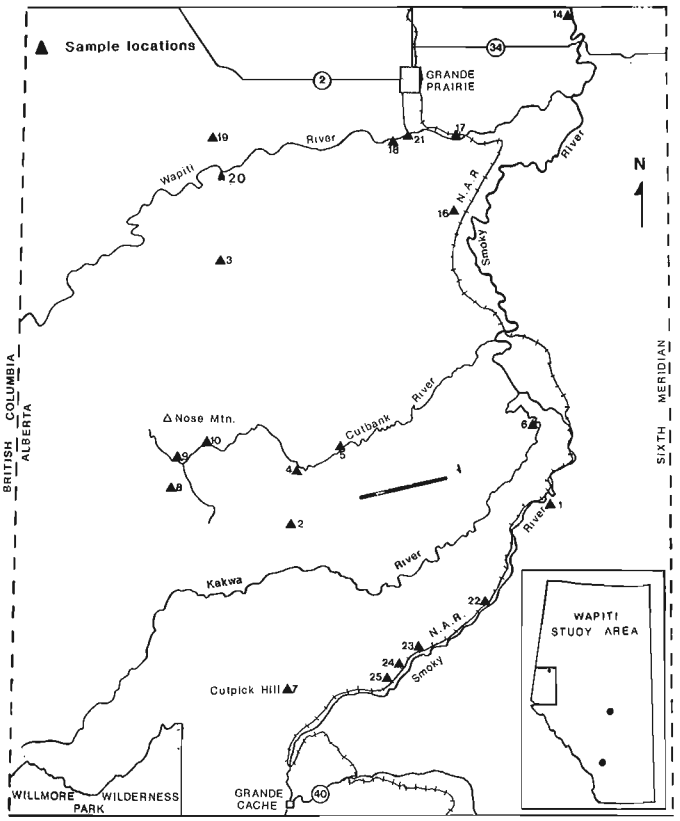

Figure 1. *Location map of Wapiti Project illustrating measured section and coal sample locations.*

indicate that significant coal resource potential exists within the Wapiti Group. Further studies are required to firmly establish the stratigraphic framework within which the coals occur and the depositional settings that controlled the distribution and character of these coals.

The geographic regions examined will be expanded to the northwest, and into the Alberta basin to the south and east. The context of the coal deposits of the Wapiti Group in the Fox Creek and Whitecourt regions in north-central Alberta will be integrated into the geological framework established for the current study area. Subsequently, the northward extension of the Wapiti Group into British Columbia and Yukon Territory will be examined.

Ultimately, a multidisciplinary geological report of the entire Wapiti Group will be published. This report will address the stratigraphic framework, depositional history and distribution of coal. It will present a series of maps displaying the coal resource characteristics in terms relevant to exploration, development and use of these coals.

REGIONAL STRATIGRAPHY

The clastic rocks that outcrop along the numerous rivers and creeks in the region between Grande Prairie and Grande Cache belong to the Wapiti Group of Maastrichtian to Early Paleocene age. Sediments were derived from the Laramide uplift to the west and form a thick clastic wedge thinning from west to east. Average thickness of the Wapiti Group is approximately 1700 m along the western margin. Underlying the Wapiti Group is the predominantly marine Wapiabi Formation of the Smoky Group. The contact is gradational, consisting of a coarsening upwards sequence of siltstones and sandstones, as observed on the Smoky River, northeast of Grande Prairie. The upper contact of the Wapiti Group with the overlying Paskapoo Formation was not observed within the project area. However, the high escarpment south of the Smoky River is thought to represent the resistant units of the Paskapoo.

The Wapiti Group consists of interbedded sandstones, siltstones and mudstones derived from the rapidly rising mountain regions of the Laramide Orogeny to the west. Thick coarse grained sandstones, (greater than 20 m thick), of channel origin frequently downcut into the underlying finer grained sequences. Stratigraphic units are highly variable in thickness and lateral distribution. Preliminary results of sedimentological studies conducted by T. Jerzykiewicz of the Institute of Sedimentary and Petroleum Geology, indicate that the depositional environment of the Wapiti Group was predominantly fluvial, with a lacustrine component. A.R. Sweet of the Institute of Sedimentary and Petroleum Geology has conducted biostratigraphic studies of field samples collected during the 1988 field season. He has determined that the strata of the Wapiti Group are Cretaceous to early Paleocene in age.

Numerous coal zones have been recognized throughout the Wapiti Group stratigraphic succession. Coal zones, up to 6 m thick, outcrop on the Smoky, Cutbank, and Kakwa rivers. These coal zones appear to be similar in age and stratigraphic position to the coals of the Saunders Group in west-central Alberta (McLean and Jerzykiewicz, 1978). Palynology and sedimentology studies that are currently underway by Jerzykiewicz and Sweet (1988), may allow correlation between the two regions.

REGIONAL STRUCTURE

Wapiti strata within the project area appear to have gentle dips in the east to more moderate dips along the western margin. A broad synclinal structure trends northwest through the eastern half of the project area. This structure may be the northward extension of the Alberta Syncline to the south. Strata on both limbs of the fold dip at generally less than 10 degrees. A series of anticlinal and synclinal folds with dips up to 25 degrees occur along the western margin of the project area, near the deformed belt of the Foothills . A structural contour map of the base of the Wapiti Group indicates that these folds trend to the northwest. Immediately to the west, a high angle reverse fault has thrust Upper Cretaceous strata of the Alberta Group upon the Wapiti strata. This fault delineates the western margin of the project. There does not appear to be significant faulting eastward of this feature into the core of the Alberta Syncline. Minor folds and faults, with limited displacement, probably exist within the stratigraphic sequence; however, no surface expressions have been recognized to date.

COAL DISTRIBUTION

Coal zones have been recognized in outcrop as well as in the subsurface throughout most of the Wapiti Group stratigraphic succession. The thickest zones occur in two major intervals within the upper third of the section (Fig. 2). In the lower two thirds of the Wapiti Group, repetitive cycles of medium to coarse grained sandstone overlain by a fine grained sequence of mudstone with minor coal have produced multiple thin coal zones (up to 2 m thick). Outcrops along the Smoky and Wapiti rivers indicate that at least three cycles of coarse grained and fine grained units are present in

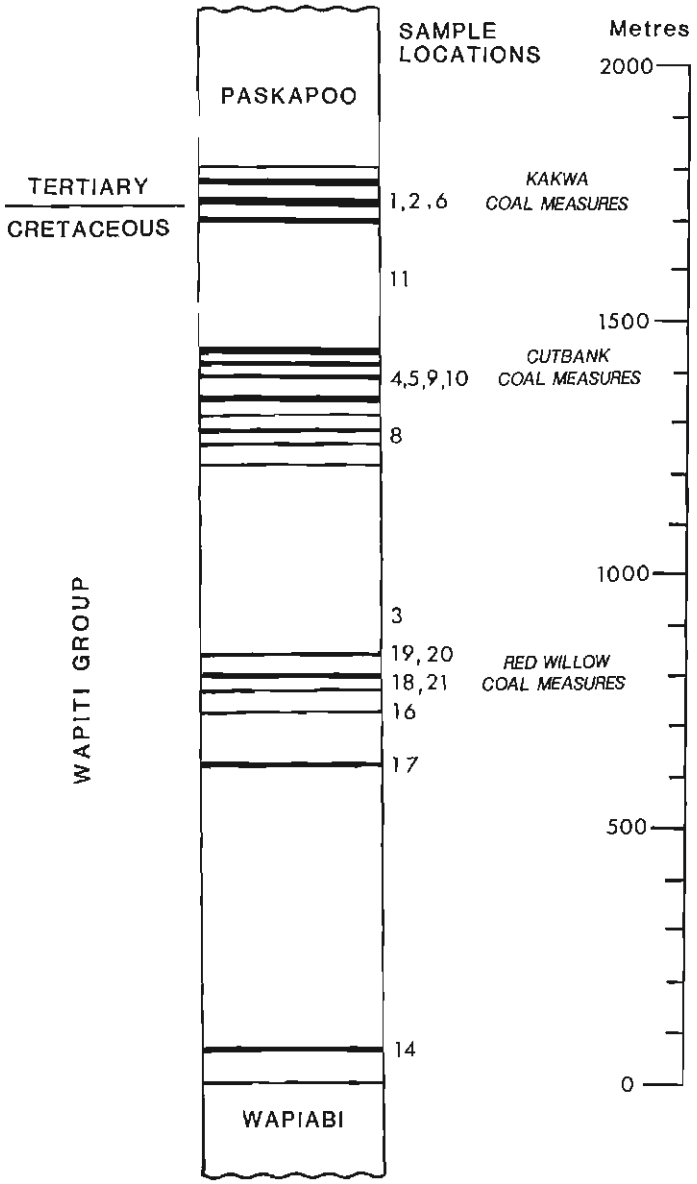

Figure 2. *Stratigraphic column of the Wapiti Group.*

the lower Wapiti strata. The coal zones that occur in these strata (Sample locations 14, 17, 18, 19, 21, Fig.2), appear to be widely variable in thickness and limited laterally to isolated deposits with an areal extent of approximately 5 to 10 km.

The first major coal-bearing interval lies approximately 1300 m above the base of the Wapiti Group. These strata contain up to 6 coal zones over an interval of approximately 100 m. Coal zones up to 6 m thick have been observed in outcrop and exploration boreholes. Sample localities 4, 5, 9, 10 represent coal seams within this interval. This coal-bearing sequence has been informally defined as the Cutbank coal measure. It may be correlative with the Brazeau coal zone of the Saunders Group in west-central Alberta and the Carbon Thompson coal zone of the Alberta Plains.

Approximately 190 to 250 m above the Cutbank coal measure, is another thick sequence of coal-bearing strata similar to the lower interval. Informally defined as the Kakwa coal measure, the interval is approximately 100 m thick. Up to seven individual coal zones have been observed, with zone thickness ranging from 1 to 6 m. Sample locations 1, 2, 6 were measured within this interval. Preliminary biostratigraphic data indicate that the Cretaceous-Tertiary boundary lies near the base of this coal measure. The presence of this time marker indicates that this upper coal horizon is correlative with the Upper Coalspur Formation in west-central Alberta, and the Ardley coal zone of the Alberta Plains. A subsurface correlation of coal exploration data based upon this coal interval has been undertaken. Preliminary results, (Fig. 3), indicate that the individual coal zones can be correlated over long distances (greater than 30 km). However, individual seams are widely variable in thickness.

COAL CHARACTERISTICS

During the 1988 field season, 31 coal samples were collected from outcrops along the river valleys (Fig. 1). These samples represent most of the coal zones within the Wapiti Group (Fig. 2). The coal zone sections were measured at the outcrop, and the coal seams and partings were sampled in detail. Only the coal samples were analysed by proximate and ultimate analyses, and by petrography (rank and petrographic composition). For sample preparation and analytical procedures used, see Bustin et al. (1985). The data shown in Table 1 represent averaged values for the coal interval at each of the locations sampled.

PETROGRAPHIC CHARACTERISTICS

Vitrinite reflectance

The random vitrinite reflectance ranges from 0.46 to 0.74%. This reflectance range indicates, for most of the coals, a high volatile C and B bituminous rank (0.47-0.71%, Davis, 1978). One sample (location 9) is of high volatile A bituminous rank, and one sample (location 14), with a reflectance level of 0.46%, is at the transition from subbituminous to high volatile C bituminous rank. In the southern part of the study area, the Kakwa coal measure appears to have the lowest reflectance levels (0.50-0.59%), whereas the Cutbank coal measure tends to have slightly higher reflectance (0.63-0.74%, Fig. 4). For the samples from the lower and middle part of the Wapiti Group, (locations 3, 8, 14, 17, 18, 19, 20 and 21), which were collected mainly in the northern part of the study area (Fig. 1), there is a trend of decreasing reflectance values from the southwest to the northeast (0.67-0.46%, Fig. 4), except for sample 3, which has a relatively low reflectance value of 0.61%. Further sampling of Wapiti Group coals is required to understand the regional rank variations with respect to depth of burial of the strata and the effect of Laramide deformation (Kalkreuth and McMechan, in press).

Petrographic Composition

Maceral group variations (averaged) for the Wapiti Group coals are shown on Table 1 and Figure 4. Most of the coals are characterized by high amounts of vitrinite macerals, (75-94 vol. %), moderate amounts of inertinite macerals, (4-21 vol. %), and low amounts of liptinite macerals, (2-8 vol. %). Exceptions are the coal zones at locations 2 and 6, which show decreased vitrinite contents, and significantly increased inertinite contents of up to 39 vol. % (Fig. 4). Within the inertinite group, the macerals semifusinite, fusinite and inertodetrinite are the main components. Within the liptinite group, the maceral sporinite is most common (up to 7 vol. %). Other liptinite macerals were determined only in minor amounts.

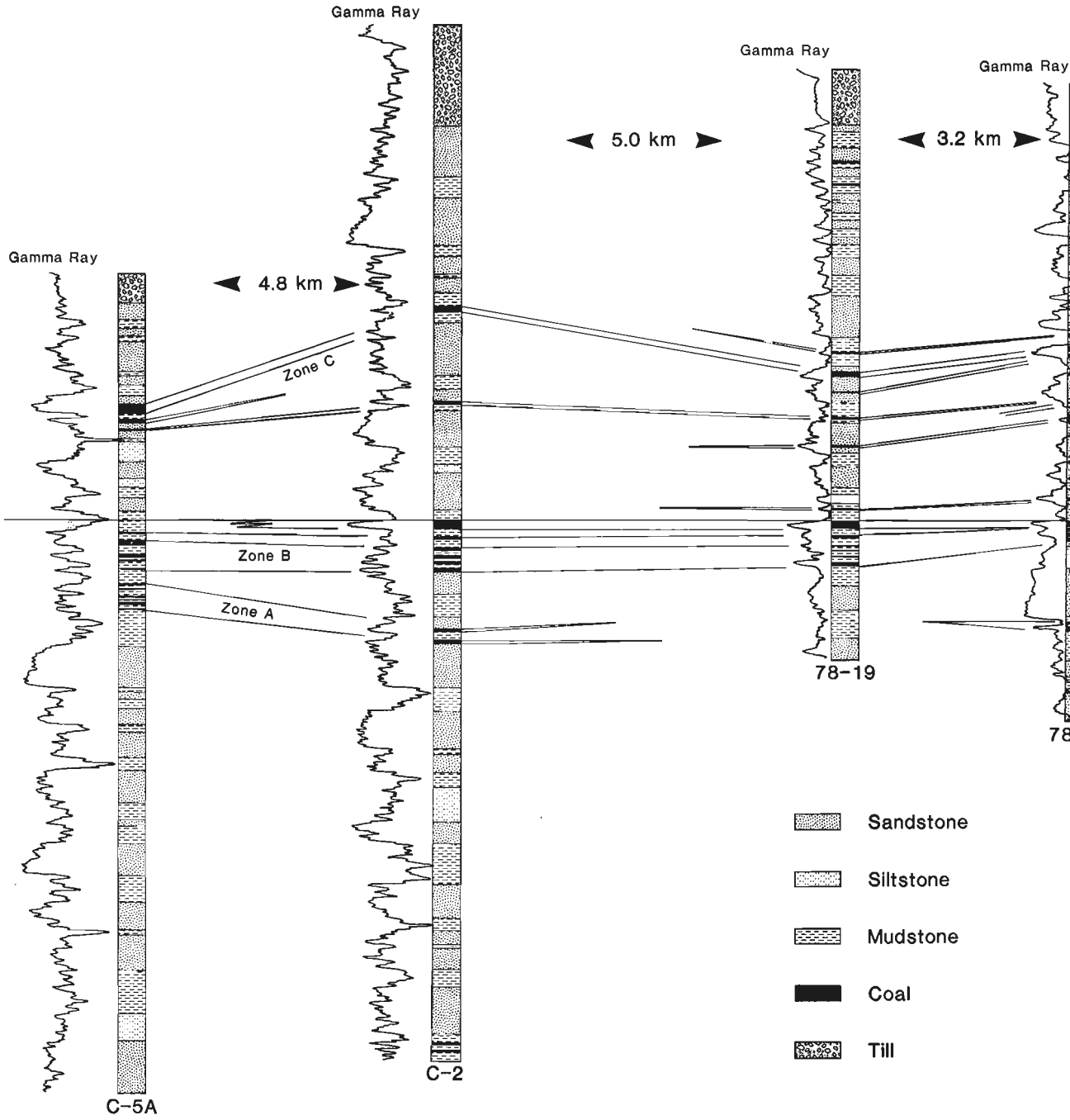
Gamma Ray
Gamma Ray
Gamma Ray
Gamma Ray
4.8 km
5.0 km
3.2 km
Zone C
Zone B
Zone A
C-5A
C-2
78-19
78
Sandstone
Siltstone
Mudstone
Coal
Till

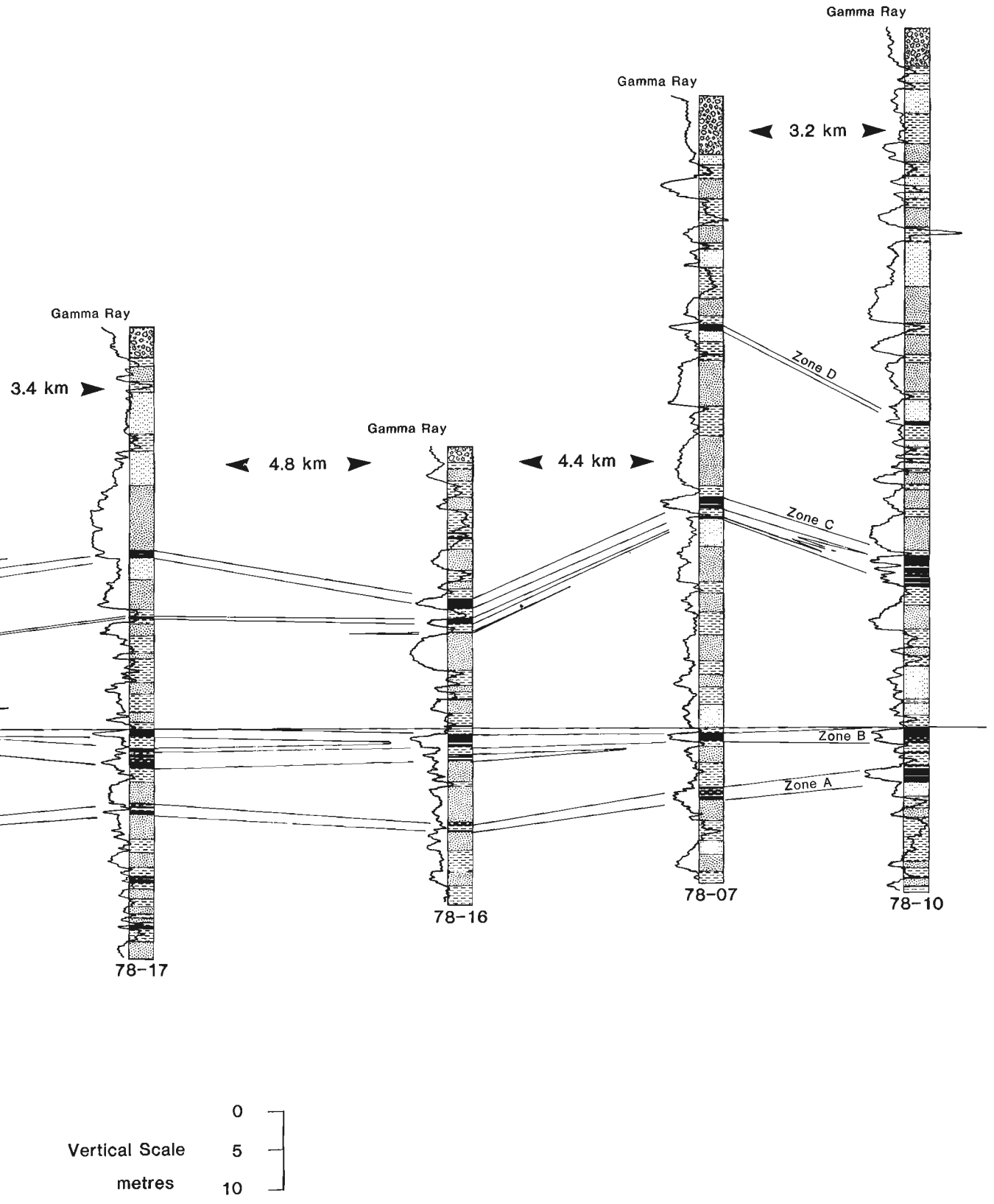

Figure 3. Detailed correlation of the Kakwa coal measures section A-A¹.

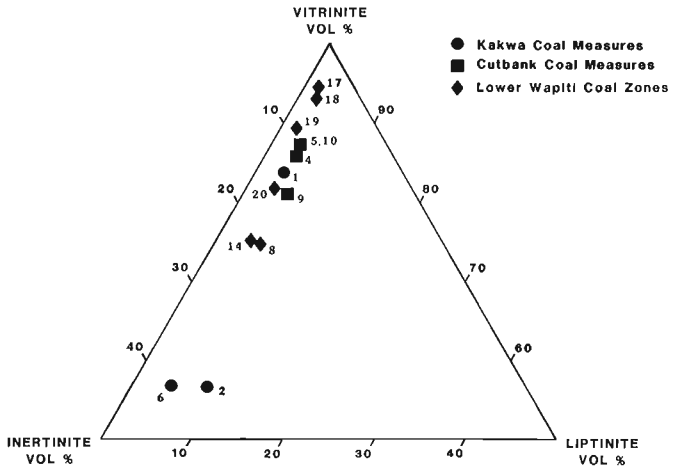

Figure 4. Maceral distribution diagram, Wapiti coal samples.

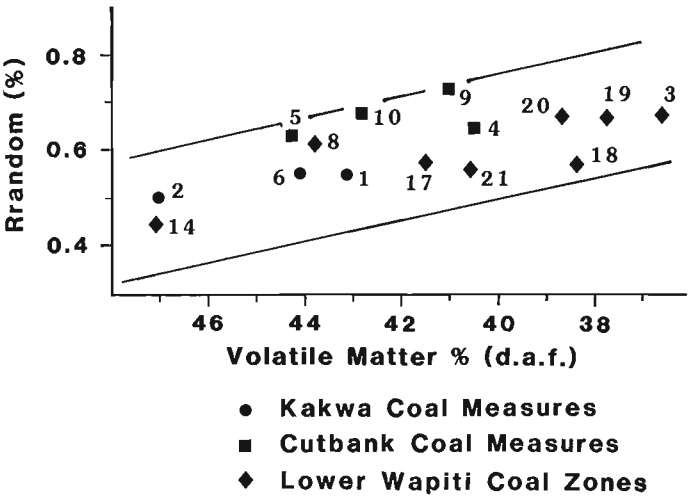

Figure 5. Relationship of reflectance to volatile matter, Wapiti coal samples.

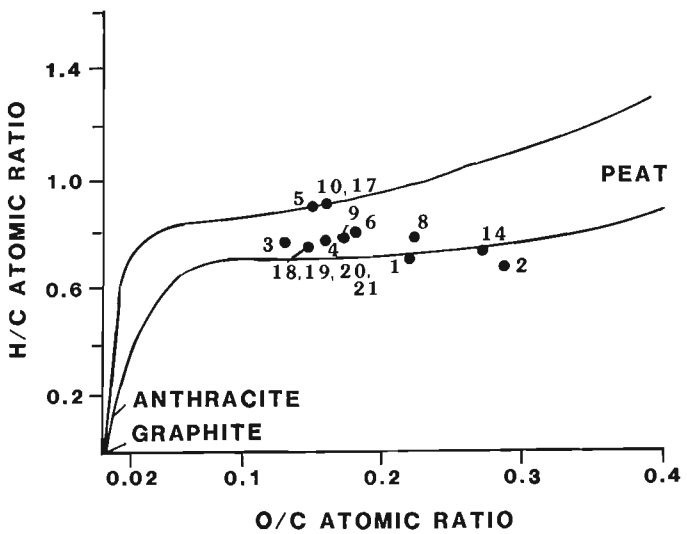

Figure 6. Hydrogen-carbon/oxygen-carbon crossplot of Wapiti coal samples.

The high vitrinite contents determined in many of the Upper Cretaceous Wapiti Group coals make them markedly different from the Lower Cretaceous Gates Formation coals of the same area. Many of the Gates coals accumulated in coastal swamps (Kalkreuth and Leckie, in press and this volume), in which relatively low water tables allowed the enrichment of inertinite macerals, indicative of oxidizing conditions (semifusinite and fusinite). The preliminary results on maceral distribution in the Wapiti coals and corresponding gelification and tissue preservation indices (Diessel, 1986), that these coals accumulated in a more fluvial depositional environment.

CHEMICAL CHARACTERISTICS

Proximate analyses

The results from proximate analyses are shown in Table 1. Ash contents are highly variable, (5.5-36%) as are the other parameters (moisture, volatile matter, fixed carbon and sulphur). Sulphur contents are low to moderate (0.11-0.79%). The volatile matter contents have been recalculated on a dry, ash-free basis and are shown in respect to random vitrinite reflectance values (Fig. 5). Despite a fairly large scatter of data points (most likely related to weathering of some samples and differences in petrographic composition), the volatile matter contents decrease quite regularly as vitrinite reflectances increase.

Ultimate Analyses

Results from ultimate analyses are shown on Table 1 and Figure 6. The atomic H/C and O/C ratios, (Fig. 6), confirm the rank determinations based upon vitrinite reflectance. Lowest rank levels are indicated for the samples from locations 2 and 14. The higher rank samples are characterized by a significant drop in the atomic O/C ratios (Fig. 6), which reflects the loss of oxygen with increasing rank, while at the same time carbon contents increase.

Technological Properties

Technological properties of coals are to a large extent a direct function of the rank and petrographic composition of the parent coals. The low rank levels of the Wapiti Group coals (0.46-0.74% Rrandom), place these coals in a rank range suitable for thermal coal utilization. The high amounts of reactive macerals (vitrinite and liptinite macerals), determined in many of the coals make them also suitable for coal conversion such as hydrogenation and pyrolysis (see Kalkreuth et al., this volume).

TABLE 1

Chemical and petrographical characteristics of Wapiti coal samples

Coal Zone	Thickness (m) Coal/Zone	Proximate Analyses (wt. %)					Ultimate Analysis Atomic Ratios		Petrographic Characteristics Maceral Group Analysis (Vol.%, mmf.)			
		Moisture	Ash	V.M.%	F.C.	S	H/C	O/C	R random	Vitrinite	Liptinite	Inertinite
Location 1 (Kakwa Zone)	5.0/6.4	11.3	14.4	29.6	44.6	0.25	0.75	0.22	0.59	84	3	13
Location 2 (Kakwa Zone)	> 1/3.00	27.3	9.1	30.0	33.6	0.11	0.63	0.29	0.50	57	8	35
Location 3	1.55/1.70	9.2	15.2	27.7	47.9	0.22	0.76	0.13	0.67	78	4	18
Location 4 (Cutbank Zone)	1.17/2.70	9.2	21.7	27.9	41.2	0.27	0.79	0.16	0.65	86	3	11
Location 5 (Cutbank Zone)	1.50/1.50	7.4	36.1	25.0	31.5	0.34	0.88	0.15	0.63	87	3	10
Location 6 (Kakwa Zone)	1.00/1.30	11.6	27.7	26.8	34.0	0.31	0.80	0.18	0.55	57	4	39
Location 8	0.60/0.60	11.9	12.1	33.3	42.7	0.29	0.75	0.22	0.61	75	5	20
Location 9 (Cutbank Zone)	1.30/1.30	8.2	8.0	34.4	49.4	0.37	0.77	0.17	0.74	81	5	14
Location 10 (Cutbank Zone)	2.65/3.25	8.1	22.2	29.4	40.3	0.28	0.83	0.16	0.68	87	3	10
Location 14*	0.45/0.45	30.5	10.4	27.9	31.3	0.30	0.72	0.27	0.46	75	4	21
Location 17	0.20/0.20	12.9	21.9	27.0	38.1	0.79	0.84	0.16	0.57	94	2	4
Location 18	0.20/0.20	17.2	5.5	29.7	47.6	0.52	0.78	0.15	0.56	93	2	5
Location 19	1.10/1.40	9.1	20.8	30.4	50.1	0.31	0.79	0.14	0.66	89	2	9
Location 20	0.30/0.30	7.2	17.1	29.3	46.5	0.38	0.79	0.14	0.67	82	3	15
Location 21	0.30/0.30	13.3	11.4	30.7	44.7	0.49	0.77	0.15	0.56	84	2	14

Note * Data analyses based upon coal samples only, excluding rock partings. Analysis based upon average of samples for each location.
* Location 14 is highly weathered giving rise to anomalous moisture value.

FURTHER RESEARCH

The Wapiti project area extends from northeastern British Columbia southeast to the Berland River in western Alberta. Phase 1 of the study examined the coal potential of the region from Grande Prairie to Grande Cache, west of the sixth meridian. Thick coal seams, (up to 6 m) have been observed within two coal-bearing intervals within the upper third of the Wapiti Group. Preliminary studies indicate the coals to be of high volatile bituminous to subbituminous rank. Further work is required to better define the stratigraphic framework within which coal beds occur, and to better understand depositional and tectonic controls on the distribution and character of the coals. The arbitrary geographic limits to the present study will be extended to the north and southeast in future.

REFERENCES

Allan, J.A. and Carr, J.L.
1946: Geology and coal occurrences of the Wapiti-Cutbank Area, Alberta. Research Council of Alberta, Report 48.

Bustin, R.M., Cameron, A.R., and Kalkreuth, W.D.
1985: Coal Petrology - Its Principles, Methods and Applications. Geological Association of Canada, Short Course Notes, v. 3, 2nd ed. 273 p.

Davis, A.
1978: The measurement of reflectance of coal macerals - its automation and significance. Pennsylvania State University Technical Report 10, 88 p.

Dawson, G.M.
1878: Report on an exploration from Fort Simpson on the Pacific Coast to Edmonton on the Saskatchewan, embracing a portion of the northern part of British Columbia and the Peace River country. Geological Survey of Canada, Report of Progress, 1879-80, Part B.

Diessel, C.F.K.
1986: On the correlation between coal facies and depositional environments. Proceedings of the 20th Newcastle Symposium, University of Newcastle, Australia, p. 19-22.

Jerzykiewicz, T. and Sweet, A.R.
1988: Sedimentological and palynological evidence of regional climatic changes in the Campanian to Paleocene sediments of the Rocky Mountain Foothills, Canada. Sedimentary Geology, v. 59, p. 29-76.

Kalkreuth, W.D. and McMechan, M.E.
in press: Burial history and thermal maturity, Rocky Mountain Foothills and Foreland, east-central British Columbia and adjacent Alberta. American Association of Petroleum Geologists, Bulletin.

Kalkreuth, W.D. and Leckie, D.A.
in press: Sedimentological and petrographical characteristics of Cretaceous strandplain coals: a model for coal accumulation from the North American Western Interior Seaway. International Journal of Coal Geology.

Kalkreuth, W.D., Leckie, D.A., and Labonté, M.
1988: Gates Formation (Lower Cretaceous) Coals in Western Canada: a Sedimentological and Petrographical Study. This volume.

Kalkreuth, W.D., Roy, C. and Stellar, M.
1988: Conversion characteristics of selected Canadian coals based on hydrogenation and pyrolysis experiments. This volume.

Kramers, J.W. and Mellon, G.B.
1972: Upper Cretaceous-Paleocene coal-bearing strata, northwest central Alberta Plains. Proceedings of the First Geological Conference on Western Canadian Coal, Research Council of Alberta Information Series no. 60, p. 109-124.

McLean, J.R. and Jerzykiewicz, T.
1978: Cyclicity, tectonics and coal: some aspects of fluvial sedimentology in the Brazeau-Paskapoo formation, Coal Valley area, Alberta, Canada. In Fluvial Sedimentology, A.D. Miall (ed.); Canadian Society of Petroleum Geologists, Memoir 5, p. 441-468.

Distribution and character of coal in the Battle River Coalfield, east-central Alberta

F.M. Dawson, A.R. Cameron, and T. Jerzykiewicz
Institute of Sedimentary and Petroleum Geology, Calgary

Dawson, F.M., Cameron, A.R., and Jerzykiewicz, T., Distribution and character of coal in the Battle River Coalfield, east-central Alberta. In Contributions to Canadian Coal Geoscience, Geological Survey of Canada, Paper 89-8, p. 49-61, 1989.

Abstract

The Battle River Coalfield contains substantial subbituminous coal in the Upper Cretaceous Horseshoe Canyon Formation. Ten coal zones have been correlated, of which five appear to be of mineable thickness. The Battle-River and Paintearth coal zones within member A of the Horseshoe Canyon Formation are the most continuous beds in the stratigraphic sequence. Discontinuous coal zones such as the Halkirk, Castor and Sullivan lie within member B of the formation.

The coals of the Horseshoe Canyon Formation in the Battle River Coalfield are of subbituminous B and C rank, suitable for electric power generation. The Battle-River and Paintearth coal zones are rich in huminite, and low in inertinite, suggesting that the coals were formed in a marginal marine marsh type facies. Sedimentological studies support this interpretation of the depositional history.

Résumé

Le bassin houiller de Battle River contient des charbons subbitumineux en quantité substantielle dans la formation de Horseshoe Canyon du Crétacé supérieur. Dix zones de charbon ont été corrélées parmi lesquelles cinq zones semblent être d'une épaisseur suffisante pour en rendre l'exploitation rentable. Les zones charbonnières de Battle-River et de Paintearth situées à l'intérieur du membre A de la formation de Horseshoe Canyon sont les couches les plus continues dans la séquence stratigraphique. Les zones discontinues comme celles de Castor, Halkirk et Sullivan se trouvent à l'intérieur du membre B de la formation.

Les charbons du bassin houiller de Battle River dans la formation de Horseshoe Canyon sont de rang subbitumineux B et C, convenant à l'alimentation des centrales électriques. Les zones charbonnières de Battle-River et de Paintearth sont riches en huminite et pauvres en inertinite, ce qui semble indiquer que les charbons ont été formés dans des milieux marins et paraliques de type marécageux. Des études sédimentologiques appuyent cette interprétation de l'histoire sédimentaire.

INTRODUCTION

The Alberta Plains contains vast resources of subbituminous coal suitable for conventional coal-fired electric power generating stations. The Upper Cretaceous Horseshoe Canyon Formation accounts for a large portion of these resources. The Energy Resources Conservation Board (ERCB, 1988) has designated thirteen fields which account for the coal resources within the Horseshoe Canyon Formation. The Battle River Coalfield is the largest of these fields. This paper is based on information from the GSC Open File Report "Coal Geology of the Battle River Coalfield". It addresses only the geology of the coal-bearing strata and character of the coals. Other data pertaining to exploration potential and resource quantities are available in the open file report.

The Battle River Coalfield is located in east-central Alberta, approximately 180 km northeast of Calgary. The study area exceeds 3500 km^2 and encompasses townships 32 to 43, ranges 13 to 17 west of the 4th Meridian (Fig. 1). Currently, two open pit coal mines, Vesta and Paintearth, are operating in the region, producing in excess of 1.5 megatonnes annually for electric power generation.

The Battle River Coalfield was initially chosen for study because of the large amount of geological information available for analysis. Subsurface coal exploration data (in excess of 4400 boreholes), in conjunction with surface mapping and coal seam sampling, have provided the data upon which geological studies have been based (Fig. 2).

PREVIOUS WORK

In 1886 coal-bearing strata of Late Cretaceous age were observed along the banks of the Red Deer River by Tyrrell (1887). Tyrrell's "Edmonton Series" rocks were subsequently studied during the early 1900's by Allan (1922), Allan and Sanderson (1945) and Sternberg (1947), with particular reference to the coal resources and dinosaur fossils of the area. In 1970, Irish (1970) elevated the Edmonton Formation to group status and introduced new formation names for the sequence of rocks between the marine Bearpaw Formation and the Paleocene Paskapoo Formation. The name Horseshoe Canyon Formation was applied to the lower 400 m of this stratigraphic interval (Fig. 3). Recent works by Shepheard and Hills (1970), Campbell (1975), Gibson (1977), Rahmani (1981), Hughes (1984), and McCabe (1987) have focused on the sedimentological variations and depositional setting of the Horseshoe Canyon Formation strata in the geographical areas north and southeast of the Battle River Coalfield. Limited studies have been undertaken within the limits of this project's boundaries.

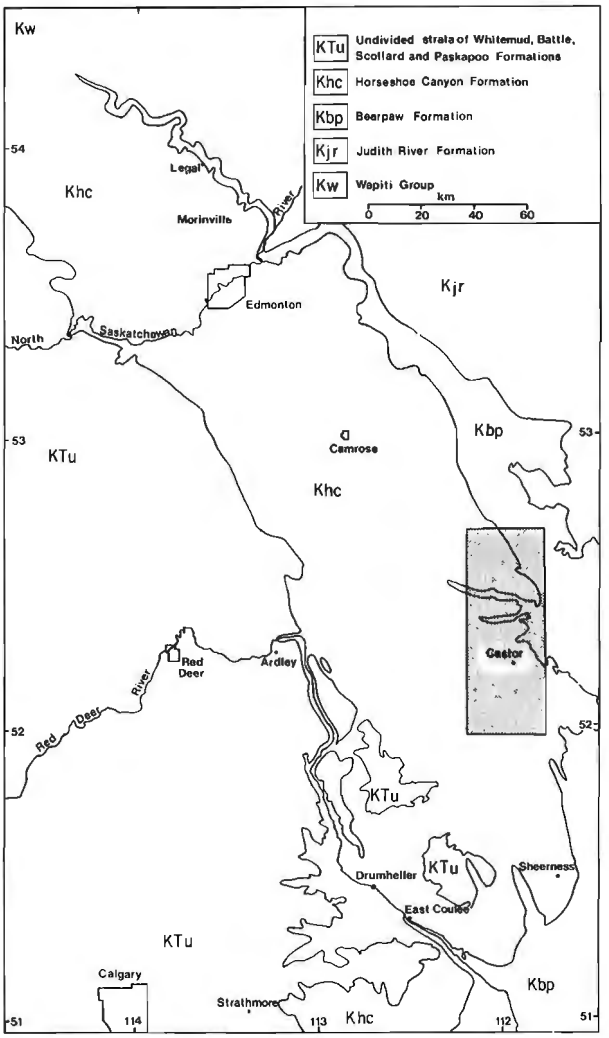

Figure 1. *General location map of Battle River project. Shaded part is study area.*

REGIONAL STRATIGRAPHY

In the Battle River study area, Upper Cretaceous strata are assigned to the Bearpaw and Horseshoe Canyon formations (Fig. 3). The Bearpaw Formation consists of marine and marginal marine strata that represent the last major transgression of the Late Cretaceous sea within Alberta. The Horseshoe Canyon Formation comprises clastic sediments derived from a source to the west during Laramide orogenesis, and deposited during regression of the Bearpaw Sea (Williams and Burk, 1964).

West of the project area, the Horseshoe Canyon Formation is overlain by the predominantly fluvial and lacustrine sediments of the Whitemud and Battle formations (Irish, 1970). No outcrops of these strata are present within the study area.

The Battle River project was initiated to examine the geology of the coal-bearing sequence of the lower 200 m of the Horseshoe Canyon Formation. The basal 50 m of strata represent the gradational contact with the underlying Bearpaw Formation and are informally defined as the "transition zone" (Shepheard and Hills, 1970). The upper 150 m of strata are predominantly continental in origin. True marine rocks of the Bearpaw Formation below the "transition zone" were not observed in either outcrop or borehole, due to the limited outcrop exposures along the eastern edge of the project area, and to the shallow depths of the exploration boreholes.

Up to 10 coal zones have been observed within the Horseshoe Canyon Formation. The 50 m interval immediately above the "transition zone" has been informally defined as member A, and contains up to six correlated coal horizons. Strata above the highest coal bed in member A have been informally defined as member B (Fig. 4).

Bearpaw-Horseshoe Canyon formations contact

The transition between the marine Bearpaw Formation and the overlying, predominantly continental strata of the Horseshoe Canyon Formation is gradational and a specific contact is difficult to define. This contact is arbitrarily chosen where marine fossils last appear and is thought to be immediately below the coarsening-upward cycle of sandstone and siltstone. In the Battle River project area, up to five coarsening-upward cycles have been observed in the subsurface data. However, only the upper two have been examined in outcrop. In some cases, each cycle is capped by a thin to thick coal, or concretionary bed. Each cycle is approximately 15 to 20 m thick and displays a distinctive natural gamma geophysical log response (Fig. 5). This easily recognized gamma-ray response is characteristic of the basal unit of the Horseshoe Canyon Formation and is recognizable in the subsurface throughout central and southern Alberta.

Member A

The lower 50 m of the Horseshoe Canyon Formation above the "transition zone" have been informally defined as member A (Fig. 4). This stratigraphic interval contains up to six coal zones, two of which are considered to be of economic importance. The coal sequences are stratigraphically divided into two major repetitions (Fig. 6). Cycle 1 begins with the coarsening-upward sequence of siltstone and sandstone lying above the Ryley marker seam. This interval is approximately 15 m thick and is capped by the regionally extensive Battle-River coal zone. The Battle-River zone represents the major economic coal horizon in the study area. Approximately 10 m above this unit lies a thin, laterally continuous coal bed defined as the Gadsby zone. This unit can be used as a marker bed throughout much of the project area, and marks the top of the first cycle.

The second cycle begins with another sequence of coarsening-upward siltstone and sandstone, capped by another thick, regionally extensive coal horizon referred to as the Paintearth coal zone. The Paintearth zone is similar to the Battle-River zone in terms of lateral continuity and seam thickness. As with cycle one, a thin coal bed (Cordel zone) lies approximately 10 m above the Paintearth horizon in cycle two.

Member B

In the Battle River study area, member B of the Horseshoe Canyon Formation is defined as the stratigraphic sequence from the top of member A to subcrop, an interval of up to 100 m (Fig. 4). Four coal zones have been recognized in this interval, of which three contain potentially mineable coal deposits. Unlike member A, where the coal beds are laterally extensive, the coals in member B are discontinuous and widely variable in thickness. The base of

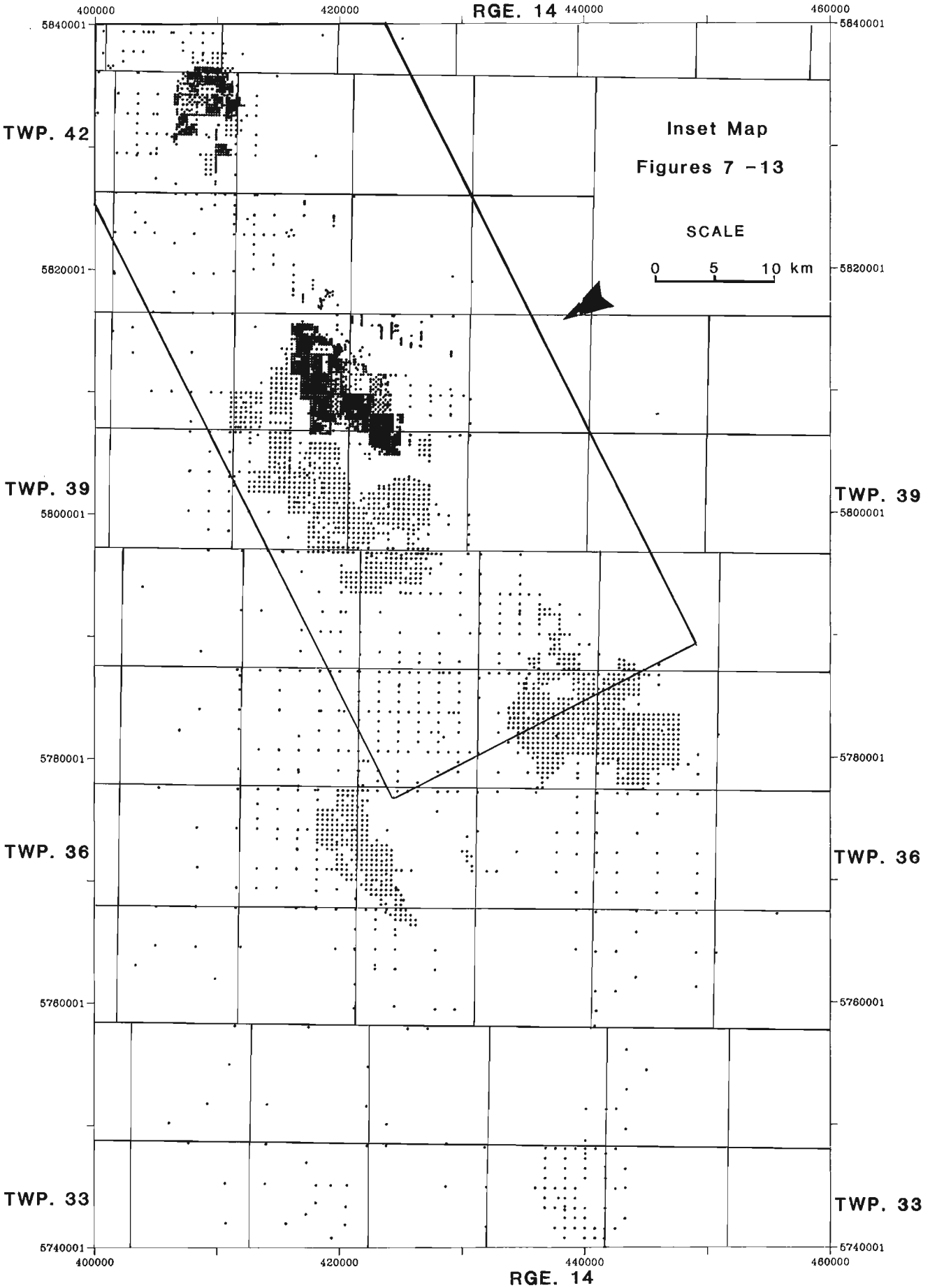

Figure 2. *Detailed map of project area illustrating distribution of borehole data and location of inset map.*

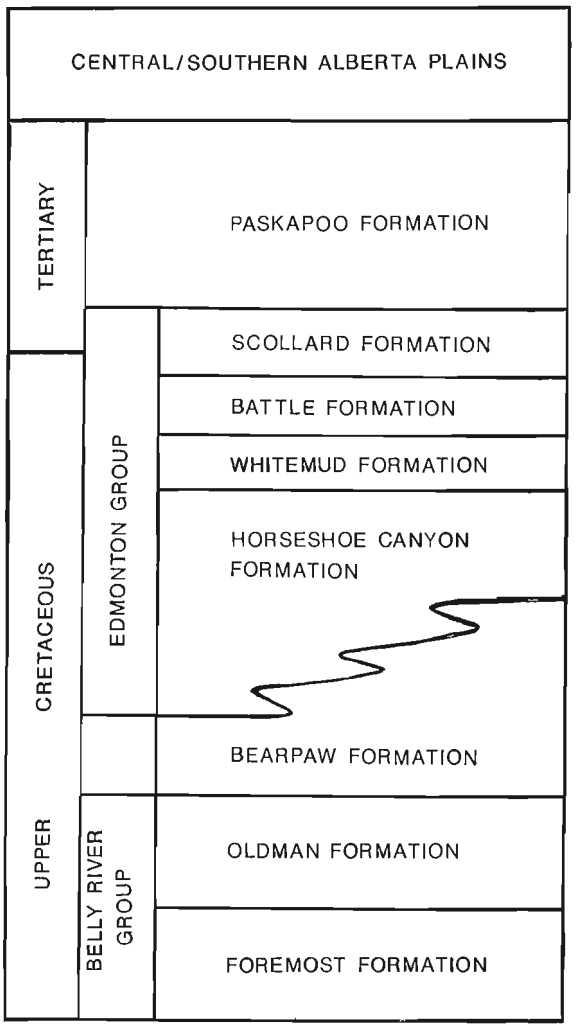

Figure 3. *Regional stratigraphic nomenclature of Upper Cretaceous strata for the southern Alberta plains.*

member B has been placed at the top of the Cordel coal bed. The Halkirk coal zone lies approximately 10 to 20 m above this contact. Three other coal zones that occur stratigraphically above the Halkirk zone are the Castor, Sullivan and Leo. Stratigraphic separation between these units is widely variable and is controlled to a large extent by the presence and distribution of sandstone bodies. Above the Leo coal zone, several coal beds have been observed. However, lack of sufficient data prevents detailed study of these units.

COAL GEOLOGY

Ryley zone

The lowest coal zone observed within the Battle River study is the Ryley (Fig. 4). The Ryley zone is present at the top of a 10 to 15 m thick coarsening-upward cycle immediately below member A. The zone is usually less than 0.5 m thick, and is commonly replaced by concretionary beds. No coal beds of potentially mineable thickness were found within the Ryley zone.

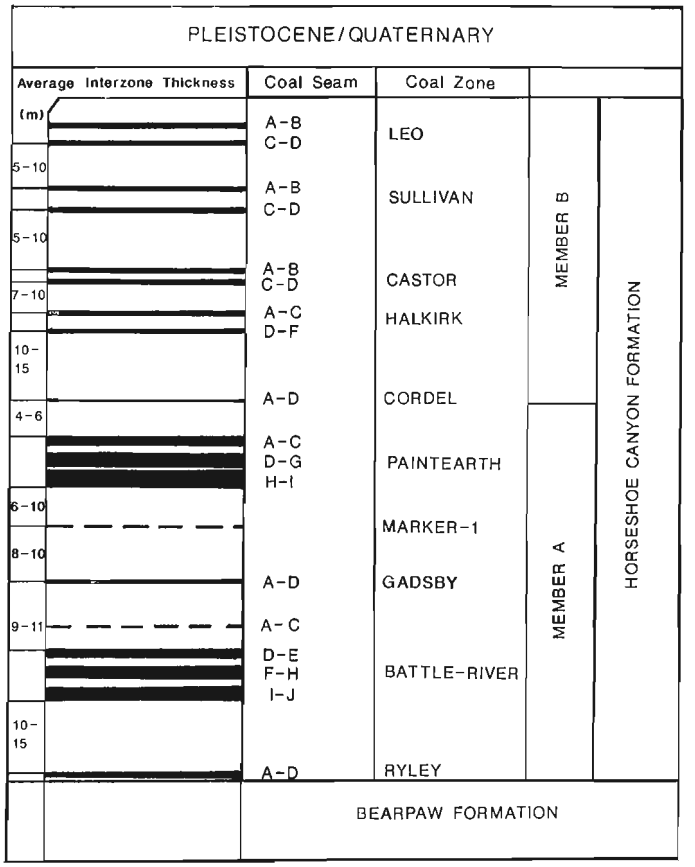

Figure 4. *Coal seam nomenclature for the Battle River Coalfield.*

Battle-River zone

The Battle-River coal zone appears to contain the greatest resource potential in the region. Ten individual coal beds have been recognized within the zone, each ranging up to 2.8 m in thickness. Four seam packages of coalesced beds are commonly developed. The lower three are laterally persistent throughout much of the project area. Locally, occasional thin partings divide these seams into thinner coal beds. In Township 40, Ranges 15 and 16, the three lower coal beds coalesce to form a single coal unit, up to 4.87 m in thickness. To the southeast and northwest of this location, the coal splits into numerous beds. In Township 37, Range 13, only one coal seam is present and is less than 0.5 m thick. In Township 42, Range 17, the Battle-River coal zone consists of three splits, each less than 0.5 m thick.

Locally, a discontinuous coal seam up to 2.8 m in thickness, but averaging less than 0.5 m, is present approximately 2 to 3 m above the main coal seam. In Township 35, Range 17, the Battle-River coal zone is very well developed, and this upper seam has an aggregate thickness up to 2.8 m over a stratigraphic interval of 9.8 m.

Gadsby coal zone

The Gadsby coal zone is a thin, carbonaceous stringer that lies approximately 8 to 11 m above the Battle-River coal zone. Aggregate coal thickness rarely exceeds 1.0 m and is locally split into two seams. The Gadsby coal zone is considered to be of insufficient thickness to be mineable.

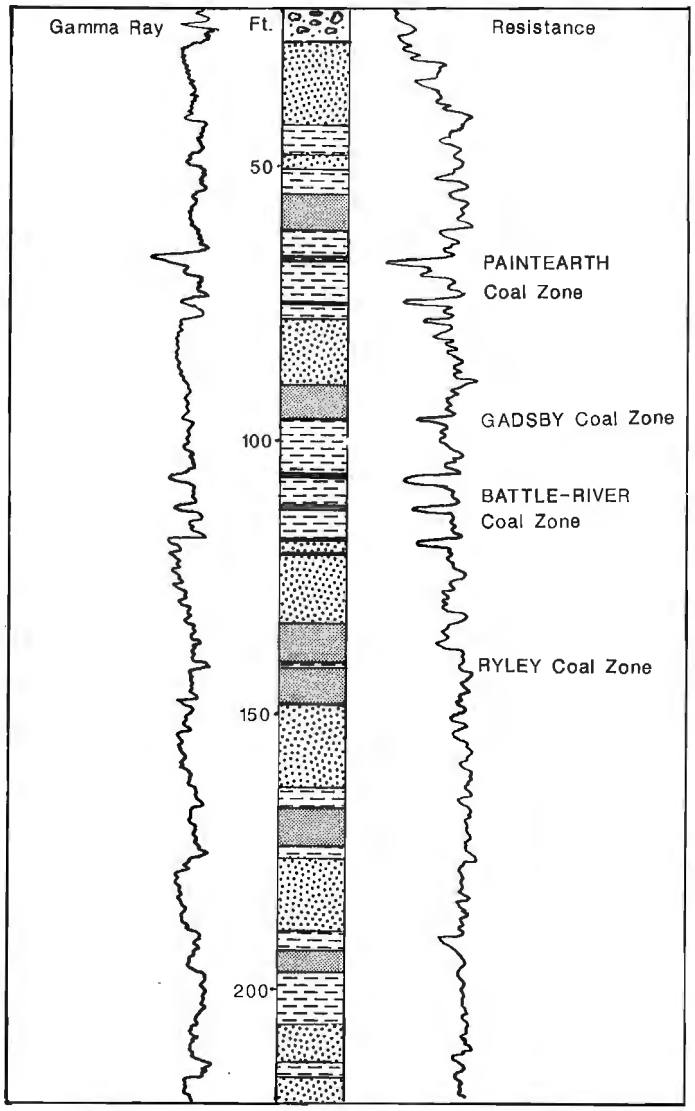

Figure 5. *Typical geophysical log response for the "Transition Zone" at the base of the Horseshoe Canyon Formation.*

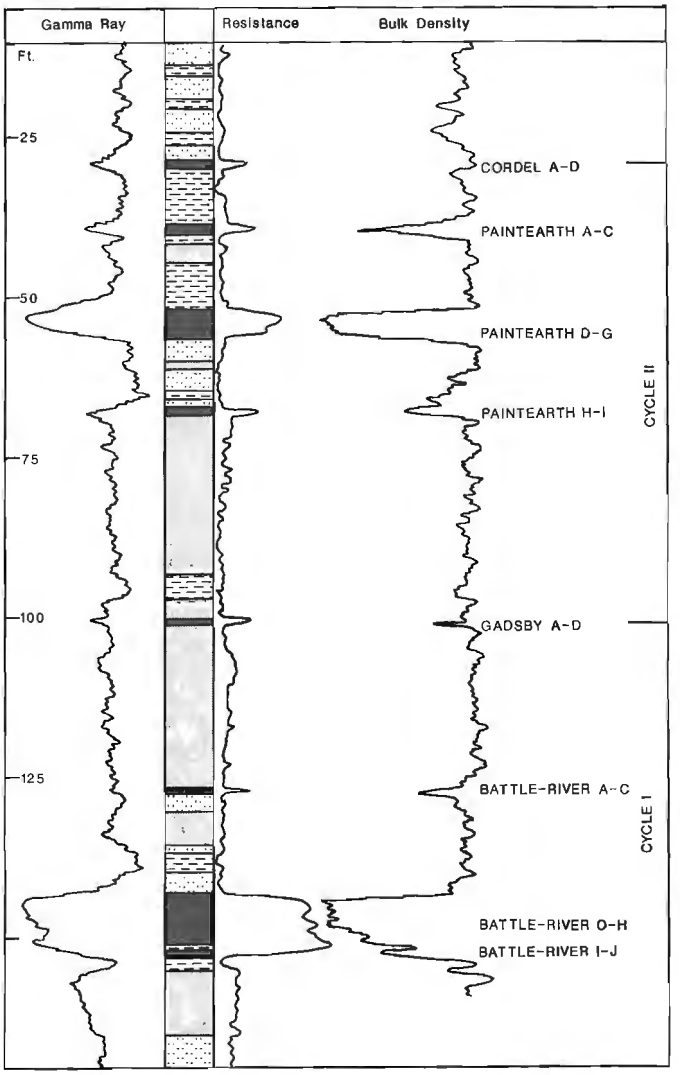

Figure 6. *Typical geophysical log response for Member A of the Horseshoe Canyon Formation.*

Paintearth coal zone

The Paintearth coal zone is similar in thickness and distribution to the Battle-River beds. The zone consists of up to nine individual coal beds with a cumulative thickness of greater than 5.0 m, over a maximum stratigraphic interval of 15 m. Throughout much of the project area, the zone can be divided into two main seams. The upper seam is well developed in Township 40, Range 15, and also in Township 42, Range 17. The seam varies in thickness up to 2.4 m, and coalesces with the underlying lower seam in Township 42, Range 17. Locally it contains several partings, and throughout most of the project area is separated from the lower seam by 1 to 4 m of muddy siltstone.

Distribution and continuity of the lower coal seam is similar to that of the lower seam of the Battle-River zone. The seam is laterally continuous; however, coal development and thickness is widely variable. The seam commonly splits into three coal beds, each separated by thin partings of mudstone and siltstone. In Township 40, Range 16, the individual coal seams coalesce into a thick (>3.0 m) unit. Toward the southeast from this locality, the seam splits into three individual beds that tend to thin and pinch out farther to the south in Township 38, Range 13. Toward the northwest, in Township 42, Range 17, the upper and lower Paintearth seams coalesce to form a single coal bed in excess of 4.0 m thick. Farther to the northwest, in Township 43, Range 17, the lower seam splits and pinches out over a short distance.

Cordel coal zone

The Cordel coal zone is a thin, discontinuous, coaly bed lying 3 to 7 m above the Paintearth zone, similar to the Gadsby zone overlying the Battle-River coal zone. The coal is poorly developed, consisting primarily of carbonaceous shale, and rarely exceeds 0.5 m of coal thickness.

Halkirk coal zone

The lowest coal horizon within member B of the Horseshoe Canyon Formation is the Halkirk coal zone (Fig. 4). This coaly unit is commonly split into two main seams separated by a muddy siltstone up to 11.7 m thick. In places, the lower seam splits into three beds, each up to a maximum of 0.6 m in thickness. In most cases, the beds coalesce into one unit, with a maximum thickness of 1.5 m as observed in Township 37, Range 15. The upper seam averages 0.5 m in thickness, with a maximum thickness of 2.0 m in Township 38, Range 16. The Halkirk coal zone appears to be more laterally discontinuous, and has a wider variability of thickness than the Paintearth or Battle-River coal zones. This variance may be due to a change in depositional setting. The Halkirk coal zone probably formed in a more unstable environment, with greater influence by fluvial depositional systems.

Castor coal zone

Approximately 7 to 15 m above the Halkirk coal zone lies the Castor coal zone. This carbonaceous bed is similar to the Halkirk, in that the zone is split into two main seams. In some places, these seams split into two beds, each attaining a thickness up to 1.5 m. Throughout much of the project area, a prominent kaolinitic mudstone unit separates the two main zones. This parting varies in thickness up to 13.26 m. In Township 35, Range 16, where the seams have coalesced, the coal is greater than 3.0 m in thickness.

Sullivan coal zone

The Sullivan coal zone represents the highest correlated unit in the stratigraphic section that was penetrated in a sufficient number of coal exploration boreholes to enable subsurface mapping. The zone lies approximately 7 to 15 m above the Castor zone and is similar in thickness and distribution. Coal seam thickness is widely variable with small localized pods of coal greater than 3.0 m in thickness. As with the Castor zone, the Sullivan coal zone is divided into two main seams. The parting separating these two main beds varies in thickness up to 15.85 m. Both the upper and lower seams range in thickness up to 2.5 m.

Leo coal zone

The Leo coal zone lies approximately 10 to 15 m above the Sullivan coal sequence. The unit is laterally discontinuous and lies approximately 150 m above the base of the Horseshoe Canyon Formation. The horizon subcrops along the western edge of the project area and, hence, has not been penetrated in many exploration boreholes. No subsurface maps have been produced for this horizon because of the limited available data.

SEDIMENTOLOGY AND DEPOSITIONAL SETTING

Coal deposition in the Battle River Coalfield is largely associated with three types of sedimentary sequences, namely: coarsening-upward sequences (CUS), thick sandstone intervals (TSI), and fining-upward sequences (FUS).

The coarsening-upward sequences (CUS) are generally characterized by interbedding with increasing thickness of the coarse beds upward. Claystone, mudstone and siltstone of the lower portion of the coarsening-upward sequences reveal delicate rhythmic laminae that resemble lacustrine rhythmite facies. Sandstone in the upper portion of the sequences is commonly parallel to subparallel bedded. This bedding may be classified in terms of "heterolithic stratification" (Thomas et al., 1979).

A thick (greater than 20 m) sandstone interval (TSI) has been observed below the Paintearth coal seam in Township 38, Range 14 (ST-9). This interval exhibits decimetre-scale trough crossbedding, small-scale cut-and-fill structures, and small channels. Small-scale crossbedding and current ripple laminae are also present in the upper portion. This interval of medium grained sandstone is overlain by a thin unit of rooted, coaly mudstone and coal. Crossbed paleocurrent data from the sandstone beds indicate a unimodal, northeasterly trend consistent with trends observed in the subsurface.

Fining-upward sequences (FUS), grading from medium grained sandstone to coaly mudstone and coal, occur in the upper part of the lower Horseshoe Canyon Formation.

The sequences described above (CUS, TSI and FUS), may be interpreted as components of one, large deltaic environment. In river deltas, the delta plain, comprising the distributary channels and intervening bays, has a wide areal extent (Fisher, 1969; Wright and Coleman, 1973). Modern interdistributary bay sequences resulting from infilling of the bay are very similar to the CUS observed within the lower Horseshoe Canyon Formation.

There are three processes by which sediment-laden floodwaters can be transferred to the bay: overbank flooding, crevassing and avulsion. The process of overbank flooding operates during a single flood event. Sediment-laden waters spill over the channel banks as a sheet flow, with no breaches or crevasse channels (Coleman, 1969). Fine grained, suspended sediment is deposited over the entire bay, and coarser sediment, if supplied, is confined to the bay margins and contributes to levee development. The muds and silts found at the bases of the coarsening-upward sequences result from overbank floods, although in open bays some of this sediment may be supplied by marine currents. Levee sediments generally comprise rapidly alternating coarse and fine grained beds (Allen, 1965). Each of the coarse grained beds results from an overbank flood (or crevasse splay), has a sharp base, and grades upward into the fine interval. Farther away from the channel margin, encroachment of the levee into the bay produces a coarsening-upward sequence characterized by interbedding, and increasing thickness of the coarse grained beds upward.

The crevasse splay is caused by a sudden, discrete incursion of sediment-laden floodwaters into a limited area of the bay (average of 2 km in the Mississippi delta bays; Arndorfer, 1973). The sediment may be deposited in numerous, small, anastomosing streams. Alternatively, the flow may become unconfined farther down the levee slope and acquire the characteristics of a sheet flood. Crevasse splay deposits are generally lobe-shaped sand bodies. The lobes extend across the lower part of the levee and beyond, thus contributing to levee development (Coleman, 1969; Arndorfer, 1973). Crevasse splay lobes (sheet and/or channel varieties) occur at the tops of some CUS of the lower Horseshoe Canyon Formation. The small-scale fining-upward sequences (FUS) that occur in the Castor coal zone may also be interpreted in terms of crevasse splay channels, although the general increase in grain size of the sediments indicates the increased influence by fluvial depositional systems.

It is likely that the TSI sequence measured at section ST-9 represents a major distributary channel. Thick coal development in Townships 40 and 29 probably represents the center of the interdistributary bays on either side of this distributary channel.

The interdistributary bay interpretation for the coarsening-upward sequences at the Bearpaw-Horseshoe Canyon transition is consistent with the general paleogeographic situation across the basin. The nature of the interdistributary bay (coastal lake ? lagoon ?) cannot be defined on a sedimentological basis alone. Further paleontological studies are needed to establish the upper limit of the marginal marine conditions of deposition in the Battle River Coalfield section. It seems likely, however, that the influence of brackish waters may extend as high as the uppermost observed CUS in the section. If this is true, the stratigraphic subdivision of the lower Horseshoe Canyon Formation into members A and B, as defined from subsurface studies, would be supported by sedimentological observations.

COAL COMPOSITION

As part of the study on the Battle River coals, a series of samples was collected for petrographic and chemical analyses (Fig. 7). Sites selected for sampling included active mines and outcrop sections, so that the resulting sample population consisted of relatively fresh, unoxidized coal along with weathered coal from outcrop exposures. In sampling the outcrop sections, trenches were dug to remove the more obviously weathered material, yet the analytical results, particularly from the chemical analyses, indicate oxidized coal at these sites. The majority of the samples were from the two main coal zones of the area, namely the Paintearth and Battle-River sequences. The Halkirk or Castor zones were sampled at five sites (Fig. 7), but results on these coals are not included in the present report. The seams exposed at each site were sampled incrementally, that is, natural sedimentological breaks such as partings or shaly coal beds were used as sample boundaries. These high ash units were sampled separately, but have not been analyzed for the present study. Table 1 lists the stations sampled on the Paintearth and Battle-River zones along with location data and the number of samples collected.

ANALYTICAL METHODS

For the chemical characterization of these coals, proximate analyses and determination of total sulphur and calorific value were carried out according to the standard ASTM procedures (American Society for Testing and Materials, 1979). Petrographic analyses consisted of maceral determinations on all coal samples, and a selected number of these were chosen for reflectance measurements. These petrographic analyses were performed on material crushed to minus 20 mesh (840 μm), molded in pellets with epoxy resin and polished according to standard procedures (ASTM, 1979). Analyses were carried out in reflected light, using oil immersion, on a Leitz Orthoplan microscope with MPV II photometric accessories at a magnification of X625.

The maceral nomenclature followed that proposed for low rank coals by the International Committee for Coal Petrology (ICCP, 1971). In this classification system, the huminite maceral group (precursor of vitrinite in higher rank coals) is divided into a variety of maceral types. The most important of these is eu-ulminite (material retaining vestiges of original woody tissue structure), densinite (finely fragmented and partially gelified huminite material) and gelinite (huminite matter in which tissue structure has been virtually destroyed, or material which may have passed through a colloidal phase). Inertinite and liptinite macerals were also identified. Diagnostic characteristics for these latter named macerals are essentially the same for both low and high rank coals (ICCP, 1971).

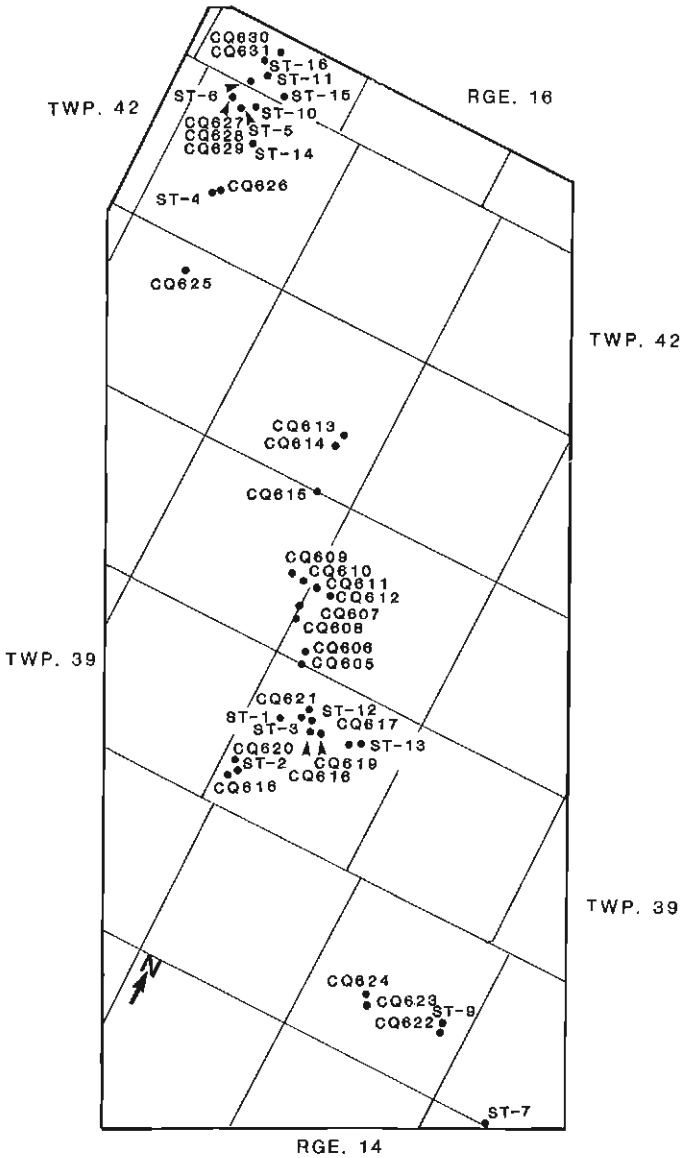

Figure 7. *Inset location map illustrating measured sections (ST) and sample sites (CQ). Sites CQ 620, 623, 624, 627 and 628 are on Halkirk or Castor zones.*

Maceral quantities were determined by point count (500 points per sample) and then calculated to per cent values. Reflectance measurements were determined in the random mode (R_o random) and the values reported are averages of 50 measurements per sample.

RESULTS AND DISCUSSION

A. Chemical

Ash and sulphur data are presented in Figures 8, 9 and 10. Average values for both ash and sulphur were calculated for the main part of both zones, that is, the thickest and most laterally persistent coal unit of each zone within the study area. These averaged values for each sampling station are recorded on Figures 8 and 9. In terms of these average values, ash content (dry basis) in the Paintearth zone ranges from 11.3% (Stn. CQ625) to 29.1% (Stn. CQ618), (Fig. 8A). Higher values for the Paintearth zone appear to be toward

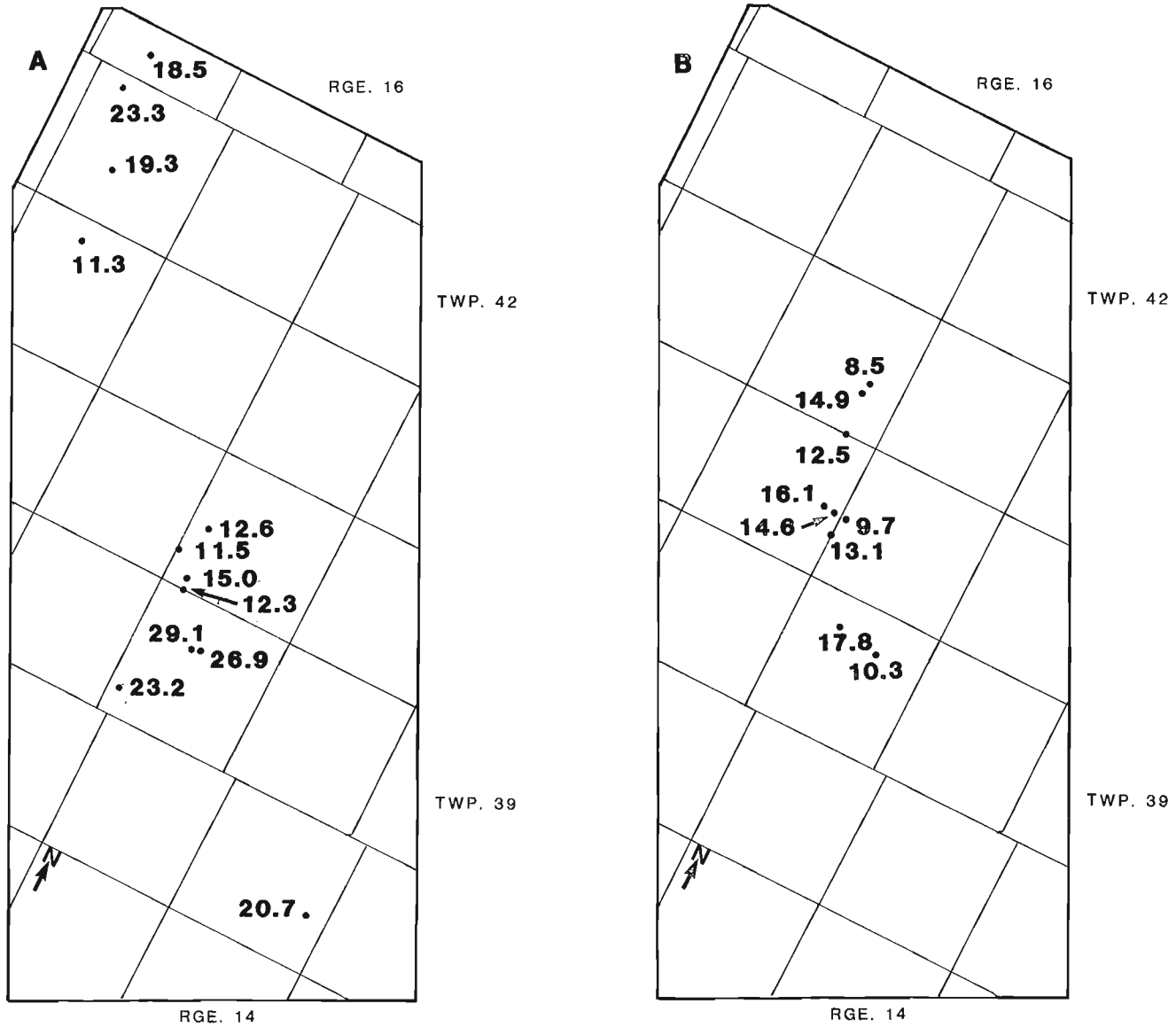

Figure 8. *Distribution of ash contents (dry basis) for Paintearth (Fig. 8A) and Battle-River (Fig. 8B) sampling stations.*

the southern end of the sampled area (Stns. CQ616, 618, 619 and 622). Subsurface data indicate that the Paintearth coal zone pinches out and is replaced by a channel sandstone immediately south of sites CQ616, 618 and 619. Apparently this is reflected in the ash content. The sampling sites in the Battle-River zone are confined to a smaller area than those in the Paintearth zone. Average ash contents on the main part of the zone are shown in Figure 8B. They range from 8.5% to 17.8% and indicate no discernable pattern.

Figure 9 (A and B) illustrates average sulphur contents for the Paintearth and Battle-River coal zones, again calculated for the main parts of both zones. The Paintearth values range from 0.32% to 0.74% whereas the Battle-River values range from 0.47% to 0.97%. The two highest values for the Battle-River zone are in the most southern stations sampled, namely CQ617 and CQ621.

Figure 10 summarizes ash and sulphur data for the Paintearth and Battle-River zones, by grouping data according to arbitrarily chosen ash and sulphur values and plotting the results in cumulative frequency histograms. For example, Figure 10A shows that 11.2 m, or over half the total thickness of Paintearth coal sampled, had ash contents of 10 to 20%, whereas for the Battle-River zone, over 8 m of the total sampled had ash contents between 0 and 10%. The numbers indicate that the Paintearth zone has higher ash values but slightly lower sulphur than the Battle-River zone. Average values are calculated separately for mine and outcrop samples. There is a marked difference in ash contents of these two kinds of samples from the Paintearth seam, with the outcrop samples averaging 21.0 per cent ash, whereas the mine samples show a mean content of 12.0 per cent. On the other hand, Battle-River outcrop and mine data are virtually identical (12.9 to 12.6 per cent). There are three possible reasons for the higher ash contents of the outcrop samples from the Paintearth zone:

1. The mine samples have come from areas where the Paintearth coal is of better quality;
2. Deposition of mineral matter in fractures by groundwater in near-surface (outcrop) coals; and

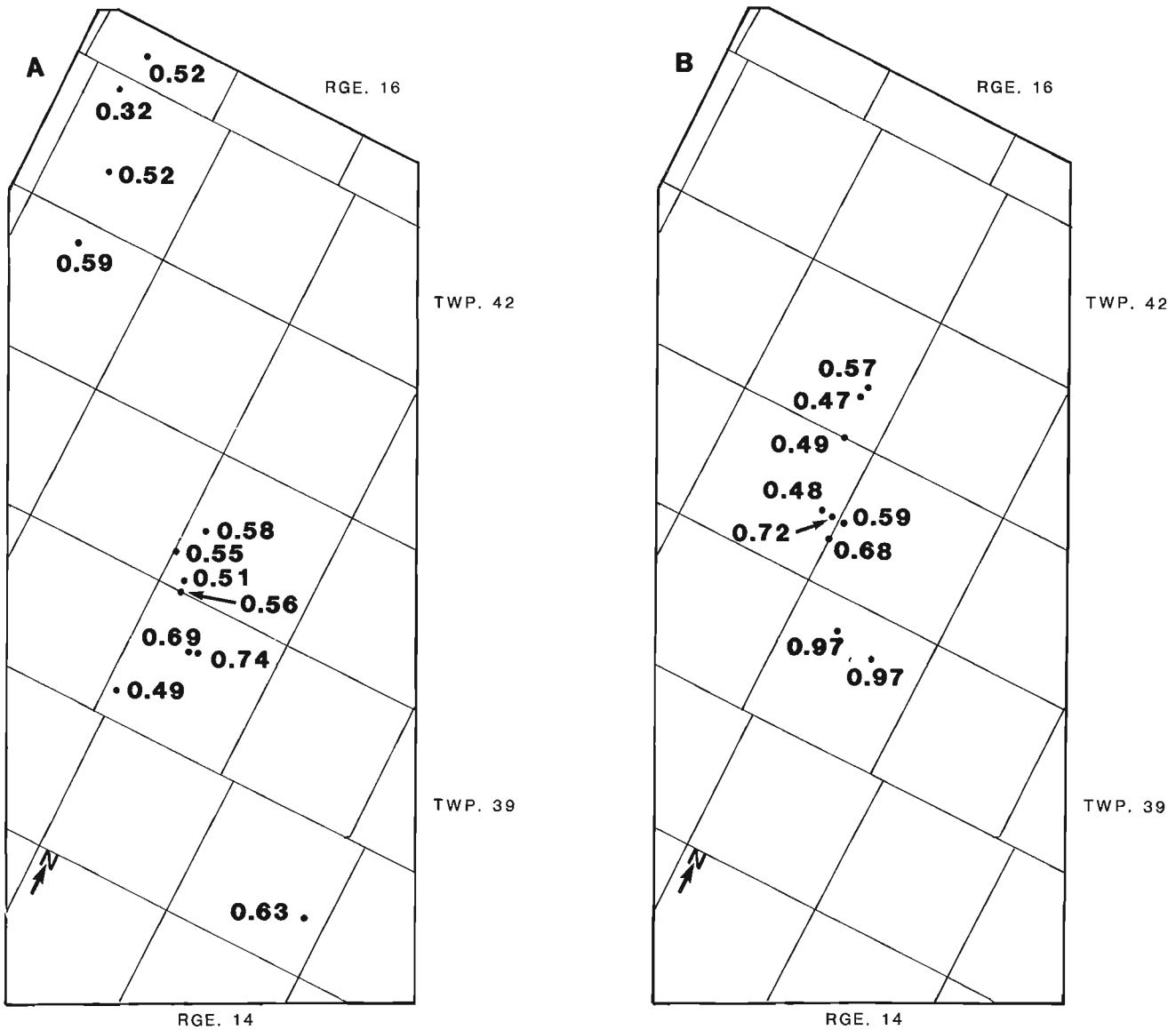

Figure 9. *Distribution of sulphur contents (dry basis) for Paintearth (Fig. 9A) and Battle-River (Fig. 9B) sampling stations.*

3. In weathered sections it is more difficult to distinguish clean coal layers from high ash layers and a number of the latter may have been included in the analyses.

Outcrop samples affected by weathering are indicated in Figure 10 by the shaded areas on the diagrams.

In Figure 11 volatile matter contents and calorific values are also plotted in the form of frequency diagrams. In this figure, the influence of weathering is clearly shown. The outcrop samples for both the Paintearth and Battle-River coal zones show elevated volatile matter contents and reduced calorific values relative to samples from currently active mines. Calorific values (mmf) for the unweathered samples in both zones range from 20.1 to 24.0 MJ/kg indicating coal ranks (ASTM) of subbituminous C and B with some coal layers approaching the subbituminous B/A boundary.

B. Petrography

Maceral distribution data for the Paintearth and Battle-River coal zones are plotted on Figure 12. Nearly all samples are uniformly high in huminite, with most of the Paintearth samples and all of the Battle-River samples containing over 80% huminite on the mineral-free basis. This agrees with results of a study of Horseshoe Canyon Formation coals by Parkash et al. (1985). Liptinite is relatively low in most samples, roughly averaging about 4%. Inertinite contents in the majority of samples are below 10%. On the basis of gross maceral composition, it is not possible to distinguish between the Paintearth and Battle-River coals. Figure 12 shows that the Battle-River samples form a somewhat more compact population than the Paintearth samples, but it is not clear whether or not this is a function of fewer Battle-River samples from a smaller area than the Paintearth, or the fact that a larger proportion of the Paintearth samples are from outcrop and weathered to varying degrees. Depending on the degree of severity, weathering can hinder proper identification of macerals.

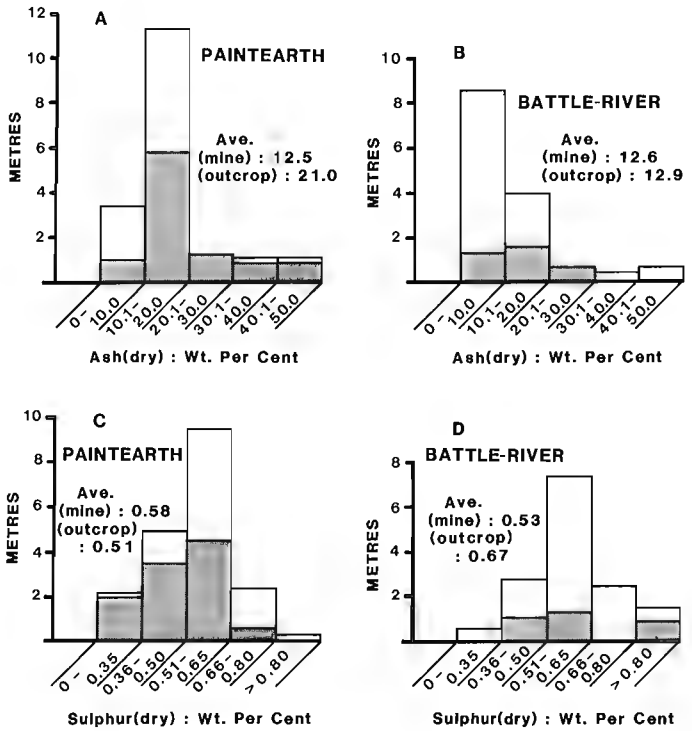

Figure 10. Cumulative thickness plots summarizing ash and sulphur contents in Paintearth and Battle-River coals. Hatched pattern indicates outcrop samples.

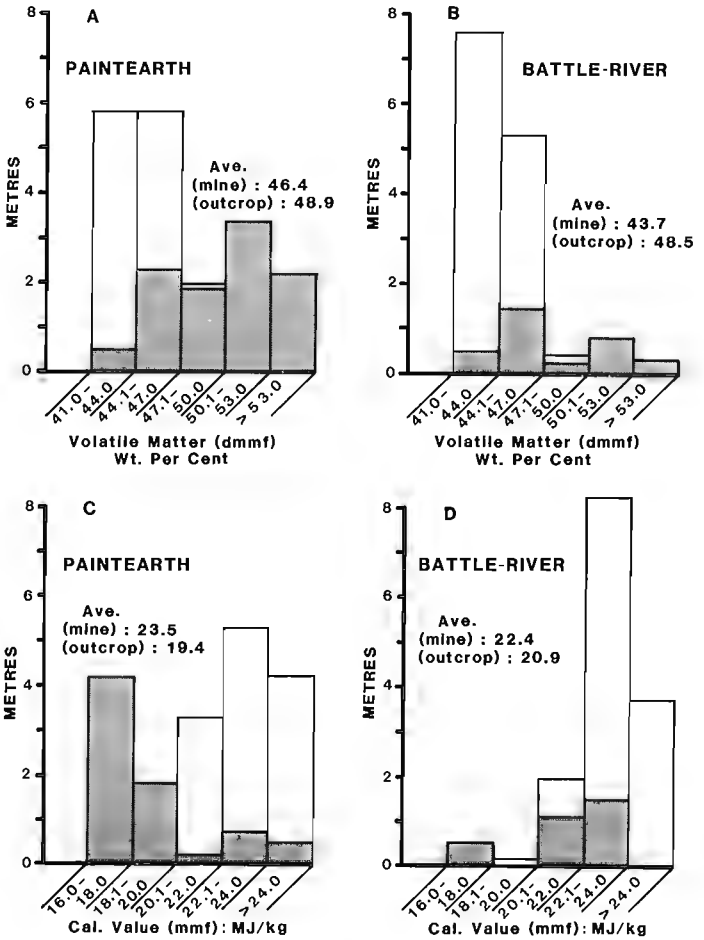

Figure 11. Cumulative thickness plots summarizing volatile matter and heating value data for Paintearth and Battle-River coals. Hatched pattern indicates outcrop samples.

Diessel (1986) proposed a model relating variations in petrographic composition of coal to differences in the swamp types in which the parent peats were deposited. His model is graphically expressed by cross-plotting two indices which he called the Gelification Index (GI) and Tissue Preservation Index (TPI). These indices are calculated from maceral distribution data and relate, as their names imply, to the degree to which plant tissue structure is preserved or is destroyed through processes of gelification. Good tissue preservation on the one hand, or gelification as an alternative, are determined by variations in the biological, chemical and physical conditions in the peat swamp and, as Diessel suggested, may be related to different sedimentological settings. Diessel's model was based upon compositional characteristics of Australian bituminous coals. In this report the model is applied to the subbituminous coals of the Battle River study.

The GI and TPI are calculated from the maceral data (mmf) of the Battle River coals as follows:

$$GI = \frac{\text{Total Huminite and Macrinite}}{\text{Semifusinite and Fusinite and Inertodetrinite}}$$

$$TPI = \frac{\text{Eu-ulminite and Semifusinite and Fusinite}}{\text{Densinite and Macrinite and Inertodetrinite}}$$

These indices were calculated for the main part of each coal zone at each station and the resulting data are displayed on Figure 13. Each point on the diagram represents a sampling station.

Several observations may be made regarding the position of these points. First it should be noted that the GI is uniformly high, indicating generally wet conditions of deposition for both the Paintearth and Battle-River coal zones. Diessel has suggested that such coals form in a lower delta plain environment. In general, that agrees with the sedimentological analyses of the study area. A second point to note is that the Battle-River zone appears to have a somewhat higher TPI than the Paintearth zone. According to Diessel (1986), this indicates for the Battle-River, a swamp environment with greater density of trees than the Paintearth coals which appear to have been deposited in a more open marsh environment, possibly with a more herbaceous plant community.

The effect of weathering on the ability to discriminate among macerals during analysis may also be influential in the positioning of points on Figure 13. The outcrop samples in both Paintearth and Battle-River populations show lower TPI values than samples collected from active mines. This means, in part, that lower amounts of structured huminite (eu-ulminite) were detected in the weathered samples, most likely a function of the masking by weathering of fine tissue texture in coal particles. Two sets of Paintearth samples (CQ618 and CQ619) stand out because their GI values (below 4.00) are much lower than the other samples. These two

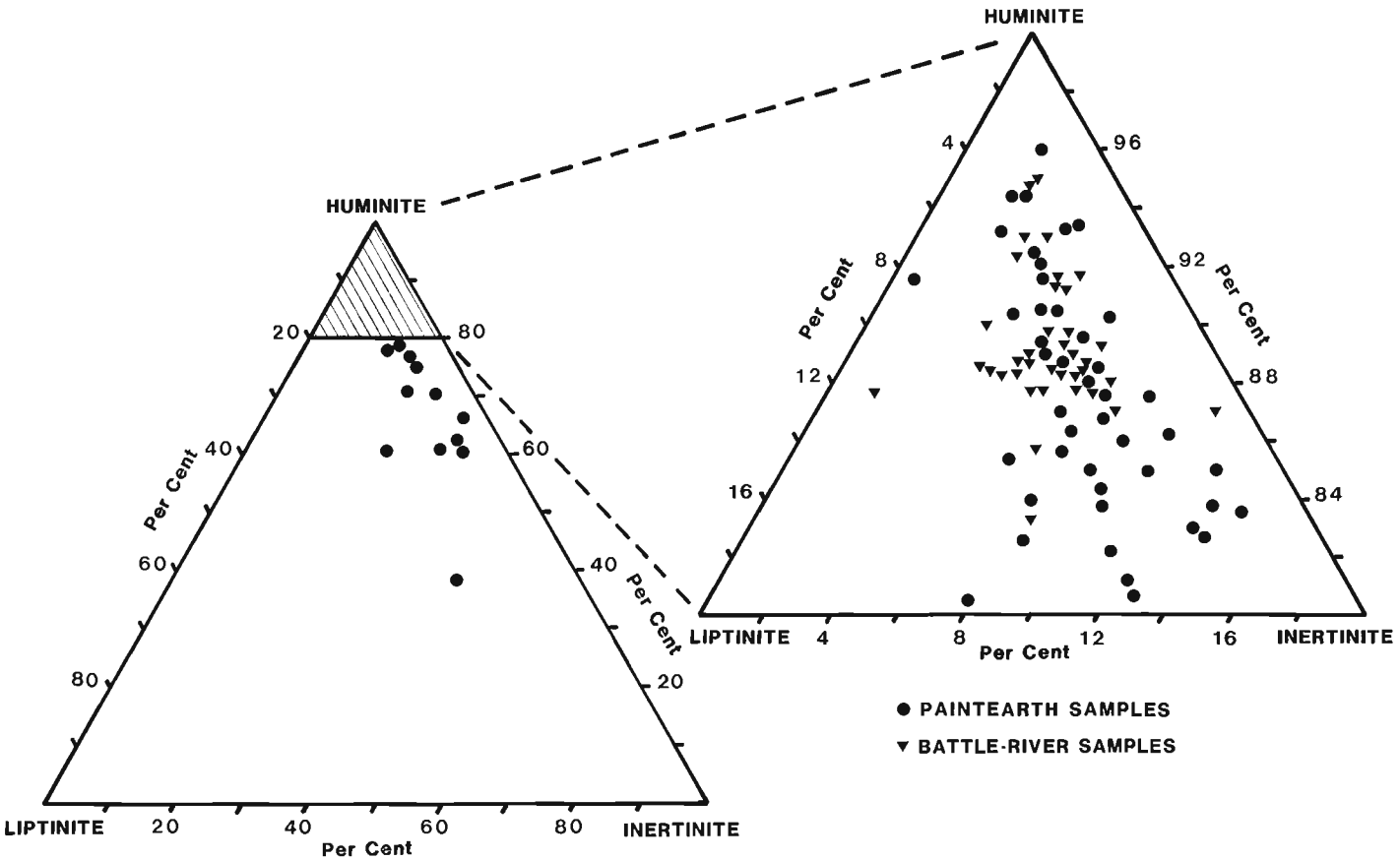

Figure 12. Ternary diagram showing maceral distribution (mineral-free basis) for Paintearth and Battle-River coals.

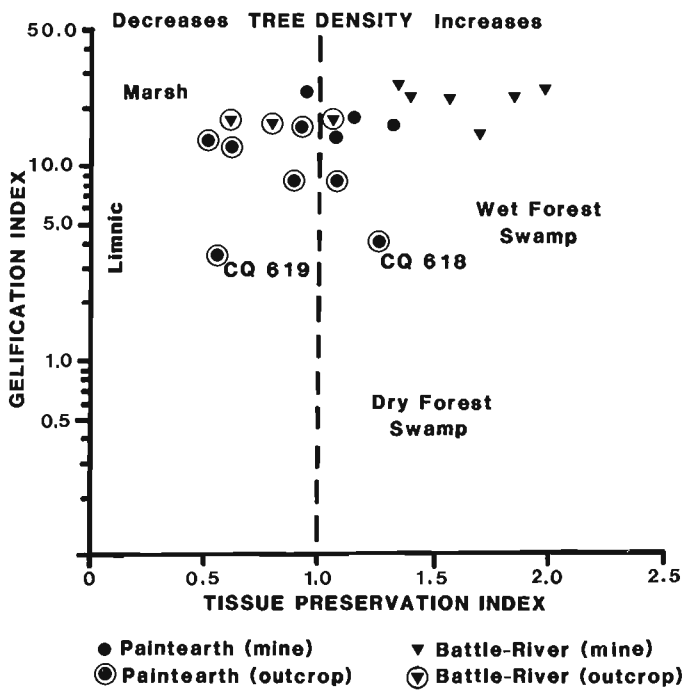

Figure 13. Relationship of summarized maceral compositional data (Paintearth and Battle River) to possible environments of accumulation. Basic diagram modified from Diessel (1986).

sample suites are high in inertinite. They are located geographically close to each other (Fig. 7) and their positions on Figure 13 indicate formation in somewhat drier conditions than most of the other Paintearth and Battle-River samples. In this case, the inertinite contents are believed to be accurate despite the fact that CQ618 and CQ619 are outcrop sections. Inertinite is more easily identified in weathered coals than are the finer discriminations within the huminite group.

Reflectance data on these coals are recorded in Table 2. For the Paintearth samples, these range from 0.42 to 0.62 R_o random. In the unweathered samples, the range is from 0.49 to 0.52 R_o random. Reflectances in the Battle-River samples are roughly similar ranging from 0.47 to 0.53 R_o random. These reflectance data, except for CQ626, are indicative of coal ranks close to the boundary of subbituminous A and B (Teichmüller and Teichmüller, 1982).

ACKNOWLEDGMENTS

The authors are appreciative of the technical review of this paper by G.G. Smith and J.M. MacGillivray. Word processing was provided by Donna Smith.

TABLE 1

Location of sample stations - Paintearth and Battle-River coal zones

Station Number	Northing[1]	Easting	Zone Thickness[2] Net coal thickness (M)	No. of Coal Samples
Paintearth Zone				
CQ605	5807160	421990	2.05 (1.76)	5
CQ606	5807500	421900	0.96 (0.78)	4
CQ608	5809500	421210	2.36 (1.95)	8
CQ612	5811000	421700	2.71 (2.50)	7
CQ616	5799300	422640	2.02 (1.77)	4
CQ618	5804250	424820	2.36 (1.07)	5
CQ619	5804250	424950	1.86 (0.51)	2
CQ622	5790700	439900	1.46 (0.69)	3
CQ625	5824470	405700	1.48 (1.45)	4
CQ626	5829810	405280	2.66 (1.88)	9
CQ629	5834140	404650	2.54 (2.53)	7
CQ630 CQ631	5936010	404040	11.40 (1.49)	4
Battle River Zone				
CQ607	5809700	421120	2.39 (2.20)	6
CQ609	5811040	420170	2.27 (2.11)	5
CQ610	5811020	420590	2.00 (1.68)	4
CQ611	5811020	420960	2.29 (2.29)	4
CQ613	5819500	418600	1.39 (1.36)	3
CQ614	5819350	418650	1.59 (1.58)	6
CQ615	5816000	419870	2.83 (2.37)	6
CQ617	5803900	427520	0.50 (0.50)	1
CQ621	5804300	424580	0.70 (0.46)	2

[1] All in zone 11
[2] Numbers in parenthesis represent net coal

TABLE 2

Summary of reflectance data for the Paintearth and Battle-River coal zones

Sample Location	Coal Zone	R_o Random	Standard Deviation
CQ605	Paintearth	0.52	0.04
CQ606	Paintearth	0.49	0.03
CQ608	Paintearth	0.51	0.03
CQ612	Paintearth	0.51	0.04
CQ616	Paintearth	0.49 *	0.04
CQ618	Paintearth	0.42 *	0.04
CQ619	Paintearth	0.46 *	0.04
CQ622	Paintearth	0.48 *	0.03
CQ625	Paintearth	0.52 *	0.03
CQ626	Paintearth	0.62 *	0.05
CQ629	Paintearth	0.50 *	0.03
CQ607	Battle River	0.50	0.04
CQ609	Battle River	0.52	0.03
CQ611	Battle River	0.52	0.04
CQ613	Battle River	0.52	0.04
CQ614	Battle River	0.53	0.04
CQ615	Battle River	0.52 *	0.04
CQ617	Battle River	0.50 *	0.04
CQ621	Battle River	0.47 *	0.03

* Outcrop

REFERENCES

Allan J.A.
1922: Geology of the Drumheller Coalfield, Alberta. Research Council of Alberta, Report 4.

Allan, J.A. and Sanderson, J.O.G.
1945: Geology of the Red Deer and Rosebud sheets, Alberta. Research Council of Alberta, Report No. 13.

Allen, J.R.L.
1965: Late Quaternary Niger delta and adjacent areas: sedimentary environments and lithofacies. American Association of Petroleum Geologists, Bulletin, v. 49, p. 547-600.

Arndorfer, D.J.
1973: Discharge patterns in two crevasses in the Mississippi River delta. Marine Geology, v. 15, p. 269-287.

ASTM (American Society for Testing and Materials)
1979: Annual book of ASTM standards, part 26. Gaseous Fuels; Coal and Coke; Atmospheric Analysis. American Society for Testing and Materials, Philadelphia, Pa.

Campbell J.D.
1975: Coal Resources, Tofield-Donalda area, Alberta. Research Council of Alberta, Report 75-8.

Coleman, J.M.
1969: Bramaputra River: channel processes and sedimentation. Sedimentary Geology, v. 3, p. 129-239.

Diessel, C.F.K.
1986: On the correlation between coal facies and depositional environments. Proceedings of the 20th Newcastle Symposium, University of Newcastle, Australia, p. 19-22.

ERCB (Energy Resources Conservation Board)
1988: Reserves of Coal Province of Alberta. ERCB ST88-31.

Fisher, W.L.
1969: Facies characterization of Gulf Coast Basin delta systems with some Holocene analogues. Transcripts of Gulf Coast Association, Geological Society, v. 19, p. 239-261.

Gibson, D.W.
1977: Upper Cretaceous and Tertiary coal-bearing strata in the Drumheller-Ardley region, Red Deer River Valley, Alberta. Geological Survey of Canada, Paper 76-35, 41 p.

Hughes, J.D.
1984: Geology and depositional setting of the Late Cretaceous, Upper Bearpaw and Lower Horseshoe Canyon formations in the Dodds-Round Hill Coalfield of central Alberta - A computer-based study of closely-spaced exploration data. Geological Survey of Canada, Bulletin 361, 81 p.

ICCP (International Committee for Coal Petrology)
1971: International Handbook of Coal Petrography, First Supplement to Second Edition. Centre National de la Recherche Scientifique, Paris, France, n.p.

Irish, E.J.W.
1970: The Edmonton Group of south-central Alberta. Bulletin of Canadian Petroleum Geology, v. 18, no. 2, p.125-155.

McCabe P.E.
1987: Facies studies of coal and coal-bearing strata. In Coal and Coal-bearing Strata: Recent Advances, A.C. Scott (ed.); Geological Society Special Publication, No. 32, p. 51-66.

Parkash, S., Lali, K., and Cameron, A.R.
1985: Petrography of subbituminous coals from Alberta (Canada) Plains. Journal of Coal Quality, v. 4, no. 1, p. 84-91.

Rahmani, R.A.
1981: Facies relationships and paleoenvironments of a Late Cretaceous tide-dominated delta, Drumheller, Alberta. In Field guides to geology and mineral deposits; GAC-MAC annual meeting, Calgary, May 1981, p. 159-176.

Shepheard, W.W. and Hills, L.V.
1970: Depositional environments Bearpaw-Horseshoe Canyon (upper Cretaceous) transition zone, Drumheller "Badlands", Alberta. Bulletin of Canadian Petroleum Geology, v. 18, no. 2, p. 166-215.

Sternberg, C.M.
1947: The upper part of the Edmonton Formation of the Red Deer Valley, Alberta. Geological Survey of Canada, Paper 47-1.

Teichmüller, M. and Teichmüller, R.
1982: The geological basis of coal formation. In Coal Petrology, 3rd edition, E. Stach, M.Th. MacKowsky, M. Teichmüller, G.H. Taylor, D. Chandra, and R. Teichmüller, (eds.); Gebrüder Borntraeger, Stuttgart, Berlin, p. 5-85.

Thomas, R.G., Smith, D.G., Wood, J.M., Visser, J., Calverley-Range, E.A., and Koster, E.H.
1979: Inclined heterolithic stratification - terminology, description, interpretation and significance. Sedimentary Geology, v. 53, p. 123-179.

Tyrrell, J.B.
1887: Report on a part of northern Alberta and portions of adjacent districts of Assiniboia and Saskatchewan. Geological Survey of Canada, Annual Report 1886, v. II, Pt. E, 176 p.

Williams, G.D. and Burk, C.F. Jr.
1964: Upper Cretaceous. In Geological History of Western Canada, R.G. McCrossan and R.P. Glaister (eds.); Alberta Society of Petroleum Geologists Special Publication, p. 169-190.

Wright, L.D. and Coleman, J.M.
1973: Variations in morphology of major river deltas as function of ocean wave and river discharge regimes. American Association of Petroleum Geologists, Bulletin, v. 57, p. 370-398.

Coal resource potential in the Arctic Islands: 1. Paleocene coastal plain coals from Strathcona Fiord

B.D. Ricketts
Institute of Sedimentary and Petroleum Geology, Calgary

Ricketts, B.D., Coal resource potential in the Arctic Islands: 1. Paleocene coastal plain coals from Strathcona Fiord. In Contributions to Canadian Coal Geoscience, Geological Survey of Canada, Paper 89-8, p. 62-67, 1989.

Abstract

Speculative lignite and subbituminous coal resources totalling more than one billion tonnes are estimated at two localities along Strathcona Fiord, western Ellesmere Island, providing an important addition to Canada's long-term resource base. The coals, with cumulative thickness up to 18 m and individual seam thicknesses up to 12 m, are part of an upper Paleocene - lower Eocene coastal plain succession in the Eureka Sound Group. Locally the coals contain up to 5% resin. These and other coal-bearing successions in the Eureka Sound Group, are potential souces of hydrocarbons in equivalent strata beneath the Polar continental shelf.

Résumé

Des ressources spéculatives en lignites et en charbons subbitumineux, se chiffrant à plus d'un milliard de tonnes, pouvraient se trouver à deux emplacements le long du fjord Strathcona, dans l'ouest de l'île d'Ellesmere. Elles augmenteraient de manière importante les approvisionnements à long terme du Canada. Les charbons, dont les épaisseurs cumulatives atteignent jusqu'à 18 m et celles des couches individuelles jusqu'à 12 m, font partie d'une succession de plaine côtière datant du Paléocène supérieur et de l'Éocène inférieur, dans le groupe d'Eureka Sound. Les charbons contiennent jusqu'à 5 % de résine par endroits. Ces charbons ainsi que les successions de couches charbonnières du groupe d'Eureka Sound constituent des sources potentielles d'hydrocarbures dans les couches équivalentes situées sous la plate-forme continentale Polaire.

RATIONALE

There can be little doubt that development of Arctic coal resources is economically non-viable, at least in the near future. However, the role of the Geological Survey of Canada coal geoscience program is not just to provide data of immediate relevance to government and industry, although there is no question that this is a critical function of the program. Indeed, an additional and important task of the coal program is to develop coal databases that are relevant to long-term policy and descision making, and perhaps this task is best rationalised in the following terms:

- All non-renewable resources have a finite abundance. Eventually, existing resource bases will have to be extended into those regions which at present have little economic viability.
- The components of industry that utilise coal require assurance of supply for periods of time that commonly extend to decades.
- Technological advances in coal extraction and use could make this resource increasingly attractive.
- Future development of the Canadian Arctic would benefit from the availability of indigenous sources of fossil fuels.

An overview of potential coal resources in the Arctic Archipelago, Canada's most remote resource bearing region, has been presented in an earlier report (Ricketts and Embry, 1984). Several areas of potentially important coal resources have been identified in the Axel Heiberg - Ellesmere Island region during stratigraphic, sedimentological and structural analysis of the Late Cretaceous - Paleogene Eureka Sound Group. In the first of a series of papers, thick coal seams are described from the Strathcona Fiord area on western Ellesmere Island (Fig. 1).

STRATIGRAPHIC FRAMEWORK

The middle-late Campanian to Eocene Eureka Sound Group contains coal in all of its formations (Fig. 1), although many of these occurrences would be deemed sub-economic. Analysis of the Late Cretaceous-Early Tertiary Eureka Sound Group on Ellesmere and Axel Heiberg islands has permitted the delineation of several third-order depositional sequences.

Initial filling of Fosheim Foredeep, a northwest-facing remnant of the Sverdrup Basin, began in the middle Campanian to lower Maastrichtian with wave-dominated deltas on western Axel Heiberg Island, and a thin wedge of coastal plain deposits on the eastern basin margin on Fosheim Peninsula (in the lower member, Expedition Formation).

Erosion during the late Maastrichtian produced a basin-wide unconformity, and removed some or all of the lower Expedition member. This event corresponds to changes in sea floor spreading in the Canada Basin and northern Labrador Sea.

Relative sea-level rise in the early Paleocene gave rise to a second episode of delta, coastal plain and estuarine accumulations (upper member, Expedition Formation). The accumulations expanded to the east and south, overstepping bedrock of the Franklinian Mobile Belt.

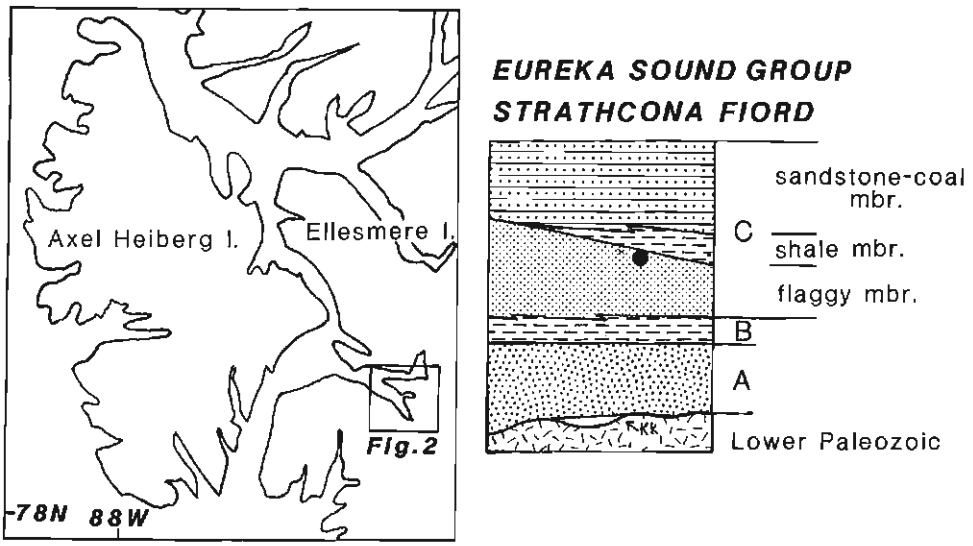

Figure 1. *General location map and stratigraphic framework of the Eureka Sound Group at Strathcona Fiord. Member designation for the Iceberg Bay Formation (C) is informal. The approximate stratigraphic position of the thick coal seams is indicated by a solid circle. Formation names are those indicated in Figure 2. Kk = Kanguk Formation.*

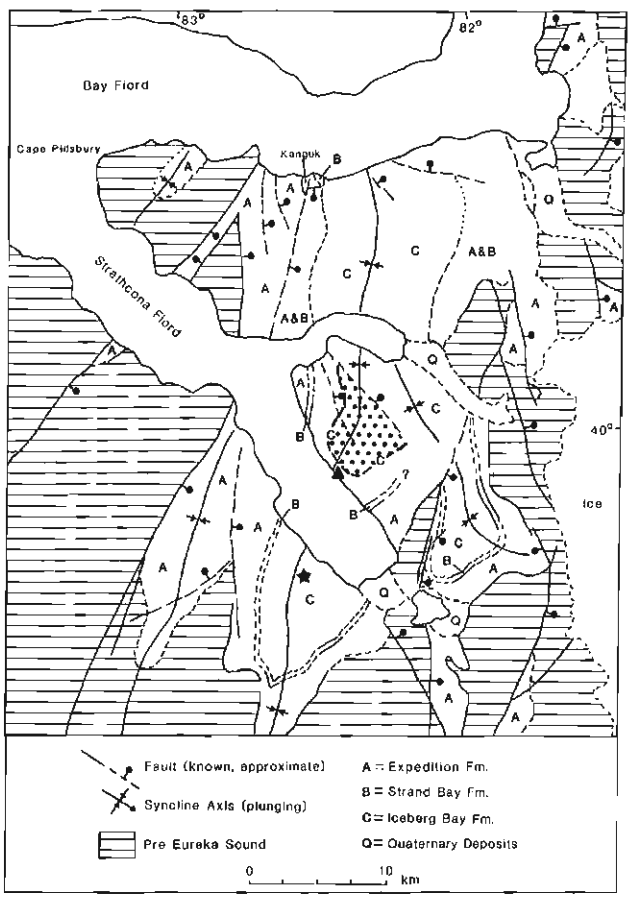

Figure 2. *Geology map of the Eureka Sound Group in the Bay Fiord - Strathcona Fiord area, from Ricketts (1986). Formation designation is indicated on Figure 1. The south shore location (RAK 4-84) is indicated by a star; the area covered on the north shore location by stipple. Section RAK 5-85 indicated by a triangle.*

Regional transgression in the mid to upper Paleocene (Strand Bay Formation) and the subsequent regressive package (Iceberg Bay Formation, upper Paleocene to lower Eocene) produced river-dominated deltas in the west and shallow shelf deposits in the east. During the period of maximum flooding, a temporary but shallow seaway may have connected the Arctic and newly formed Labrador-Baffin Bay seas. The upper Iceberg Bay Formation (lower to middle Eocene), is the final phase of extensive river-dominated, delta plain-coastal plain accumulations. Basin subsidence and sedimentation rates were probably greatest during Strand Bay and Iceberg Bay times, heralding the climactic phase of Eurekan tectonism.

During middle Eocene time, formation of major arches (Princess Margaret and Cornwall arches) and folding and faulting, fragmented Fosheim Foredeep into several narrow, synorogenic intermontane basins, filled by coarse alluvial sediment (Buchanan Lake Formation), (Ricketts, 1987).

Coal-forming environments within the Eureka Sound Group ranged from wave- and fluvial-dominated deltas (e.g. western Axel Heiberg Island; Ricketts, in press), coastal plains, lagoons, estuaries, and alluvial braidplains and meanderplains.

Only the upper member of the Expedition Formation occurs in the Strathcona Fiord region, where Paleocene strata overstep Lower Paleozoic, Franklinian bedrock. The Expedition is overlain successively by the Strand Bay and Iceberg Bay formations. Particularly thick coal seams occur within the Iceberg Bay Formation on both the north and south shores of Strathcona Fiord (Fig. 2), at the top of a succession of coarsening-upward, calcareous, flaggy mudstone, siltstone and sandstone parasequences, up to 12 m thick. These coals are abruptly overlain by a thick unit of shale (Figs. 1, 3). The lower part of the flaggy siltstone succession is of open marine - shelf origin, as indicated by a diverse assemblage of calcareous foraminifera (Wall et al., 1988). Thin, shaly coal and carbonaceous shale beds become increasingly common towards the top of the flaggy unit, where they usually cap the coarsening upward parasequences. This lithological transition

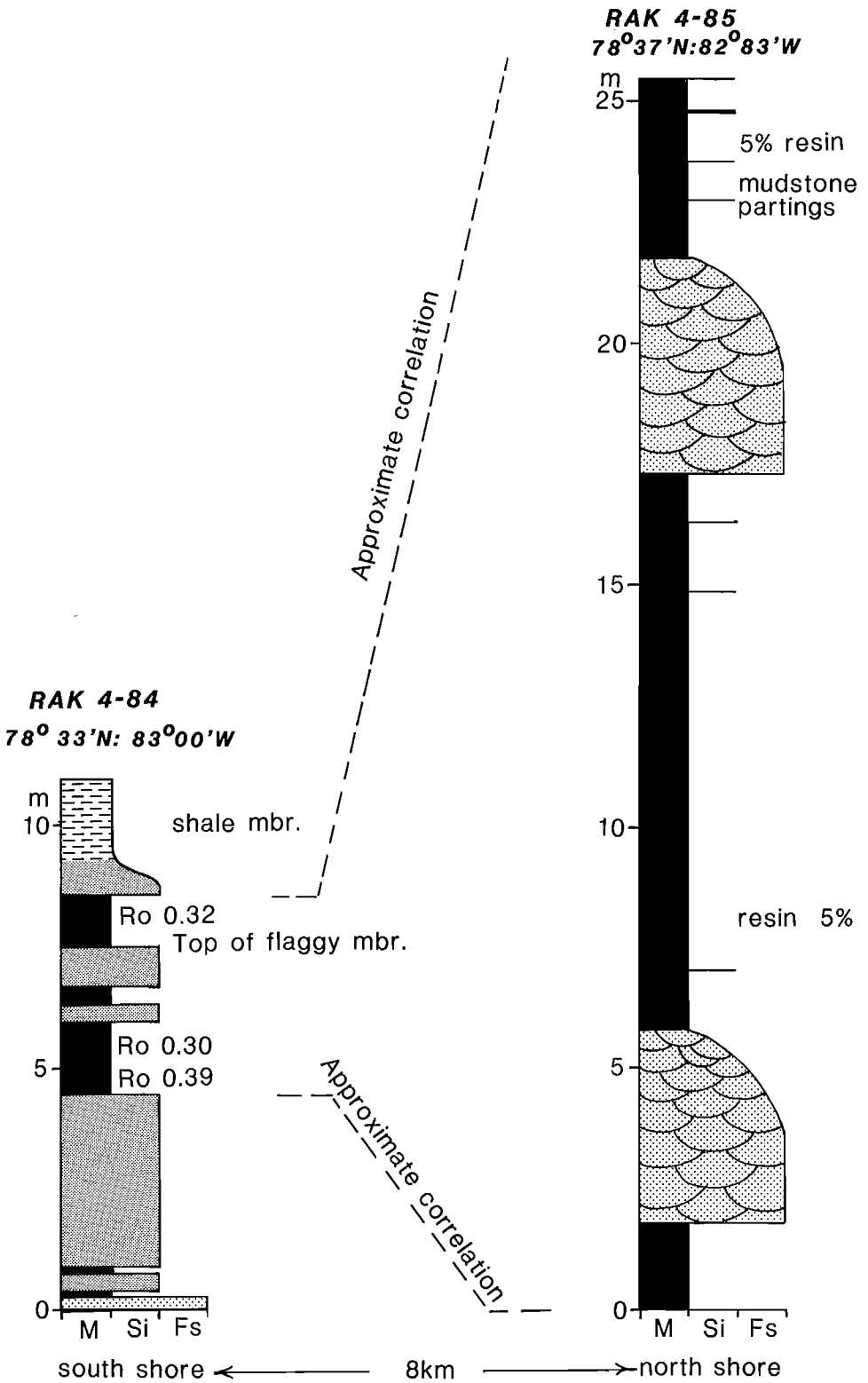

Figure 3. *Schematic representation of measured sections on the north and south shores of Strathcona Fiord and their approximate correlation. Solid black areas are coal. M = shale; Si = siltstone; Fs = fine sandstone, according to the Wentworth grain size scale.*

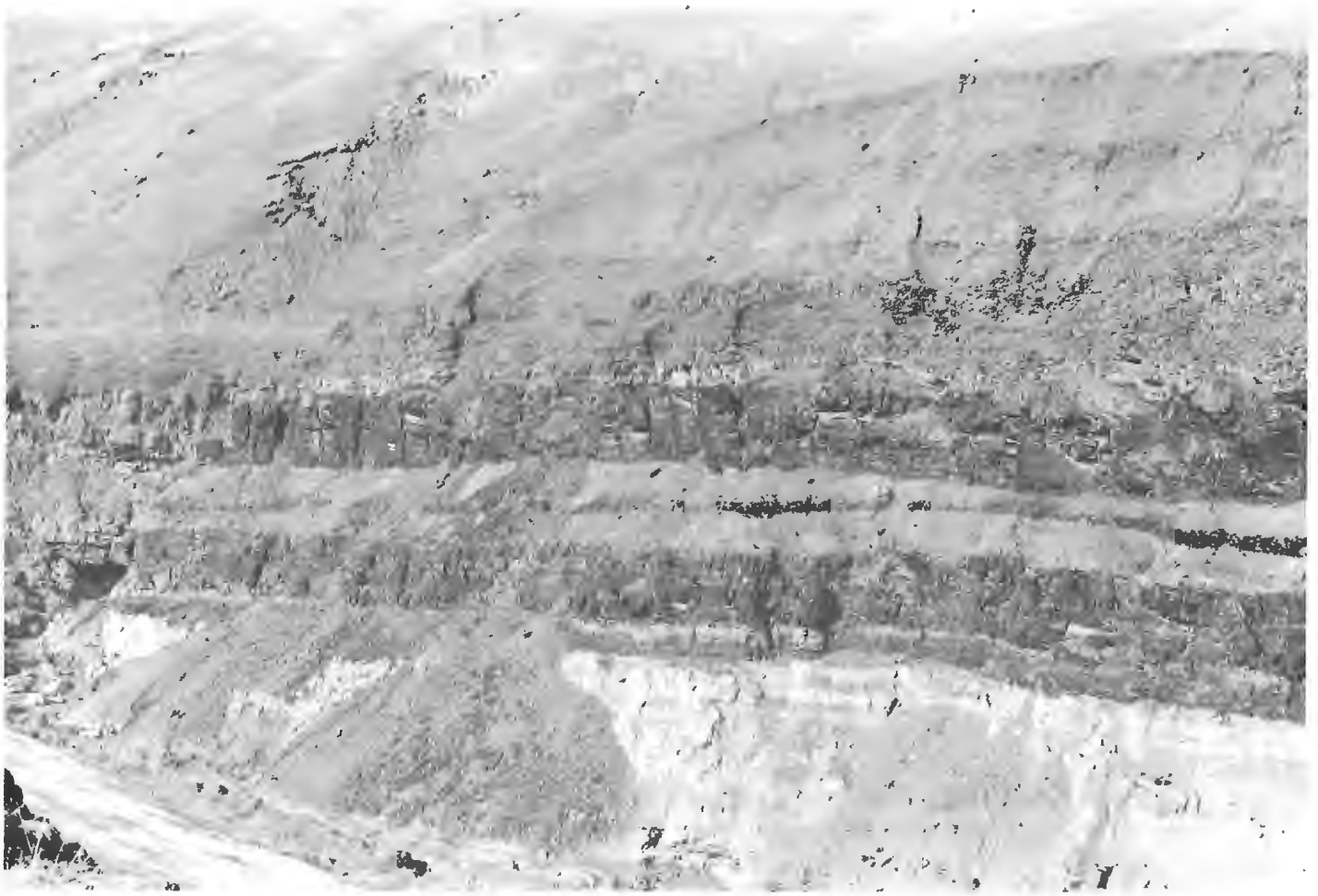

Figure 4. View of the two main coal seams at the south shore location. Note the abrupt contact with the overlying shale member, and the resistant, permineralized tree stumps and roots at the top of the upper seam. Upper seam is 1.2 metres thick, and the lower seam 1.5 metres thick.

coincides with an overall regressive trend and a change from shallow shelf conditions to coastal plain, with broad, intervening sand-mud tidal flats. The thick coal seams thus represent maximum development of the prograding coastal plain facies (a more detailed analysis of the depositional and paleogeographic setting is under way).

Grey shales that abruptly overlie the coals have a minimum thickness of 105 metres (top not exposed). Although contact with the overlying coal-sandstone succession of the upper Iceberg Bay Formation is poorly exposed, general stratigraphic relationships suggest that the shale unit is of prodelta origin. Contact between the thick coal seams and shales (e.g. Figs. 3, 4) represents a surface of maximum flooding, or transgression. There is no obvious subaerial unconformity below this surface and it seems likely that the subaerial and ravinement surfaces coincide.

COAL SEAM DISTRIBUTION AND CHARACTERISTICS

Thick seams that occur on both the north and south shores of Strathcona Fiord are considered to be stratigraphically equivalent given their positions immediately below a thick unit of shale.

South Shore Coals

Exposure of these coal seams is confined to small gullies on the west side of an unnamed valley (Figs. 2, 4). Two main seams up to 1.5 m thick, and several stringers of carbonaceous shale are separated by thinly bedded, laminated and rippled siltstone. A few mud flasers and lenticular bedforms suggest possibly weak tidal influences. Some bioturbation is also present.

In one 8 m section the cumulative thickness of coal is 3 m (Fig. 3). The two thickest seams consist mostly of blocky fracturing, woody coal, and in the lowest seam teardrop shaped resin is abundant. Random vitrinite reflectances on three samples range from 0.30 to 0.39%, corresponding to lignite and subbituminous C ranks (A.R. Cameron, pers. comm.).

Conspicuous bright orange-weathering, permineralized tree stumps and roots, in growth position, occur in the upper half of the upper coal seam (Fig. 4). The remnants of similarly preserved forests of Eocene age have also been reported from a valley a few kilometres west of this location, from which conditions of high rainfall and temperate climate were inferred (Francis, in press).

Figure 5a. *Panorama of the north shore of Strathcona Fiord, showing the thick, laterally continuous coal seams.*

Figure 5b. *View of the upper zone coals, north Strathcona Fiord. (RAK 4-85).*

North Shore Coals

Coal seams up to 12 m thick are well exposed along the steep north shore of Strathcona Fiord, and can be traced laterally for at least 8 km (Figs. 2, 5a, b). Two main zones of coal-bearing strata are present, referred to here as the 'upper' and 'lower' zones.

The lower zone is poorly exposed and control on seam thickness is correspondingly poor. It consists of multiple seams separated by mudstone and white quartz sandstone interbeds. In terms of cumulative thickness the lower zone is potentially as valuable as the upper zone.

Although structurally simple on a regional scale (Fig. 2), the seams are cut by numerous normal faults with displacements usually less than a metre. Larger faults, with downthrown blocks to the north, are oriented approximately normal to the major syncline axis.

The upper coal zone comprises three main seams with a cumulative thickness of 18 m (Fig. 3). Distinctive, white quartz sandstone beds with abundant trough crossbedding and fining-upward character, separate the main seams. These channel deposits are probably of fluvial or estuarine origin. Coals in the upper zone are mostly blocky weathering and locally woody with scattered, permineralized wood fragments. Resin is usually concentrated in layers a few centimetres thick and constitutes upwards of 5% of those layers. Mudstone partings a few millimetres thick comprise about 5% to 10% of the total thickness; some of the mudstones grade upward into highly carbonaceous shale.

ESTIMATE OF SPECULATIVE RESOURCES

The following resource estimate is classified as 'future interest' and 'speculative' as defined by Bielenstein et al. (1979) and Smith (1989). Only the upper coal zone along the north shore of Strathcona Fiord is considered here because it is best constrained by thickness and lateral extent. The areal extent used for the calculation is shown on Figure 2 (40 km^2). An in situ bulk density of 1.3 g/cm^3 represents between 15% and 20% ash for lignite and low rank subbituminous coal (G.G. Smith, pers. comm.). Maximum depth of the seam has been projected to 350 m, assuming a constant northward dip of five degrees.

For the upper coal zone the total tonnage is estimated at 936 million tonnes. Although figures are not available for the lower coal zone, it is likely that combined, the two zones would contain well in excess of a billion tonnes.

The coal seams are located near the deep waterway of Strathcona Fiord, which during the summer months, is partly or completely ice-free. Notwithstanding the problems inherent in mining this region (for example environmental impact, engineering problems associated with permafrost, and brief summer access to the Arctic sea lanes), the seams described here and at other localities on western Ellesmere Island, represent an important long term resource for Canada.

REFERENCES

Bielenstein, H.U., Chrismas, L.P., Latour, B.A., and Tibbetts, T.E.
1979: Coal resources and reserves of Canada. Energy Mines and Resources Canada, Report ER 79-9.

Francis, J.E.
in press: A Tertiary fossil forest on Ellesmere Island, Canadian high Arctic. Arctic.

Ricketts, B.D.
1986: New formations in the Eureka Sound Group, Canadian Arctic Islands. Geological Survey of Canada, Paper 86-1B, p. 363-374.

198?: Princess Margaret Arch: re-evaluation of an element of the Eurekan Orogen, Axel Heiberg Island, Arctic Archipelago. Canadian Journal of Earth Sciences, v. 24, p. 2499-2505.

in press: Delta evolution in the Eureka Sound Group, western Axel Heiberg Island: the transition from wave-dominated to fluvial-dominated deltas. Geological Survey of Canada, Bulletin.

Ricketts, B.D. and Embry, A.F.
1984: Summary of geology and resource potential of coal deposits in the Canadian Arctic. Bulletin of Canadian Petroleum Geology, v. 32, p. 359-371.

Smith, G.G.
1989: Coal resources of Canada. Geological Survey of Canada, Paper 89-4, 146 p.

Wall, J.H., McNeil, D.H., Ricketts, B.D., and McIntyre, D.J.
1988: Paleocene foraminifera from the Eureka Sound Group, eastern Sverdrup Basin, Canadian Arctic Archipelago. Geological Society of America, Program and Abstracts.

Coalification patterns in Jurassic-Lower Cretaceous strata (Minnes, Bullhead and Fort St. John groups), Rocky Mountain Foothills and foreland, east-central British Columbia and adjacent Alberta

W. Kalkreuth and M. McMechan
Institute of Sedimentary and Petroleum Geology, Calgary

Kalkreuth, W. and McMechan, M., Coalification patterns in Jurassic-Lower Cretaceous strata (Minnes, Bullhead and Fort St. John groups), Rocky Mountain Foothills and foreland, east-central British Columbia and adjacent Alberta. In Contributions to Canadian Coal Geoscience, Geological Survey of Canada, Paper 89-8, p. 68-79, 1989.

Abstract

The regional coalification pattern of Jurassic-Lower Cretaceous strata has been determined by vitrinite reflectance measurement. Vitrinite reflectances range from 0.73 - 2.67% Rmax (high volatile A bituminous-semianthracite). Regionally there is, for any of the coal-bearing sequences, a trend from low reflectances in the Inner Foothills to increased values in Outer Foothills and Alberta Syncline. To the east and north of the Alberta Syncline reflectances decrease rapidly. Time-depth (burial) curves suggest that the regional coalification pattern results largely from variations in the depth and/or duration of burial beneath Maastrichtian-Tertiary foredeep deposits.

ASTM rank maps for the Bluesky-Gething Formation indicate high volatile A bituminous to low volatile bituminous rank for localities in the Inner Foothills, where seams of mineable thickness occur at or near surface. This rank places many of the Gething coals in a rank range suitable for the production of metallurgical coal.

Résumé

Il a été possible de déterminer la structure de la carbonification régionale des couches du Jurassique et du Crétacé inférieur à l'aide de mesures du taux de réflectance de la vitrinite. Les taux de réflectance de la vitrinite varient de 0,73 à 2,67 % Rmax (charbon de type bitumineux A à haute teneur en matières volatiles et houille anthraciteuse). Sur le plan régional, il existe, pour chacune des séquences carbonifères, une tendance allant de taux de réflectance faibles dans les contreforts intérieurs à des taux plus élevés dans les contreforts extérieurs et dans le synclinal d'Alberta. Vers l'est et le nord du synclinal d'Alberta, les taux de réflectance diminuent rapidement. Les courbes de la chronologie de l'enfouissement semblent indiquer que la structure de la carbonification régionale est surtout le produit de variations dans la profondeur ou dans la durée de l'enfouissement au-dessous des sédiments de l'avant-fosse du Maastrichtien et Tertiaire, ou les deux.

Les cartes de rang (selon l'ASTM), pour la formation de Bluesky-Gething, indiquent la présence de charbons bitumineux A dont la teneur en matières volatiles varie de haute à faible pour certains emplacements dans les contreforts intérieurs des Rocheuses, où des couches exploitables se trouvent à, ou près, de la surface. Ces observations établissent que plusieurs des couches de charbon de Gething sont d'un rang qui conviendrait à la production de charbon métallurgique.

INTRODUCTION

The Canadian Rocky Mountain Front Ranges and Foothills contain a number of Jurassic-Cretaceous coal-bearing strata for which measured and indicated coal resources are in the order of 4955 megatonnes and 5260 megatonnes, respectively (Smith, 1989).

The purpose of this paper is to outline local and regional rank variations for Jurassic-Lower Cretaceous coals from the Peace River Coalfield, British Columbia, and adjacent parts of Alberta. The study area is situated in the Foothills of Alberta and British Columbia and adjacent foreland (Alberta Syncline and Alberta Plateau), between 53 and 57 degrees North latitude (Fig. 1). The Foothills are divisible into two belts: the Inner Foothills, a topographically high belt characterized by folded and faulted Lower Cretaceous and older strata; and the Outer Foothills, a topographically subdued belt with folded Upper Cretaceous strata predominant. The rocks of the outer belt merge with the essentially undeformed rocks of the Alberta Syncline and the Alberta Plateau to the east.

Coalification data for this paper are based on vitrinite reflectance (Rmax) measurements and come from the Lower Cretaceous Fort St. John Group (Boulder Creek and Gates formations), the Lower Cretaceous Bullhead Group (Bluesky-Gething and Cadomin formations), the Jurassic-Lower Cretaceous Minnes Group, and their stratigraphic subsurface equivalents (Fig. 2). Detailed studies on the stratigraphy and sedimentology of the Jurassic-Cretaceous systems of the study area have been published by Stott (1983, 1984), McLean (1982), and Gibson (in press).

Strata in the study area are complexly folded and cut by numerous thrust faults. Deformation is thought to have proceeded from southwest to northeast (Price, 1981) and is estimated to have reached the Foothills during the Paleocene (Kalkreuth and McMechan, 1984).

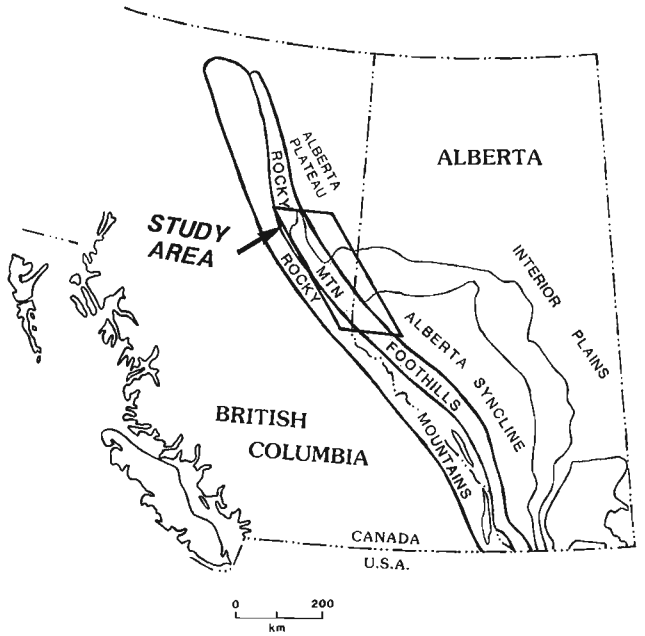

Figure 1. *Location of study area in relation to major subdivisions of the Rocky Mountains and near-surface coal-bearing belts (stippled pattern) in Alberta and British Columbia.*

Previous coal rank studies in and near the study area suggest that coalification occurred mainly before Late Cretaceous-Tertiary Laramide deformation (Hacquebard and Donaldson, 1974). Coal rank studies in the Rocky Mountain Foothills, Front Ranges, and Alberta Syncline, north and west of Grande Cache, Alberta (Kalkreuth and McMechan, 1984, 1988) showed that the level of maturation of organic matter in Carboniferous to Cretaceous strata decreased markedly to the west across the Foothills, from a maximum near the eastern limit of deformation. Modelling using time-depth (burial) curves suggested that this westward decrease in rank is due to a westward decrease in the duration and depth of burial beneath Upper Cretaceous-Tertiary foredeep deposits, largely as a consequence of diachronous west to east deformation. Coal rank also decreases significantly to the north because of a northward thinning of the Maastrichtian-Tertiary section. Locally the overall coalification pattern was found to be influenced by variations in geothermal gradients across the study area and by reactivation of old basement structures associated with the Peace River arch. Local thrusting does not appear to have affected significantly coalification levels established by former depth of burial (Kalkreuth et al., in press).

The present paper focuses on:

1. The regional coalification pattern of the Lower Cretaceous Boulder Creek, Gates, Bluesky-Gething and Cadomin formations and the Jurassic-Lower Cretaceous Minnes Group.

2. The relationship of coal rank to depth of burial and timing of deformation for the Lower Cretaceous Bluesky-Gething Formation.

3. Discussion of ASTM rank ranges for top and base of Bluesky-Gething Formation.

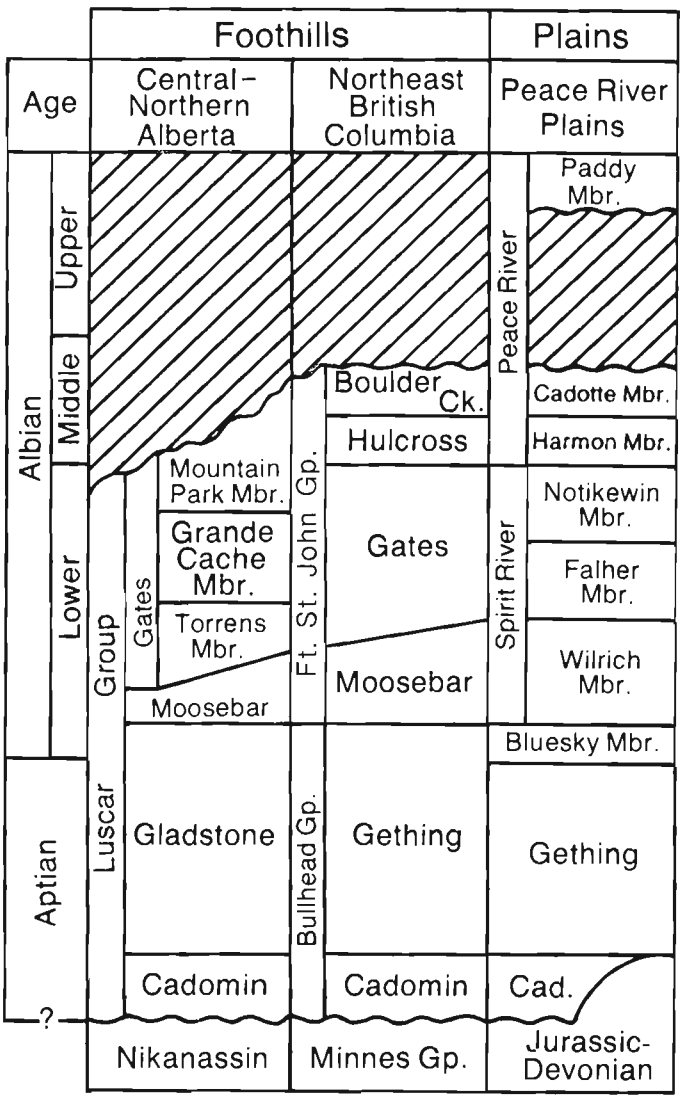

Figure 2. *Stratigraphic nomenclature used in this study (modified from McLean and Wall, 1981 and Langenberg and McMechan, 1985). Stratigraphic units are formations, unless specified otherwise; from Kalkreuth et al. (in press).*

SAMPLES AND METHODS

Collection

Coals from outcrop and mine sites were collected as channel or grab samples. Coals from the subsurface were obtained from shallow coal exploration coreholes or as cuttings hand picked from petroleum exploration wells. Details on sample locations, stratigraphic positions, depth intervals, etc. will be published in Kalkreuth and McMechan (in prep.).

Sample preparation and analytical methods

The coals were crushed to a maximum particle size of 850 µm (20 mesh), mounted in epoxy resin, then ground and polished according to standard procedures (Bustin et al., 1985). Rank was determined by measuring maximum vitrinite reflectances using a Leitz MPV II microscope under standardized conditions and following the procedures outlined in Bustin et al. (1985). American Society for Testing and Materials (ASTM) rank classes and groups based on

reflectance values were obtained by using the maximum reflectance limits for ASTM ranks as published by Davis (1978).

RESULTS AND DISCUSSION

Regional rank variations, Fort St. John Group (Lower Cretaceous)

Boulder Creek Formation/Paddy and Cadotte members, Peace River Formation

One hundred and ten coals were analysed from the Boulder Creek Formation and Paddy and Cadotte members. The locations for the samples and the regional variations in the vitrinite reflectances are shown in Figure 3A. In the Inner Foothills the reflectances range from 0.73 to 1.15% Rmax, indicating ASTM rank groups from high volatile A to medium volatile bituminous. In the Outer Foothills south of Peace River and east of Mt. Bickford (Fig. 3A), the reflectances are in the order of 0.94 to 1.26% Rmax (high volatile A - medium volatile bituminous). Much higher rank levels are indicated by reflectances farther to the south. The values of 1.71 and 1.67% Rmax, respectively, indicate low volatile bituminous coals (Fig. 3A). Coal rank data east of the Foothills are sparse. The values range from 1.71% Rmax (low volatile bituminous) near the eastern limit of deformation in the southern part of the area, to 0.91% Rmax (high volatile A bituminous) near Dawson Creek. A further decrease in rank eastward is indicated by a reflectance value of 0.55% Rmax for a coal collected from the type section of the Paddy and Cadotte members near the town of Peace River (Fig. 3A). The reflectance value indicates high volatile C bituminous rank.

Gates Formation/Falher and Notikewan members, Spirit River Formation

One hundred ninety-three coals were analysed from the Gates Formation or its subsurface correlatives the Falher and Notikewan members of the Spirit River Formation. The sample material includes the economically important coal seams from the presently operating open pit mines (Smoky River Coal near Grande Cache, Alberta in the southern part of the study area, and the Bullmoose and Quintette mines in northeastern British Columbia near Tumbler Ridge in the central part of the study area). Sample locations and regional variations in the vitrinite reflectances for the Gates coals are illustrated in Figure 3B. In the Inner Foothills the reflectances range from 0.79 to 1.98% Rmax, indicating a coalification range from high volatile A bituminous to low volatile bituminous. In the southeastern part of the Inner Foothills not all available data points have been shown due to space limits. For this area the reader is referred to Kalkreuth and Langenberg (1986), in which detailed coal rank data have been reported for the Gates coals from the Grande Cache area. In the Outer Foothills the reflectance values range from 0.94 to 1.97% Rmax. According to the reflectance levels most of the Outer Foothills coals from the Falher and Notikewan members are medium to low volatile bituminous. The highest reflectances for coals from the Gates-Spirit River interval were recorded near the western limit of the Alberta Syncline (2.15% Rmax), indicating semi-anthracite at this location. East of and parallel to the deformed Foothills belt, a gradual northwest trend to lower reflectances is apparent. The values decrease from 1.85 to 2.15% Rmax (low volatile bituminous - semianthracite) in the Alberta Syncline to 0.84 to 0.90% Rmax (high volatile A bituminous west of Dawson Creek; (Fig. 3B). Relatively low vitrinite reflectance values of 0.96 to 1.01% Rmax (high volatile A bituminous) were recorded for coals collected near the eastern limit of the study area (Fig. 3B).

Regional rank variations, Bullhead Group (Lower Cretaceous)

Bluesky-Gething Formation

In this study, coal rank variations in the Lower Cretaceous Bluesky-Gething Formation are based on analyses of 664 coal samples. The regional variations in vitrinite reflectances for the Bluesky-Gething coals are shown in Figure 4A. The vitrinite reflectance values range from 0.76% Rmax (high volatile A bituminous) to 2.55% Rmax (semianthracite).

In the Inner Foothills the reflectances range from 0.85 to 1.87% Rmax (high volatile A - low volatile bituminous). In the south and central parts of the study area the low rank Bluesky-Gething coals tend to occur close to the western limit of exposure, whereas the higher rank Bluesky-Gething coals occur to the east, close to the transition into the Outer Foothills. Relatively low reflectances occur across the Inner Foothills immediately south of Williston Lake and to the north of it (Fig. 4A).

A similar coalification pattern occurs for the Bluesky-Gething coals collected from the Outer Foothills (Fig. 4A). The reflectances here range from 0.96 to 2.55% Rmax indicative for ASTM rank groups ranging from high volatile A bituminous to semianthracite. Coals of high volatile A to medium volatile bituminous rank occur north of Peace River, whereas most of the coals south of Peace River are low volatile bituminous or semianthracites.

East of the Foothills (Fig. 4A) the highest reflectance levels were recorded for Bluesky-Gething coals from the central part of the Alberta Syncline (2.34-2.52% Rmax, semianthracite). From there the reflectances decrease markedly to the east (1.05-1.07% Rmax, high volatile A bituminous). Along the centre of the Alberta Syncline there is also a trend to lower reflectances to the northwest. Reflectance values decrease gradually from 2.52% Rmax to values of less than 1% Rmax north of Peace River in the Alberta Plateau (Fig. 4A) In terms of ASTM rank, this marks a change from semianthracites in the south to high volatile A bituminous coals in the north.

At two locations, Bluesky-Gething coals were collected from hanging and footwalls of thrust faults. In the southern example (Fig. 4A, locality A) there are virtually no significant differences in reflectances in coals collected from hanging and footwall. In the northern example (Fig. 4A, locality B) there is a significant increase in reflectances for coals from the footwall (1.65-1.79% Rmax) as compared to values of 1.25 to 1.35% Rmax for coals collected from the hanging wall. These preliminary observations form part of a current study on the relationships between thrusting and coalification and will not be discussed here.

Cadomin Formation

Occasionally thin coal seams and/or coalspars are associated with the conglomerates of the Cadomin Formation. A total of 23 samples of these were analysed for vitrinite reflectance. The locations of the samples and the regional variations in vitrinite reflectances are shown in Figure 4B. In the Inner Foothills, the reflectances range from 0.98 to 1.91% Rmax, indicating a coalification range from high volatile A bituminous to low volatile bituminous. Two samples were analysed from the Outer Foothills. North of Peace River the reflectance level of 1.24% Rmax indicates a medium volatile bituminous coal. South of Peace River the reflectance value of 2.25% Rmax corresponds to the semianthracite range. The one sample analysed east of the Foothills shows an intermediate rank level of 1.21% Rmax (medium volatile bituminous).

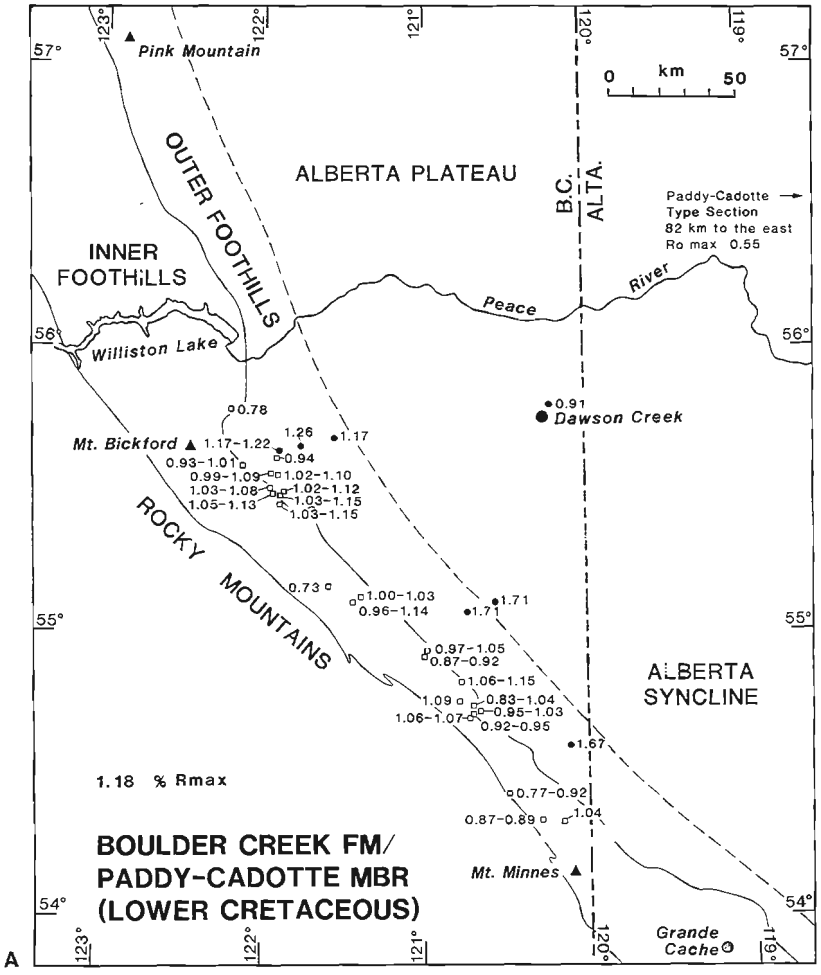

Figure 3.

A. Reflectance data for Lower Cretaceous Boulder Creek Formation and subsurface equivalent (Paddy and Cadotte members, Peace River Formation); from Kalkreuth and McMechan (1988).

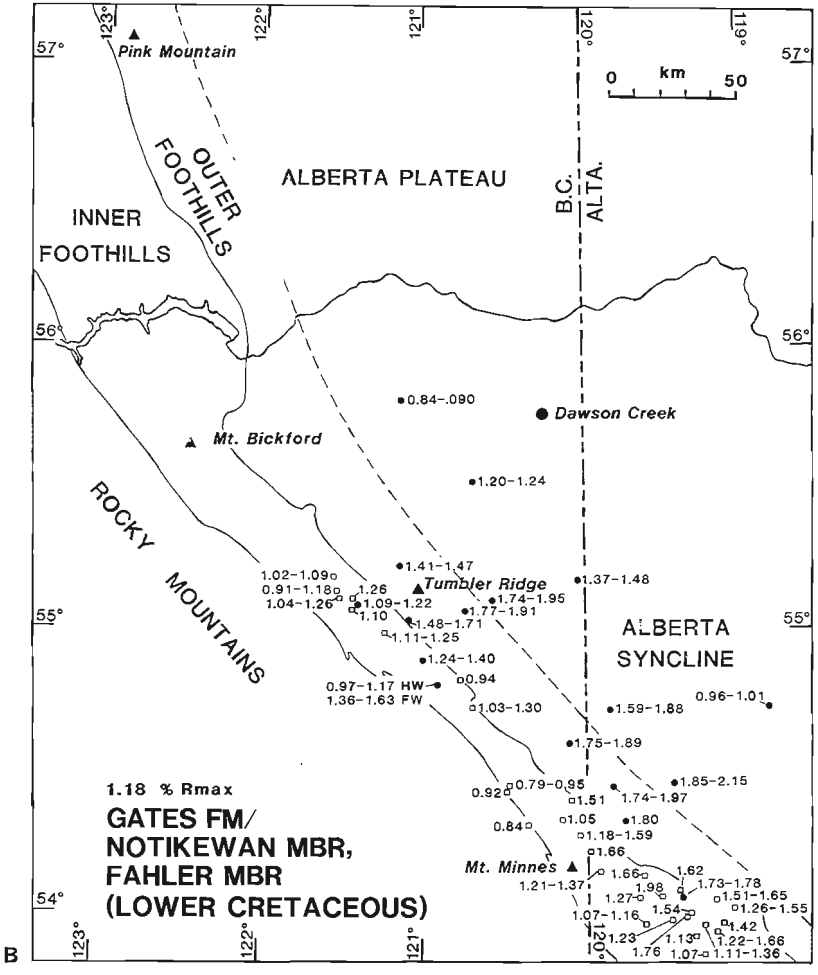

B. Reflectance data for Lower Cretaceous Gates Formation and subsurface equivalents (Falher and Notikewan members, Spirit River Formation). HW - hanging wall, FW -footwall; from Kalkreuth and McMechan (1988).

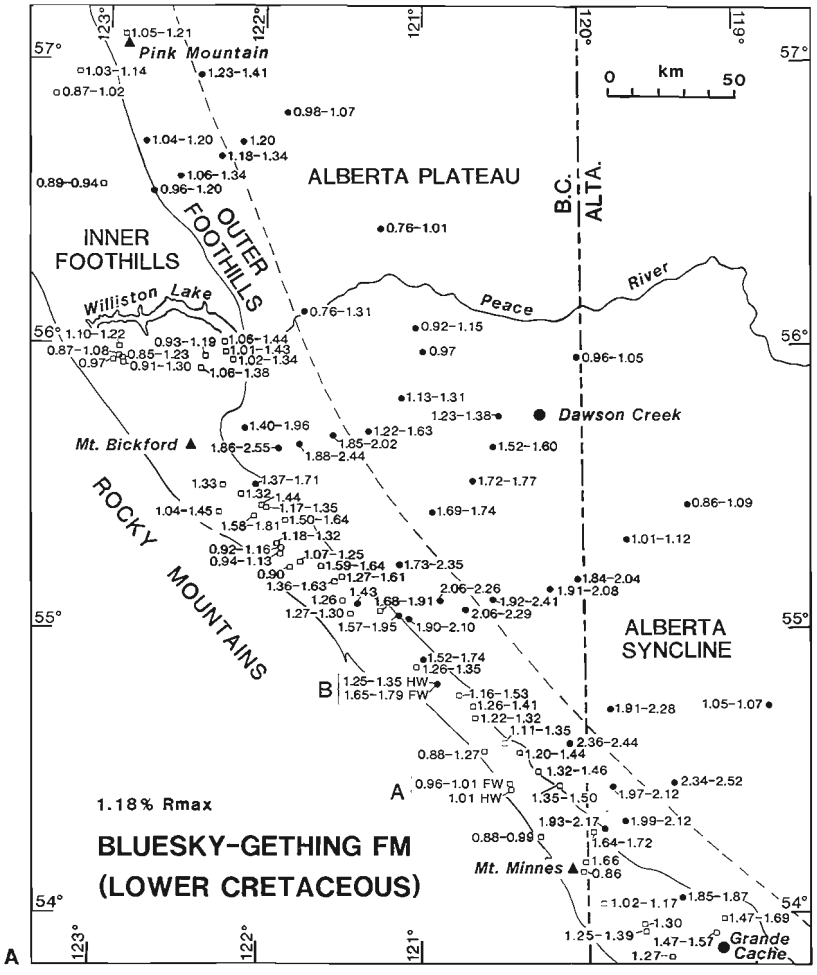

Figure 4.

A. *Reflectance data for Lower Cretaceous Bluesky-Gething Formation. A and B, location where rank was determined in both the hanging walls and footwalls of thrust faults; from Kalkreuth and McMechan (1988).*

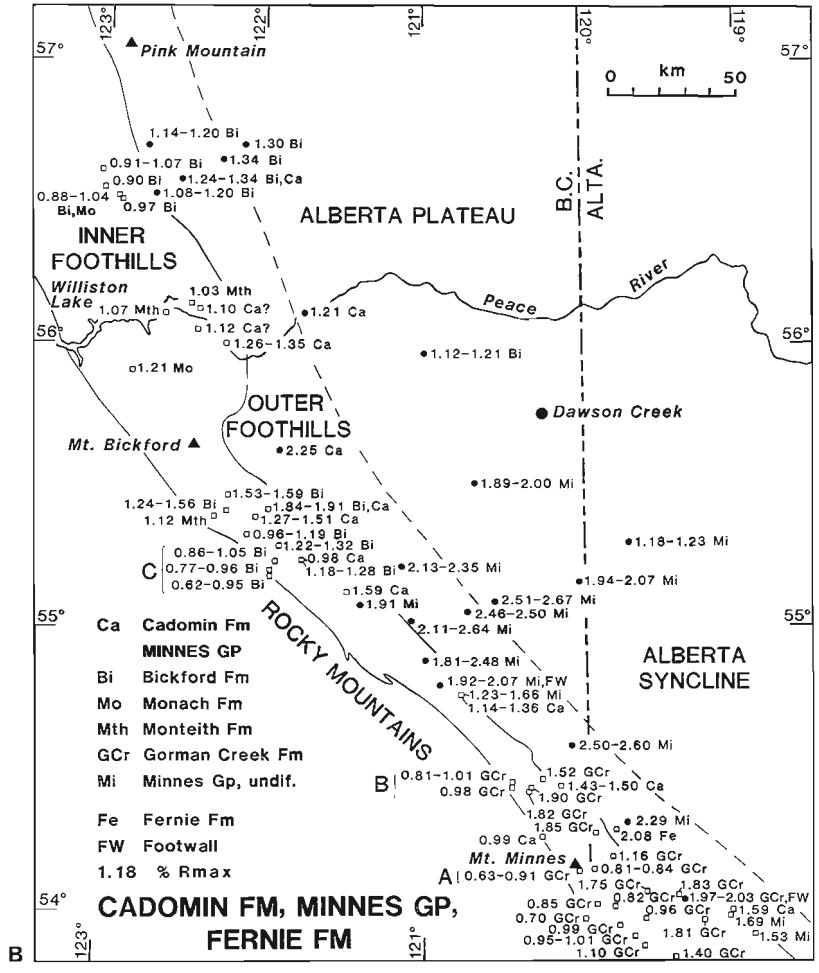

B. *Reflectance data for Lower Cretaceous Cadomin Formation, Jurassic-Lower Cretaceous Minnes Group and Jurassic Fernie Formation. A, B and C denote locations where vitrinite reflectances were found to be depressed (Kalkreuth, 1982a); from Kalkreuth and McMechan (1988).*

Regional rank variations, Minnes Group (Jurassic-Lower Cretaceous)

Bickford, Gorman Creek, Monach and Monteith formations

Two hundred thirty-six coals were analysed from the Minnes Group, the majority of which were obtained from the coal-bearing Gorman Creek and Bickford formations (Stott, 1981). In the central and northern part of the study area, a few samples were also collected from the Monach and Monteith formations, which in general are non-coal-bearing sequences.

The regional distribution of sample locations and the vitrinite reflectance ranges for the various formations of the Minnes Group are given in Figure 4B. At three locations, marked A, B, C in Figure 4B, coals from the upper Minnes Group were found to be characterized by anomalously low reflectances. For locations A and C it has been demonstrated that these coals contain large amounts of liptinite macerals, which tend to decrease the reflectance of the associated vitrinite (Kalkreuth, 1982a). The same holds true for the Minnes coals collected from location B, which also contain large amounts of liptinite macerals. Because of the peculiar coalification pattern of these coals, the samples from locations A, B and C were excluded from consideration of regional rank changes in the study area.

In the Inner Foothills the reflectance levels range from 0.88 to 2.07% Rmax indicating a range from high volatile A bituminous to semianthracite. The lowest reflectances occur north of and in the vicinity of Williston Lake and in the south, near the western margin of the Inner Foothills west of Grande Cache (Fig. 4B). Reflectance values < 1.10% Rmax indicate that many of the coals in these areas are of high volatile A bituminous rank. The reflectance values increase generally to the east with some of the coals attaining semianthracite rank (reflectance values >2.05% Rmax).

In the Outer Foothills south of Peace River the rank of the Minnes coals is greater than in the Inner Foothills. The vitrinite reflectance levels range from 2.11 to 2.60% Rmax (Fig. 4B), indicating semianthracite rank. North of Peace River the rank levels are considerably lower. The reflectances range from 1.14 to 1.34% Rmax, indicating medium volatile bituminous coals.

Data for Minnes coals from the Alberta Syncline and the Alberta Plateau are sparse. The highest reflectance was determined on a coal from the western limb of the Alberta Syncline (2.67% Rmax, semianthracite). Lowest reflectances were determined on Minnes coals northwest of Dawson Creek (1.12-1.21% Rmax, medium volatile bituminous, Fig. 4B).

Fernie Formation

One hand-picked coaly fragment from the Jurassic Fernie Formation was analysed for vitrinite reflectance. The sample was collected from a glauconite sandstone sequence (Green Beds) near the base of the Fernie Formation in the Alberta part of the Outer Foothills (Fig. 4B). The vitrinite reflectance value of 2.08% Rmax indicates semianthracite.

Burial (temperature) history, Bluesky-Gething Formation

Time-depth (burial) curves

Since the work of Karweil (1956) it has been recognized that the rank of a coal is related to temperature and to the time the coal has been exposed to that temperature in its geological history. Because reaction rates in the coalification process approximately double for each 10°C increase in temperature (Lopatin, 1971), temperature is the main factor affecting coalification. Consequently, a coal that has been exposed to high temperatures for relatively short time will have higher rank than a coal that has been at low temperatures for a long time. Pressure does not appear to have a significant effect on coalification after the initial compression, loss of volume and loss of moisture that occur in the early stages of coalification (Teichmüller, 1962; Bostick, 1973; Hood and Castaño, 1974; Lyons et al., 1985).

Several methods have been proposed that relate temperature, time and organic maturation/coalification (Karweil, 1956; Lopatin, 1971; Bostick, 1973, 1979; Hood et al., 1975; Waples, 1980). The present study used the extended Lopatin method published by Waples (1980). For details the reader is referred to Kalkreuth and McMechan (1984, 1988).

In the study area, one episode of deep burial and subsequent uplift corresponding to the deposition and (partial) erosion of Laramide foredeep deposits in the Late Cretaceous to early Tertiary, dominates the time-depth (burial) history for the Bluesky-Gething Formation. Maximum rates of rank increase and, therefore, the greatest proportion of the total rank occurred around the time of deepest burial.

Burial history curves were constructed for the base of the Lower Cretaceous Bluesky-Gething Formation using the available geological information. Thicknesses of preserved stratigraphic units were determined directly from well logs east of the Foothills. Within the Foothills and Front Ranges these thicknesses were generally obtained from nearby measured sections by Stott (1968, 1973, unpub.), Gibson (in press, unpub.) and Leckie (unpub.). The estimated ages and time spans of the various stratigraphic units found in the study area were generally obtained from the sources listed above. In areas where pre-Maastrichtian units are eroded, the original thicknesses of these units were estimated by extrapolating thickness trends from areas where these strata are preserved. The youngest strata found in the study area are Maastrichtian in age. The total original thickness of Maastrichtian and Tertiary sediments was initially estimated following the geological constraints described in Kalkreuth and McMechan (1984).

For the calculation of Time-Temperature-Indices (TTI-values, Waples, 1980), up to 30 stratigraphic control points have been incorporated into a horizon's history. Each control point was represented by a new layer in the computer program. TTI and Rmax values were calculated for all layers. The measured reflectance values used in calibration of the time-depth (burial) curves were taken from coalification profiles. These profiles were based on first order regression lines where the sampled interval was thin (usually < 1000 m), and second order regression curves where thicker intervals were sampled. Time-depth (burial) curves were constructed for 45 localities that include 37 petroleum exploration wells. Localities modelled generally were chosen to form five transverse and one longitudinal section. Calibrated time-depth (burial) curves for the base of the Bluesky-Gething Formation at 15 locations are shown in Figure 5 and will be contrasted with the isoreflectance maps of the top and base of the Bluesky-Gething Formation (Figs. 6A and B).

Surface temperatures and geothermal gradients

In the present study the initial TTI calculations were made using an initial surface temperature of 20°C and a paleogeothermal gradient equal to the present-day geothermal gradient (Kalkreuth and McMechan, 1984). The present gradient was estimated, where possible, from bottom hole temperatures corrected using a Horner temperature plot (Dowdle and Cobb, 1975) as determined from petroleum exploration well logs, or else from the American Association of Petroleum Geologists/United States Geological Survey Geothermal Gradient Map (1976). In general the present-day geothermal gradient is lower in the west in the topographically high Mountains and Foothills, and increases gradually eastward. Gradients tend to be higher east of the Foothills in the northern part of the area as compared to the south. If using the present-day geothermal gradients as the initial estimate for the paleogeothermal gradient resulted in coalification gradients markedly different from the measured coalification gradients, the estimated paleogeothermal gradient and the estimated thickness of unpreserved Maastrichtian to Eocene sediments were modified to obtain a more reasonable fit. Change in the estimated thickness of unpreserved sediments was limited by the necessity to maintain a burial history geologically consistent with adjacent wells.

Calibrated time-depth (burial) curves (Fig. 5) suggest that the Late Cretaceous-early Tertiary paleogeothermal gradients were approximately the same as the present average geothermal gradients in most of the study area. However, paleogeothermal gradients of the order of one and a half times the present average geothermal gradient are indicated for an area located approximately 100 km west of Dawson Creek, where a local coalification maximum of concentric pattern occurs (Figs. 6A and B). Similarly, the eastward deflection in isoreflectance lines for the Bluesky-Gething Formation 60 km south of Dawson Creek (Figs. 6A and B) is probably a reflection of higher paleogeothermal gradients across the Bluesky-Gething interval in this area.

Regional rank changes

The regional pattern of rank variation for the Bluesky-Gething Formation shows a maximum near the eastern limit of deformation (Figs. 6A and B). Reflectance values decrease from there to the east and also the west across the Foothills. Calibrated time-depth (burial) curves (Fig. 5) suggest that the westward decrease in rank across the Foothills is largely due to a westward decrease in the depth and duration of sedimentary burial beneath Upper Cretaceous-Lower Tertiary foredeep deposits. This decrease in rank is related to diachronous west to east deformation (Kalkreuth and McMechan, 1984) and partially due to a general westward decrease in the paleogeothermal gradient. This westward decrease in paleogeothermal gradients is indicated by comparison of measured and calculated coalification gradients, and is also consistent with the present-day geothermal gradient distribution (American Association of Petroleum Geologists/United States Geological Survey Geothermal Gradient Map (1976)).

Comparison of coalfication gradients is, however, complicated by the fact that the rate of increase in vitrinite reflectance varies with rank. The curves for the Bluesky-Gething horizon (Fig. 5) show also that the time of maximum depth of burial (coalification) has migrated to the east. In the sections to the west [Schooler (10), Hook (90) and Hannington (135)], maximum depth of burial occurred around 70-75 Ma B.P., whereas in the sections to the east [Goldenrod (5), Pouce (19), Sinclair (58) and Steep Creek

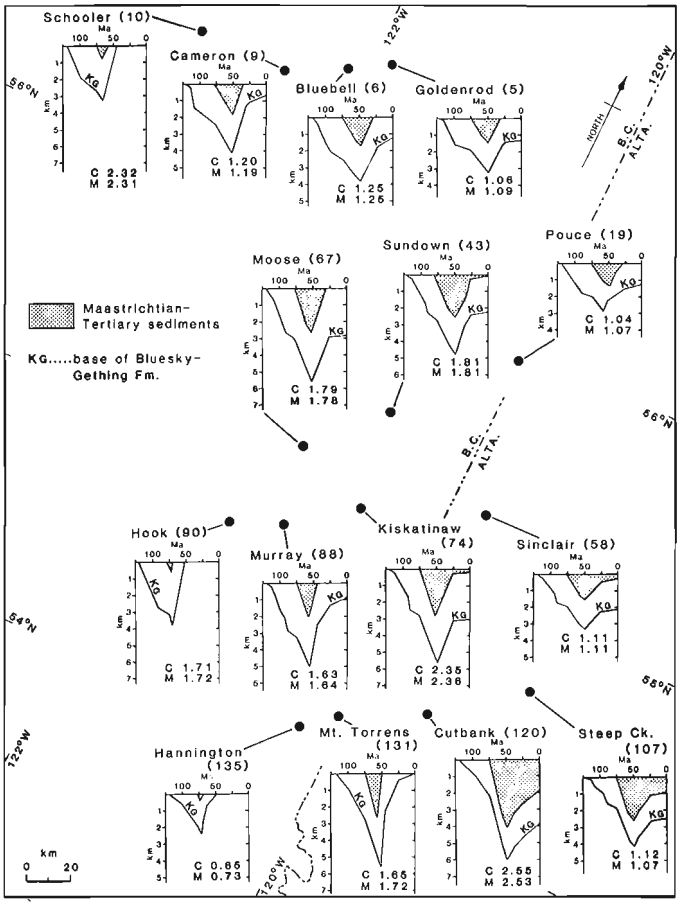

Figure 5. *Representative time-depth (burial) curves for study area. Localities 10, 90, 135 (Inner Foothills and Front Ranges); localities 9, 67, 88, 131 (Inner and Outer Foothills); localities 6, 43, 74, 120 (Alberta Plateau and Alberta Syncline) are in similar structural positions. C and M, calculated and measured reflectance values, respectively, for K_g (base of Bluesky-Gething Formation). Measured values are based on first- or second-order regression lines where these were available; modified from Kalkreuth and McMechan (1988).*

(107)], maximum depth of burial occurred 50-55 Ma B.P., about 20 Ma years later. The curves also suggest that the eastward decrease in rank, from a maximum near the eastern limit of deformation, is largely due to eastward thinning of the Cretaceous-Tertiary sedimentary wedge. For example, compare the time-depth (burial) curve for the Bluesky-Gething horizon at location Sundown (43) with location Pouce (19), and the time-depth (burial) curve at location Cutbank (120) with the location Steep Creek (107) (see Fig. 5). However, because of the exponential dependence of reaction rates on temperature, the amount and rate of the eastward decrease in coal rank also depends on the eastward change in the paleogeothermal gradient. The change in the paleogeothermal gradient and the change in wedge thickness dictate the magnitude of the eastward change (decrease) in the Bluesky-Gething temperature history. The amount that this temperature change affects the coal rank depends on the maximum temperatures attained at the eastern limit of deformation. These temperatures are in turn controlled by the thickness of the overlying sedimentary wedge and by the paleogeothermal gradient. At the level of the Bluesky-Gething Formation, the maximum amount and rate of eastward decrease in coal rank occurs in the southern part of the study area, where paleogeothermal gradients were nearly constant and burial at the eastern limit of deformation was

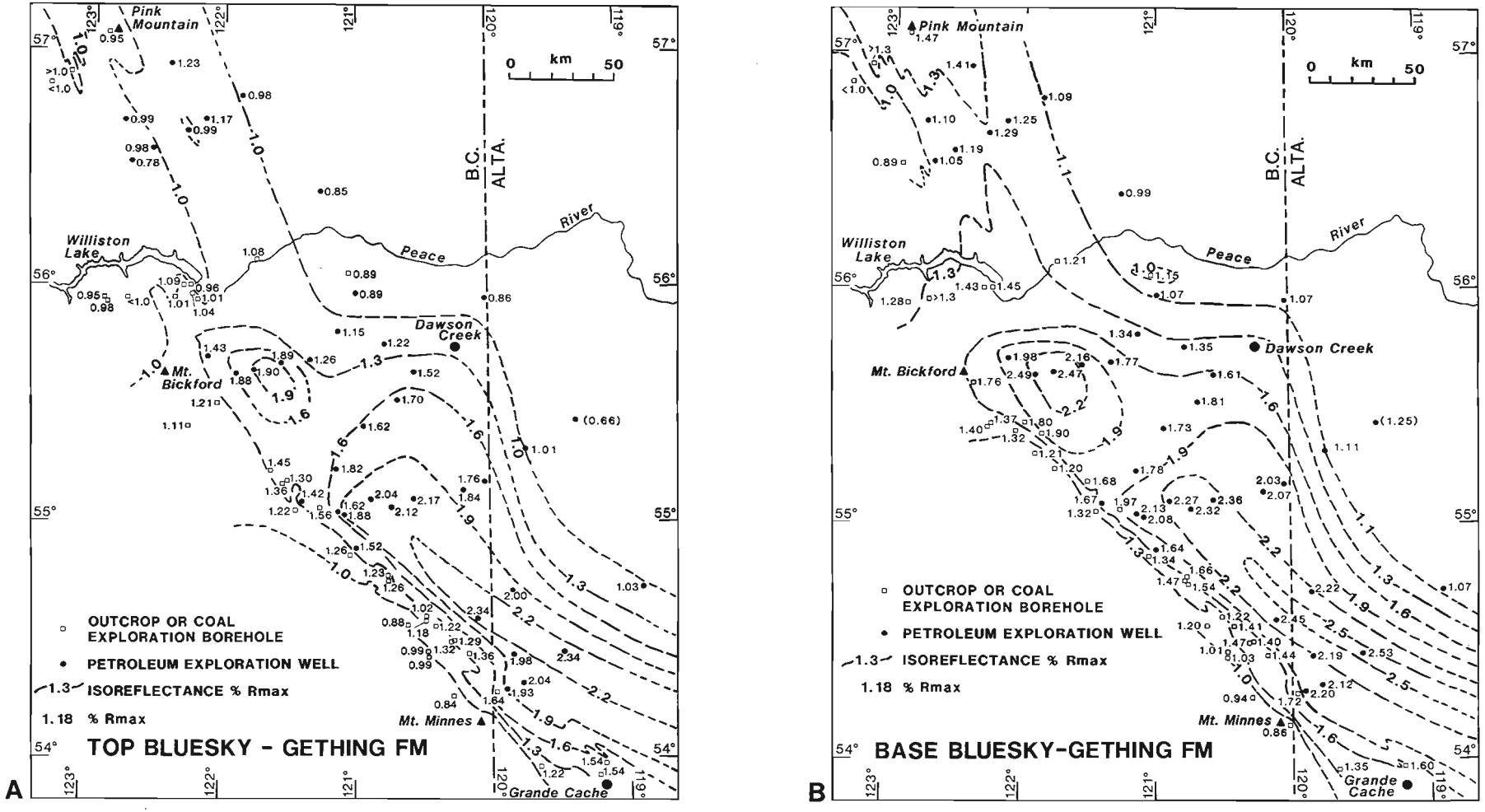

Figure 6. Isoreflectance lines for top (A) and base (B) of Lower Cretaceous Bluesky-Gething Formation; from Kalkreuth and McMechan (1988).

greatest. A much smaller decrease occurs in the north where paleogeothermal gradients increase to the east and the estimated maximum burial is approximately half of that in the south. In the northern area the increased paleogeothermal gradients towards the east have partially compensated for decreased burial.

Alberta Syncline and Alberta Plateau

East of the Foothills, the regional pattern of rank variation for the Lower Cretaceous Bluesky-Gething Formation shows a general decrease in reflectance values along strike from the southern part of the study area to the region north of Peace River, with a relatively rapid northward decrease in reflectance values in the region west of Dawson Creek (Figs. 6A and B). The calibrated time-depth (burial) curves suggest that the overall northward decrease in rank is largely due to reduced Maastrichtian (uppermost Cretaceous)-early Tertiary subsidence and burial in the north (Fig. 5, location 6) as compared to the south (approx. 2 km vs 4 km) near the eastern limit of deformation (Fig. 5, locations 74 and 120). Over most of the area, the estimated along-strike (northward) thinning of the Maastrichtian-Lower Tertiary sedimentary wedge is very gradual (<10 m/km). However, west of Dawson Creek, at the zone of rapid change in reflectance values, there appears to be a zone of relatively rapid northward thinning (40-50 m/km), across which approximately half the total estimated northward thinning of the Maastrichtian-early Tertiary sedimentary wedge occurs. The magnitude and rate of thinning suggest that this zone overlies the margin of a (series of) basement normal fault block(s) that had north-side-up movement in the Maastrichtian and early Tertiary. Seismic data indicate that a local zone of steeper south plunge in the sedimentary basin coincides with the proposed zone of Maastrichtian-Tertiary thickness change.

Rocky Mountain Foothills

In the Foothills, the regional distribution of reflectance values along strike for the base of the Bluesky-Gething Formation shows a relatively complex pattern. In the Inner Foothills, values gradually increase northward along strike to a maximum in the area south of Mt. Bickford (Fig. 6A, B). Values then decrease northwards to a low north of Williston Lake and then gradually increase to the north at Pink Mountain (Fig. 6A, B).

In the Outer Foothills, reflectance values generally decrease northward along strike to the area west of Dawson Creek (Figs. 6A and B). There they increase to form a secondary maximum that is apparently due to a local paleogeothermal gradient anomaly (see previous discussion). Continuing north, reflectance values decrease to a low north of Williston Lake and then gradually increase.

Calibrated time-depth (burial) curves (Fig. 5) suggest that regions of northward increase in reflectance values for the base of the Bluesky-Gething Formation correspond to regions of significant northward thickening of the Bluesky-Gething-Moosebar interval documented by Stott (1968, 1973, pers. comm., 1986) and Gibson (in press). In these regions the increase in rank caused by thickening of the Bluesky-Gething-Moosebar interval more than offsets the decrease caused by thinning of the Maastrichian-Tertiary sedimentary wedge.

Coal rank (ASTM) maps for top and base of Gething Formation

ASTM coal rank maps for the top and base of the Bluesky-Gething Formation are shown in Figures 7A and B. The maps are based on 60 coalification profiles through the Gething strata for which, by using 1st and 2nd order regression lines, the reflectance levels at the base (Gething/Cadomin contact) and for the top (Gething/Moosebar contact) were calculated. The first step was to create isoreflectance maps for the two stratigraphic horizons as shown in Figures 6A and B. The second step was to apply the reflectance limits of the ASTM rank, as published by Davis (1978), to the isoreflectance maps. In the following discussion, the regional changes in ASTM rank for the Bluesky-Gething Formation will be outlined with emphasis on the areas where seams of economic interest occur at or near the surface (Inner Foothills).

In the Inner Foothills, coal resources of the Bluesky-Gething Formation indicate measured resources of immediate interest of 300 megatonnes (British Columbia Geological Survey Branch, W. Kilby, pers. comm., 1987). Resources of immediate interest in the Canadian Rocky Mountains (Hughes et al., in press) refer to beds >0.60 m (surface mining, stripping ratio <20:1) and to beds >1.50 m up to 600 m depth (underground mining). In the Inner Foothills, where the seams of the Bluesky-Gething Formation occur at or near the surface, five areas are known to contain seams of immediate economic interest (Fig. 7A, B, locations 1, 2, 3, 4, 5).

At, and in the vicinity of, Peace River Canyon east of Williston Lake (Fig. 7A, B, location 1) the Bluesky-Gething Formation contains up to 40 seams (Stott, 1969), some attaining thicknesses of 0.90 to 1.30 m. In the Carbon Creek Basin to the west (Fig. 7A, B, location 2), more than 100 seams have been reported by Gibson (1985). However, only 14 of these were found to have sufficient thicknesses to be considered of economic interest. North of Williston Lake, seams occur less abundantly in the Bluesky-Gething Formation, the thicknesses rarely exceeding 0.50 m (Kalkreuth, 1982b). To the south, seams of economic interest have been reported for the Pine Valley area (Fig. 7A, B, location 3), the Sukunka area (Fig. 7A, B, location 4) and for the Monkman-Stoney Lake area (Figs. 9A and B, location 5). In these localities thick seams are developed in the upper part of the Bluesky-Gething Formation and have thicknesses of 1 to 5 m. One exceptionally thick coal zone (19 m) has been reported by Gibson (in press) to occur in the Pine Valley area (Fig. 7A, B, location 3).

Farther to the south, between the Monkman-Stoney Lake area (Fig. 7A, B, location 5) and Grande Cache, seams in the Bluesky-Gething Formation are presently not considered to be of economic interest.

ASTM rank groups, Top of Bluesky-Gething Formation (Fig. 7A)

The ASTM rank groups at the top of the Bluesky-Gething Formation range from high volatile A bituminous coal to semianthracite. In the south, a large coalification maximum is developed along the eastern edge of the deformed Outer Foothills belt. A second coalification maximum is indicated in the Outer Foothills east of Mt. Bickford (Fig. 7A). For the areas of economic interest, high volatile A bituminous coal is indicated at the top of the formation at Peace River Canyon and in the Carbon Creek Basin (Fig. 7A, locations 1 and 2). In Pine Valley (Fig. 7A, location 3), a transitional zone from high volatile A bituminous coal to low volatile bituminous coal is indicated. For the Sukunka and Monkman-Stoney Lake areas to the south (Fig. 7A, locations 4 and 5), medium volatile bituminous rank is indicated for coals occurring at the top of the formation.

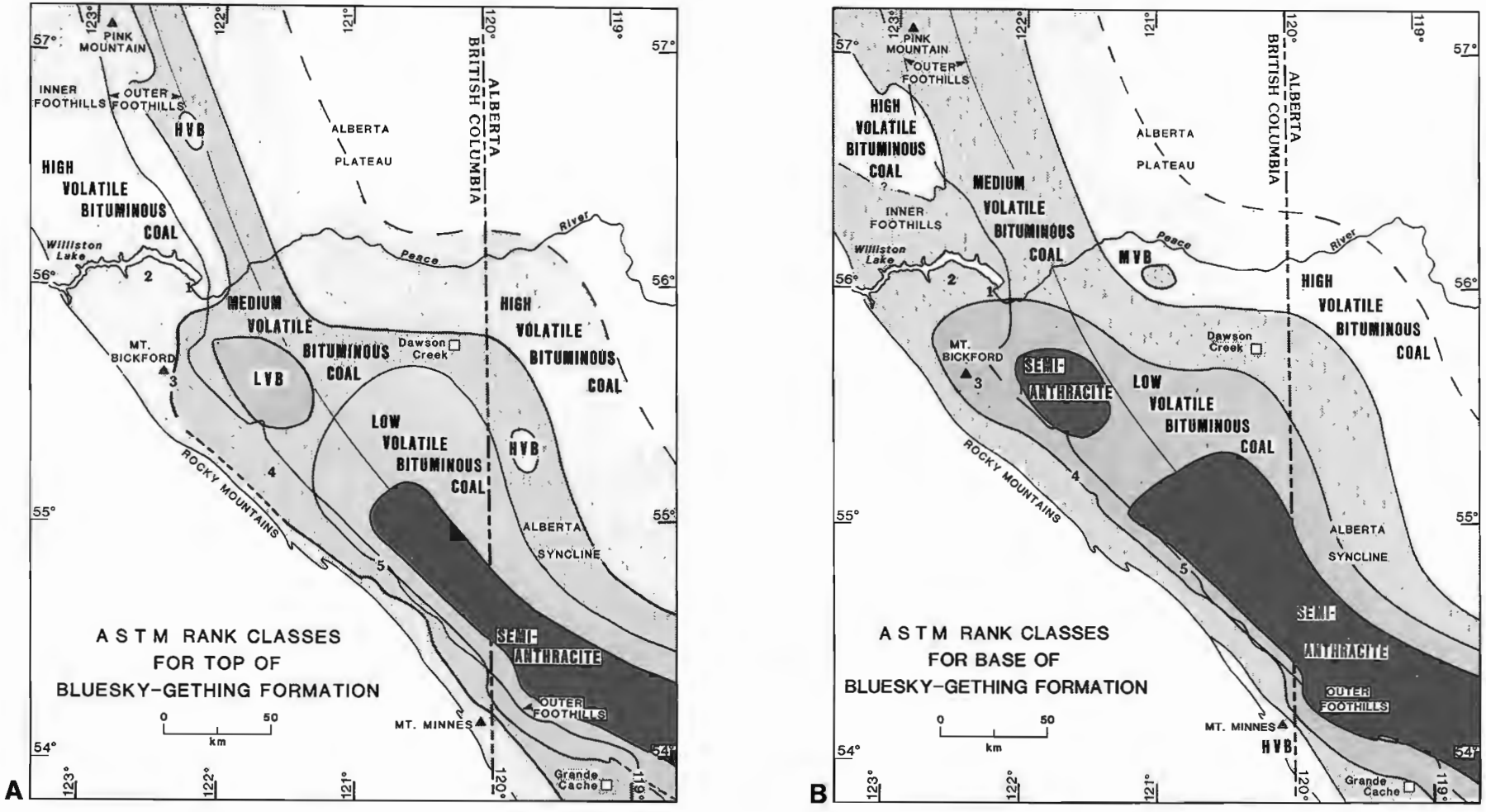

Figure 7. *Maps showing ASTM ranks for top (A) and base (B) of Bluesky-Gething Formation. 1-5, areas of immediate economic potential: 1 = Peace River Canyon area; 2 = Carbon Creek Basin; 3 = Pine Valley area; 4 = Sukunka area; 5 = Monkman-Stoney Lake area, from Kalkreuth et al. (in press).*

ASTM rank groups, Base of Bluesky-Gething Formation (Fig. 7B)

The ASTM ranks at the base of the Bluesky-Gething Formation range from high volatile A bituminous coal to semianthracite. However, the regional extent of semianthracite rank along the eastern limit of the Outer Foothills has increased significantly (compare Figs. 7A and B). Similarly, the rank of the second coalification maximum east of Mt. Bickford has increased from low volatile bituminous at the top of the Bluesky-Gething Formation to semianthracite at the base (compare Fig. 7A, B). In conformity with the higher reflectance levels at the base of the formation (Fig. 6A. B), the areal extent for high volatile A bituminous rank has decreased significantly both in the Inner Foothills to the west and in the Alberta Plateau and Alberta Syncline to the northeast and east, respectively. Lowest coal rank (high volatile A bituminous) occurs southeast and northwest of Dawson Creek in the Alberta Syncline and the Alberta Plateau. High volatile A bituminous coal is also indicated for an area in the northwestern part of the study area (Fig. 7B, southwest of Pink Mountain) and for an area in the southwest, where high volatile A bituminous rank is indicated for parts of the western Inner Foothills (near Mt. Minnes). For the areas of economic interest, medium volatile bituminous coals at the base of the Bluesky-Gething Formation are indicated for the Peace River Canyon and the Carbon Creek Basin (Fig. 7B, locations 1 and 2). Higher rank levels (low volatile bituminous) are indicated for the areas to the south [Fig. 7B, location 3 (Pine Valley), location 4 (Sukunka area) and location 5 (Monkman-Stoney Lake area)].

CONCLUSIONS

1. *Regional Rank Variations.* Reflectance values determined in coal-bearing sequences of the Fort St. John, Bullhead and Minnes Groups range from 0.73-2.67% Rmax (high volatile A bituminous - semianthracite). The regional coalification pattern indicates low reflectance levels in the Inner Foothills, higher reflectance in the Outer Foothills and highest reflectance values in the Alberta Syncline. From there, reflectances decrease rapidly to the east and also to the north (Alberta Plateau).

2. *Burial (temperature) history, Bluesky-Gething Formation.* Time-depth (burial) curves for the Lower Cretaceous Bluesky-Gething Formation suggest that the regional rank pattern for the top of the formation results largely from variations in the depth and/or duration of burial beneath Maastrichtian-Tertiary foredeep deposits. Rank increases from west to east across the Foothills because of diachronous Laramide deformation that resulted in an eastward increase in duration and depth of burial. Maximum rank occurs near the eastern limit of deformation. Rank decreases further east as a consequence of eastward thinning of the Late Cretaceous-early Tertiary sedimentary wedge. Rank also decreases significantly along strike because of northward thinning of the Maastrichtian-early Tertiary section.

   The rank pattern is more complicated for the base of the Bluesky-Gething Formation because local thickness changes in the Lower Cretaceous (Moosebar, Bluesky-Gething formations) intervals have a greater effect on the rank than does the regional change in thickness of Maastrichtian-Tertiary sedimentary wedge.

3. *ASTM Rank Maps, Bluesky-Gething Formation.* Coalification maps created for the base and top of the Bluesky-Gething Formation indicate the areal extent of ASTM ranks, ranging from high volatile A bituminous coal to semianthracite. For areas of economic interest in the Inner Foothills, where Bluesky-Gething seams occur at or near the surface, medium to low volatile bituminous rank is indicated for coals occurring close to the base of the formation. High volatile A bituminous to medium volatile bituminous coal occurs close to the top of the formation.

ACKNOWLEDGMENTS

The authors thank J.E. Barclay, H. Geldsetzer, D.W. Gibson, D.A. Leckie, B.C. Richards and D.F. Stott (all from the Institute of Sedimentary and Petroleum Geology, Calgary, Alberta) for providing stratigraphic information and samples. The authors wish to thank personnel of Smoky River Coal Ltd., Bullmoose Mine, and Quintette Mine for assistance in the collection of samples from their properties. Crows Nest Resources Ltd., BP Exploration Canada Ltd., Esso Resources Canada Ltd., Gulf Canada Resources Ltd., Petro-Canada and Utah Mines Ltd., provided many of the coals from the Lower Cretaceous Bluesky-Gething Formation and the authors acknowledge the co-operation of staff of these companies during the course of the study. K.E. Mottershead (ISPG) wrote the computer program used in the TTI calculations and K. Pratt (ISPG) provided technical assistance in sample preparation and analysis.

REFERENCES

American Association of Petroleum Geologists (AAPG) and United States Geological Survey (USGS)
1976: Geothermal gradient map of North America. Scale 1:5 000 000.

Bostick, N.
1973: Time as a factor in thermal metamorphism of phytoclasts (coaly particles). Septième Congrès International de Stratigraphie et de Géologie du Carbonifère (Krefeld, Aug. 23-28, 1971), Compte Rendu, 2, p. 183-193.

1979: Microscopic measurement of the level of catagenesis of solid organic matter in sedimentary rocks to aid exploration for petroleum and to determine formal burial temperatures. Society of Economic Paleontologists and Mineralogists, Special Publication, no. 26, p. 17-43.

Bustin, R., Cameron, A., Grieve, D., and Kalkreuth, W.
1985: Coal Petrology - Its principles, methods and applications. Geological Association of Canada, Short Course Notes, v. 3, Victoria, 1983, Second revised edition, 230 p.

Davis, A.
1978: The measurement of reflectance of coal macerals - its automation and significance. Pennsylvania State University Technical Report 10, 88 p.

Dowdle, W.L. and Cobb, W.M.
1975: Static formation temperature from well logs - an empirical method. Journal of Petroleum Technology, v. 27, p. 1326-1330.

Gibson, D.W.
1985: Stratigraphy and sedimentology of the Lower Cretaceous Gething Formation, Carbon Creek Coal Basin, northeastern British Columbia. Geological Survey of Canada, Paper 80-12, 29 p.

in press: The stratigraphy, sedimentology, coal geology and depositional environment of the Lower Cretaceous Gething Formation, northeast British Columbia and west-central Alberta. Geological Survey of Canada, Bulletin.

Hacquebard, P.A. and Donaldson, J.
1974: Rank studies of coals in the Rocky Mountain and Inner Foothills Belt, Canada. In Geological Society of America, Special Paper 153, p. 75-94.

Hood, A. and Castaño, J.
1974: VIII, Organic metamorphism: its relationship to petroleum generation and applications to studies of authogenic minerals. United Nations ESCAP CCOP Technical Bulletin, v 8, p. 87-118.

Hood, A., Gutjahr, C. and Peacock, R.
1975: Organic metamorphism and the generation of petroleum. American Association of Petroleum Geologists, Bulletin, v. 59, p. 986-996.

Hughes, J.D., Klatzel-Mudry, L. and Nikols, D.
in press: A standardized coal resource/reserve reporting system for Canada. Geological Survey of Canada, Paper 88-22.

Kalkreuth, W.D.
1982a: Rank and petrographic composition of selected Jurassic-Lower Cretaceous coals from British Columbia, Canada. Bulletin of Canadian Petroleum Geology, v. 30. p. 112-139.

1982b: Preliminary results on rank and composition of coals from the Gething Formation north of Peace River, northeastern British Columbia. In Current Research, Part C, Geological Survey of Canada, Paper 82-1C, p. 65-69.

Kalkreuth, W.D. and Langenberg, W.
1986: The timing of coalification in relation to structural events in the Grande Cache area, Alberta, Canada. Canadian Journal of Earth Sciences, v. 23, p. 1103-1116.

Kalkreuth, W.D., Langenberg, W., and McMechan, M.E.
in press: Regional coalification pattern of Lower Cretaceous coal-bearing strata, Rocky Mountain Foothills and foreland, Canada - implications for future exploration. International Journal of Coal Geology.

Kalkreuth, W.D. and McMechan, M.E.
1984: Regional pattern of thermal maturation as determined from coal-rank studies, Rocky Mountain Foothills and Front Ranges north of Grande Cache, Alberta - implications for petroleum generation. Bulletin of Canadian Petroleum Geology, v. 32, no. 3, p. 249-271.

1988: Burial history and thermal maturity, Rocky Mountain Foothills and Foreland, east-central British Columbia and adjacent Alberta. American Association of Petroleum Geologists, Bulletin, v. 72, no. 11, p. 1395-1410.

in prep: Regional rank studies of Jurassic-Cretaceous strata, Peace River Coalfield and adjacent parts of Alberta. Geological Survey of Canada, Bulletin.

Karweil, J.
1956: Die Metamorphose der Kohlen vom Standpunkt der physikalischen Chemie. Zeitschrift der Deutschen Geologischen Gesellschaft, v. 107, p. 132-139.

Langenberg, C.W. and McMechan, M.E.
1985: Lower Cretaceous Luscar Group (revised) of the northern and north-central Foothills of Alberta. Bulletin of Canadian Petroleum Geology, v. 33, p. 1-11.

Lopatin, N.
1971: Temperature and geologic time factors in coalification. Akademiya Nauk SSSR Izvestiia, Seriia geologicheskaia, v. 3, p. 95-106.

Lyons, P., Hatcher, P., Brown, F., Krasnow, M., and Larson, R.
1985: Role of static load (overburden) pressure in coalification of bituminous and anthracitic coal. Proceedings of International Conference on Coal Science, October 28-31, 1985, Sydney, N.S.W., Australia, Pergamon Press, p. 620-623.

McLean, J.
1982: Lithostratigraphy of the Lower Cretaceous coal-bearing sequence, Foothills of Alberta. Geological Survey of Canada, Paper 80-29, 46 p.

McLean, J. and Wall, J.
1981: The Early Cretaceous Moosebar Sea in Alberta. Bulletin of Canadian Petroleum Geology, v. 29, no. 3, p. 334-337.

Price, R.A.
1981: The Cordilleran Foreland Thrust and Fold belt in the southern Canadian Rocky Mountains. In Thrust and Map Tectonics, K. McClay and N. Price (eds.); Geological Society of London, Special Publication, v. 9, p. 427-448.

Smith, G.
1989: Coal Resources of Canada. Geological Survey of Canada, Paper 89-4, 146 p.

Stott, D.F.
1968: Lower Cretaceous Bullhead and Fort St. John Groups, between Smoky and Peace River, Rocky Mountain Foothills, Alberta and British Columbia. Geological Survey of Canada, Bulletin, v. 152, 279 p.

1969: The Gething Formation at Peace River Canyon, British Columbia. Geological Survey of Canada, Paper 68-28, 30 p.

1973: Lower Cretaceous Bullhead Group between Bullmoose Mountain and Tetsa River, Rocky Mountain Foothills, northeastern British Columbia. Geological Survey of Canada, Bulletin, v. 219, 228 p.

1981: Bickford and Gorman Creek, two new formations of the Jurassic-Cretaceous Minnes Group, Alberta and British Columbia. Geological Survey of Canada, Paper 81-1B, p. 1-9.

1983: Late Jurassic-Early Cretaceous foredeeps of northeastern British Columbia. Transactions of the Royal Society of Canada, Series IV, v. XXI, p. 143-153.

1984: Cretaceous Sequences of the Foothills of the Canadian Rocky Mountains. In The Mesozoic of Middle North America, D.F. Stott and D. Glass (eds.); Canadian Society of Petroleum Geologists Memoir, v. 9, p. 85-107.

Teichmüller, R.
1962: Zusammenfassende Bemerkungen über die Diagenese des Ruhrkarbons and ihre Ursachen. Fortschritte in der Geologie von Rheinland und Westfalen, v. 3, p. 725-734.

Waples, D.
1980: Time and temperature in petroleum formation; Application of Lopatin's method to petroleum exploration. American Association of Petroleum Geologists, Bulletin, v. 64, p. 916-926.

Controls on coal quality variation in the Cadomin-Luscar Coalfield, Alberta

C.W. Langenberg[1], D. Macdonald[1], and W. Kalkreuth
Institute of Sedimentary and Petroleum Geology, Calgary

Langenberg, C.W., Macdonald, D., and Kalkreuth, W., Controls on coal quality variation in the Cadomin-Luscar Coalfield, Alberta. In Contributions to Canadian Coal Geoscience, Geological Survey of Canada, Paper 89-8, p. 80-87, 1989.

Abstract

The economic Jewel Seam (Lower Cretaceous) has a stratigraphic thickness of about 10 m. Its depositional setting was on a coastal plain, well removed from marine clastic influences. Shortening by subsequent folding and thrusting of the strata amounted to 50 per cent, often resulting in structural thickening of the Jewel Seam along the hinges of folds. Average disseminated ash is 14 per cent. Sulphur contents are low and average 0.3 per cent. Volatile matter and vitrinite reflectance are largely determined by depth and duration of burial and to some extent by deformation. Rank of the Jewel Seam ranges from high to medium volatile bituminous, where the highest rank is found in the central part of the study area. The intersections of isorank surfaces and the Jewel Seam indicate components of syndeformational coalification. A contoured map of vitrinite reflectance predicts rank and volatile matter of the Jewel Seam for unexplored parts of the Cadomin-Luscar Coalfield.

Résumé

Le filon économiquement rentable de Jewel (Crétacé inférieur) possède une épaisseur stratigraphique d'environ 10 m. Sa sédimentation s'est produite sur une plaine côtière, bien loin des influences clastiques marines. Des plissements et chevauchements subséquents ont produit un raccourcissement s'élevant jusqu'à 50 % de la couche, qui s'est traduit par un épaississement structural du filon de Jewel le long des charnières des plis. La moyenne des cendres disséminées est de 14 %. La teneur en soufre est faible avec une moyenne de 0,3 %. Les matières volatiles et les taux de réflectance de la vitrinite sont largement déterminés par la profondeur et la durée de l'enfouissement et, jusqu'à un certain point, par la déformation. Le rang du filon de Jewel varie, allant de charbons bitumineux à teneur élevée en matières volatiles aux charbons bitumineux à teneur moyenne en matières volatiles; le rang le plus élevé se trouve dans la partie centrale de la région étudiée. Les intersections des surfaces d'isorangs et du filon de Jewel indiquent la présence d'éléments de carbonification s'étant produits pendant la déformation. Une carte isograde des taux de réflectance de la vitrinite extrapole les rangs et les teneurs en matières volatiles du filon de Jewel pour ce qui est des régions inexplorées du bassin houiller Cadomin-Luscar.

INTRODUCTION

The objectives of this study are to document coal quality variations (including rank, chemical constituents, petrographic composition and thickness) in the Cadomin-Luscar Coalfield and to establish geological models that explain these variations. The study area is located in west-central Alberta, between latitudes 53° and 53°8' and longitudes 117°17' and 117°34' (Fig. 1). The area forms part of the Cadomin (NTS 83F/3) and Miette (NTS 83F/4) map sheets and covers approximately 100 km^2. It conforms closely to the Cadomin-Luscar Coalfield.

The Jewel Seam is the most important seam in the coalfield and its existence has been known since the turn of the century. An underground mine was developed at Cadomin in 1917 and at Luscar in 1921. These mines operated until the mid 1950s. The Cardinal River Mine at Luscar (open pits) was opened in 1970 and the Gregg River Mine (also open pits) started shipping coal in 1983.

The Cadomin area was mapped by the Geological Survey of Canada (MacKay, 1929, 1930). Mountjoy (1959) mapped the Miette mapsheet. The area east of Gregg River was mapped by Hill (1980). The sections along the McLeod River at Cadomin have often been used in stratigraphic studies (e.g. Mellon, 1967; McLean, 1982). Preliminary data on petrographic characteristics of the coals have beeen reported by Kalkreuth (1988).

GENERAL GEOLOGY

The Cadomin-Luscar Coalfield is situated in the Inner Foothills. The area is largely underlain by Lower Cretaceous rocks of the Luscar Group as defined by Langenberg and McMechan (1985). The coal-bearing Luscar Group was deposited in an overall regressive sequence, during Aptian-Albian time. This sequence represents a major, western sourced, Cretaceous clastic wedge, which prograded into the

[1]Alberta Geological Survey, Alberta Research Council
Box 8330, Station 'F', Edmonton, Alberta, T6H 5X2

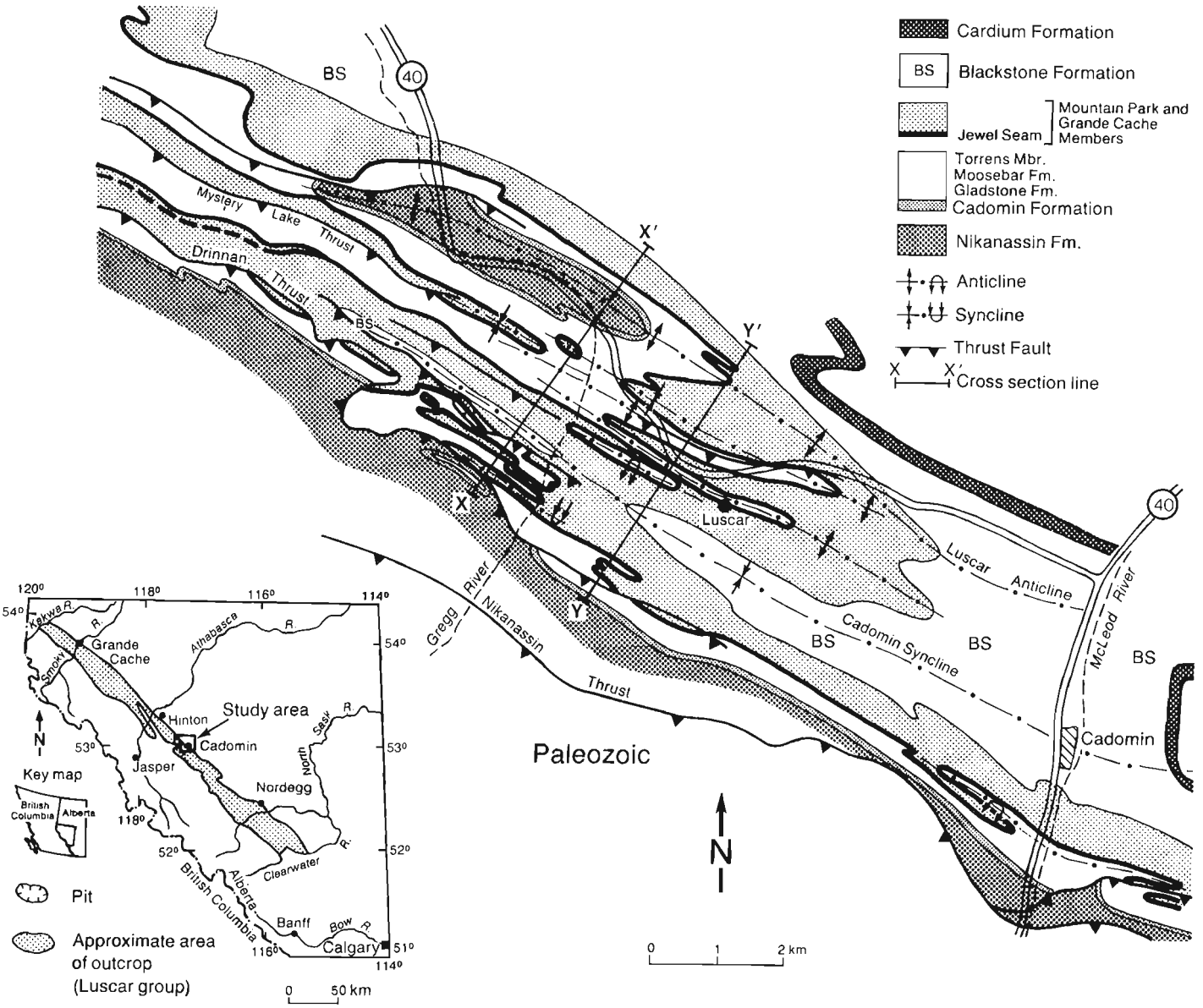

Figure 1. *Simplified geological map of the Cadomin-Luscar Coalfield, compiled and modified from Hill (1980) and Karst (Gregg River Resources, unpublished).*

Interior Cretaceous seaway. The Luscar Group comprises the Cadomin, Gladstone, Moosebar and Gates formations (Fig. 2). The Cadomin Formation consists of alluvial conglomerates. The Gladstone Formation consists of alluvial sandstone, shale and minor coal. The Moosebar Formation contains marine shale and minor sandstone. The largely nonmarine Gates Formation consists of sandstones, shales and coal and can be divided into three members, the Torrens, Grande Cache and Mountain Park members, in ascending order. The Grande Cache Member comprises coastal plain sandstones, shales and major economic coal seams. It grades into the Mountain Park Member, which consists of fluvial, fining-upward sandstones, shales, and minor coal seams. Four regional marine sedimentation cycles can be distinguished in the transition from Moosebar to Gates formations (Macdonald et al., 1988).

Two open pit coal mines (operated by Cardinal River Coals Ltd. and Gregg River Resources Ltd.) are presently producing from the Grande Cache Member. All production comes from the 10 m thick Jewel Seam at the base of this member and a total of 4.4 million tonnes of raw metallurgical coal were produced in 1987. The rank of the Jewel Seam is mainly medium volatile bituminous. The R Seam (named Ryder Seam by Cardinal River and Ruff Seam by Gregg River) is situated about 60 m above the Jewel Seam. The R Seam is highly variable in thickness and mineral matter content and is presently not being mined. The other stratigraphic units contain additional, generally thin coal seams.

DEPOSITIONAL ENVIRONMENTS

Outcrop studies in the marine to nonmarine transition of the Moosebar and Gates formations, in the Cadomin and Grande Cache areas, together with subsurface studies in the time-equivalent Spirit River Formation (Deep Basin), have

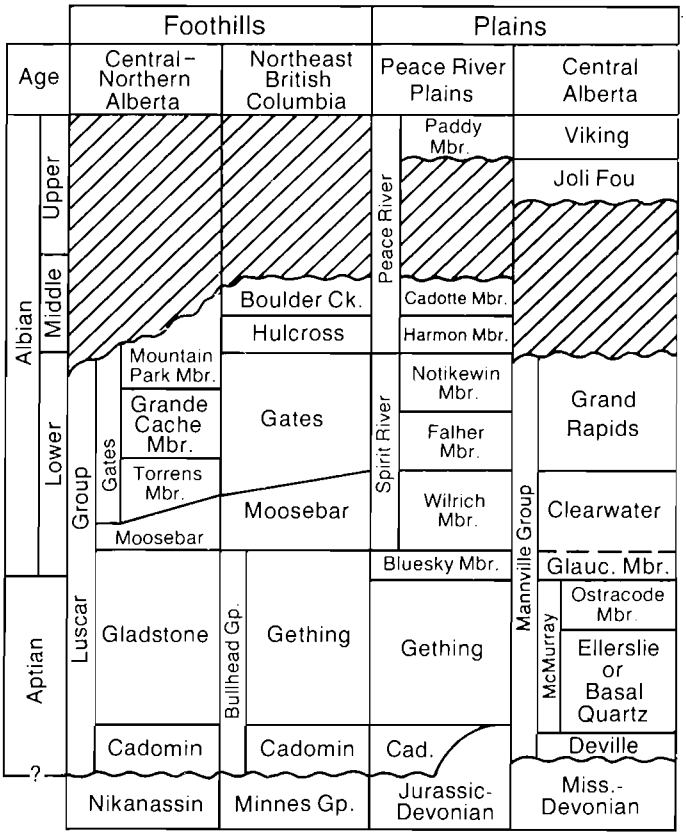

Figure 2. *Lower Cretaceous stratigraphic nomenclature of north-central Alberta and northeastern British Columbia.*

shown several transgressive-regressive cycles in an overall prograding shoreline sequence (Macdonald et al., 1988). Four fourth-order marine cycles are recognized in outcrop in the Cadomin area; the lower three associated with possible wave dominated prograding deltas and strandlines, and the upper one having a more brackish (lagoonal, tidal channels, etc.) association. Some of these cycles can be correlated with Falher and Wilrich cycles in the Deep Basin, indicating that they are contemporaneous (Fig. 3).

Sedimentological examination of the lower three cycles in the Cadomin area shows a progression of offshore to shoreface to foreshore environments (strandplains), culminating in the deposition of coal seams. This interpretation is supported by the coal facies (Kalkreuth and Leckie, in press and Kalkreuth, et al., this volume). Seaward stepping of coastal shoreline sediments was the most common stratigraphic architectural style. A variety of physical and biogenic sedimentary structures are present, such as hummocky cross-stratification and *Skolithos* ichnofacies, indicating shallow marine conditions. Interpretation of the upper cycle is based primarily on limited trace fossils and foraminifera.

The deposition of organic matter, which resulted in the 10 m thick Jewel Seam, is closely related to the underlying strandplain sandstones of the Torrens Member (Kalkreuth et al., this volume). In the western part of the study area the Jewel Seam is split into an upper and lower seam (Fig. 1). The siltstone and sandstone split is up to 25 m thick.

STRUCTURAL SETTING

The rocks of the area are highly deformed by folding and faulting, including major structures such as the Cadomin Syncline, the Luscar Anticline and the Drinnan Thrust (Fig. 1). In the south, the area is bounded by the Nikanassin Thrust, which forms the boundary between Foothills and Mountains in the region.

The geological map (Fig. 1) and cross sections (Fig. 4) show the nature of the deformation in the area. The cross sections show overturned folds, which are in places tight. The shortening has been calculated to be around 50 per cent. Folding has had a profound effect on coal seams as a resulting of thickening in fold hinges, where the original thickness of the Jewel Seam (cf about 10 m) is locally increased up to 30 m. The mechanism of this process was described in detail for the Grande Cache area to the north (Langenberg et al., 1987). The examples show that coal has flowed into these hinges from the nearby limbs. This process can be seen to have taken place by the extensive shearing of the coal. Most open pits in the Cadomin-Luscar area have been developed along the hinges of folds, indicating the economic significance of this thickening.

COAL QUALITY, SEDIMENTATION AND DEFORMATION

Coal quality will be discussed in terms of ash, sulphur and volatile matter contents, and percentage of vitrinite reflectance. Ash and sulphur contents are largely determined by the original sedimentary environment. Amounts of volatile matter, fixed carbon, ultimate carbon, hydrogen and vitrinite reflectance are largely determined by subsequent burial and to some extent by deformation. For further details the reader is referred to Langenberg et al. (1988).

Ash

Ash in the Jewel Seam comes either from visible rock partings or from finely disseminated mineral matter within the coal. In places the disseminated ash content may have increased by tectonic shearing. In general, ash contents have increased both by the shearing process and possibly by precipitation of mineral matter by percolating groundwater (see also Bustin, 1982). However, exceptions to this general tendency can be observed in several places. These factors make prediction of ash content difficult. Average disseminated ash content of the Jewel Seam is about 14 per cent, calculated from values ranging from 4 to 30 per cent. Vertical successions with upward increase in ash content and low ash zones in the middle of the seam (generally continuous on pit scale) can be explained by the original acidity of the swamp.

The overall depositional setting of the Jewel Seam is believed to have been on a coastal plain, perhaps up to 100 km inland from the shorelines. Thus the Jewel Seam attained its large thickness well removed from marine clastic influences. Smaller fluvial or tidal channels may have dissected or been adjacent to the Jewel swamp, providing the visible partings. For mining purposes, a two metre sampling interval of the Jewel Seam results in a good characterization of ash variation.

Ash values in the R Seam tend to be high, and are more likely related to nearby clastic environments than to the original acidity of the swamp.

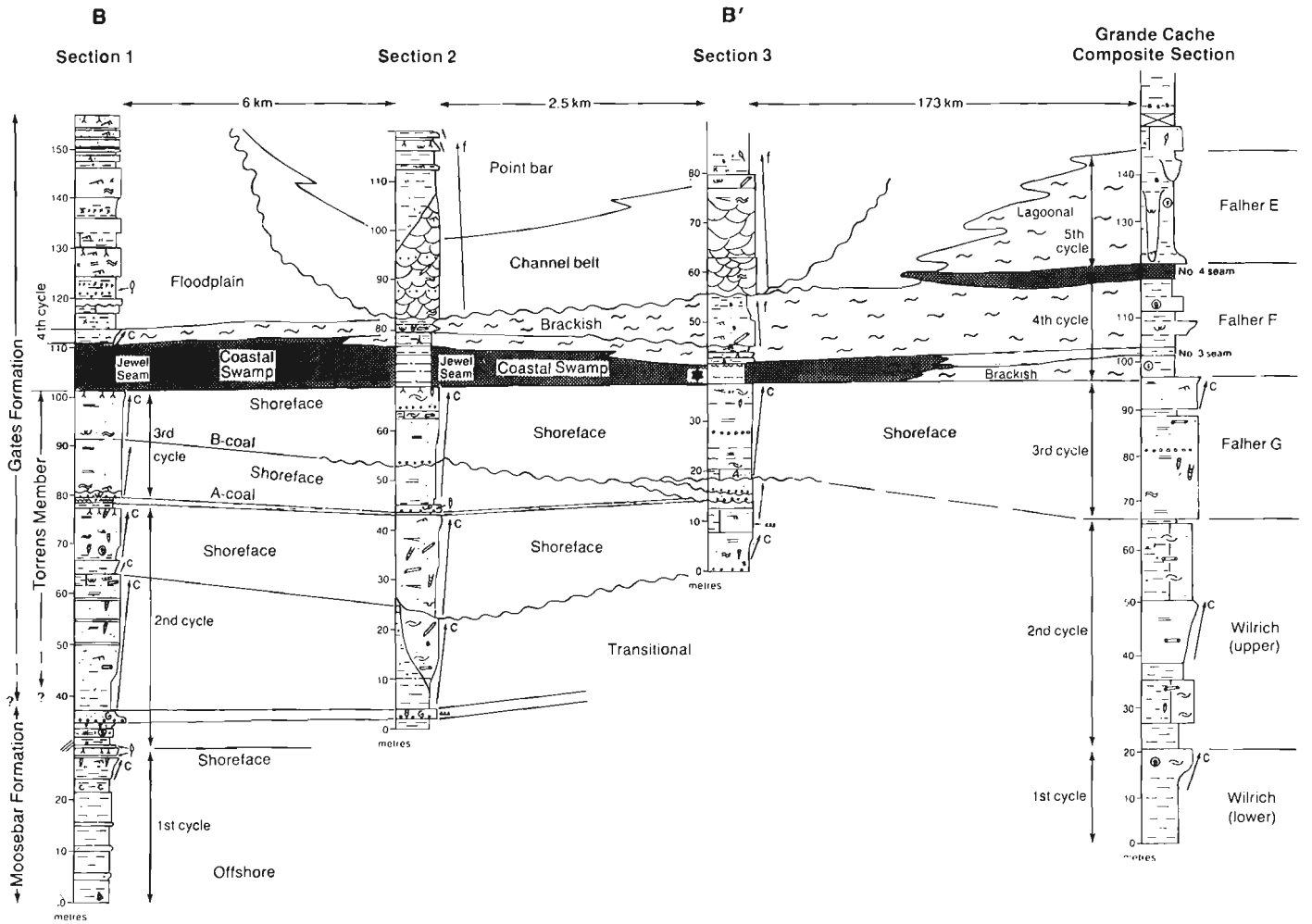

Legend:

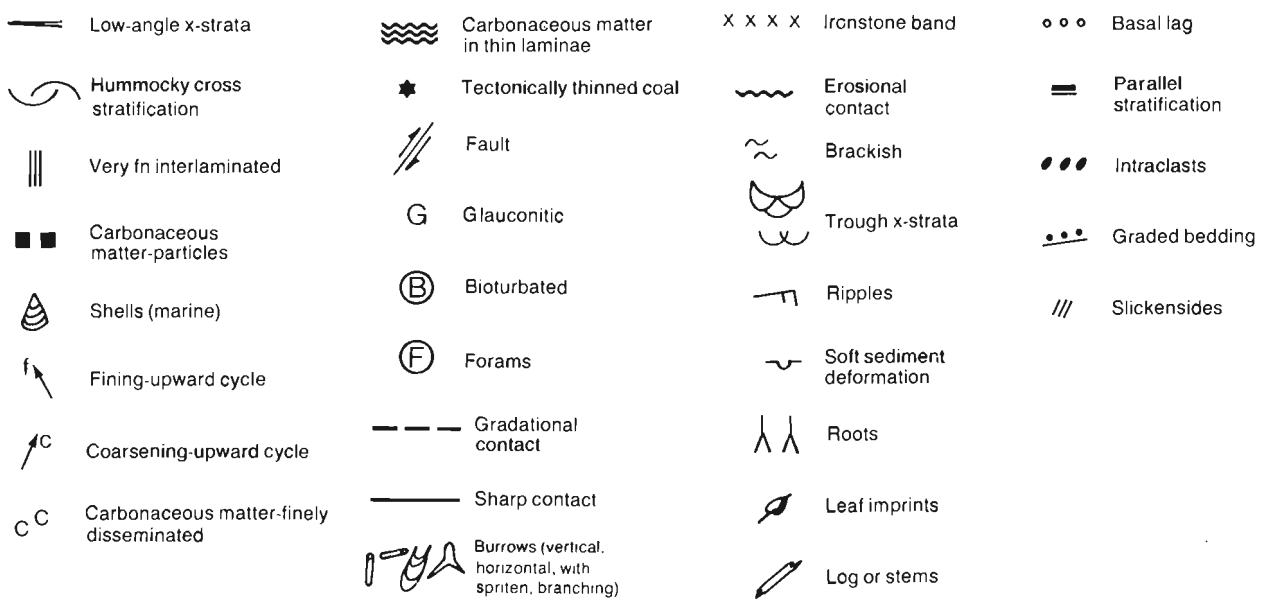

Figure 3. *Stratigraphic cross section through the Cadomin and Grande Cache areas (from Macdonald et al., 1988). The part of the section in the Cadomin area (BB') is along section line YY', which is shown on Figure 1.*

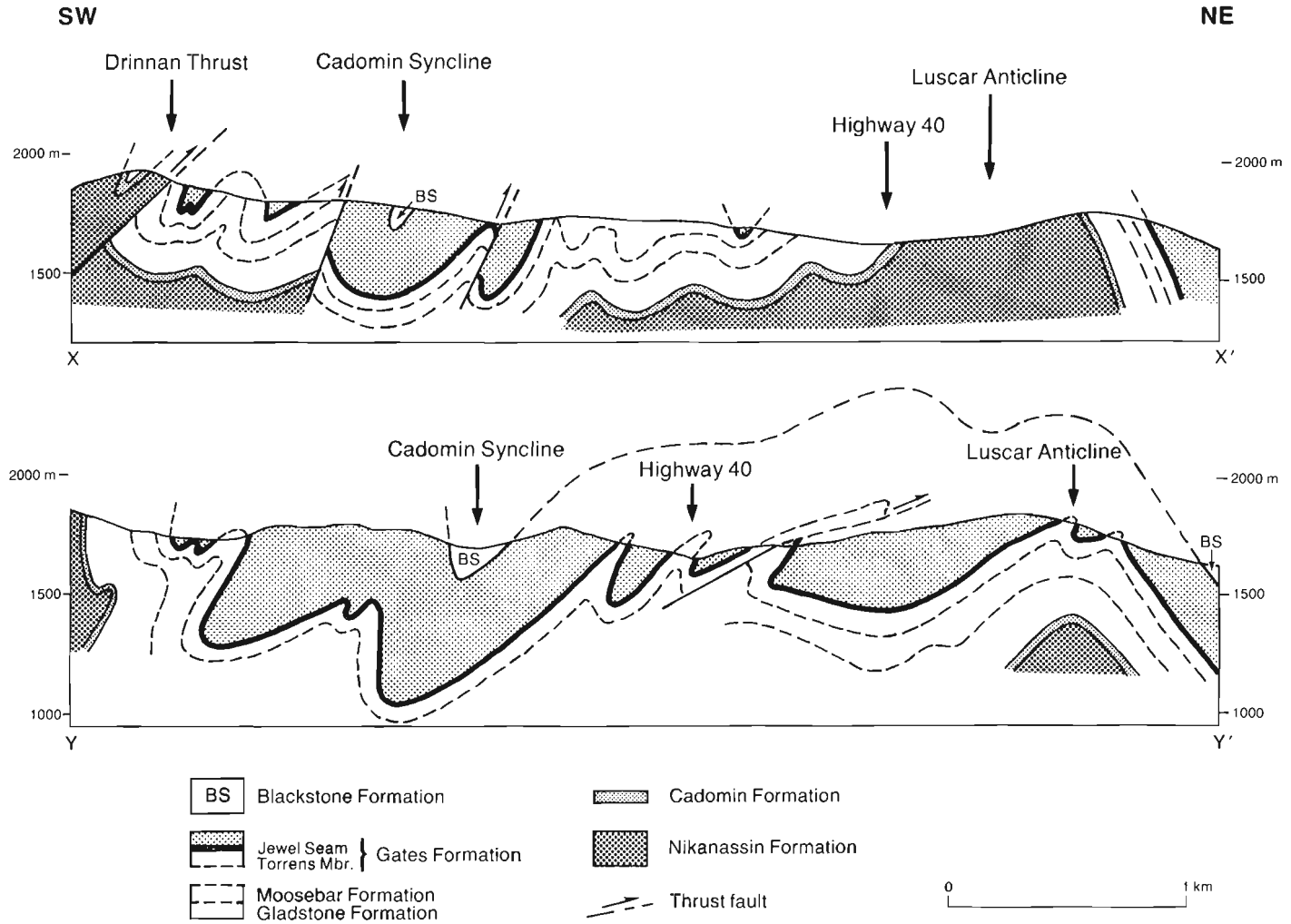

Figure 4. *Cross sections XX' and YY' through the Cadomin-Luscar Coalfield. Section XX' is on the Gregg River property (after Karst, Gregg River Resources, unpublished). Section YY' is on the Cardinal River property (modified from Hill, 1980). The lines of section are shown on Figure 1.*

Sulphur

Sulphur contents of the Jewel Seam are low, averaging 0.3 per cent. Low sulphur combined with moderately high ash and high inertinite contents point to acidic swamps, with intermittent aerobic conditions (Cecil et al., 1979). Sulphur, which is mostly organic in the Jewel Seam, is often slightly more abundant at the base, and to some extent at the top of the seam. Elevated sulphur values at the top of the seam may be related to overlying thick channel or brackish water deposits. A very low sulphur zone (i.e. <0.2 per cent, dry) is often found in the middle of the Jewel Seam, particularly where there are few partings.

Sulphur values in the R Seam (alluvial plain setting) are generally about 0.4 per cent.

Volatile Matter

Volatile matter content (dry and ash free) of the Jewel Seam ranges from 19.3 to 31.8% for unoxidized coal and up to 39.8% for oxidized coal. This range indicates predominantly medium volatile bituminous rank for the unoxidized coal. There is a systematic variation of rank (and volatile matter) in the study area, where the central part has the highest ranks (Fig. 5). Consequently, volatile matter (dry and ash free) can be predicted fairly precisely by extrapolation of existing data, based on the location of the coal.

Vitrinite Reflectance

Maximum vitrinite reflectance for the Jewel Seam ranges from 0.97 to 1.43% (high volatile A to medium volatile bituminous coals). The highest rank is found in the central part of the study area, along the southwest limb of the Luscar Anticline (Fig. 5). High volatile A bituminous coals are present in the southeast. The intersection of isorank lines and the folded Jewel Seam, as illustrated in Figures 5 and 6, shows that some of the coalification is syndeformational. However, higher rank in the central part of the coalfield could be due to deeper burial. It should also be noted that the highest ranks are not along the axis of the Cadomin Syncline as would be expected in the syn-deformational coalification model, but along the southwestern flanks of the Luscar Anticline (Fig. 5). This might be explained by a late stage adjustment of the

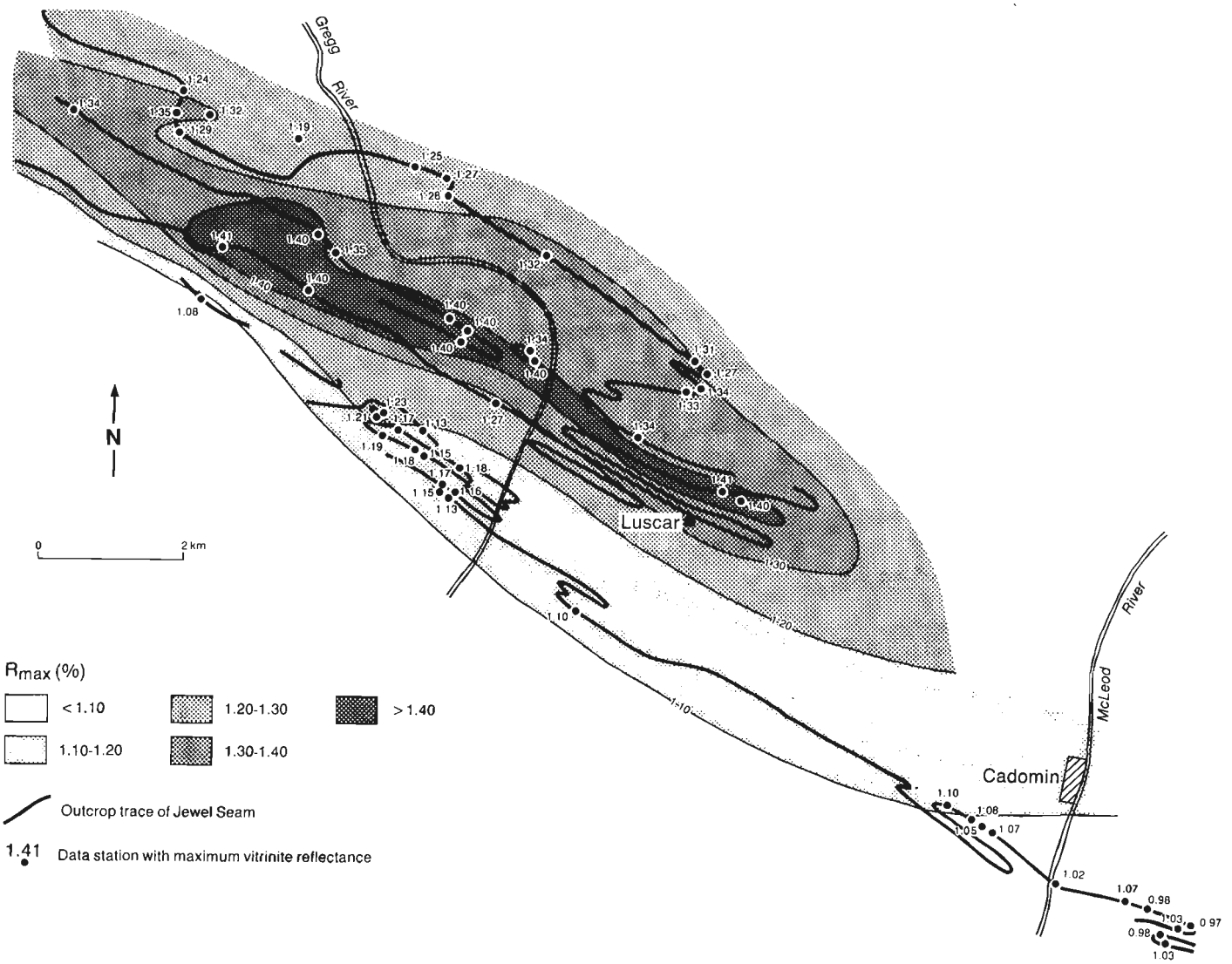

Figure 5. *Regional vitrinite reflectance variations of the Jewel Seam.*

structure, where parts of the Cadomin Syncline have moved upwards by secondary folding and thrusting (Mystery Lake Fault and fault near Luscar).

A good linear correlation between maximum vitrinite reflectance and volatile matter (dry and ash free) is observed (Fig. 7), enabling volatile matter to be determined from vitrinite reflectance. The map of maximum vitrinite reflectance variation (Fig. 5) can be used to predict rank and volatile matter of the Jewel Seam for unexplored parts of the Cadomin-Luscar Coalfield.

CONCLUSIONS

Part of the Luscar Group of the study area is characterized by transgressive-regressive cycles of an overall prograding shoreline succession. The development of the thick Jewel Seam is closely related to underlying strandplain sandstones. Folding of the strata during Laramide deformation has formed open to tight anticlines and synclines. The shortening resulting from folding and faulting is approximately 50 per cent. The Jewel Seam shows significant thickening in fold hinges. Ash contents are moderate, averaging 14%. Sulphur contents are low (average 0.3%), with slightly increased values at the base and top of the seam. A tentative geochemical model of the peat swamp (Cecil et al., 1979) explains some of these variations.

Volatile matter and vitrinite reflectance indicate a rank range from high volatile A bituminous to medium bituminous coals. The highest ranks are found in the central part of the study area along the southwest limb of the Luscar Anticline. Intersection of isoranklines with the folded Jewel Seam reflects components of syndeformational coalification for the area. The observed rank pattern and structural deformation model for the study area allow prediction of coal rank variation for unexplored parts of the Cadomin-Luscar Coalfield.

ACKNOWLEDGMENTS

This study has been partly funded by the Alberta Office of Coal Research and Technology. Personnel of Gregg River Resources Limited and Cardinal River Coals Limited are thanked for providing access to their mine sites.

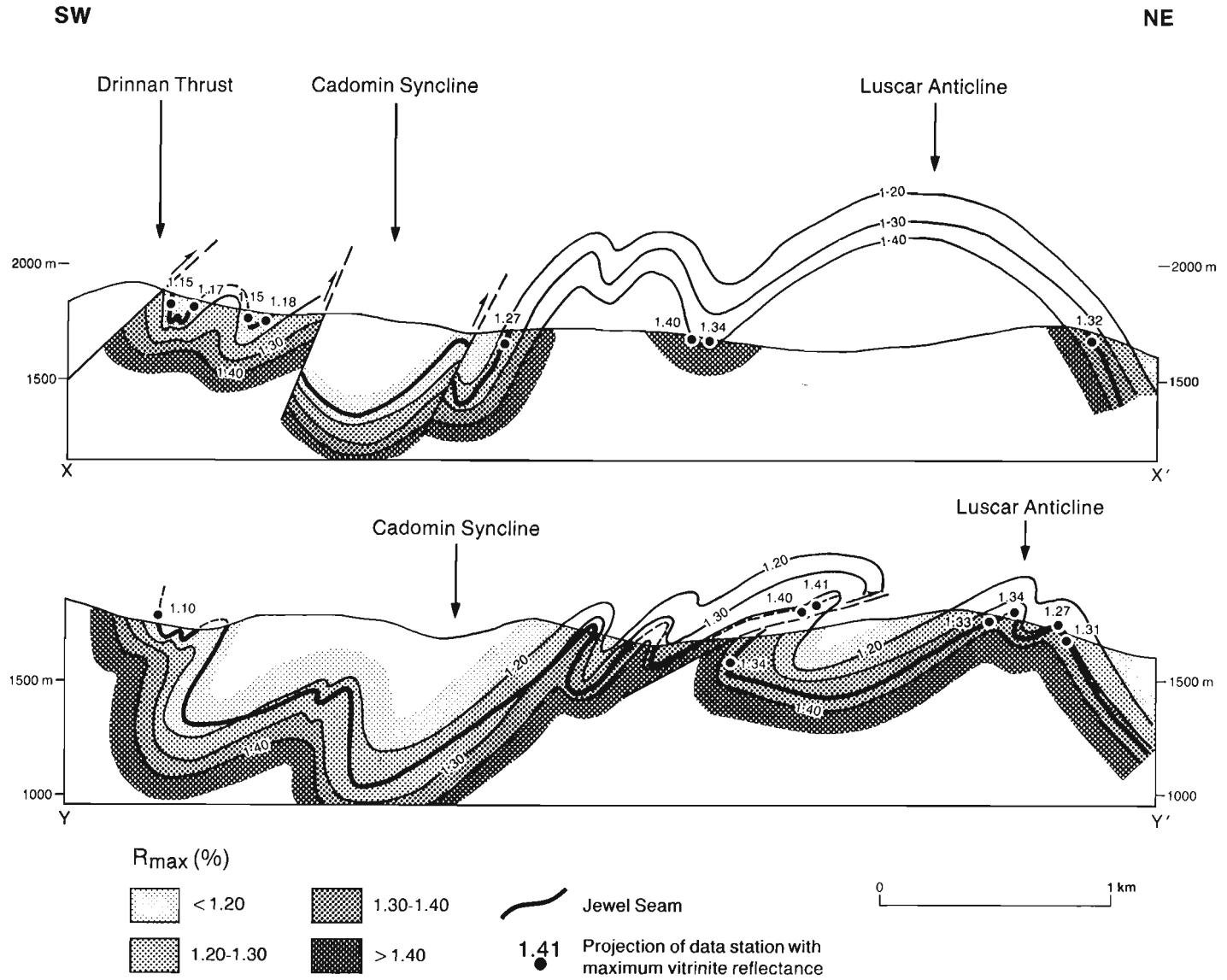

Figure 6. Cross sections, simplified from Figure 4, showing the relation between coal rank of the Jewel Seam and deformed strata.

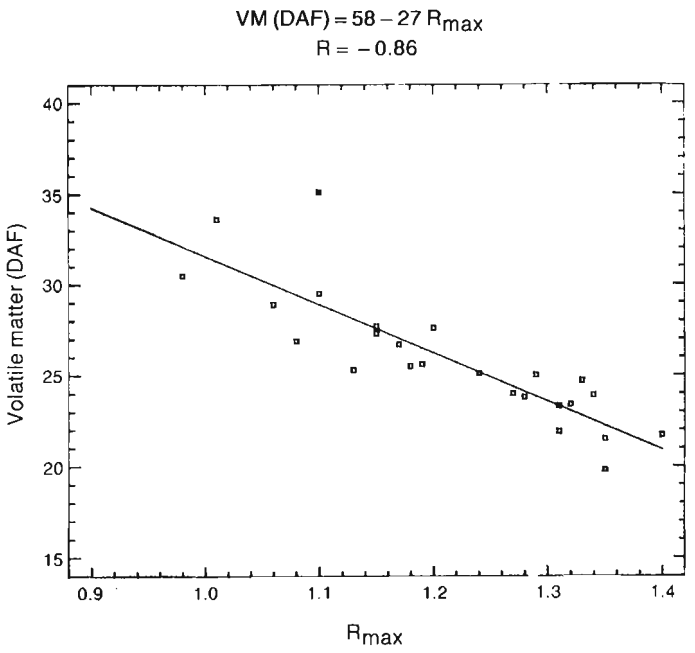

Figure 7. Cross plot and best fit linear correlation between volatile matter (dry and ash free) and maximum vitrinite reflectance. Plot is based on 25 samples of which 16 are from the Jewel Seam.

REFERENCES

Bustin, R.M.
1982: The effect of shearing on the quality of some coals in the southeastern Canadian Cordillera. Canadian Mining and Metallurgical Bulletin, v. 75, no. 841, p. 76-83.

Cecil, C.B., Stanton, R.W., Dulong, F.T., and Renton, J.J.
1979: Geologic factors that control mineral matter in coal. In Carboniferous coal short course and guidebook, v. 3, A.C. Donaldson, M.W. Presley, and J.J. Renton (eds.); American Association of Petroleum Geologists field seminar, West Virginia Geological Survey, Bulletin B-37-3, p. 43-56.

Hill, K.C.
1980: Structure and stratigraphy of coal-bearing strata near Cadomin, Alberta. University of Alberta, unpublished M.Sc. thesis, 191 p.

Kalkreuth, W.
1988: Kanadische Kreidekohlen-Inkohlungsgrad und petrographische Zusammensetzung Kanadischer Kreidekohlen in den Rocky Mountain Foothills von NE-British Columbia und Westzentral Alberta. Erdöl und Kohle, v. 41, p. 2, p. 61-70.

Kalkreuth, W. and Leckie, D.A.
in press: Sedimentological and petrographical characteristics of Cretaceous strandplain coals: A model for coal accumulation from the North American Western Interior seaway. International Journal of Coal Geology.

Kalkreuth, W., Leckie, D.A., and Labonté, M.
1989: Gates Formation (Lower Cretaceous) coals in western Canada: a sedimentological and petrological study. This volume.

Langenberg, C.W. and McMechan, M.E.
1985: Lower Cretaceous Luscar Group (revised) of the northern and north-central Foothills of Alberta. Bulletin of Canadian Petroleum Geology, v. 33, p. 1-11.

Langenberg, C.W., Kalkreuth, W., and Wrightson, C.B.
1987: Deformed Lower Cretaceous coal-bearing strata of the Grande Cache area, Alberta. Alberta Research Council, Bulletin 56, 54 p.

Langenberg, C.W., Macdonald, D.E., Kalkreuth, W., Strobl, R.S., and Bahnsen, B.
1988: An initial assessment of controls on coal quality variation in the Cadomin-Luscar coalfield. Alberta Research Council, Open File Report 1988-06.

Macdonald, D.E., Langenberg, C.W., and Strobl, R.W.
1988: Cyclic marine sedimentation in the Lower Cretaceous Luscar Group and Spirit River Formation of the Alberta Foothills and Deep Basin. In Sequences, Stratigraphy, Sedimentology: Surface and subsurface, D.P. James and D.A. Leckie (eds.); Canadian Society of Petroleum Geologists, Memoir 15, p. 143-154.

MacKay, B.R.
1929: Cadomin, Alberta. Geological Survey of Canada, Map 209A.

1930: Stratigraphy and structure of the bituminous coalfields in the vicinity of Jasper Park, Alberta. Canadian Mining and Metallurgical Bulletin, no. 222, Transactions Section, p. 1306-1342.

McLean, J.R.
1982: Lithostratigraphy of the Lower Cretaceous coal-bearing sequence, Foothills of Alberta. Geological Survey of Canada, Paper 80-29, 46 p.

McLean, J.R. and Wall, J.H.
1981: The Early Cretaceous Moosebar sea in Alberta. Bulletin of Canadian Petroleum Geology, v. 29, p. 334-377.

Mellon, G.B.
1967: Stratigraphy and petrology of the Lower Cretaceous Blairmore and Mannville groups, Alberta Foothills and Plains. Alberta Research Council, Bulletin 21, 270 p.

Mountjoy, E.W.
1959: Miette, Alberta. Geological Survey of Canada, Map 40-1959.

Petrology and sedimentology of Gates Formation coals, northeastern British Columbia: preliminary results

M.N. Lamberson[1], W. Kalkreuth, and R.M. Bustin[1]
Institute of Sedimentary and Petroleum Geology, Calgary

Lamberson, M.N., Kalkreuth, W., and Bustin, R.M., Petrology and sedimentology of Gates Formation coals, northeastern British Columbia: preliminary results. In Contributions to Canadian Coal Geoscience, Geological Survey of Canada, Paper 89-8, p. 88-95, 1989.

Abstract

Reported herein are the preliminary results of a petrological and sedimentological study of bituminous coals of the Gates Formation in northeastern British Columbia. Banded lithotypes predominate in all of the seams studied. No fibrous coal (fusain) in thick enough accumulations to constitute a lithotype occur. Maceral analyses indicate that the seams are vitrinite-rich; liptinite occurs in trace amounts. Of the inertinite maceral group, semifusinite is in greatest concentration.

Résumé

Le présent rapport comprend les résultats préliminaires d'une étude pétrologique et sédimentologique des charbons bitumineux de la formation de Gates du nord-est de la Colombie-Britannique. Des charbons lithotypes zonés sont prédominants dans tous les filons étudiés. Il n'y a pas de charbons ligneux (fusain) dans les filons assez épais pour constituer un lithotype. Des analyses macérales indiquent que les filons sont riches en vitrinite; il y a aussi des indices de liptinite. Dans le groupe macéral de type inertinite, la semifusinite est l'élément qui présente la plus grande concentration.

INTRODUCTION

The technological characteristics of coal are fundamentally controlled by composition. In order to develop a methodology for predicting more accurately variations in coal quality within a mine, a petrological and sedimentological study of coal samples collected from the Lower Albian Gates Formation in the Bullmoose and Quintette areas (Fig. 1) of northeastern British Columbia is in progress. The objectives of this study are: (1) to document the lateral and stratigraphic variation in the organic (maceral, microlithotype and lithotype) and inorganic (trace and minor elements) facies of the coals and associated strata in the Foothills of northeastern British Columbia; and (2) to determine the factors that control the variation. Fieldwork, including sample collection and analysis, began during the summer of 1988. This report presents preliminary results on lithotype variations, maceral analyses and reflectance ranges for selected seams from the Bullmoose and Quintette areas in northeastern British Columbia (Fig. 1). The results are based on a limited number of samples and do not necessarily reflect the current product of either Bullmoose or Quintette Mine.

SITE LOCATION AND GEOLOGY

The study area is in northeastern British Columbia in the Rocky Mountain Foothills and Great Plains between 54°45' and 55°30' North latitude, and 120°15' and 121°30' West longitude (Fig. 1). The regional geology of the area was described by Stott (1968, 1982). Leckie (1983) and Carmichael (1983) studied the regional sedimentology of the Gates Formation. Lower Cretaceous strata consist of a series of transgressive-regressive clastic wedges deposited in response to periodic uplift of the Cordillera (Smith et al., 1984). The Moosebar (marine) and Gates (nonmarine and nearshore marine) formations and their subsurface equivalents, the Wilrich, Falher and Notikewin members of the Spirit River Formation (Fig. 2), form one of the transgressive-regressive sedimentary packages. Moosebar sediments were deposited as the Boreal sea advanced southward to the vicinity of the Elbow River, Alberta (McLean, 1982). Renewed uplift and erosion in the Cordillera resulted in a northward progradation of the Gates Formation sediments over the Moosebar sediments. The northward advance was not uniform; Leckie (1986) recorded seven individual coarsening-upward regressive cycles within the Moosebar-Gates interval.

The Gates Formation crops out in the Foothills from north of the study area at the "Gates" of the Peace River near Hudson Hope, British Columbia, southeastward across the B.C.-Alberta border to within the vicinity of the Clearwater River area (Langenberg and McMechan, 1985). The northern limit of economic coal deposits in the Gates Formation is in the vicinity of the Bullmoose Mine leases. North of the Bullmoose Mine, the strata consist primarily of marine shelf sediments (Stott, 1982; Leckie and Walker, 1982). Within the study area there is extensive intertonguing of marine and nonmarine facies.

Within the study area, no formal subdivision of the Gates Formation has been widely accepted. Informally, three major subdivisions (Fig. 2) are made (Rance, 1985; Leckie, 1986; Carmichael, 1988): Torrens member (lower Gates); middle Gates; and upper Gates. Carmichael (1988) correlated the Torrens member with the Falher cycle "F", the middle Gates with Falher cycles "E" through "A" and the upper Gates with the Notikewin member of the Spirit River Formation (subsurface terminology, Fig. 2). The coal seams currently being mined at Bullmoose and Quintette are found within the middle Gates. Thinner (non-economic) seams are found within the upper Gates.

[1]Department of Geological Sciences University of British Columbia Vancouver, B.C. V6T 2B4

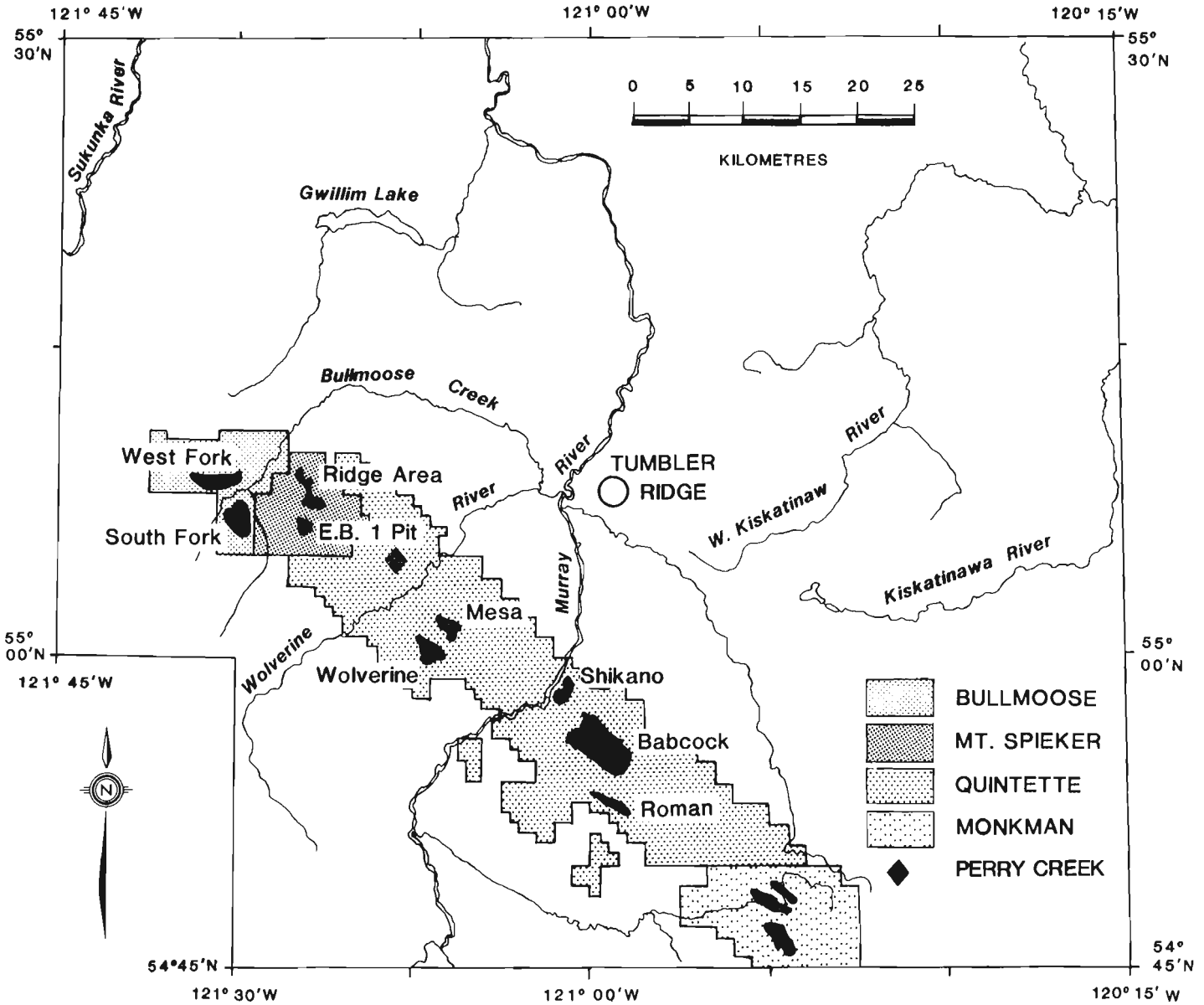

Figure 1. *Location map of study area. Shaded areas indicate major coal leases. Diamond indicates location of outcrop sample of J seam on Perry Creek Road. Named areas are current production sites or areas of proposed development. Modified from Matheson (1986).*

No correlation of seams from mine to mine in the study area has been published. Nine coal seams are recognized in the Quintette area (Rance, 1985); from youngest to oldest, the seams are referred to as A, B, C, D, E, F, G/I, J and K. Seams A, B and C are found within the upper Gates, are thin and are not mined. Five seams of economic thickness are present in the Bullmoose area (Drozd, 1985); the seams are designated, from oldest to youngest A (A1 and A2), B, C, D and E. Upper Gates coals are present at Bullmoose, but are not named. Details of the pit geology and mining methods, as well as gross chemical and compositional characteristics of the seams at Quintette and Bullmoose can be found in Rance (1985) and Drozd (1985), respectively. Petrographic characteristics and a discussion of technological properties of selected Gates coals from the study area are discussed in Steller et al. (1987) and Kalkreuth (1988). A discussion of coal facies and depositional environments based on channel samples collected from many of the Gates coal seams are discussed in Kalkreuth and Leckie (in press) and in Kalkreuth et al. (this volume).

The Gates Formation is inferred to represent a wave and tide-dominated linear clastic shoreline deposit (Leckie and Walker, 1982). The Lower Cretaceous coastlines are believed to have been characterized by arcuate-shaped wave-dominated deltas and associated strandplains (Kalkreuth and Leckie, in press). Thick, laterally extensive peat (coal) deposits accumulated on the delta plain setting shoreward of thick (15-35 m), regionally extensive sheets of shoreface sand and gravel (traceable along strike for about 230 km).

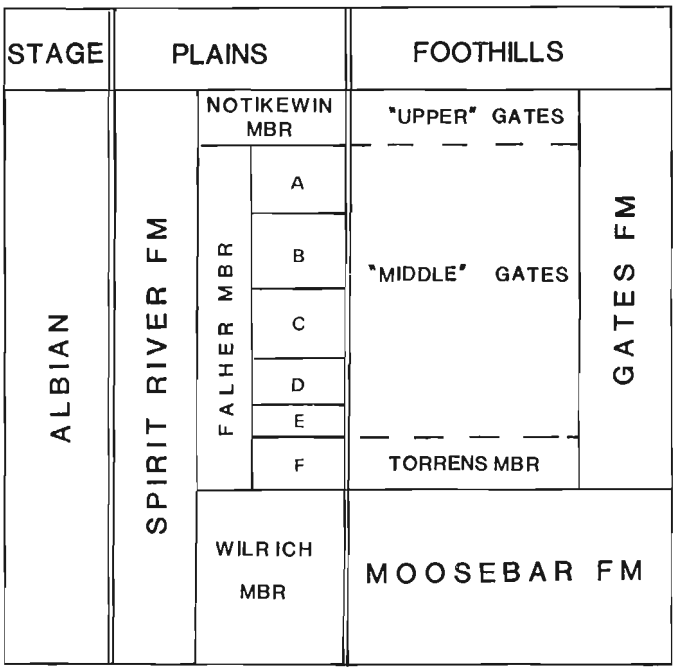

Figure 2. Stratigraphic chart of Lower Cretaceous formations in northeastern British Columbia. Modified from Leckie (1986) and Carmichael (1988).

METHODS

During June, July and August of 1988, channel samples of all of the Quintette seams exclusive of G/I, column (bench) samples of all of the Bullmoose seams with the exception of B, 50 coal grab samples (from core) and representative coal and carbonaceous rock fragments in the cuttings of 20 Deep Basin petroleum wells were collected. Approximately 1300 samples of strata associated with the coal were taken from outcrop and core. In addition, a number of plant fossils were collected.

Lithotype descriptions of the A, B, C, E1, E2, E3, F, K1 and K2 seams (Shikano area, Fig. 1) were made at the collection site and a channel sample of each seam was taken. In addition to the lithotypes description, a column sample of the E2 seam was removed from the Wolverine area. A channel sample of the Quintette J seam was collected from an outcrop on the Perry Creek road (between Mount Spieker and the Wolverine River, Fig. 1).

Bench samples of seams A1 (two sites), A2, C, D, and E at Bullmoose were collected. Lithotype descriptions of the Bullmoose samples were made in the laboratory after returning from the field.

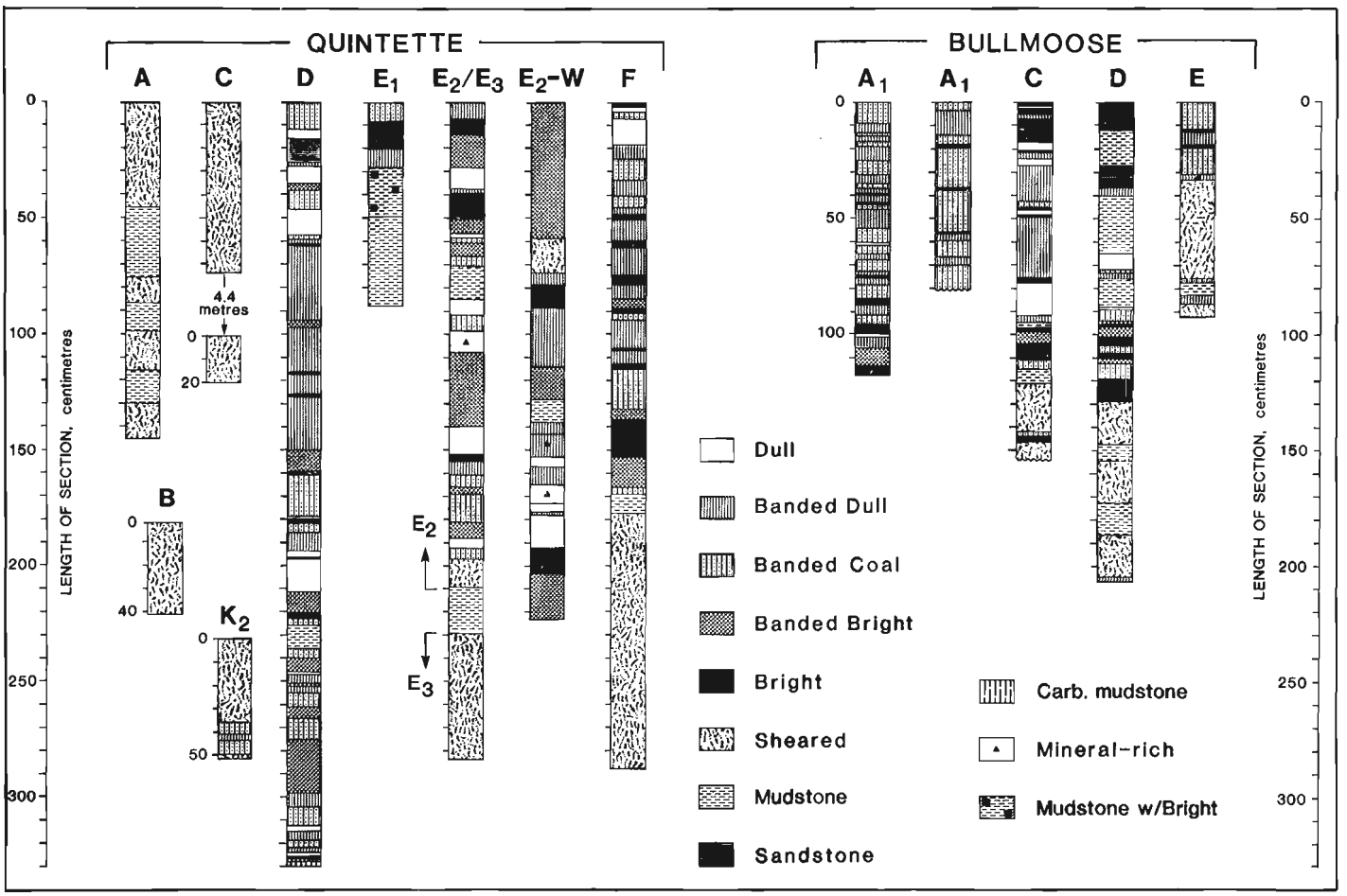

Figure 3. Lithotype columns for selected bench seam samples collected during 1988 from the Bullmoose and Quintette areas. Seam designation at top of column. All of the Quintette seams, with the exception of E2-W, were collected from Shikano pit. E2-W was collected from Wolverine pit. The base of the shale in seam E2 is in contact with the E2/E3 section (drawn to the right of E1).

Coal lithotypes (layers of different brightness or texture within the coal seam) were described using a modified version of the Australian classification scheme (Diessel, 1965; Marchioni, 1980). Seven lithotypes were distinguished: bright, banded bright, banded coal, banded dull, dull, fibrous and sheared. A minimum band thickness of one centimetre was used in defining lithotypes. Mineral partings in the seam were noted. The seven lithotypes are illustrated in Plate 1, and are described in Table 1.

A crushed particle pellet was prepared for each of the channel samples taken (Quintette). Maceral and vitrinite reflectance analyses were performed on each pellet. All of the maceral analyses are based on 500 points, and both inorganic and organic matter was counted. With the exception of sample 705, C seam (Fig. 3), all of the vitrinite reflectance values are based on 50 measurements per sample; C seam is mineral-rich, and only 25 grains were analysed. Table 2 lists the sample number, thickness, vitrinite reflectance and maceral composition of the channel samples.

TABLE 1

LITHOTYPE CLASSIFICATION SCHEME
(modified from Diessel, 1965 and Marchioni, 1980)

BRIGHT	subvitreous to vitreous lustre, conchoidal fracture, less than 10% dull coal laminae
BANDED BRIGHT	predominantly bright coal with 10-40% dull laminae
BANDED COAL	interbedded dul and bright coal in approximately equal proportions
BANDED DULL	dull coal with approximately 10-40% bright laminae
DULL	matte lustre, uneven fracture, less than 10% bright coal laminae, hard
FIBROUS	satin lustre, very friable, sooty to touch
SHEARED COAL	variable lustre, disturbed bedding, numerous slip/slickenside surfaces, very brittle

RESULTS

Lithotype Variations

Bullmoose Area

Lithotype descriptions of Bullmoose seams A1 (two locations), C, D and E are graphically illustrated in Figure 3. Other bench samples collected are currently being analysed. Banded lithotypes predominate in the seams studied; fibrous coal in accumulations thick enough to be separated out as a distinct lithotype do not occur in any of the seams. Fibrous material (fusain in Stopes-Heerlan terminology) is present, however, as scattered fragments and very thin laminae (Plate 1, fig. F). No consistent pattern of repetition of the lithotypes appears to exist with respect to position within seams. The basal portions of three out of the four seams studied are sheared such that the original lithotype stratigraphy is indistinguishable. Additional analysis and sample collection is necessary.

The two column samples of seam A1 were taken approximately 50 m apart. Although the basal section of seam A1 was not exposed at the more southerly collection site, it appears that the seam stratigraphy is relatively consistent over the 50 m. The seam is primarily composed of banded coal and banded dull layers. Bright layers at both sites are lenticular in nature. Thicker bright layers occur within the basal portion of the seam. In contrast, the bright layers in seams C and D are relatively thick and occur in the middle and upper sections of the seams. Both C and D contain several mineral partings, as well as dull layers (absent in A1), indicating that the wetland environments of the two seams may have been subject to flooding, as well as to dry conditions with more intense degradation levels. Seam E is similar to A1, in that there are fewer mineral partings and thinner bright layers than are observed in seams C and D. However, pyrite was observed on some bedding surfaces of seam E, indicating that there may have been a marine influence.

Quintette Area

Lithotype profiles of the seams collected from the Shikano area, and the E2 seam from the Wolverine area (E2-W) are shown in Figure 3. The seams sampled are thicker in the Quintette area than in the Bullmoose area. Seams A, B and C (not mined at Quintette) are separated from seam D by 67 m of conglomerate and marine shelf sandstones. The interval represents a marine transgression, and separates the middle Gates from the Upper Gates (Carmichael, 1988).

No fibrous coal is present in accumulations thick enough to represent a single lithotype. The thinner seams, i.e., A, B and C, as well as the upper 36 cm of seam K2, are extensively sheared. The basal portions of the Shikano E3 seam and F seam are also sheared. Like the Bullmoose seams, there does not appear to be a consistent pattern of repetition of lithotypes with respect to position within the seam. However, both the D seam, and the upper 1.7 m of the F seam (above the mineral parting, Fig. 3) exhibit a gradual decrease in the bright and banded bright lithotypes towards the top of the seam and a concomitant increase in the dull and banded dull lithotypes. In contrast, the E2 seam does not show the aforementioned trend at either collection site; rather, the stratigraphy alternates between banded bright and bright, and dull and banded dull layers. Individual layers in seam E2 are not correlatable over the 12 km distance which separates the two collection sites (Fig. 1).

Maceral and Reflectance Analyses

Maceral and reflectance analysis results are given in Table 1. Mean maximum reflectance in oil ranges from 1.04% (B seam) to 1.51% (K2 seam), indicating a rank range of high volatile A bituminous to medium-low volatile bituminous. Reflectance tends to increase with stratigraphic depth. However, there is some variation that might reflect the varying amounts of mineral matter, oxidation levels, etc. within the sample material.

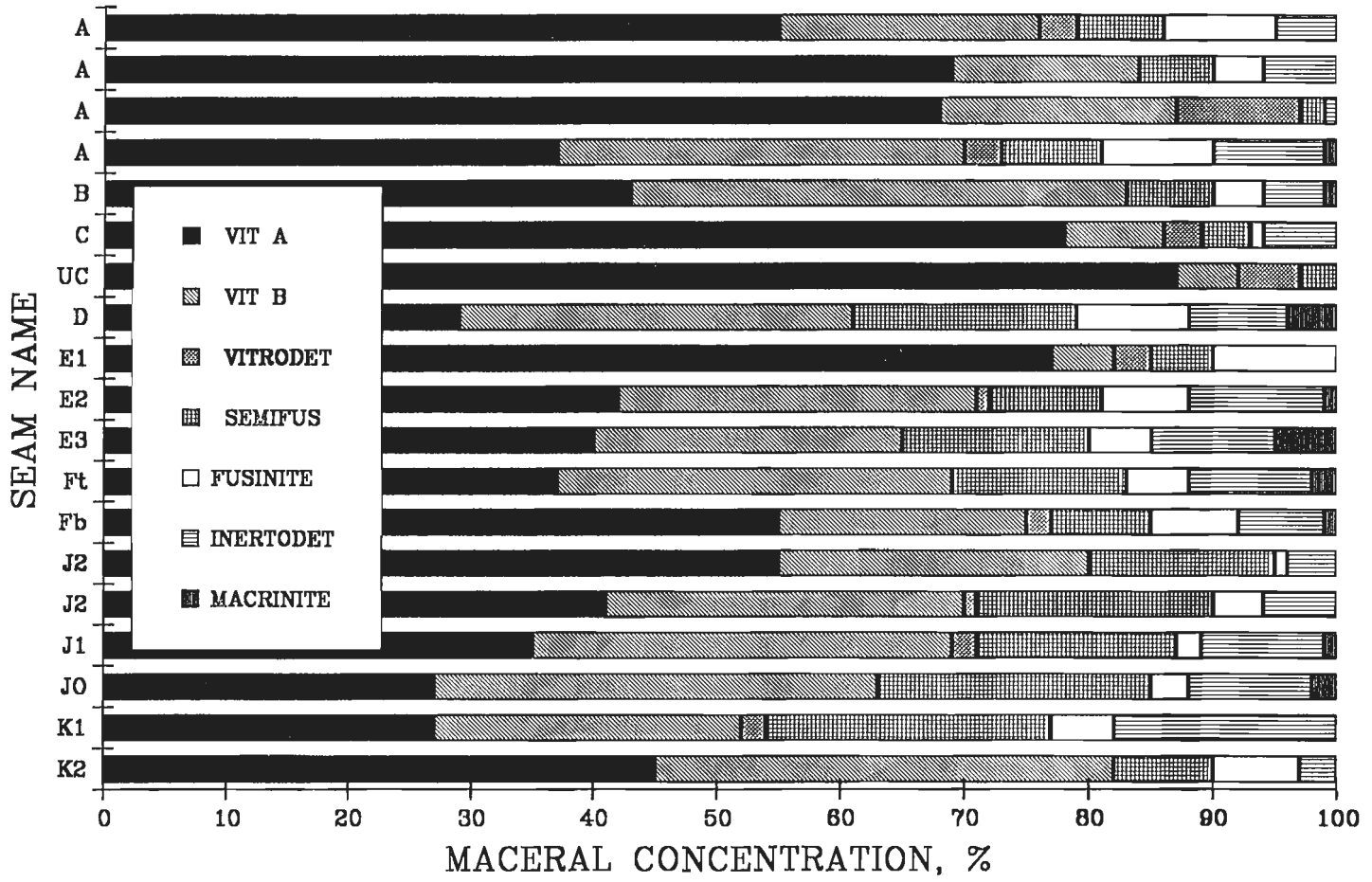

Figure 4. Bar graph illustrating the maceral composition of the channel samples collected from coal seams in the Shikano pit (Quintette). Seam numbers are given to the left of the corresponding bar. Maceral concentrations expressed on mineral matter-free basis. Height of bars is not indicative of thickness. VIT A = vitrinite A; VIT B = vitrinite B; VITRODET = vitrodetrinite; SEMIFUS = semifusinite; INERTODET = inertodetrinite.

Figure 4 is a schematic representation of the variation in maceral composition, on a mineral matter-free basis, of the sampled seams. The seams are shown in stratigraphic order, but no relative thickness is implied. Liptinite occurs in trace amounts (<1% by volume). Vitrinite, present as vitrinite A, vitrinite B and vitrodetrinite, dominates the maceral counts and ranges in concentration from 54 to 97%. The vitrodetrinite is composed of fragments of vitrinite A, and is present in the form of stringers parallel to bedding. Semifusinite is the dominant inertinite maceral; macrinite concentrations are quite low. Quartz and clay are the most common minerals; pyrite was observed in seams D and E, but only in trace concentrations.

FUTURE RESEARCH

Currently, the bench and spot coal samples are being processed for further analysis. The bench samples will be split. Half of the sample will be kept intact, polished and microlithotypes described. Each lithotype of the other half of the bench samples will be analysed petrographically and by Rock-Eval pyrolysis. The spot samples will also be analysed petrographically and by Rock-Eval pyrolysis.

In order to properly evaluate compositional variation in terms of organic depositional environment, it will be necessary to collect additional bench samples. Future field work will concentrate in the Bullmoose and Mt. Spieker areas

PLATE 1

EXAMPLES OF COAL LITHOTYPES
Scale bar in photos is in centimetres

A. DULL COAL – <10% bright coal. Note dull, grey, matte appearance. Bright streak in upper part of photograph is <1 cm thick. E seam, Shikano pit, Quintette mine.

B. BANDED DULL – 10-40% bright coal. Bright material appears as black streaks in coal. Grey background material with waxy lustre is dull coal matrix. D seam, Bullmoose mine.

C. BANDED COAL – approximately 50% dull, 50% bright layers. Bright coal appears black with glassy lustre, conchoidal fracture. D seam, Bullmoose mine.

D. BANDED BRIGHT COAL – 10-40% dull coal. Thick bright layers with thin streaks of dull coal. E seam, Shikano Pit, Quintette mine.

E. BRIGHT COAL – <10% dull coal. Note glassy lustre, black color, conchoidal fracture. Material is quite brittle. D seam, Bullmoose mine.

F. FIBROUS COAL – bedding plane surface. Note charcoal-like appearance. Friable, sooty to touch. E seam, Shikano pit, Quintette mine.

G, H. SHEARED COAL – Two examples of sheared coal. Note random orientation of layers, slickenside surfaces. Material is quite friable, falls apart easily to touch.

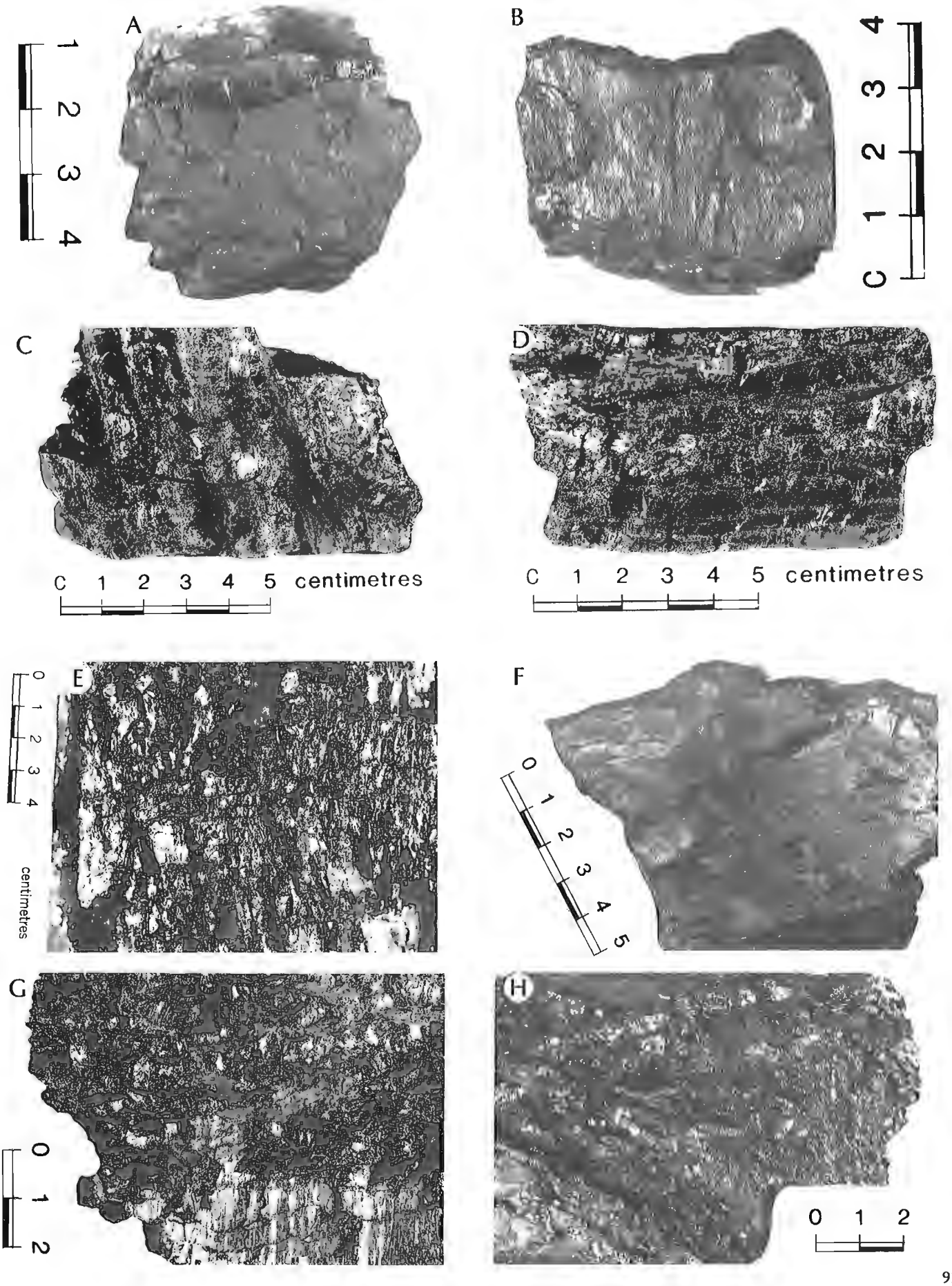
A
B
C
D
E
F
G
H
centimetres
centimetres

TABLE 2

Thickness, vitrinite reflectance and maceral composition (mineral matter-free basis) of coal channel samples, Shikano Pit, Quintette Mine (results shown do not necessarily reflect the current product of Quintette Coal)

SN	SEAM	THICK (cm)	REFLECTANCE %		VITA %	VITB %	V'DET %	SFUS %	FUS %	I'DET %	MAC %	TV %	TI %
			MEAN	S.D.									
710/88	A	45	1.08	0.04	37	33	3	8	9	9	1	73	27
709/88	A	11	1.05	0.04	68	19	10	2	0	1	0	97	3
708/88	A	17	1.16	0.04	69	15	0	6	4	6	0	84	16
707/88	A	15	1.10	0.04	55	21	3	7	9	5	0	79	21
711/88	B	40	1.04	0.05	43	40	0	7	4	5	1	83	17
705/88	C	73	1.14	0.04	87	5	5	3	0	0	0	97	3
706/88	UC	20	1.18	0.04	78	8	3	4	1	6	0	89	11
721/88	D	510	1.14	0.04	29	32	0	18	9	8	4	61	39
720/88	E1	36	1.16	0.04	40	25	0	15	5	10	5	65	35
719/88	E2	194	1.23	0.04	42	29	1	9	7	11	1	72	28
718/88	E3	54	1.14	0.04	77	5	3	5	10	0	0	85	15
717/88	Fu	192	1.45	0.05	37	32	0	14	5	10	2	69	31
716/88	Flo	110	1.42	0.04	55	20	2	8	7	7	1	77	23
715/88	Jo	110	1.33	0.05	27	36	0	33	3	10	2	63	37
714/88	J1	140	1.33	0.05	35	34	2	16	2	10	1	71	29
713/88	J2	150	1.34	0.04	41	29	1	19	4	6	0	71	29
712/88	J2	55	1.38	0.05	55	25	0	15	1	4	0	80	20
703/88	K1	100	-	-	27	25	2	23	5	18	0	54	46
704/88	K2	52	1.51	0.04	45	37	0	8	7	3	0	82	18

SN = channel sample number; THICK = channel thickness; REFLECTANCE = mean maximum in oil; VIT = vitrinite; V'DET = Vitrodetrinite; SFUS = semifusinite; FUS = fusinite; I'DET = inertodetrinite; MAC = macrinite; TV = %total vitrinite; TI = % total inertinite

where tectonic deformation is minimal and there is an opportunity to sample from nonmarine, transitional and marine depositional environments.

Laboratory research will focus on characterizing the coal lithotypes in terms of maceral composition. The variation in type and quantity of organic matter in the lithofacies associated with the coals will be investigated. The rock samples will be analysed in terms of the same parameters as the coal samples and organic facies delineated. In order to further aid in understanding the types and evolution of the wetland depositional environments, fossil plant assemblages will be determined.

ACKNOWLEDGMENTS

Dr. D.L. Marchioni of Petro-Logic Services performed the maceral analyses reported in this paper. The authors would like to thank Mr. D. Johnson and the staff at the Charlie Lake core storage facility (B.C. Ministry of Energy, Mines and Petroleum Resources) for their assistance with petroleum and coal drill core. We would also like to thank the exploration and production geological staff at Quintette and Bullmoose Mines for their help with sample collection and access to areas within the mines. Mr. Murray Gant and Mr. John Whittles provided excellent assistance in the field and are gratefully acknowledged. Support for this project was in part provided by the Geological Survey of Canada.

REFERENCES

Carmichael, S.M.M.

1983: Sedimentology of the Lower Cretaceous Gates and Moosebar formations, northeast coalfields, British Columbia. University of British Columbia, unpublished Ph.D. thesis, 285 p.

1988: Linear estuarine conglomerate bodies formed during a Mid-Albian marine transgression: "Upper Gates" Formation, Rocky Mountain Foothills of northeastern British Columbia. In Sequences, Stratigraphy, Sedimentology: Surface and Subsurface, D.P. James and D.A. Leckie (eds.); Canadian Society of Petroleum Geologists, Memoir 15, p. 49-62.

Diessel, C.F.K.

1965: Correlation of macro- and micropetrography of some New South Wales coals. In Proceedings-General, Vol. 6, J.T. Woodcock, R.T. Madigan and R.G. Thomas (eds.); 8th Commonwealth Mineralogical and Metallurgical Congress, Melbourne, p. 669-677.

Drozd, R.

1985: The Bullmoose mine project. In Coal in Canada, T.H. Patching (ed.); Canadian Institute of Mining and Metallurgy, Special volume 31, p. 263-268.

Kalkreuth, W.
1988: Kanadische Kreidekohlen-Inkohlungsgrad und petrographische Zusammensetzung kanadischer Kreidekohlen in den Rocky Mountain Foothills von NE-British Columbia und Westzentralalberta. Erdöl und Kohle, v. 41, no. 2, p. 61-70.

Kalkreuth, W. and Leckie, D.A.
in press: Sedimentological and petrographical characteristics of Cretaceous strandplain coals: a model for coal accumulation from the North American Western Interior Seaway. International Journal of Coal Geology.

Kalkreuth, W., Roy, C., and Steller, M.
1989: Conversion characteristics of selected Canadian coals based on hydrogenation and pyrolysis experiments. This volume.

Langenberg, W. and McMechan, M.
1985: Lower Cretaceous Luscar Group (revised) of the northern and north-central Foothills of Alberta. Bulletin of Canadian Petroleum Geology, v. 33, no. 1, p. 1-11.

Leckie, D.A.
1983: Sedimentology of the Moosebar and Gates formations (Lower Cretaceous). McMaster University, unpublished Ph.D. thesis, 515 p.

1986: Rates, controls, and sand-body geometries of transgressive-regressive cycles: Cretaceous Moosebar and Gates formations, British Columbia. American Association of Petroleum Geologists, Bulletin, v. 70, p. 516-535.

Leckie, D.A. and Walker, R.G.
1982: Storm- and tide-dominated shorelines in the Cretaceous Moosebar-lower Gates interval - outcrop equivalents of Deep Basin gas traps in western Canada. American Association of Petroleum Geologists, Bulletin, v. 66, p. 138-157.

Marchioni, D.L.
1980: Petrography and depositional environment of the Liddell Seam, Upper Hunter Valley, New South Wales. International Journal of Coal Geology, v. 1, p. 35-61.

Matheson, A.
1986: Coal in British Columbia. British Columbia Ministry of Energy, Mines and Petroleum Resources; Paper 1986-3, 170 p.

McLean, J.R.
1982: Lithostratigraphy of the Lower Cretaceous coal-bearing sequence, Foothills of Alberta. Geological Survey of Canada, Paper 80-29, 31 p.

Rance, D.C.
1985: The Quintette coal project. In Coal in Canada, T.H. Patching (ed.); Canadian Institute of Mining and Metallurgy, Special Volume 31, p. 254-262.

Smith, D.G., Sneider, R.M., and Zorn, C.E.
1984: The paleogeography of the Lower Cretaceous of western Alberta and northeastern British Columbia in and adjacent to the Deep Basin of the Elmworth Area. In Elmworth-Case Study of a Deep Basin Gas Field, J.A. Masters (ed.); American Association of Petroleum Geologists, Memoir 38, p. 79-114.

Steller, M., Kalkreuth, W., and Hodek, W.
1987: Hydrogenation characteristics of selected subbituminous and bituminous coals - micropetrological and chemical studies on feedstock and reaction residues. Erdöl und Kohle, v. 40, no. 9, p. 383-393.

Stott, D.F.
1968: Lower Cretaceous Bullhead and Fort St. John groups between Smoky and Peace rivers, Rocky Mountain Foothills, northeastern British Columbia. Geological Survey of Canada, Bulletin, v. 152, 279 p.

1982: Lower Cretaceous Fort St. John Group and Upper Cretaceous Dunvegan Formation of the Foothills and Plains of Alberta, British Columbia, District of Mackenzie and Yukon Territory. Geological Survey of Canada, Bulletin 328, 124 p.

Organic petrology of thermally altered coals from Telkwa, British Columbia

F. Goodarzi and A.R. Cameron
Institute of Sedimentary and Petroleum Geology, Calgary

Goodarzi, F. and Cameron, A.R., Organic petrology of thermally altered coals from Telkwa, British Columbia. In Contributions to Canadian Coal Geoscience, Geological Survey of Canada, Paper 89-8, p. 96-103, 1989.

Abstract

Alteration of coal by dyke intrusion has been examined in the Telkwa Coalfield of British Columbia. The coal exhibits progressively greater alteration with increasing proximity to the dyke. Temperature of alteration at dyke contact is estimated to exceed 575°C. At a distance of 120 cm from the dyke unaltered coal was observed. Alteration characteristics include: increased maximum reflectance, from 0.78 in the unaltered coal to 8.30 in the coke; increase in bireflectance ($R_o max - R_o min$) and development of coke mosaic structure. Assimilation of less reactive components by reactive components was observed in the altered coal, which also contains spherulitic and layered pyrolytic carbon formed by thermal cracking of coal tar. Spherulitic carbon in the contact zone suggests localized temperatures significantly higher than 575°C. Development of fluidity and mosaic texture in semi-inert macerals (pseudovitrinite) indicates high heating rates as does the strong anisotropy developed in some liptinite macerals.

Résumé

L'altération que subissent les charbons lors de l'intrusion d'un dyke a été étudiée dans le bassin houiller de Telkwa en Colombie-Britannique. On a remarqué que l'altération du matériel charbonnier se fait plus prononcée, et de façon progessive, plus on se rapproche du dyke. Le niveau de la température d'altération des charbons en contact avec le dyke a été estimé à plus de 575°C. À une distance de 120 cm du dyke, on a trouvé des charbons qui n'avaient subi aucune modification. Les caractéristiques de l'altération comprennent: un taux de réflectance maximum accru, allant de 0,78 % dans le charbon non modifié à 8,30 % dans le coke; une augmentation du taux de bi-réflectance ($R_o max - R_o min$) et le développement d'une structure en forme de mosaïque typique au coke. Une assimilation des composants moins réactifs par des composants réactifs a été observée dans le charbon altéré, qui contient d'ailleurs du carbone pyrolitique caractérisé par la présence de sphérulites et de stratifications formées par la fissuration thermique du goudron de houille. Le carbone sphérulitique dans la zone de contact laisse supposer des températures locales beaucoup plus élevées que 574°C. L'apparition d'un comportement fluidal et la présence d'une texture en forme de mosaïque dans des macéraux semi-inertes (pseudovitrinite) indiquent des taux de chauffage élevés, comme en témoigne également la forte anisotropie que l'on observe dans certains macéraux de type liptinite.

INTRODUCTION

Thermally metamorphosed coals have been reported from many areas of the globe, for example Antarctica (Brown and Taylor, 1961; Kisch and Taylor, 1966; Schapiro and Gray, 1966); Australia (Taylor, 1961); England (Marshall, 1936; Aganoglu, 1972; Melvin, 1974; Jones and Creaney, 1977; Creaney, 1980); Germany (Stach, 1952) and South Africa (Mackowsky, 1968).

Thermally metamorphosed coals are formed due to intrusion of dykes and sills, or by invasion of plutonic or volcanic rocks. The temperature of metamorphism can be up to 1000°C (Chandra and Taylor, 1982) and the metamorphism is greatest in the contact zone with the invading igneous rocks (Jones and Creaney, 1977; Chandra and Taylor, 1982).

Jones and Creaney (1977) have examined thermally metamorphosed coals from northeast England (see also Creaney, 1980, and found that reflectance increased slowly with decreasing distance towards the contact.

The morphology of coal changes progressively towards the contact in the following sequence:

a) Liptinite becomes vesiculated and telocollinite develops some small slits.

b) Coal becomes plastic, vitrinite develops primary vesiculation.

c) Coal becomes brecciated and liptinite disappears.

d) Semi-coke showing mosaic structure develops.

e) Secondary vesiculation in granular coke develops; graphite with reflectance of 16.0% in oil begins to develop (Creaney, 1980).

The present paper discusses results of a study of thermally metamorphosed coal from a seam in the Telkwa Coalfield, British Columbia (Fig. 1). The coal occurs in the Red Rose Formation of Early Cretaceous age (Koo, 1983, 1984). The predominant rank of unaltered coal in this field is high volatile bituminous. According to Koo (1983) a granodiorite and quartz monzonite stock of Late Cretaceous age intrudes the coal measures at one end of the field, and elsewhere, mafic dykes of unknown age cut some of the coal seams. The suite of samples reported on in this paper comes from the vicinity of one of the dykes. The dyke is 2.4 m wide and has been identified as alkali basaltic in composition according to criteria proposed by Irvine and Baragar (1971).

EXPERIMENTAL

Samples were collected from the immediate contact of the dyke and also from distances of 5, 25, 37, 65, 90, 120, 210 and 420 cm from the dyke. Samples were ground to 20 mesh (<850 μm), mounted in cold-set resin and polished following the method described by Mackowsky (1982). Ultimate analyses were carried out according to standard procedures (ASTM, 1979).

Maximum and minimum reflectances in oil (n oil = 1.518 at 546 nm) were determined on the polished samples using a Zeiss M.P.M. II microscope fitted with white (halogen), and fluorescence (HBO) light sources. Data were recorded on a Zonax microcomputer. The number of reflectance measurements on each sample was fifty. Bireflectance ($R_o$max-$R_o$min) was calculated for all samples. Reflectance data along with results from ultimate analysis are reported in Table 1.

Photomicrographs were taken with plane polarised light and partially crossed polars.

RESULTS AND DISCUSSION

The optical characteristics of the thermally altered coal at Telkwa can be better understood by first briefly reviewing published results of laboratory studies on the thermal treatment of coal macerals.

Coal macerals can be divided into two groups based on their behaviour during carbonization:

1. Macerals which show fluidity, become anisotropic and produce granular mosaic, for example, vitrinite (desmocollinite and telocollinite) in coal of bituminous rank [%C(daf) = 80-91], and liptinite (Goodarzi and Murchison, 1973, 1976a, 1978; Goodarzi, 1981, 1984a, b).
2. Macerals which have almost no fluidity and remain essentially isotropic or develop basic anisotropy during carbonization. Vitrinite in low rank coal [%C(daf) = <80] and most of the inertinite macerals belong to this group (Goodarzi and Murchison, 1973; Creaney, 1980; Goodarzi, 1984c).

However, there are exceptions to this grouping. Goodarzi and Murchison (1978) found that some macerals that are virtually non-fluid at low heating rates became fluid at higher heating rates. As an example, they found that a low rank vitrinite [%C(daf) = <80] was non-fluid at a heating rate of 1°C/min but became fluid at a rate of 60°C/min and developed cenospheres and devolatilization vacuoles. Pseudovitrinite is almost non-fluid and retains its original botanical structure at 1°C/min, but becomes fluid when carbonized at 60°C/min (Goodarzi and Murchison, 1976b). The naturally heated sample series of the present study shows a number of these carbonization characteristics.

The Telkwa samples become progressively more altered with decreasing distance from the dyke. Reflectance is a conspicuous aspect of this alteration and reflectance data are plotted on Figure 2. This figure shows that coal sample 4 taken 90 cm from the dyke contact has the same reflectance as the unaltered coal of sample 1, taken over 4 m away from the contact. Sample 4 was affected in other ways as will be shown later, but its reflectance has not changed appreciably. However, samples taken at progressively shorter distances from the contact show a conspicuous increase in maximum reflectance and an equally conspicuous change in bireflectance ($R_o$max-$R_o$min).

The results of chemical (ultimate) analysis (Table 1) also show significant changes in the concentration of elements, especially hydrogen. The variation in chemical data between "fresh" and altered coal is more clearly shown in Figure 3 where atomic H/C is plotted against atomic O/C. The "fresh" samples (1 through 4) plot in one area of the graph that is quite distinct from the altered population (5 through 9). As will be discussed later, sample 4 does not really belong to the "fresh" population.

TABLE 1

Chemical and reflectance data on Telkwa samples

Sample	Distance from dyke (in cm)	Ultimate Analysis (daf): per cent by wt.					Per cent Reflectance (Max. - Min.)		
		C	H	N	S	O [1]	Mf [2]	Mm [3]	P.C. [4]
9	contact	88.8	0.8	0.7	1.5	6.0	6.80-2.54	9.13-5.20	11.30-1.20
8	5	91.0	1.6	0.8	2.3	4.3	7.00-2.50	-	-
7	25	86.0	1.9	0.6	5.8	5.7	8.30-2.09	-	8.1-2.0
6	37	94.1	1.8	0.8	1.4	1.8	6.01-2.27	-	-
5	65	93.0	2.4	1.1	2.5	1.2	5.00-1.96	6.60-2.40	-
4	90	82.4	4.9	0.9	4.0	7.8	0.82-0.78	-	-
3	120	85.4	5.0	1.0	1.5	7.1	0.80-0.78	-	-
2	210	84.4	5.3	1.0	1.3	8.0	0.78-0.72	-	-
1	420	83.0	5.2	0.9	2.2	8.6	0.80-0.69	-	-

1. Oxygen by difference; 2 and 3 fine grained (Mf) and medium grained (Mm) mosaic respectively (definitions after Grint and March 1981)
4. P.C. = pyrolytic carbon

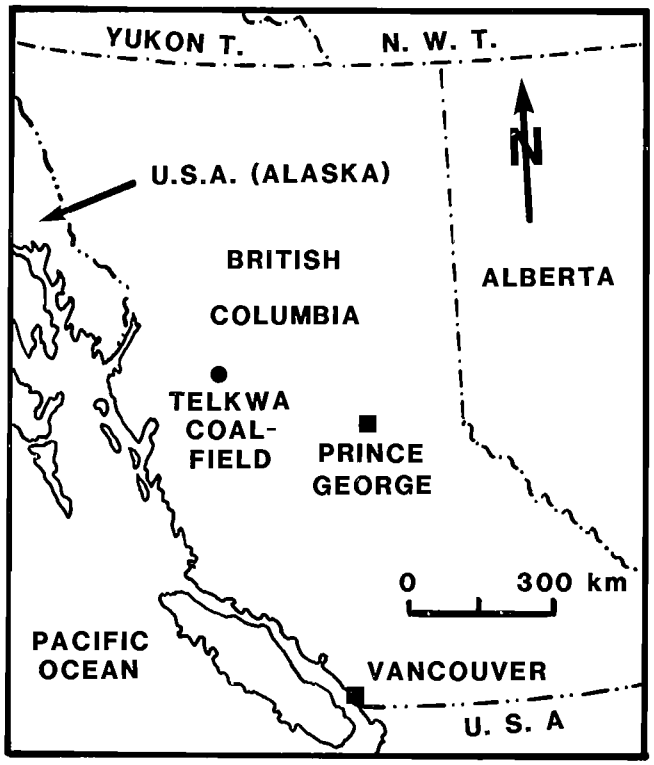

Figure 1. Location of Telkwa Coalfield in British Columbia.

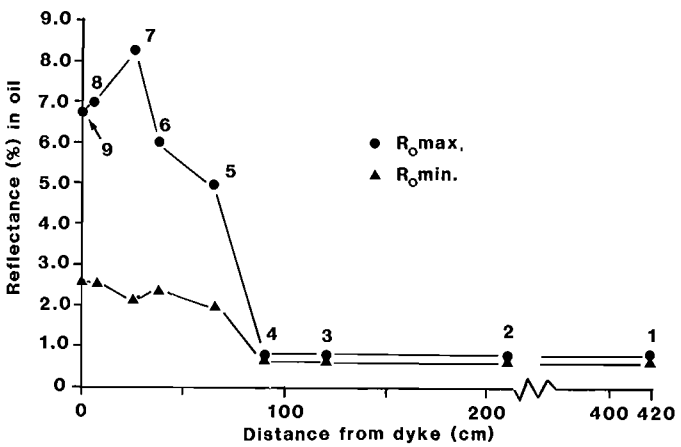

Figure 2. Reflectance data (maximum and minimum) plotted according to distance from dyke; 1, 2, 3, etc. represent sample identification numbers

Based on reflectance parameters and a variety of morphological/textural features observed optically, the Telkwa samples can be divided into four groups:

Group 1. Unaltered coal. This group includes samples 1, 2 and 3. The vitrinite in these samples has a reflectance range of 0.78 to 0.80% $R_o$max (Table 1, Fig. 2), and shows all the features of normal vitrinite for this rank of coal (Fig. 4).

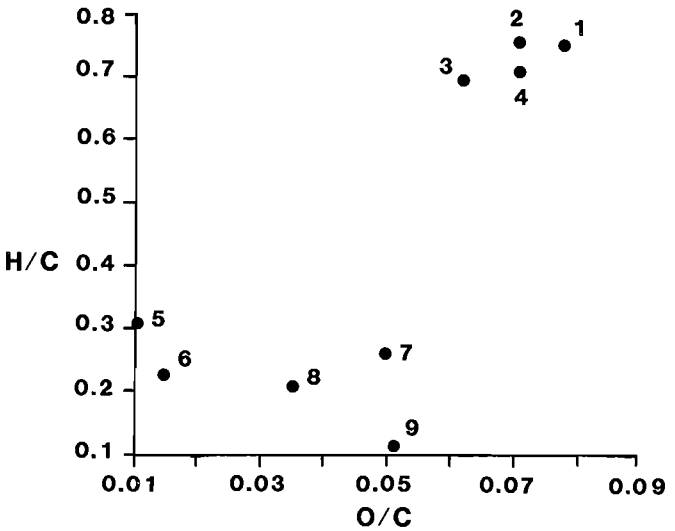

Figure 3. Cross plot of atomic hydrogen/carbon (H/C) and atomic oxygen/carbon (O/C) for Telkwa samples.

Group 2. Altered coal is represented by sample 4. Here, the vitrinite has reflectance (0.82%) almost identical to samples 1, 2 and 3 as well as similar H/C and O/C values, but microscopically the vitrinite shows the development of small vesiculation, and the beginning of slight basic anisotropy (Fig. 5).

Group 3. Brecciated coke ($R_o$max = 5.0-6.0%, Figs. 2 and 3). It includes angular fragments with granular (fine to coarse grained mosaic) anisotropic texture annealed together (Figs. 6a and 7a). This material is found in samples 5 and 6.

Group 4. Coherent coke ($R_o$max = 6.8-7.28%, Table 1, Fig. 2). It consists of coke with medium to coarse grained mosaic texture (Figs. 6b, 7a, 7b). This type of material is first found in sample 5, but its proportion of the total material in the sample increases as the dyke is approached via samples 6 through 9. Other characteristics of the coherent coke are the presence of pyrolytic carbons, in spherulitic, rosette and layered forms (Figs. 7c, 9b, c and 10 c, d).

All macerals have become fluid to some degree. Pseudovitrinite developed coherent coke, devolatilisation vacuoles and anisotropy (Figs. 6c, 9a, 10c). Very coarse grained mosaic was found in coke fragments enclosed by the igneous material.

Chandra and Taylor (1982) classified the organic components of thermally metamorphosed bituminous coals into:

a) "Groundmass" that comprised the alteration products of the vitrinite and liptinite maceral groups. The groundmass remained almost similar to unaltered macerals at temperatures <300°C. At temperatures of 300 to 500°C the groundmass developed granular anisotropy.

b) "Original constituents" were the inertinite group of macerals that remained unchanged even at 300°C. Above this temperature the alteration was limited to distortion and fracturing of inertinite particles.

Figure 4. *Fresh coal, 120 cm from contact.*

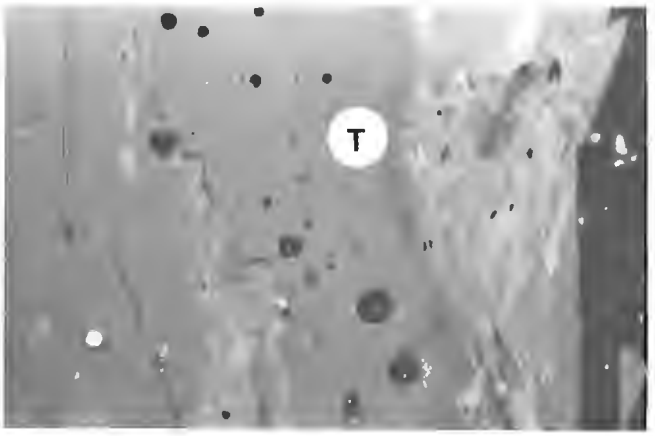

Figure 5. *Altered coal showing vesiculation in telocollinite (t), 90 cm from contact.*

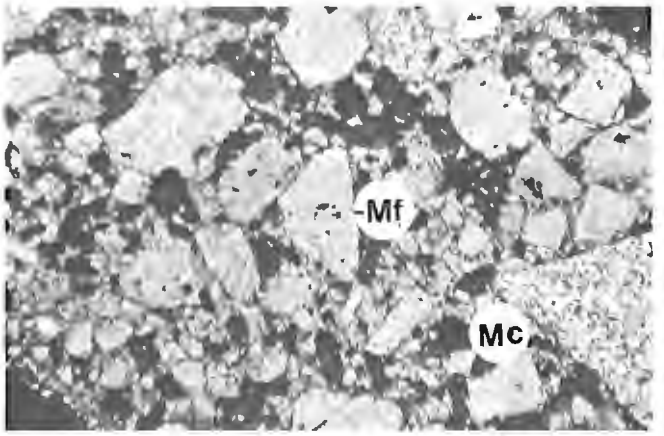

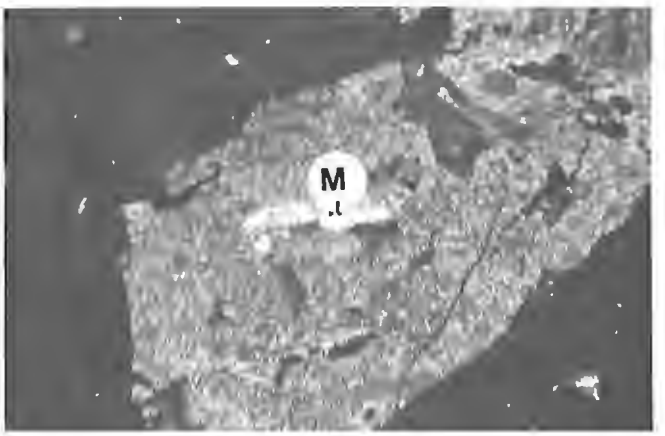

Figure 6. *Altered coal 65 cm from contact.*

a) In situ transformation of angular coal fragments to fine grained (Mf) and coarse grained (Mc) coke.

b) Microspore (M) in altered coal showing stronger anisotropy than the granular mosaic in the matrix.

c) "Newly-formed constituents" included the by-products of thermal treatment, for example coal tar (Sanyal, 1965), which could further thermally crack into pyrolytic carbons.

Thermally metamorphosed coals from Telkwa contain all three of these components (Fig. 5-10). However, a further subdivision of the "groundmass" components can be made utilizing differences in morphology and anisotropy. A detailed study of these components provides clues as to the temperatures reached and the rates of heating. Cutinite in heat-affected coals often retains its original morphology but it developes granular anisotropy (Creaney, 1980; Goodarzi, 1984b). Resinite lenses develop strong basic to domain type anisotropy at low temperatures (450°C), and banded resinite develops coarse grained mosaic (Melvin, 1974; Creaney, 1980; Goodarzi, 1984b). Sporinite often retains its original morphology while showing high anisotropy under rapid heating rates (Kisch and Taylor, 1966; Creaney, 1980). Liptinite macerals in the heat affected coals from Telkwa show the retention of morphological identity, for example sporinite (Fig. 6b). This retention is facilitated by the fast rates of heating associated with contact metamorphism.

The coke in Figure 6c shows two types of optical texture, isotropic in inertinite fragments and an anisotropic texture containing two optical phases: a fine grained phase formed from semi-reactive macerals (e.g. semifusinite) and a coarse grained phase formed from reactive macerals (e.g. vitrinite). The retention of morphological botanical features in macerals during carbonization can be related to the rate of heating. Goodarzi (1984a, b) found that retention of such features in coke was due to a high rate of heating, for example 10° and 60°C/min. Such rates of heating facilitate the differentiation of optical texture, such as size, form of mosaic and degree of anisotropy. Contact metamorphism results in carbonization of coal at heating rates >10°C/min due to the sudden exposure of coal to hot igneous rock. Evidence for this in the Telkwa samples is the presence of morphologically intact sporinite and cutinite fragments showing stronger anisotropy than the vitrinitic coke matrix (Fig. 6b, c). Semi-reactive coal macerals, for example pseudovitrinite, become reactive, develop anisotropy with increasing proximity to the contact (Figs. 6c, 7d, 9a, 10b) and devolatilisation vacuoles which become more numerous.

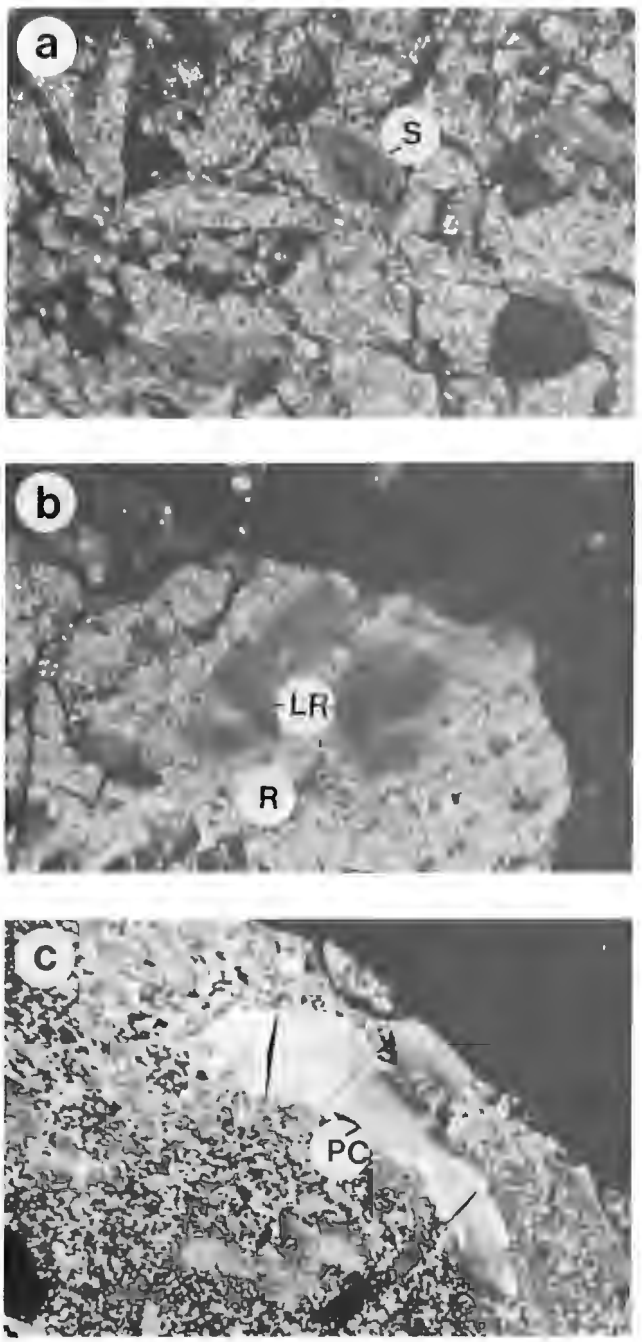

Figure 7. *Altered coal 37 cm from contact.*

a) Brecciation of granular coke, sclerotinite (S) is present.

b) Assimilation of less reactive components (LR) in reactive component (R).

c) Anisotropic pyrolytic carbon (PC) in granular coke.

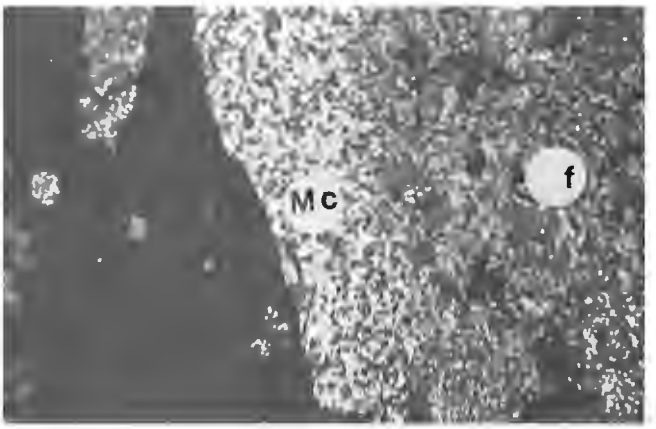

Figure 8. *Altered coal 25 cm from contact.*

Coke showing fine grained (Mf) and coarse grained (Mc) mosaic.

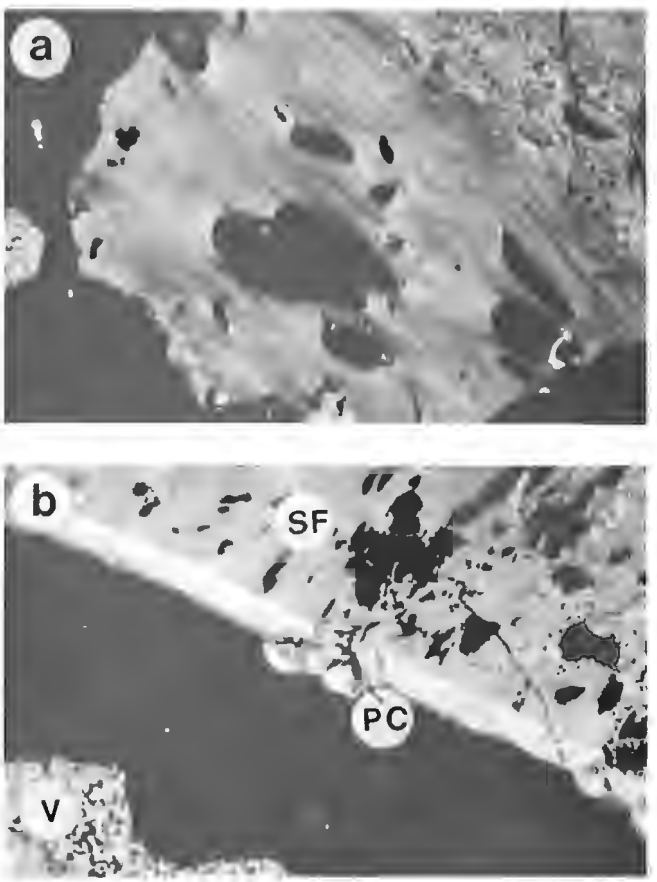

Figure 9. *Altered coal 5 cm from contact.*

a) Pseudovitrinite coke retains its botanical structure (centre) and shows fine granular-basic anisotropy.

b) The edge of isotropic semifusinite (SF) coke is lined by anisotropic layered pyrolytic carbon (PC). Vitrinite coke (V) shows granular anisotropy.

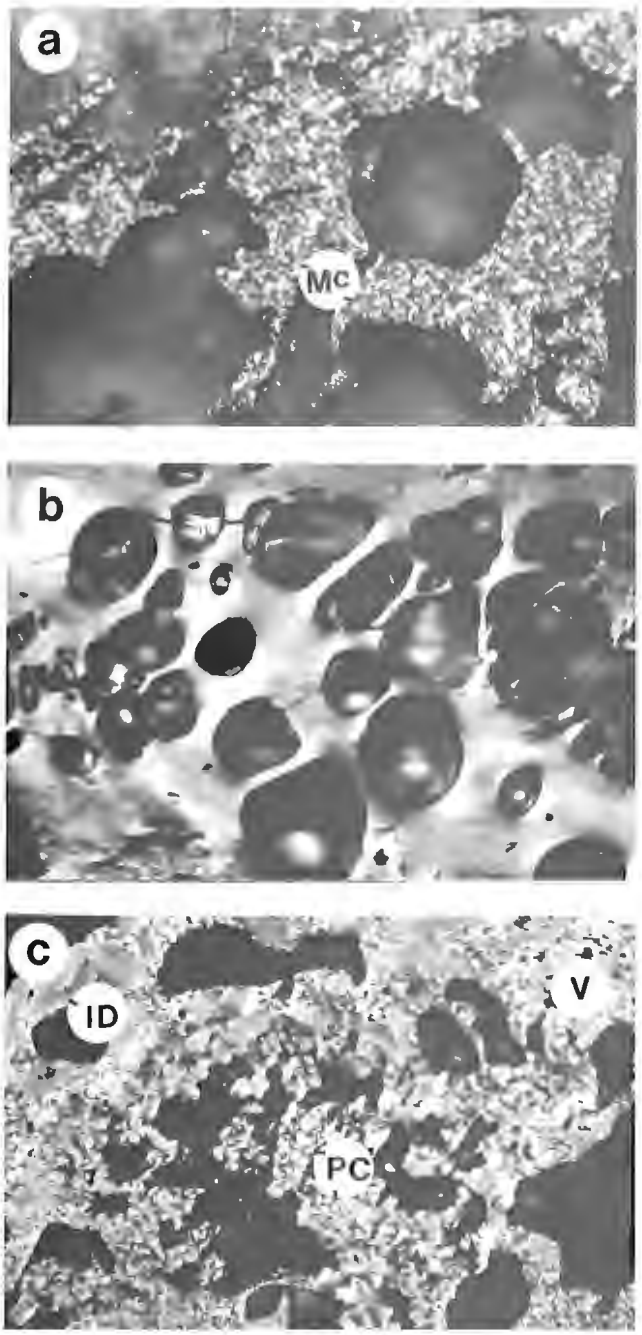

Figure 10. *Altered coal from contact with dyke.*

a) Coarse grained (Mc) mosaic in intrusive matrix.

b) Natural coke retains its botanical structure (centre) and shows basic anisotropy and pores, probably represents pseudovitrinite.

c) Pyrolytic carbon (PC) lines the pores in vitrinite (V) coke; inertodetrinite (ID) fragments are present.

The presence of well developed pyrolytic carbon Figs. 9b, 10c, d), particularly the spherulitic type (Fig. 10d), in coke at the dyke contact, might indicate a temperature approaching 1000°C. Brown et al. (1966) have stated that spherulitic pyrolytic carbon is almost absent in material coked at 700°C and becomes more abundant at about 1000°C. In the Telkwa coals spherulitic pyrolytic carbon is present at the dyke contact (Fig. 10d), but changes to the layered type a short distance (5 cm) from the dyke in sample 8 (Fig. 9b), suggesting a decrease in temperature over this very short distance. Reflectance of pyrolytic carbon increases steadily towards the contact (Table 2). Goodarzi (1985) noted pyrolytic carbon in some other Canadian coals.

Assimilation of less reactive components of coal, e.g. semifusinite, by reactive coal components (vitrinite) was observed in the altered coal (Fig. 7b). This is similar to experimental results of Goodarzi (1981), who co-carbonized less reactive vitrinite (less fluid) with reactive sporinite (more fluid) and found that vitrinite became assimilated in the more fluid sporinite.

The temperature of formation of these natural cokes can be estimated by superimposing the maximum and minimum reflectance (Table 1) on Goodarzi's (1975) maximum and minimum reflectance curves for a high volatile bituminous vitrinite, (% Ro = 1.1). These were carbonised in the laboratory at heating rates of 1°C, 10°C and 60°C/min in the range of 400°C to approximately 900°C (Fig. 11). It is evident that coal at distances greater than 90 cm from the dyke is little affected by the intrusion (Samples 1 through 4, Table 1). Samples 5 and 6 taken at 65 cm and 37 cm, respectively, from the dyke have been coked at temperatures ranging between 575° and 615°C. At 25 cm from the dyke the coal (sample 7) was exposed to temperatures between 650° and 700°C. Samples 8 and 9 are even closer to the contact than 7 and were likely subjected to higher temperatures than sample 7, yet their position on Figure 11 is anomalous. One reason for this may be that because of the highly developed mosaic texture and granularity of these samples, it was difficult to get good maximum and minimum reflectance values and the positioning of samples on Figure 11 is dependant on those values.

It should be noted that decreases in reflectance of samples at dyke contacts are apparently a very common phenomenon (Creaney,1980; Raymond and Murchison, in press). It has also been observed in coal tested in the laboratory at high temperature (Goodarzi, 1984c).

Figure 11 also suggests that different rates of heating prevailed during this carbonizing event, depending on the distance from the intrusion. The position of sample 7 on this plot relative to points 1 through 6 suggests a change in direction of the trend line and it is projected to cut across the 60°C/min rate of heating contour. This implies that samples farther away from the dyke experienced lower heating rates than those close to, or in contact with, the dyke. This is to be expected. Coal at the dyke contact may have been more or less shock heated, whereas at greater distances the heating rate would progressively decrease.

The petrological examination of the present suite of samples indicates that coal at a distance greater than 120 cm from the dyke contact was not affected by heat generated from the intrusion. This contrasts with observations of some other authors (Dow, 1977) who suggest that the organic material at a distance of twice the dyke width would be affected. Accordingly, one would look for the zone of altered coal at Telkwa to be 4.8 m wide given a dyke width of 2.4 m. However, according to other authors the width of the altered coal aureole enveloping dykes appears to be highly

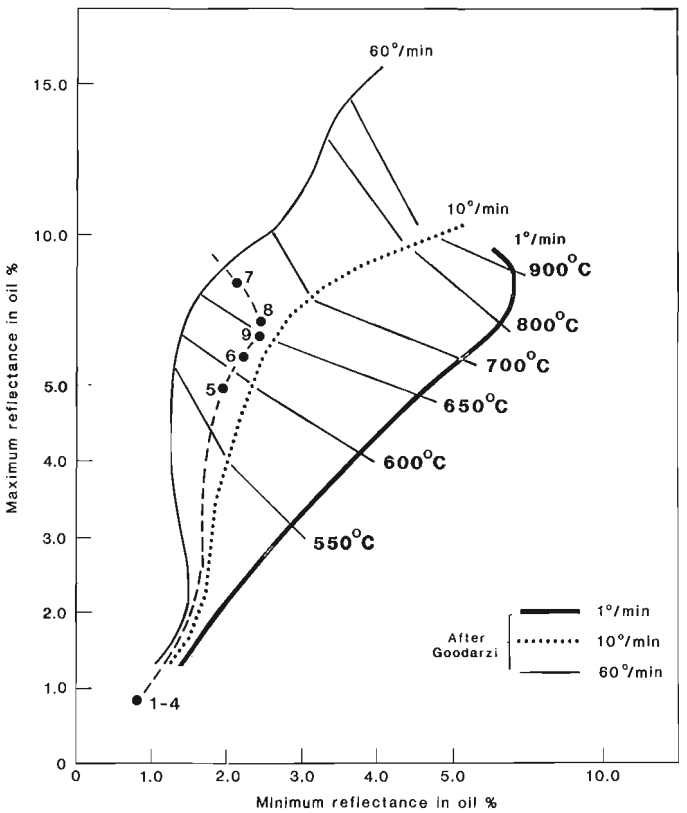

Figure 11. *Maximum and minimum reflectance data for Telkwa samples superimposed on rate of heating, temperature and reflectance diagram developed by Goodarzi, 1975. Original diagram based on laboratory experiments in which coal was carbonised at different heating rates. The isotherms (550°C, 600°C, etc.) were derived from these experiments.*

variable. Based on a study of some dykes in Colorado, Bostick and Pawlewicz (1984) found that organic matter appeared to be affected for little more than the width of the associated dyke. They also commented regarding the influence of prevailing conditions on the degree of thermal alteration, i.e. conductivity of the invaded rock, degree of crystallization of the magma, and the amount of material introduced and rate of flow into the country rock. Undoubtedly it makes a difference if the dyke is the product of a single short-lived intrusion or was instead formed in a conduit through which molten material flowed for a relatively long time. Clegg (1955) in an earlier paper on dykes in the Illinois Basin suggested a narrow alteration zone, 4 to 5 inches (10-13 cm) for an 18 inch (46 cm) dyke. On the other hand Dutcher et al. (1966) reported alteration effects, including reflectance changes, some 900 feet (274 m) from a 25 foot (7.6 m) dyke in Colorado. In short, published observations indicate that the width of the alteration aureole is quite variable and that the rather narrow zone at Telkwa is not unique.

The data for the Telkwa samples suggest a high temperature gradient between the dyke/coal contact and the site of the nearest unaltered coal (sample 3), 120 cm from the dyke. A temperature at the dyke of at least 600°C is suggested by the petrographic data. The temperature at the sample 3 site is difficult to estimate but may have been about 200°C based on calibration curves by Bostick and Pawlewicz (1984). It could not have remained long at that temperature, otherwise certain optical changes such as reflectance increase would be observed in samples as close to the contact as site 3. It suggests that the emplacement of this Telkwa dyke was a single phase event and did not source a persistent high heat regime.

CONCLUSIONS

1) The temperature of coal alteration at contact with the dyke was greater than 575°C and may have approached 1000°C.

2) Although the dyke is 2.4 m wide, coal beyond 90 cm from the contact appears to be little affected.

3) Pseudovitrinite became reactive, developed higher fluidity and stronger anisotropy with increasing proximity to the dyke.

4) The liptinite group of macerals developed stronger anistropy than the granular "groundmass" and some retained their original morphology.

5) Pyrolytic carbon changed from spherulitic type at the contact with the dyke to layered type at a relatively short distance from the dyke.

6) Assimilation of some less reactive components by the more active components was observed.

REFERENCES

Aganoglu, K.
1972: A comparison of the thermal metamorphism of coal seams in northeast England. University of Newcastle-upon-Tyne, unpublished M.Sc. thesis.

ASTM (American Society for Testing and Materials)
1979: Annual book of ASTM standards: Part 26, Gaseous Fuels: Coal and Coke - Atmospheric Analysis. American Society for Testing and Materials, 1916 Race Street, Philadelphia, Pa.

Bostick, N.H. and Pawlewicz, M.J.
1984: Paleotemperatures based on vitrinite reflectance of shales and limestones in igneous dike aureoles in the Upper Cretaceous Pierre shale, Walsenburg, Colorado. In Hydrocarbon Source Rocks of the Greater Rocky Mountain Region, J. Woodward, F.F. Meisner and J.L. Clayton (eds.); Rocky Mountain Association of Geologists (Denver), p. 387-392.

Brown, H.R. and Taylor, G.H.
1961: Some remarkable Antarctic coals. Fuel, v. 40, p. 211-224.

Brown, H.R., Hesp, W.R., and Taylor, G.H.
1966: Carbons obtained by thermal and catalytic cracking of coal tars. Carbon, v. 4, p. 193-194.

Chandra, D. and Taylor, G.H.
1982: Thermally altered coals. In Coal Geology, E. Stach et al. (eds.); Gebrüder Borntraeger, Berlin, p. 206-209.

Chatterjee, N.N., Chandra, D., and Ghosh, T.K.
1964: Reflectance of Poniati Seam affected by mica peridotite dyke. Journal of Mines, Metals, Fuel, v. 12, no. 11, p. 346-348.

Clegg, K.E.
1955: Metamorphism of coal by peridotite dykes in southern Illinois. Illinois State Geological Survey, Report of Investigations, 178, 18 p.

Creaney, S.
1980: Petrographic texture and vitrinite reflectance variation on the Alston block, northeast England. Proceedings of the Yorkshire Geological Society, v. 42, pt. 4, no. 32, p. 533-580.

Dow, W.
1977: Petroleum source beds on continental slopes and rises. In Geology of Continental Margins; AAPG Continuing Education Course Note Series 5, AAPG Continuing Education Program, American Association of Petroleum Geologists, Tulsa, Oklahoma, 37 p.

Dutcher, R.R., Campbell, D.L., and Thornton, C.P.
1966: Coal metamorphism and igneous intrusives in Colorado. In Coal Science, Advances in Chemistry Series 55, R.F. Gould (ed.); American Chemical Society, Washington, D.C., p. 708-723.

Goodarzi, F.
1975: Some factors influencing the behaviour of the optical properties of carbonised macerals. University of Newcastle-Upon-Tyne, Ph.D. Thesis, England, 348 p.

1981: Optical properties of carbonised sporinites. In Organic Maturation Studies and Fossil Fuel Exploration, J. Brooks, (ed.); p. 75-87, Academic Press.

1984a: Optical properties of carbonised sporinite in vitrinite sporinite blends. Fuel, v. 63, p. 827-833.

1984b: Retention of liptinitic structure in vitrinite chars. Fuel, v. 63, p. 239-244.

1984c: Optical properties of high temperature heat treated vitrinites. Fuel, v. 63, p. 820-826.

1985: Characteristics of pyrolytic carbon in Canadian coals. Fuel, v. 64, p. 1177-1178.

Goodarzi, F. and Murchison, D.G.
1973: Optical properties of carbonised preoxidized vitrinites. Fuel, v. 52, p. 164-167.

1976a: Petrography and anisotropy of carbonised pre-oxidized coals. Fuel, v. 55, p. 141-147.

1976b: Plant-cell structure in vitrinite chars. Journal of Microscopy, v. 106, pt. 1, p. 49-58.

1978: Influence of heating - rate variation on the anisotropy of carbonised vitrinites. Fuel, v. 57, p. 273-284.

Grint, A. and Marsh, H.
1981: Carbonisation of coal blends. Fuel, v. 60, p. 1115-1120.

Irvine, T.N. and Baragar, W.R.A.
1971: A guide to the chemical classification of the common volcanic rocks. Canadian Journal of Earth Sciences, v. 8, p. 523-548.

Jones, J.M. and Creaney, S.
1977: Optical character of thermally metamorphosed coals of Northern England. Journal of Microscopy, v. 109, pt. 1, p. 105-118.

Kisch, H.J. and Taylor, G.H.
1966: Metamorphism and alteration near an intrusive contact. Economic Geology, v. 61, p. 343-361.

Koo, W.E.
1983: Telkwa Coalfield, west-central British Columbia. In British Columbia Ministry of Energy, Mines and Petroleum Resources, Geological Fieldwork 1982, Paper 1983-1, p. 113-121.

1984: The Telkwa, Red Rose and Klappan coal measures in northwestern British Columbia. In British Columbia Ministry of Energy, Mines and Petroleum Resources, Geological Fieldwork 1983, Paper 1984-1, p. 81-90.

Mackowsky, M. Th.
1968: European Carboniferous coalfields and Permian Gondwana coalfields. In Coal and Coal-bearing Strata, D.G. Murchison and T.S. Westoll (eds.). Oliver and Boyd, Edinburgh, p. 325-345.

1982: Preparation of polished surfaces; in Stach's Textbook of Coal Petrology, E. Stach et al. (eds.); Gebrüder Borntraeger, Berlin, p. 296.

Marshall, C.E.
1936: Alteration of coal seams by the intrusion of some igneous dykes in the Northumberland and Durham coalfields. Institute Mining Engineers, Transactions, London, v. 91, p. 235.

Melvin, J.N.
1974: Thermal metamorphism and carbonisation of coals in relation to petrology. University of Newcastle-Upon-Tyne, unpublished Ph.D. thesis.

Raymond, A.C. and Murchison, D.G.
in press: Organic maturation and its timing in a Carboniferous sequence in the central Midland Valley of Scotland: comparisons with northern England. Fuel.

Sanyal, S.P.
1965: Nature of a thin vein of solidified tarry matter formed during natural carbonisation of coal from Victoria West Collieries, Raniganj Coalfield, India. Fuel, v. 44, p. 333-338.

Schapiro, N. and Gray, R.J.
1966: Physical variation in highly metamorphosed Antarctic coals. In Coal Science, F.E. Gould (ed.); Advances in Chemistry, Series 55, American Chemical Society, Washington, p. 196-217.

Stach, E.
1952: Mikroskopie natürlicher kokse. In Handbuch der Mikroskopie in der Technik, H. Freund, (ed.); v. 2, pt. 1, p. 411-422, Umschau-Verlag, Frankfurt/M.

Taylor, G.H.
1961: Development of optical properties of coke during carbonisation. Fuel, v. 40, p. 465-471.

The nature of thermally altered coal from Mount Granger, Whitehorse area, Yukon Territory

F. Goodarzi and T. Jerzykiewicz
Institute of Sedimentary and Petroleum Geology, Calgary

Goodarzi, F. and Jerzykiewicz, T., The nature of thermally altered coal from Mount Granger, Whitehorse area, Yukon Territory. In Contributions to Canadian Coal Geoscience, Geological Survey of Canada, Paper 89-8, p. 104-107, 1989.

Abstract

A suite of thermally altered coal samples from mount Granger, near Whitehorse, Yukon Territory was examined using reflected light microscopy. The coal in contact with a rhyolitic sill was coked at >600°C at a rate of heating of 60°C/min and developed granular anisotropy. The alteration zone of coal is more than twice the thickness of the intruding body. The residue at a distance of >65 cm from the intrusion represents the weathered portion of the coal seam. The original rank of coal as determined by the optical texture developed in coal, i.e. flow type mosaic, is medium to low volatile bituminous ($R_o max$ = 1.2-1.6%).

Résumé

Une série d'échantillons de charbon altéré thermiquement et provenant du mont Granger près de Whitehorse, dans le territoire du Yukon, a été examinée par la méthode de la microscopie en lumière réfléchie. Le charbon en contact avec un filon-couche rhyolitique, a été cokéfié à une température de > 600°C et à un taux de chauffage de 60°C/min, et a ainsi développé une anisotropie granulaire. La zone d'altération du charbon atteint plus de deux fois l'épaisseur de la masse intrusive. Le résidu, à une distance de >65 cm de l'intrusion, représente la partie altérée du filon de charbon. Le rang original du charbon a été déterminé comme bitumineux à teneur en matières volatiles de moyenne à faible, ainsi que l'établit la texture optique qui se développe dans les charbons dans de telles situations, soit un type d'écoulement en mosaïque. ($R_o max$ = 1,2 à 1,6 %).

INTRODUCTION

Coal thermally altered by intrusions of sills and dykes provides information about the temperature of the intrusive body and the behaviour of coal macerals during natural metamorphism (Chatterjee et al., 1964; Kisch and Taylor, 1966; Aganoglu, 1972; Jones and Creaney, 1977; Creaney, 1980; Chandra and Taylor, 1982; Goodarzi and Jerzykiewicz, 1986; Goodarzi et al., 1988).

In this paper the variation of reflectance and morphology of samples from a coal seam intruded by a Tertiary rhyolitic is examined. The affected coal is from an exploration pit at Mount Granger near Whitehorse in the Yukon Territory (Fig. 1). The coal measure at Mount Granger is in the Tantalus Formation of Upper Jurassic to Lower Cretaceous age. The rhyolite is related to the leucokratic granite of Cretaceous-Tertiary age which has intruded the coal-bearing strata and is exposed nearby at the top of Mount Granger (Wheeler, 1961). Further general information on the intrusive rock (Coast intrusions) and the comagmatic rhyolites is provided by Souther (1977).

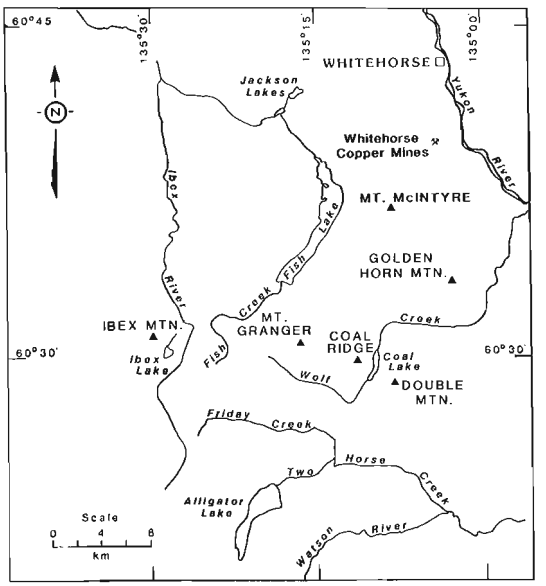

Figure 1. *Location and geological setting of Mount Granger.*

EXPERIMENTAL

Samples were collected from the sill contact and also from distances of 5, 50 and 65 cm from the sill. Samples were ground to 20 mesh (850 µm), mounted in cold set resin and polished following standard methods (Mackowsky, 1982).

Maximum and minimum reflectance on these coal samples (now turned into natural coke) were determined according to standard methods (Mackowsky, 1982) using a Zeiss MPM II microscope fitted with Zonax microcomputer and printer. Reflectance data, including bireflectance ($\%R_o max$-$\%R_o min$) for the samples and their morphology are reported in Table 1.

TABLE 1

Reflectance data on Mount Granger samples

Sample	Distance from sill (in cm)	Per cent Reflectance Max	Min	Optical Texture*
a	contact	6.36	0.94	Coarse grained mosaic
b	5	7.55	1.88	Coarse grained to flow-type mosaic
c	50	5.31	0.69	Flow-type mosaic texture
d	65	4.63	3.87	Basic anisotropy

*Definitions after Grint and March 1981

RESULTS AND DISCUSSION

Coals are divided into two groups, coking and non-coking, based on their behaviour during thermal treatment (Goodarzi, 1975).

Coking coals become fluid and develop a porous cohesive coke (Goodarzi and Murchison, 1976, 1978; Grint and Marsh, 1981). Non-coking coals develop only char that may contain devolatilisation vacuoles. The residues of non-coking coals remain almost isotopic for a rank of high volatile bituminous B and lower, or develop basic anisotropy in semianthracitic and higher rank coals (Goodarzi, 1975).

The coal from Mount Granger has undergone two types of alteration; a) regional thermal maturation due to the presence of an underlying leucokratic granite block, which perhaps resulted in an increase in the rank of coal and b) contact metmorphism due to intrusion of a rhyolitic sill. The intrusion of this sill has transformed the coal into coke up to a distance of 65 cm from the dyke (Fig. 2). This is in contrast with the observation made by Dow (1977) that the intrusive body alters the organic matter to a distance that is twice the thickness of the intrusion. The ryolitic sill in this study is about 20 cm thick, but it has altered the coal to a distance up to 65 cm, more than three times the thickness.

The coal at contact with the sill is transformed into coke, which shows high anisotropy (Table 1) and granular texture (Table 1). The anisotropy of coke decreases with increasing distance from the dyke (Fig. 3).

The coal at the contact with the sill became fluid and produced a cohesive coke (Fig. 2). However, the char (sample d) at a distance of >65 cm has the reflectance and morphology of anthracite (Table 1, Plate 1). Anthracitic coals are non-coking and do not develop granular anisotropy (Goodarzi, 1975; Goodarzi and Murchison 1978). The only explanation for this unusual behaviour of sample d is that it may represent a weathered part of the coal seam. Weathering (low temperature oxidation) destroys the fluidity of bituminous coal. An extremely weathered bituminous coal within (i.e. outcrop sample), within the coking range, behaves similarly to a non-coking coal during thermal treatment, and develops anthracitic morphology (Goodarzi and Murchison, 1976; Goodarzi and Marsh, 1980).

A sample of the unaltered coal was not available for determination of rank. However, the original rank of the heat-affected coal is medium to low volatile bituminous (%$R_o$max:1.2-1.6) based on the optical texture (coarse-flow type mosaic) observed in natural coke. Coal in this range

Figure 2. *Coal seam in Mount Granger intruded by rhyolite.*

constitutes a prime coking coal and can produce an excellent industrial coke. Such coals are highly fluid and develop medium to flow type anisotropic texture, as evident in sample c (Plate 1).

The decrease in reflectance of the sample at contact with the dyke is a common phenomenon associated with thermally altered coals (Creaney, 1980; Raymond and Murchison, in press; Goodarzi and Cameron, in press) and high temperature heat treated coals (Goodarzi, 1984).

Estimation of temperature

The coal in contact with the rhyolitic sill is reactive and has developed granular anisotropy (Plate 1). An estimation of the minimum temperature for the heat affected coals (Fig. 3) may be made by using laboratory-produced curves (Goodarzi, 1975) for a low volatile bituminous coal (%$R_o$max:1.55), (Fig. 3). This curve and reflectance data obtained in this study indicate that the sample at the contact with the sill (Fig. 3, sample a) has been altered by temperatures of >600°C at a rate of heating of >60°C/min. Samples b and c located at 15 and 55 cm from the dyke have been altered by temperatures in the range of 550 to 500°C and at the rate of heating of >60°C/min. Estimation of temperature of alteration for sample d is impossible due to preoxidation (weathering) of this sample, which has altered its coking and optical properties.

Goodarzi and Cameron (in press) have estimated the temperature of an alkali basaltic dyke at Telkwa, B.C., which intruded a high volatile bituminous coal (% $R_o$max:0.87), may have been as high as 1000°C. The sill in Mount Granger is rhyolitic, which is the lava equivalent of granite and is expected to have a temperature lower than the basaltic dyke at Telkwa, B.C. The temperature of intrusion of the sill at Mount Granger, as determined by laboratory studies of the

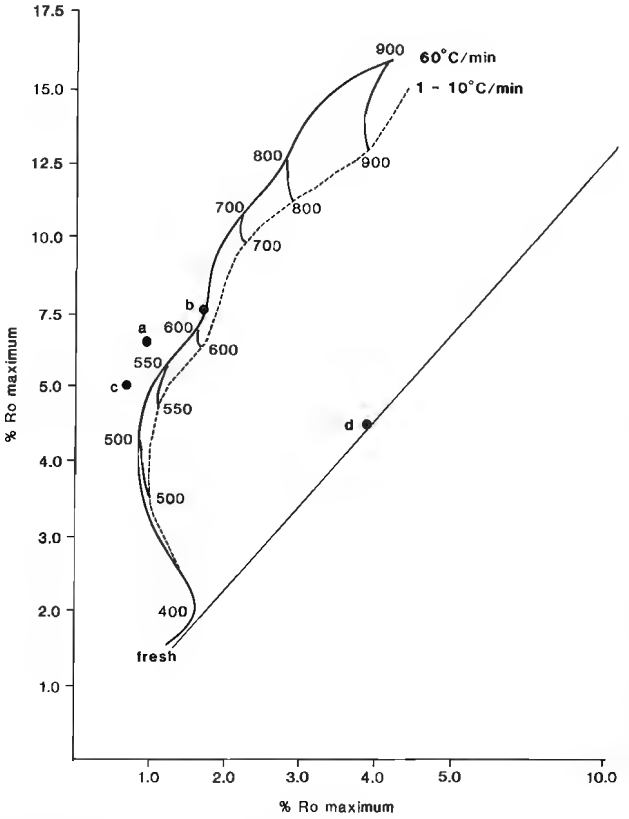

Figure 3. *Variation of maximum and minimum reflectance of heat affected coal with decreasing distance to the sill. a, b, c, d indicate samples studied for this report (see Table 1). Modified from Goodarzi, 1975.*

reflectances (%$R_o$max and $R_o$min) of heat affected medium to low volatile bituminous coal (%$R_o$max:1.2-1.6%), is >600°C, which is in agreement with temperature of intrusion of rhyolites.

CONCLUSIONS

Coal at Mount Granger has undergone both regional and contact metmorphism. The regional metamorphism has probably elevated the rank of coal and contact metmorphism has resulted in coking of the coal.

Based on the coking behaviour of the altered coal at the contact and in close proximity with the sill, the rank of the unaltered coal is estimated to be in the range of medium to low volatile bituminous, indicative of an excellent quality coking coal. However, weathering may have reduced the coking ability of these coals.

Coal in contact with the sill has been coked at a temperature of 600°C and at rate of heating of >60°C/min.

ACKNOWLEDGMENTS

We thank R. Collins and R. Hill of the Energy and Mines Branch of the Yukon Economic Development (Mines and Small Business) and personnel of Whitehorse Coal Corporation for their assistance in collecting the coal samples and for supply of valuable geological information.

PLATE 1

Morphology of heat affected coals; oil immerison; partially crossed polars; magnification: full scale of long axis of photographs = 230 microns

a) Char showing non-granular morphology and basic anisotropy. 65 cm from the sill.

b) Coke showing flow type mosaic texture and granular anisotropy. 50cm from the sill.

c) Coke showing coarse grained mosaic texture and granular anisotropy. 5 cm from the sill.

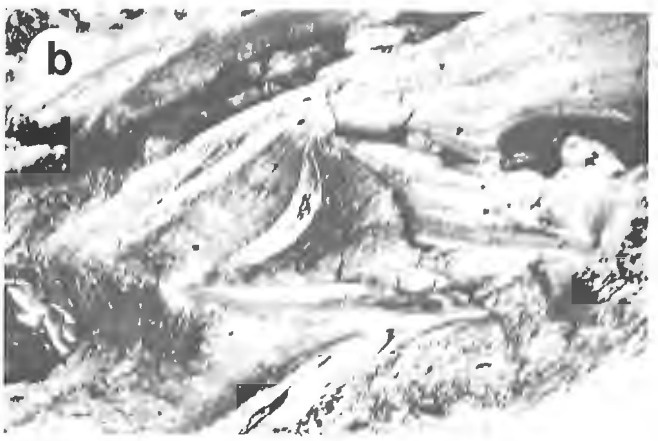

REFERENCES

Aganoglu, K.
1972: A comparison of the thermal metamorphism of coal seams in northeast England. University of Newcastle-Upon-Tyne, unpublished M.Sc. thesis, 145 p.

Chatterjee, N.N.,Chandra, D., and Ghosh, T.K.
1964: Reflectance of Poniati seam affected by mica peridotite dyke. Journal of Mines, Metals, and Fuel, v. 12, no. 11, p. 346-348.

Chandra, D. and Taylor, G.H.
1982: Thermally altered coal. In Coal Petrology, E. Stach et al. (eds.); Gebrüder Borntraeger Berlin, p. 206-209.

Creaney, S.
1980: Petrographic texture and vitrinite reflectance variation on the Alston Block, Northeast England. Proceedings of the Yorkshire Geological Society, v. 42, Pt.4, no. 32 , p. 533-580.

Dow, W.G.
1977: Petroleum source beds on continental slopes and rises. In Geology of Continental Margins; AAPG Continuing Education Course Note Series 5, American Association of Petroleum Geologists, Tulsa, Oklahoma, 37 p.

Goodarzi, F.
1975: Some factors influencing the optical properties of carbonised macerals. University of Newcastle-Upon-Tyne, unpublished Ph.D. thesis, 348 p.

1984: Optical properties of high temperature heat treated vitrinite. Fuel, v. 63, p. 827-833.

Goodarzi, F. and Cameron, A.R.
in press: Organic petrology of thermally altered coals from Telkwa, British Columbia. Contributions to Canadian Coal Science. This volume.

Goodarzi, F., Gentzis, T., and Bustin, M.
1988: Reflectance and petrology profile of a partially combusted and coked bituminous coal seam from British Columbia. Fuel, v. 67, p 1218-1222.

Goodarzi, R. and Jerzykiewicz, T.
1986: Petrology of burning bituminous coal seam. Geological Survey of Canada, Paper 86-1B, p. 421-427.

Goodarzi, F. and Marsh, H.
1980: Optical properties of carbon HTT 873 K from pre-oxidised vitrinite, carbonised under pressure of about 200 MPA. Fuel, v. 59, p. 266-267.

Goodarzi, F and Murchison, D.G.
1976: Petrology and anisotropy of carbonised pre-oxidised coals. Fuel, v. 55, p. 141-147.

1978: Influence of heating rate variation on the anisotropy of carbonised vitrinite. Fuel, v. 57, p. 273-284.

Grint, A. and Marsh, H.
1981: Carbonisation of coal blend. Fuel, v. 60, p. 1115-1120.

Jones, J.M. and Creaney, S.
1977: Optical character of thermally metamorphosed coals from northern England. Journal of Microscopy, v. 109, pt.1, p. 105-118.

Kisch, H.J. and Taylor, G.H.
1966: Metamorphism and alteration near an intrusive - coal contact. Economic Geology, v. 61, p. 343-361.

Raymond, A.C. and Murchison D.G.
in press: Organic maturation and its timing in a Carboniferous sequence in the central Midland Valley of Scotland: comparisons with northern England. Fuel.

Mackowsky, M.Th.
1982: Preparation of polished surface. In Coal Petrology, E. Stach et al. (eds.); Gebrüder Borntraeger, Berlin, p. 296-299.

Souther, G.
1977: Volcanism and tectonic environments in the Canadian Cordillera - a second look. In Volcanic Regimes in Canada, W.R.A. Baragar, L.C. Coleman, and H.J. Hall, (eds.); Geological Association of Canada, Special Paper, no. 6, p. 3-39.

Wheeler, J.O.
1961: Whitehorse map-area, Yukon Territory. Geological Survey of Canada, Memoir 312, 156 p.

Conversion characteristics of selected Canadian coals based on hydrogenation and pyrolysis experiments

W. Kalkreuth, C. Roy[1], and M. Steller[2]
Institute of Sedimentary and Petroleum Geology, Calgary

Kalkreuth, W., Roy, C., and Steller, M., Conversion characteristics of selected Canadian coals based on hydrogenation and pyrolysis experiments. In Contributions to Canadian Coal Geoscience, Geological Survey of Canada, Paper 89-8, p. 108-114, 1989.

Abstract

Hydrogenation conversion rates were found to range from 8 to 78%. The highest conversions were obtained from reactive rich subbituminous and high volatile bituminous coals. For each rank level the coal containing the highest amount of reactive macerals has also the highest conversion. Results from this study suggest that some of the higher rank Western Canadian coals can be hydrogenated successfully despite their high contents of inertinite macerals.

Vacuum pyrolysis conversion rates were found to reflect closely rank and petrographic composition of the parent coals. The highest conversion rates were obtained from the liptinite-rich lignites and subbituminous coals (30-70%), whereas the conversion rates of the higher rank coals were found to be significantly lower (32-14%). The preliminary results suggest that vacuum pyrolysis might be an effective process in which valuable tar by-products could be generated from lower rank (thermal) coals prior to burning the coal.

Résumé

Les taux de conversion de hydrogénation variaient entre 8 et 78 %. Les conversions les plus élevées ont été obtenues pour les charbons subbitumineux riches en macéraux réactifs ainsi que les charbons bitumineux à haute teneur en matières volatiles. Pour chaque rang, le charbon possédant la proportion la plus élevée de macéraux réactifs enregistrait également les conversions les plus élevées. Les résultats de l'étude semblent indiquer que certains des charbons de rang élevé provenant de l'Ouest canadien peuvent être hydrogénés avec succès malgré leur fort contenu en macéraux de type inertinite.

Les taux de conversion de pyrolyse sous vide suivaient étroitement le rang des charbons ainsi que les caractérisitiques pétrographiques des charbons d'origine. Les conversions les plus élevées (30 à 70 %) ont été obtenues pour les lignites riches en macéraux de type liptinite et pour les charbons subbitumineux. Les conversions les plus basses (14 à 32 %) ont été obtenues pour les charbons de rang élevé. Les résultats préliminaires semblent indiquer que la pyrolyse sous vide pourrait représenter une méthode valable susceptible de permettre la récupération des sous-produits contenus dans le goudron des charbons de rang faible (houilles thermiques) préalablement à leur combustion.

INTRODUCTION

Technological properties of coals are to a large extent a function of rank and petrographic composition of the parent coal. In hydrogenation, for example, the optimum rank to produce the highest liquid yields appears to be at the level of high volatile bituminous coals, while at lower and higher rank levels the degree of conversion decreases markedly (Whitehurst et al., 1980). In coals having the same rank levels, the petrographic composition determines the susceptibility to conversion (Given et al., 1975); i.e. the ratio of reactive to inert macerals.

Macerals are commonly identified by methods of incident light microscopy in which morphological characteristics and reflectance levels are used to define three major maceral groups, namely the vitrinite, liptinite and inertinite groups. In technological terms, the group of reactive components comprises the macerals of the vitrinite and liptinite groups and a portion of the maceral semifusinite. The latter consists of material which, in its properties, is thought to be at an intermediate stage between vitrinite and inertinite. The inert group comprises the macerals of the inertinite group plus mineral matter. In general, the greater the amount of reactive macerals contained in a coal the better conversion can be expected (Fisher et al., 1942).

[1]Department of Chemical Engineering
Université Laval Quebec
Québec, Canada G1K 7P4

[2]Bergbauforschung GmbH, Postfach 130140
D-3400 Essen 13, Germany.

In the present study, coals characterized by varying amounts of reactive and inert materials and ranging in rank from lignite to low volatile bituminous were tested for their susceptibility to hydrogenation and vacuum pyrolysis.

The feedcoals were characterized petrographically using incident light microscopy techniques (automatated image analysis and conventional petrographic methods). Vitrinite reflectance measurement was used to determine the rank, and maceral and microlithotype analyses to determine the petrographic composition. Chemical analyses involved the determination of elemental composition, ash contents and volatile matter contents.

The results presented here form part of a joint research project on conversion characteristics of coals between the Geological Survey of Canada, the Department of Chemical Engineering, Université Laval, Québec and Bergbau-Forschung, Essen, Germany. This paper focuses on petrographic and chemical characterization of the feedcoals and discusses their conversion rates. For further information in respect to yields (gaseous and liquid products) and the characterization of solid reaction products (solid residues), the reader is referred to Roy et al. (1985), Hébert (1986), Kalkreuth et al. (1986), Hébert et al. (1987) and Steller et al. (1987).

EXPERIMENTAL

Petrographic analyses

Coal

Rank and gross petrographic composition of the coals used in the hydrogenation experiments were established using an automated texture-analysis-system (TAS-Leitz). Details of the procedure have been described by Riepe and Steller (1984). In addition, conventional maceral analysis was used for detailed determination of macerals following the Stopes-Heerlen concept for maceral classification. Rank of the coals used in the vacuum pyrolysis experiments was determined by measuring vitrinite reflectances under standardized conditions (Bustin et al., 1985).

Hydrogenation

In the hydrogenation experiments a bench-scale autoclave (2l) was used. In each experiment 50 g of coal were mixed with 100 g of recycled oil from the Bergbau-Forschung coal hydrogenation plant and fed into the autoclave. The mixture was then reacted with hydrogen starting at 150 bar cold-pressure to approximately 350 bar at 450°C. The coal-oil mixture was kept at maximum temperature for one hour and then cooled down to room temperature. The solid residues were extracted with pyridine. Based on the amount of pyridine-insoluble residual material the degree of conversion for the coals was defined as follows:

$$\text{conversion (\%)} = \frac{\text{g coal (m.a.f.)}-\text{g residue (m.a.f.)}}{\text{g coal (m.a.f.)}} \times 100$$

Vacuum pyrolysis

The operating conditions used for the pyrolytic reactions of the coal samples have been reported in detail elsewhere (Roy et al., 1985). The pyrolysis experiments were conducted in a bench scale retort using a final decomposition temperature of about 600°C at an average heating rate of 9°C min^{-1}. The absolute pressure was kept below 2 mm Hg.

Chemical analyses

Proximate and ultimate analyses on the feedcoals were performed using standard procedures at Bergbau-Forschung, Essen and Université Laval, Québec.

RESULTS AND DISCUSSION

Hydrogenation Experiments

Petrographic analyses of feedcoals

Rank

Table 1 lists the coals according to rank. The random vitrinite reflectances as determined by TAS were found to range between 0.40 to 1.47%. In terms of ASTM rank classes, three of the coals are subbituminous, eight are high volatile bituminous, and one is low volatile bituminous.

Composition

Gross petrographic composition was determined by TAS (Table 1). Figure 1 illustrates the reflectograms for the 12 coals analysed. Highest vitrinite contents occur in the handpicked vitrains (sample 1 and sample 4), which contain 89 and 85 Vol. %. Inertinite contents range from 10-55 Vol. %. In particular, some of the Western Canadian coals have very high amounts of inertinite (Fig. 1, samples 3, 10, 12). The only other coal having a similar high inertinite content is the sample from South Africa (Table 1 and Fig. 1, sample 7). The liptinite contents are low to moderate. Only two coals have more than 10 Vol. % liptinite (Table 1 and Fig. 1, samples 8 and 9). In both reflectograms a distinct peak to the left of the major vitrinite peak indicates greater amounts of liptinite macerals (Fig. 1).

At the present time TAS cannot differentiate between macerals that might have the same reflectances but different morphologies, as, for example, some of the inertinite macerals. Traditional manual maceral analyses showed that within the inertinite group there is considerable variation in the percentage of individual macerals. The macerals micrinite, macrinite and sclerotinite are rare or absent. The same is true for inertodetrinite, which was found to occur in large amounts in sample 3 only (seam No. 6, Highvale Mine, Canada). Fusinite content is low to moderate, ranging from 1 Vol. % (sample 4, Luscar Sterco Mine, Canada) to 15 Vol. % in sample 2 (Highvale Mine, Canada, Seam No. 1). Semifusinite contents show the greatest variations of all inertinite macerals, ranging from 1 Vol. % (sample 1, Highvale Mine, Canada) to 38 Vol. % in sample 10 (Bullmoose Mine, Canada). The determination of semifusinite is of particular interest, because this maceral is believed to react, to some extent, in much the same way as vitrinite. However, the degree of reactivity is not very well defined at the present time and may vary depending on rank and origin of coal samples.

Elemental analyses of feedcoals

The results of elemental analyses are shown in Table 2. With increasing rank (samples 1-12) the carbon content increases from 68.7% in sample 3 to 90.6% in sample 12, accompanied by a drastic decrease in oxygen, from 24.6% in sample 3 to 4.4% in sample 12. The hydrogen content appears to remain fairly stable in this rank range. Two coals are characterized by high amounts of sulphur (samples 6 and

TABLE 1

Origin, A.S.T.M. rank classes, petrographic characteristics and conversion rates for feedcoals used in hydrogenation experiments

Sample	Location	Seam	A.S.T.M. Rank	Vitrinite Reflectance Rrandom (%)[4]	Maceral Analyses Vol. % (m.m.f.)[4]			Conversion (%)
					Vitrinite	Liptinite	Inertinite	
1	Highvale Mine, Canada	No. 1	subbituminous	0.40	89[1]	1[1]	10[1]	78
2	Highvale Mine, Canada	No. 1	subbituminous	0.40	71[2]	1[2]	28[2]	49
3	Highvale Mine, Canada	No. 6	subbituminous	0.41	56[3]	1[3]	43[3]	8
4	Luscar Sterco, Canada	Mynheer	high vol. C bit.	0.49	85[1]	2[1]	13[1]	71
5	Luscar Sterco, Canada	Mynheer	high vol. C bit.	0.54	71[2]	8[2]	21[2]	29
6	Prince Mine, Canada	Hub	high vol. B bit.	0.67	83	5	12	10
7	South Africa	-	high vol. A bit.	0.82	41	8	51	59
8	West Germany	Gudrun	high vol. A bit.	0.87	65	15	20	61
9	West Germany	Zollverein	high vol. A bit.	1.03	64	13	23	78
10	Bullmoose Mine, Canada	B	high vol. A bit.	1.05	64	1	55	54
11	China	-	high vol. A bit.	1.06	66	4	30	34
12	Smoky River Coal, Canada	No. 10	low vol. bit.	1.47	48	2	50	65

[1] handpicked vitrain from [2]
[2] channel sample
[3] handpicked durain
[4] by TAS (Texture Analysis System)

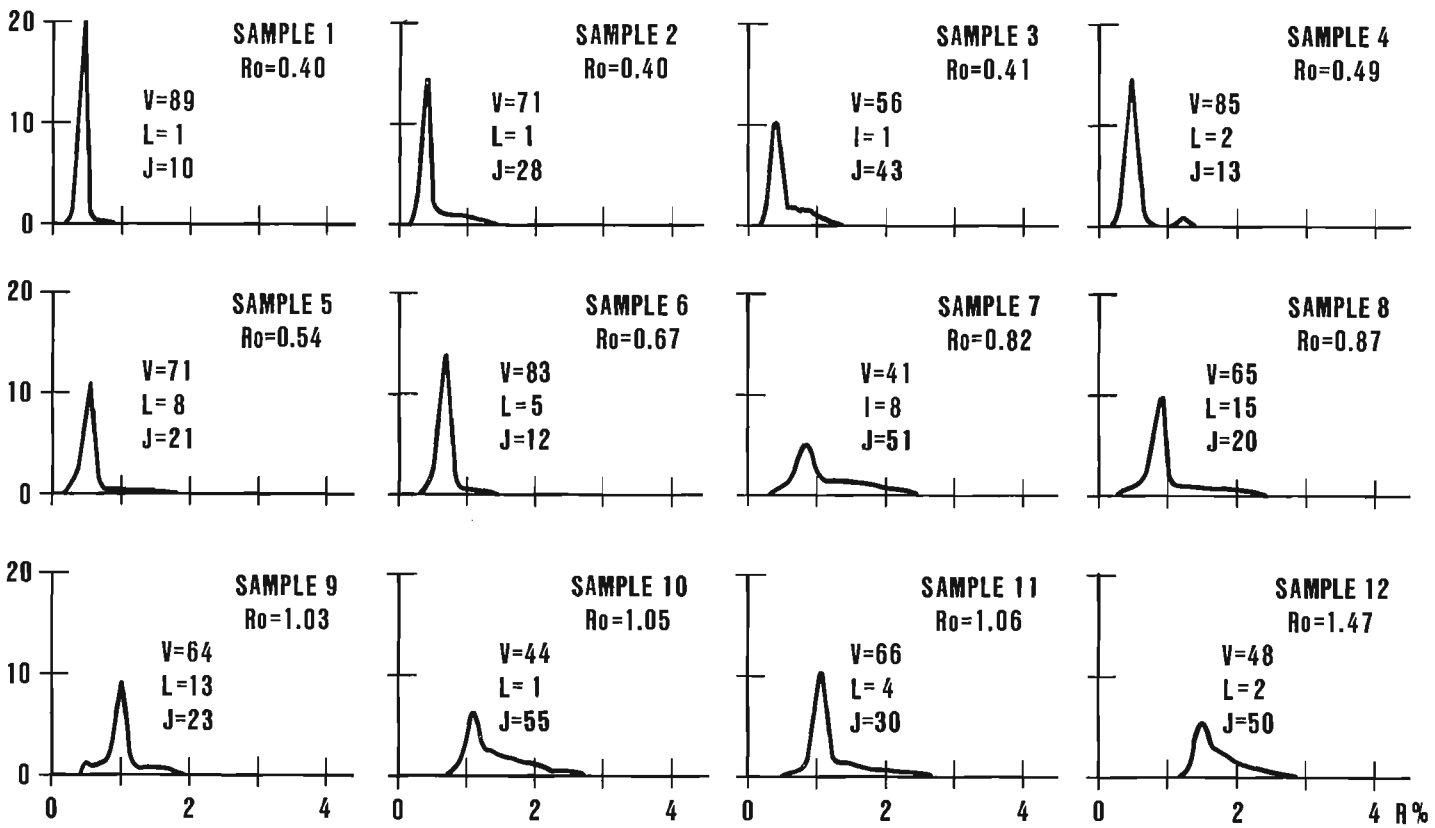

Figure 1. Diagram illustrating reflectograms as determined by TAS (Texture Analysis System), from which random vitrinite reflectances and maceral group distributions were calculated; from Steller et al. (1987).

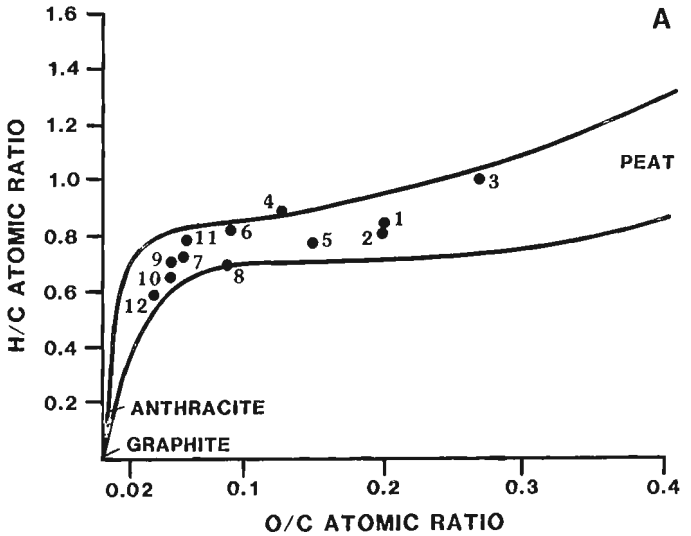

Figure 2. *van Krevelen diagram illustrating H/C - O/C atomic ratios of feedcoals used in the hydrogenation experiments in respect to ASTM rank classes. Numbers refer to samples listed in Table 1; from Steller et al. (1987).*

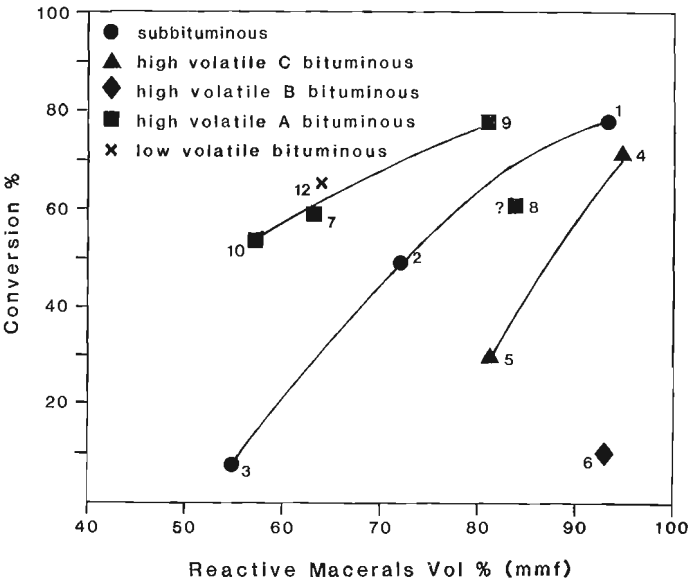

Figure 3. *Diagram illustrating relationship between conversion rates, petrographic composition and coal rank (reactive maceral contents are based on averaged values from TAS and conventional maceral analyses). Numbers refer to samples listed in Table 1; from Steller et al. (1987).*

11), which occurs mainly in the form of pyrite. The H/C-O/C atomic ratios obtained from elemental analysis confirm the rank levels determined by vitrinite reflectance measurement. All coals fall within the van Krevelen "coalification band", indicating coal ranks from subbituminous to low volatile bituminous (Fig. 2). Variations of C/H-O/C ratios in samples 1, 2 and 3, which according to vitrinite reflectance have exactly the same rank (0.40 and 0.41% respectively), can be explained by differences in composition. Sample 3, for example, contains larger amounts of inertinite macerals (43 Vol. %) and can thus be expected to have greater O/C ratios. Ash contents determined by proximate analyses range from 4.8 to 57.5% (dry).

Petrographic characteristics and conversion rates

The degree of conversion for the coals analyzed in this study ranges from 8 to 78% (Table 1). The best conversion (>70%) was determined for the vitrinite-rich, low rank coals from Canada (sample 1, Highvale Mine; and sample 4, Luscar Sterco), and for sample 9 (seam Zollverein, W. Germany) which is high volatile A bituminous in rank. The relationships between rank, petrographic composition and conversion rates for all coals are illustrated in Figure 3. This figure shows clearly that within each ASTM rank class there is a strong relationship between the conversion rate and maceral composition, i.e. the amount of reactive macerals.

In the subbituminous coals from Canada the conversion increases from 8% for the inertinite-rich and ash-rich coal (sample 3) to 78% for the handpicked vitrain (sample 1), having 93 Vol. % reactive macerals. These values are the worst and best conversion rates recorded in the present study. They were obtained from the same coal zone and are clear evidence of the importance of maceral composition in the conversion of coals. In sample 3, the high ash content may also have had an influence upon the recorded low conversion rate.

A similar pattern of conversion dependency on petrographic composition can be illustrated for the high volatile bituminous coals. Samples 4 and 5 (high volatile C bituminous) were obtained from the same seam at Luscar Sterco, Canada. Sample 4 represents a handpicked vitrain lens (94 Vol. % reactive macerals) and sample 5 represents a channel sample from the same seam (81 Vol. % reactive macerals). The degree of conversion for sample 5 appears, however, to be somewhat low, possibly indicating an incomplete conversion. This is supported by the fact that in the residual materials from this hydrogenation run, minor amounts of only slightly altered vitrinite components were observed, which is indicative of incomplete conversion.

The sole sample from high volatile B bituminous rank (Prince Mine, N.S., Canada) shows a conversion rate of only 10% although the amount of reactive macerals total 93 Vol. %. Analysis of the residual material from this coal revealed a maceral composition in the residue very similar to that of the feedcoal, and newly formed materials such as semi-coke and coagulant were absent. These observations, together with the low conversion rate, suggest that the hydrogenation experiment failed, probably due to failures in the pressure or temperature controlling system.

In the high volatile A bituminous rank, relatively high conversions were achieved even for coals containing large amounts of inertinite macerals. Sample 10 (Bullmoose Mine, Canada) has a conversion rate of 54% even though its reactive maceral content is only 57 Vol. %. The same is true for sample 7 (South Africa), which also has a considerable amount of inertinite macerals, in particular semifusinite. The highest conversion rate of 78% was determined for sample 9 (seam Zollverein, W. Germany), which has a reactive maceral content of 81 Vol. %. Deviations from the general trend are shown by sample 8 (seam Gudrun, W. Germany) and sample 11 (China) which, despite fairly high contents of reactive macerals, only have moderate conversion rates, of 61% and 34% respectively. In fact, sample 8 has not only a high content of reactive macerals but the highest amounts of liptinite macerals (15 Vol. % by TAS) within this group. At the present time, the discrepancies are not understood and further experimentation needs to be done on these two samples.

TABLE 2

Elemental composition, ash content and H/C-O/C; atomic ratios for feedcoals used in hydrogenation experiments

Sample	Elemental Analysis (d.a.f.)					Ash (dry)	Atomic Ratios	
	C	H	N	S	O		H/C	O/C
1	75.0	5.26	0.79	0.29	20.2	6.8	0.84	0.20
2	74.5	5.04	1.00	0.34	19.7	15.4	0.81	0.20
3	68.7	5.28	1.04	0.14	24.6	57.5	1.01	0.27
4	79.1	5.76	1.39	0.26	13.4	9.1	0.87	0.13
5	78.7	5.14	1.08	0.24	15.6	24.6	0.78	0.15
6	80.2	5.32	1.34	3.73	10.0	10.3	0.80	0.09
7	85.0	5.15	2.32	1.34	7.3	12.1	0.73	0.06
8	83.7	4.91	1.65	1.87	10.4	8.4	0.70	0.09
9	88.7	5.27	2.04	0.68	5.6	4.8	0.71	0.05
10	88.5	4.87	0.92	0.22	6.1	12.2	0.66	0.05
11	79.8	5.09	1.08	4.75	6.5	35.8	0.77	0.06
12	90.6	4.61	0.99	0.27	4.4	14.6	0.61	0.04

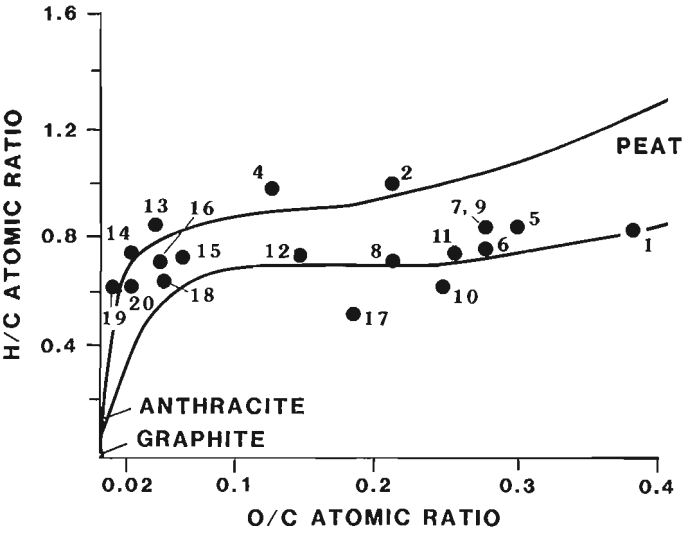

Figure 4. van Krevelen diagram illustrating H/C - O/C atomic ratios of feedcoals used in the vacuum pyrolyses experiments. Numbers refer to samples listed in Table 3.

It is interesting to note that the sole sample representing low volatile bituminous rank (sample 12, Smoky River Coal, Canada) has a conversion rate above 60%, despite the fact that it also contains considerable amounts of inert macerals, and the content of reactive macerals is low at 64 Vol. % (Fig. 3).

From the conversion rates shown for subbituminous and high volatile A bituminous coals, it is obvious that at higher rank levels the same conversion rate can be achieved with lower amounts of reactive macerals. In other words, low rank coals need a much higher content of reactive macerals to obtain acceptable conversion yields. The higher rank coals from Western Canada, which are characterized by high amounts of inertinite macerals (sample 10, Bullmoose Mine, and sample 12, Smoky River Coal) have acceptable conversion rates above 50%. These coals are currently mined and exported as coking coals. The results of the present study show that these coals also have potential for hydrogenation. Under the experimental conditions used, not only reactive-rich, high volatile bituminous coals are converted easily, but also the reactive-rich subbituminous coals. Good hydrogenation potential is also predicted for the low volatile bituminous coals.

TABLE 3

Origin, A.S.T.M. rank classes, petrographic characteristics and conversion rates for feedcoals used in vacuum pyrolysis experiments

Sample	Location	A.S.T.M. Rank	Vitrinite Reflectance (%)	Maceral Analyses Vol. % (m.m.f.)			Conversion (%)
				Vitrinite	Liptinite	Inertinite	
1	Manalta, Sask.	lignite	0.37[1]	82	4	14	31.9
2	Hat Creek, B.C.	lign./subbit.	0.41[1]	74	26	–	49.6
3	Hat Creek, B.C.	lign./subbit.	0.41[1]	–	92	8	97.9
4	Marten Ridge, B.C.	lign./subbit.	0.42[1]	21	78	<1	70.2
5	Hat Creek, B.C.	lign./subbit.	0.44[1]	95	5	–	38.4
6	Vesta Mine, Alta.	subbituminous	0.44[1]	100[3]	–[3]	–[3]	30.7
7	Vesta Mine, Alta.	subbituminous	0.45[1]	86[4]	11[4]	3[4]	34.0
8	Highvale Mine, Alta.	subbituminous	0.45[1]	61	5	34	27.7
9	Forestburg, Alta.	subbituminous	0.49[1]	94	3	3	30.6
10	Peace River Coalfield, B.C.	high vol. B bit.	0.64[2]	53	2	45	27.0
11	Coal Valley, Alta.	high vol. B bit.	0.66[2]	66	11	23	30.4
12	Prince Mine, N.S.	high vol. A bit.	0.73[2]	85	7	8	32.4
13	Elk Valley, B.C.	high vol. A bit.	0.79[2]	99	<1	<1	25.7
14	Elk Valley, B.C.	high vol. A bit.	0.87[2]	86	5	9	32.4
15	Elk Valley, B.C.	high vol. A bit.	0.89[2]	88	4	8	28.7
16	Weary Ridge, B.C.	high vol. A bit.	1.08[2]	83	4	13	23.4
17	Peace River Coalfield, B.C.	med. vol. bit.	1.09[2]	28	1	71	22.5
18	Peace River Coalfield, B.C.	med. vol. bit.	1.15[2]	34	3	63	20.4
19	Cardinal River Mine, Alta.	med. vol. bit.	1.39[2]	73	1	26	15.6
20	Weary Ridge, B.C.	low vol. bit.	1.52[2]	71	–	29	14.6

1 Mean random huminite (eu-ulminite) reflectance
2 Mean maximum vitrinite reflectance
3 handpicked vitrain from 4
4 channel sample

Vacuum pyrolysis experiments

Petrographic analyses of feedcoals

Rank

Table 3 lists the coals according to rank. The random huminite (eu-ulminite) reflectances for the lignites and subbituminous coals range from 0.37 to 0.49%. The maximum vitrinite reflectance for the bituminous coals range from 0.73 to 1.52%. The reflectances indicate a rank range from lignite to low volatile bituminous.

Composition

Table 3 lists the distribution of maceral groups (m.m.f.) for the coals used in the experiments. Macerals of the vitrinite group (huminite group in lignites and subbituminous coals) were found to range from 25 to 100 Vol. %. Liptinite macerals were found to range between nil and 11 Vol. %, except in three samples which had been selected

for extraordinary high liptinite contents: sample 2 has a resinite content of 24 Vol. %, sample 3 represents enrichment of resinite (92 Vol. %), handpicked from Hat Creek lignite, and sample 4 was chosen for a very high alginite/resinite content of 66 Vol. %. Macerals of the inertinite group were found to range between nil and 70 Vol. %. One pair of samples (nos. 7 and 8, Vesta Mine, Table 3) was chosen to compare conversion characteristics for vitrinite-rich (vitrain) layers to whole seam characteristics.

Chemical analyses of feedcoals

Results of elemental analyses are shown in Table 4. Organic carbon contents increase regularly with increasing rank except in sample 3 (handpicked resinite) and sample 17 (petrographic analysis indicated high degree of oxidation). Oxygen contents decrease with increasing rank from 31.2% in the lignite to 2.5% in the low volatile bituminous coal. Virtually no oxygen content was determined in the handpicked resinite, whereas the oxidized sample (No. 17, Table 4) is characterized by a much higher oxygen content as would be expected for its rank range (see Table 4). The variations in carbon, oxygen and hydrogen contents for the feedcoals are shown in the van Krevelen diagram, Figure 4, in which the atomic ratios of H/C and O/C are plotted. The lower rank coals plot in an area characterized by relatively high O/C and H/C ratios between 0.7 and 0.8. With increasing rank the H/C ratios remain fairly constant, whereas the O/C ratios decrease significantly as a result of decreasing oxygen contents. A few exceptions from the general trend can be explained by petrographic composition and effects of weathering. Samples 2 and 4 have relatively high H/C ratios which reflect the high amounts of liptinite macerals as observed micro-scopically (Table 3). Sample 17 (low H/C ratio and high O/C ratio) plots in an area far from the other samples of similar rank. Petrographic examination of this sample had shown a high degree of oxidation as a result of weathering of the coal seam. Sulphur contents were found to be very low in most of the samples except in the coal from Eastern Canada (sample 12, Prince Mine, sulphur = 3.66%). Ash contents determined by proximate analyses were found to range between 6.2 and 55 wt% (Table 4).

Petrographic characteristics and conversion rates

Conversion rates were found to range between 14.6% in the low volatile bituminous coal (sample 20) and 70.2% in the liptinite-rich coal at the transition from lignite to subbituminous coal (sample 4). An extremely high conversion rate of 97.9% was determined for the handpicked resinite from Hat Creek (sample 3). The conversion rates decrease in general with increasing rank of the coal (Table 3). At the same rank level the conversion rates appear to be affected particularly by the liptinite contents (samples 2, 3, 4, 7 and 8).

Conversion rates obtained from the vacuum pyrolysis experiments were correlated with chemical and petrographic properties of the feedcoals (Hébert, 1986). A good correlation was observed with chemical parameters such as the H/C atomic ratio, volatile matter contents and calorific values. For the petrographic characteristics (reflectance and maceral contents) the best correlation to conversion rates was found by using a method originally developed by Mackowsky and Simonis (1969) for the prediction of coke strength. In this method Mackowsky and Simonis (1969) concentrated macerals of various ranks, determined the volatile matter contents and then calculated a correction factor based on the percentage of liptinite macerals present. The final equation

$$X_T = \text{Vol.\% Vitrinite} \times \text{Corr}_{Vi} + \text{Vol.\% Liptinite} \times \text{Corr}_{Li} + \text{Vol. \% Inertinite} \times \text{Corr}_{In} + \text{Del}$$

TABLE 4

Elemental composition, ash content and H/C-O/C atomic ratios for feedcoals used in the vacuum pyrolysis experiments

Sample	Elemental Analysis (d.a.f.)					Ash (dry)	Atomic Ratios	
	C	H	N	S	O		H/C	O/C
1	62.5	4.10	1.70	0.49	31.2	13.0	0.79	0.37
2	70.8	6.51	1.38	1.19	20.1	21.6	1.10	0.21
3	91.0	12.08	0.50	0.85	0.0	17.8	1.59	-
4	78.1	7.13	1.38	0.85	12.5	6.7	1.10	0.12
5	66.7	4.58	1.67	1.11	25.9	19.9	0.82	0.29
6	68.7	4.39	1.65	0.39	24.8	6.5	0.77	0.27
7	68.6	4.49	1.70	0.85	24.4	7.7	0.79	0.27
8	73.3	4.30	1.42	0.54	20.4	18.2	0.70	0.21
9	68.1	4.65	2.20	0.51	24.6	8.4	0.82	0.27
10	71.4	3.58	1.62	0.31	23.1	10.7	0.60	0.24
11	77.2	4.84	1.01	0.39	16.5	25.5	0.75	0.25
12	76.2	4.63	1.60	3.66	13.9	8.3	0.73	0.14
13	85.9	6.09	3.20	1.00	3.8	55.0	0.85	0.03
14	87.9	5.57	3.47	0.34	2.8	12.0	0.76	0.02
15	85.2	5.41	2.48	0.62	6.3	12.8	0.76	0.06
16	85.9	5.04	3.85	0.99	4.3	10.3	0.70	0.04
17	75.0	3.28	3.60	0.50	17.6	6.2	0.52	0.18
18	88.7	4.72	1.76	0.36	4.5	8.7	0.64	0.04
19	93.2	4.81	1.27	0.45	0.2	13.2	0.62	0.002
20	90.6	4.65	1.92	0.45	2.9	27.0	0.62	0.02

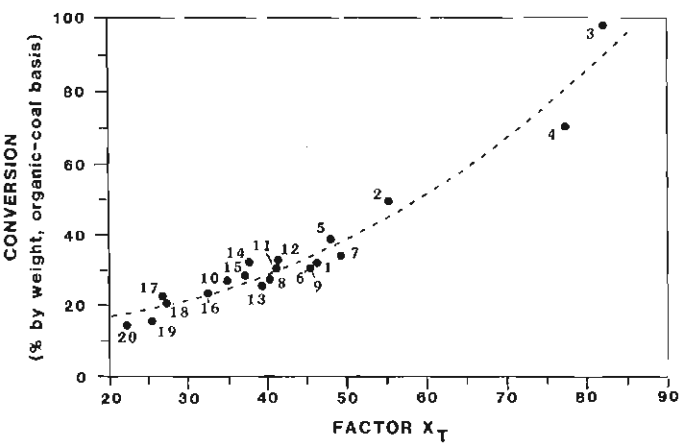

Figure 5. *Correlation of conversion rates and calculated volatile matter (X_T) calculated from maceral group analyses and rank (Mackowsky and Simonis, 1969), modified from Hébert (1986). For definition of X_T see text.*

represents the calculated volatile matter of a coal based on maceral group contents corrected for rank level ($Corr_{Vi}$, $Corr_{Li}$, $Corr_{In}$) and for liptinite contents (Del). The calculated volatile matter contents of the feedcoals using the above method matched very closely the values determined by proximate analyses (Hébert, 1986). The correlation of calculated volatile matter contents with conversion rates is shown in Figure 5. The curve has a high correlation coefficient of r = 0.997 and is valid for a reflectance range from 0.30 to 2.71% (lignite to semianthracite).

CONCLUSIONS

Hydrogenation

Feedcoals. Petrographic and elemental analyses indicated a rank range from subbituminous to low volatile bituminous coals. Maceral analyses showed wide variations in maceral contents at each rank level.

Conversion. The best conversion rates were determined for reactive-rich, subbituminous and high volatile bituminous coals. At each rank level there is a strong relationship between the rate of conversion and petrographic composition of the feedcoals, with the highest conversion rates determined for the coals rich in reactive macerals. In hydrogenation, high volatile A bituminous coals appear to be superior to subbituminous coals, because they tend to achieve acceptable conversion rates with less amounts of reactive macerals. From the preliminary results it appears also that low volatile bituminous coals with substantial amounts of inertinite macerals can be hydrogenated successfully.

Vacuum Pyrolyses

Feedcoals. Petrographic and elemental analyses indicated a rank range from lignite to low volatile bituminous coal. Maceral analyses showed wide variations in maceral contents, particularly in the lower rank ranges. Three samples were characterized by anamolously high contents of liptinite macerals. One pair of samples represented a vitrain layer and a channel sample from the whole seam.

Conversion. Best conversion rates were determined for the liptinite-rich lignites and subbituminous coals. Conversion rates decreased in general with increase in rank. Conversion properties of the coals were found to correlate best wih petrographic characteristics, volatile matter contents and H/C-atomic ratios, in that order.

ACKNOWLEDGMENTS

The authors wish to thank personnel of Bullmoose Mine, Coal Valley Mine, Highvale Mine, Luscar Mine, Prince Mine, Vesta Mine, Manalta Coal Ltd. and Smoky River Coal Ltd. for providing sample material. The authors also thank Dr. A.R. Cameron, ISPG, for providing sample material from Elk Valley and Weary Ridge, B.C.

REFERENCES

Bustin, R., Cameron, A., Grieve, D., and Kalkreuth, W.D.
1985: Coal petrology - its principles, methods and applications. Geological Association of Canada, Short Course Notes, v. 3, second revised edition, 230 p.

Fisher, C., Sprunk, A., Eisner, H., O'Donnel, H., Clarke, L. and Storch, H.
1942: Hydrogenation and liquefaction of coal, Part 2: Effect of petrographic composition and rank of coal. U.S. Bureau of Mines, Technical Paper 642, p. 1-162.

Given, P., Cronauer, D., Spackman, W., Davis, A., and Biswas, B.
1975: Dependence of coal liquefaction behaviour on coal characteristics. 2. Role of petrographic composition. Fuel, v. 54, p. 40-49.

Hébert, M.
1986: Etude pétrographique de charbons canadiens soumis à la pyrolyse sous vide. Université de Sherbrooke, unpublished M.Sc. thesis, Sherbrooke, Canada.

Hébert, M., Kalkreuth, W., and Roy, C.
1987: Vacuum pyrolysis of Canadian coal - petrographic and chemical analyses of feedstock and reaction residues. International Conference on Coal Science, J.A. Moulijn et al. (eds.); Elsevier Science Publishers B.V., Amsterdam, The Netherlands, p. 637-642.

Kalkreuth, W., Roy, C., and Hébert, M.
1986: Vacuum pyrolysis of Canadian Prince Mine coal - chemical and petrological analyses of feedcoal and solid residues. Erdöl und Kohle, v. 39, no. 5, p. 213-222.

Mackowsky, M.-Th. and Simonis, W.
1969: Die Kennzeichnung der Kokskohlen für die mathematische Beschreibung der Hochtemperaturverkokung im Horizontalkammerofen bei Schüttbetrieb durch Ergebnisse mikroskopischer Analysen. Glückauf Forschungshefte, v. 30, p. 25-37.

Riepe, W. and Steller, M.
1984: Characterization of coal and coal blends by automatic image analyses. Fuel, v. 35, p. 313-317.

Roy, C., de Caumia, B., and Kalkreuth, W.
1985: Vacuum pyrolysis of Prince Mine coal, Nova Scotia, Canada. Fuel, v. 64, p. 1662-1666.

Steller, M., Kalkreuth, W., and Hodek, W.
1987: Hydrogenation of selected subbituminous and bituminous coals - micropetrological and chemical studies on feedstock and reaction residues. Erdöl und Kohle, v. 40, no. 9, p. 383-393.

Whitehurst, D., Mitchell, T., and Farcasiu, M.
1980: Coal liquefaction. Academic Press, New York, 378 p.

A preliminary assessment of the hydrocarbon potential of selected coals using hydrous pyrolysis

H. von der Dick[1], M.G. Fowler, and W. Kalkreuth
Institute of Sedimentary and Petroleum Geology, Calgary

Dick, H. von der, Fowler, M.G., and Kalkreuth, W., A preliminary assessment of the hydrocarbon potential of selected coals using hydrous pyrolysis. In Contributions to Canadian Coal Geoscience, Geological Survey of Canada, Paper 89-8, p. 115-119, 1989.

Abstract

The initial results of hydrous pyrolysis experiments of six coal samples of different compositions indicate a strong dependence between the maceral composition and the hydrocarbon generation potential, i.e. the greater the abundance of hydrogen-rich macerals, in particular resinite, the greater the hydrocarbon potential of the coal. In the coals selected for the hydrous pyrolysis experiments, two distinct types of resinite with different maturation behaviour were found to occur.

When subjected to hydrous pyrolysis conditions used here only samples with a high resinite content generate large quantities of hydrocarbons. The discrepancy between the solvent extractable yields and hydrocarbons generated from resinite-rich samples are predominantly low molecular weight compounds (C_1-C_{15}). A sample of "pure" vitrinite with a low initial hydrocarbon potential gave low yields on hydrous pyrolysis and showed a limited change in its Rock-Eval S2 value.

Résumé

Les résultats initiaux des essais de pyrolyse hydratée sur six échantillons de charbon de compositions différentes indiquent une dépendance élevée entre la composition macérale et le potentiel de production des hydrocarbures, c.à.d. que plus la quantité des macéraux riches en hydrogène est grande, de résinite en particulier, plus la possibilité que les charbons renferment des hydrocarbures est grande. Dans les charbons choisis pour les essais de pyrolyse hydratée, on a noté la présence de deux types distincts de résinite possédant différentes caractéristiques de maturation.

Quand ils ont été soumis aux conditions de pyrolyse hydratée, seuls les échantillons possédant un taux de résinite élevé produisaient de grandes quantités d'hydrocarbures. L'écart qui existe entre la production extraite par solvant et les hydrocarbures produits à partir d'échantillons riches en résinite révèle des composés ayant surtout un poids moléculaire bas (C_1-C_{15}). Un échantillon de vitrinite "pure" possédant initialement un faible potentiel de production d'hydrocarbures a donné de bas rendements dans les essais de pyrolyse hydratée et a démontré peu de changement au niveau de sa valeur Rock-Eval S2.

INTRODUCTION

Although coals have been considered as prolific sources of natural gas (Tissot and Welte, 1984, p. 251-252), traditionally they have not been considered as significant oil source rocks because they normally contain hydrogen-poor organic matter and/or because of the difficulties of expelling hydrocarbons from coals (e.g. Durand and Paratte, 1983 and references therein). In recent years these concepts have been questioned (Durand and Paratte, 1983) and coals and coal-bearing strata have increasingly attracted attention as potential oil source rocks. Detailed geochemical studies on oils from several areas such as the Beaufort-Mackenzie Delta (Snowdon and Powell, 1982), the Mahakam Delta (Schoell et al., 1983) and the Gippsland Basin (Shanmugan, 1985) suggest they are at least partially derived from terrestrial organic matter. Furthermore, Teichmüller (1974) has observed petroleum-like substances within coal seams.

It is evident from recent studies that the maceral composition of coals is of prime importance for their hydrocarbon potential. The greater the proportion of hydrogen-rich macerals such as cutinite, sporinite and resinite, the greater the hydrocarbon potential of the coal will be (e.g. Thompson et al., 1985; Khavari Khorasani, 1987). The possibility that vitrinite, normally the predominant maceral in humic coals, might also have some potential to generate higher molecular weight compounds rather than just gas has also been considered. It is now evident that the term "vitrinite" is applied to materials with a diverse chemistry and that some vitrinites are more hydrogen-rich than others (Thompson et al., 1985; Khavari Khorasani, 1987). Although the potential of vitrinites to generate oil is generally much lower than typical oil-prone organic matter, it has been argued by some authors that its abundance in coals could compensate for this and, hence, they could be significant oil source rocks (e.g. Durand and Paratte, 1983).

[1]Canadian Hunter Exploration Ltd.
435 - 4th Avenue S.W., Calgary, Alberta T2P 3A8

The technique of hydrous-pyrolysis (heating organic matter in the presence of liquid water) has been used to examine the hydrocarbon potential of many source rocks (e.g. Winters et al., 1983). Here we use hydrous-pyrolysis to assess the ability of some coals to generate petroleum. Although extrapolation of the results obtained from hydrous pyrolysis experiments to natural systems can be disputed, at the present time this method is the best for simulating the processes associated with maturation such as hydrocarbon generation. The results presented here are preliminary and a more detailed report will be published at a later date.

Sample Material

Six coals ranging in rank from peat/lignite transition to subbituminous from Canada, Greece and West Germany were selected for this study. Their vitrinite (huminite) reflectance values range from 0.12% to 0.45% R_{max} (Table 1). The detailed petrographic composition of these coals is given in Table 2. All samples are humic coals with vitrinite as the dominant maceral. Two samples (1 and 4) are rich in resinite, sample 5 has a relatively high cutinite content, sample 3 has a mixed liptinite content, whereas sample 6 is composed entirely of vitrinite.

Analytical Techniques

Aliquots of the original coals were first taken for reflected light microscopy, Rock-Eval pyrolysis and total organic carbon (TOC) analysis. Standard Rock-Eval conditions of 300°C to 600°C at 25°C/min with a 390°C S3 cut off temperature were used. The coal samples were dried, crushed in a steel disc mill for one minute and soxhlet extracted using dichloromethane (DCM) for 24 hours. Fractionation of the resulting extract into saturated hydrocarbons, aromatic hydrocarbons, NSO compounds and asphaltenes, and gas chromatography of the saturated hydrocarbons was as previously described (Fowler and Brooks, 1987). Hydrous pyrolysis of the extracted coals was achieved using a similar method to that of Eglinton et al. (1986). Briefly, the extracted coals were enclosed in a stainless steel bomb (35 ml) which was one third filled with distilled water and then purged with nitrogen. The bomb was rapidly heated to 330°C and then held isothermal for 72 hours. The bomb was allowed to cool prior to opening. The pyrolysed coals were first extracted at room temperature with 125 ml distilled water and then five times with 125 ml DCM under ultrasonic agitation. Water soluble organic compounds and hydrocarbons floating on the water phase (if present) were then extracted into a DCM phase and combined with the DCM extract of the pyrolysed coals. This combined organic extract was subsequently fractionated and the saturate fraction examined by gas chromatography in the same way as the original extracts. Rock-Eval/TOC analysis and reflected light microscopy were also used to examine the pyrolysed coal residues.

RESULTS AND DISCUSSION

Hydrocarbon Potential of Original Coal Samples

Figure 1 shows the six original coals plotted on a pseudo van-Krevelen diagram of Hydrogen Index (HI = S2/TOC) versus Oxygen Index (OI = S3/TOC). Most of the coals plot near to the type III organic matter maturation trendline. Samples 1 and 4 with high resinite contents plot in between organic matter type II and III. Their increased hydrocarbon potential is related to their high content of resinite, as observed under the microscope.

TABLE 1

Sample locations, A.S.T.M. rank groups and huminite reflectances for feedcoals

SAMPLE	LOCATION	ASTM RANK	HUMINITE Rrandom(%)
1	Kozani, Greece[1]	Peat/Lignite	0.12
2	Joannina, Greece[1]	Peat/Lignite	0.19
3	Bergheim, Germany	Lignite	0.31
4	Bergheim, Germany[2]	Lignite	0.31
5	Hat Creek, Canada	Lignite	0.39
6	Vesta Mine, Canada[3]	Subbituminous	0.44

[1]from Cameron et al (1984)

[2]handpicked xylite

[3]handpicked vitrain, No. 3 seam

TABLE 2

Maceral-Analyses (mineral matter free) and mineral matter contents of feedcoals

	SAMPLE					
MACERAL	1[1]	2[1]	3	4[2]	5	6[3]
Textinite	45	1	-	82	-	-
Texto-ulminite	17	1	-	-	-	-
Ulminite	2	4	32	-	75	85
Gelinite	1	2	17	-	1	-
Corpohuminite	4	6	5	-	7	14
Densinite/Attrinite	4	65	27	-	3	1
Total Huminite	73	79	81	82	86	100
Sporinite	-	4	10	-	1	-
Cutinite	-	-	-	-	10	-
Resinite	26	2	1	18	-	-
Liptodetrinite	-	-	6	-	3	-
Others	1	4	-	-	-	-
Total Liptinite	27	10	16	18	14	-
Inertinite	-	11	3	-	1	-
Mineral Matter (Vol%)	2	17	4	-	41	8

[1]from Cameron et al (1984)
[2]handpicked xylite
[3]handpicked vitrain, No.3 seam

The high amount of solvent extract and S1 yields obtained from sample 1 (Table 3) appears to be the result of the high solubility and mobility, at low temperatures, of the resinite in this sample. Twenty-six per cent of the volume of the organic matter in the unextracted sample was determined to be resinite (Table 2) but no resinite was recognised in the extracted sample. The gas chromatogram of the C_{15+} saturate fraction is dominated by diterpanes, which are derived from resinites (Snowdon, 1980). Absence of optically recognizable resinite, but a high S1 value for the extracted sample (13.4 mg/g, Table 3), indicates the presence of disseminated, incorporated resinite in the coal matrix which is mobilized at a low temperature. Sample 1 is the only sample in which the maceral composition of the original coal was significantly changed by soxhlet extraction.

Sample 4, which also has a high resinite content, shows much lower extract yields and a low S1 peak. The resinite of this sample appears to be geochemically different from that of sample 1 in its low solubility and low mobility at low temperatures. Some workers have shown that resinites, depending on their biochemical origins (e.g. whether they are derived from angiosperms or gymnosperms), or their maturity, may show very different chemical and optical properties (Mukhopadhyay and Gormly, 1984; Dobell et al.,

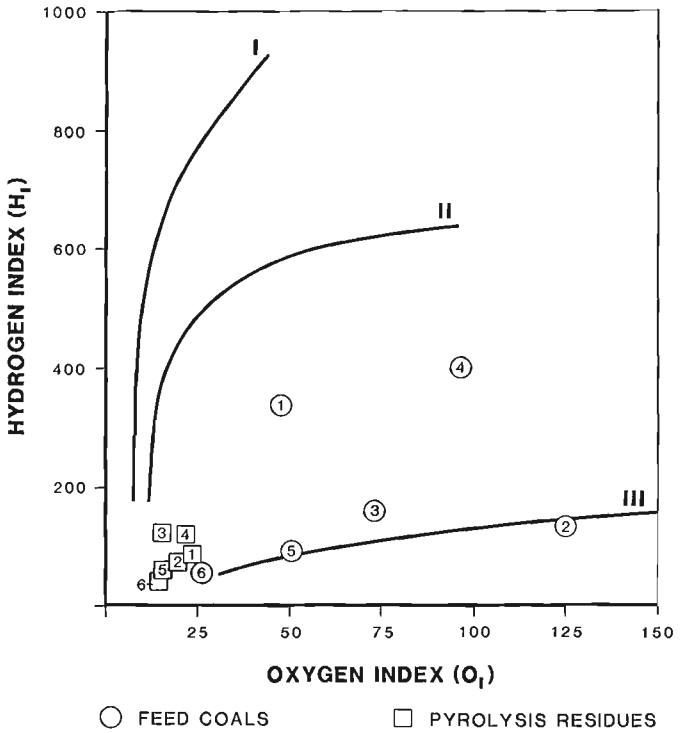

Figure 1. *Pseudo van Krevelen diagram illustrating Hydrogen and Oxygen Indices for feedcoals and pyrolysis residues.*

1984; Teerman et al., 1987). In the feedcoals of the present study, resinite was found to occur as two distinct varieties: 1) angular shaped, fracture filling and of high fluorescence intensity and, 2) *sensu stricto* occurring as oval shaped bodies in cell-tissues, characterized by lower fluorescence intensity.

The Rock-Eval Tmax values of the two resinite-rich coals are much lower (>360°C) than for the other samples (Table 3), which is probably a function of the low temperature needed to generate hydrocarbons from resinite (Powell and Snowdon, 1983). Hence, the low Tmax-values for samples 1 and 4 indicate incorporation of resinous material into the non-extractable (kerogen) fraction. The high S2 values for samples 1 and 4 (Table 3) and their overall higher hydrocarbon potential (Fig. 1), are most likely related to their resinite content since only minor amounts of other hydrogen-rich components were determined (Table 2) and vitrinite-rich samples (e.g. sample 6, Table 2) show relatively low S2 values (Table 3). The high S2 value for sample 1 can be explained by the presence of an extractable and thermally labile form of resinite. The high S2 peak but low extractability of sample 4 can be explained by the presence of a second, less thermally labile resinite type. Alternately, there might be a matrix effect by which the otherwise highly mobile resinite is adsorbed to other macerals such as vitrinite by diagenetic reactions and would, therefore, require higher temperatures and thermal disintegration of the sample for the release of resinous compounds. The latter explanation is favoured here, since it explains our observations made in the experiments: extraction removes the visible, most obvious resinite, whereas the resinous material incorporated into other macerals requires higher temperatures to be mobilized.

This concept of disseminated, incorporated resinite is also supported by samples 5 and 6 which do not contain microscopically observable resinite, but the chromatograms of their extractable C_{15+} saturate compounds reveal resinite-derived diterpanes as the major compounds. However, the amount of resinous material incorporated into these samples must be minor as they have much lower S2 and higher Tmax values than samples 1 and 4.

The extract yields of the vitrinite-rich coals do not appear to be related to their maceral content, with the exception of sample 6. This sample, which was assessed as being 100% vitrinite with no liptinitic components, gave the lowest extract yield.

Effects of Hydrous Pyrolysis

Hydrous pyrolysis at 330°C for 72 hours on immature organic-rich rocks has been shown to result in mature kerogen with a reflectance level of 0.7 to 0.8% R_{max} (Lewan, 1985; Muhamad, 1986). Reflectance measurements on the coal residues from our first experiments gave much higher values than expected (1.3-1.5%). Subsequently, several control experiments were run under different conditions, such as varying the particle size of the coal used in the pyrolysis experiments, using non-extracted coal instead of extracted coal samples, using helium instead of nitrogen as a purge gas, varying the amount of coal used in the experiments, and mixing a crude oil with the coal samples. None of these variations in the experimental conditions had any significant effect on the resulting R_{max} values. Experiments at 310°C for 72 hours resulted in somewhat lower R_{max} values (1.2-1.3%) than those at 330°C (Table 4) but were still higher than those recorded for source rock samples heated at 330°C for 72 hours. Lewan (1985) first reported this discrepancy between the reflectance values obtained after heating source rocks and coal samples. He

TABLE 3

Basic geochemical data for feedcoals

Sample	Pellet No.	TOC (wt %)	C_{15+} DCM Extract ppm	Extracts (ppm)				ROCK EVAL			
				saturates	aromatics	resins	asphaltenes	S_1 (mg/g rock)	S_2	S_3	Tmax (°C)
1	346/81	62.5	349410	19928	28832	147128	153522	93.0	210.0	31.8	358
2	503/81	43.0	4822	76	4	685	4057	5.9	39.4	55.6	419
3	85/87	57.7	15618	185	989	4419	10025	4.6	84.1	45.5	408
4	84/87	57.2	5124	47	301	2164	2612	4.8	226.2	56.7	356
5	1020/82	57.9	8016	1689	598	1794	3935	2.1	50.7	29.1	418
6	960/82	65.8	3147	330	462	1009	1346	0.15	32.3	17.6	420
1[1]	346/81	60.4						13.4	166.1	46.2	358

[1] Rock-Eval data and TOC on dichloromethane (DCM) extracted coal

attributed it to the increased refractory nature of dispersed vitrinite in sediments due to it being allochthonous whilst that in coals was more likely to be autochthonous and therefore involved in reducing reactions early in its depositional history.

The Tmax values obtained from Rock-Eval analysis of coal residues show considerable variation. Samples 2 and 3 show values in the range of those obtained from source rocks samples (around 450°C; Fowler, unpublished results) after they have been heated at 330°C for 72 hours (Table 4). The other coal residues gave much higher values that are approximately consistent with the measured reflectance values of about 1.4%. At present we have no explanation for the variation in the Tmax values.

A comparison of feedcoals with pyrolysis residues shows that only the resinite-rich samples 1 and 4 show a large decrease in their S2 values after hydrous pyrolysis and hence have generated large quantities of hydrocarbons (Fig. 1). An observation common to all coals is their significantly lower oxygen index as a result of defunctionalization of organic matter exposed to hydrous pyrolysis.

A more complicated relationship emerges when the results of extraction (Table 4) are examined. The yields of extract obtained from samples 1 and 4 are much lower than their high S1 values would suggest. In fact they are not significantly different from those of the other samples. This indicates that a large proportion of the hydrocarbons generated are not extracted and/or retained in the C_{15+} fraction. These compounds are probably being retained within the coal matrix and in a natural system might not be available for migration. A much larger fraction of the extract obtained from samples 1 and 4 was water soluble and expelled into the water phase, which also seems to be a result of their higher resinite content. Also, a large proportion of the decrease in the S2 peak of these samples cannot be accounted for by the amounts of extract and S1 values and must be presumed to be C_1-C_{15} compounds which were not measured in this work. This reflects the natural system, as the accumulations of hydrocarbons often assigned a resinite source are termed "immature condensates". This is because they are dominated by lower molecular compounds in spite of their apparent maturity being much less than that normally expected for condensates (Snowdon and Powell, 1982; Nissenbaum et al., 1985). All other samples with relatively low or no resinite contents show little change in their S2 values (Fig. 1). Sample 3, with a relatively high content of sporinite, is only marginally reduced in its hydrocarbon potential, indicating that sporinite has not yet generated significant amounts of hydrocarbons under these conditions. Sample 6, which consists of 100% vitrinite, gave the lowest yield of extract and shows very little change in its S2 value. Therefore, it must be concluded that this particular vitrinite has very little hydrocarbon potential.

CONCLUSIONS

The initial results of the hydrous pyrolysis of selected coal samples indicate the following:

1. The hydrocarbon potential of coals does depend on their maceral composition.
2. The presence of hydrogen-rich macerals, and in particular resinite, can significantly increase the hydrocarbon potential of coals.
3. Resinite-rich coals produce low amounts of C_{15+} hydrocarbons in comparison to lower molecular weight compounds.
4. The differences in the behaviour of the two resinite-rich samples during extraction and Rock-Eval analysis supports the suggestions of previous workers that there are different types of resinites, which could behave differently during thermal maturation. In addition to different origins, matrix effects probably contribute to the behaviour of resinite under thermal stress. Both aspects may explain the complex behaviour of resinites in natural systems.

TABLE 4

Basic geochemical and petrographic data for hydrous pyrolysis residues (330°C, 72 hours) residues[1]

Sample	Pellet	TOC (wt %)	Total C_{15+} DCM Extract[3] ppm	Water Extract ppm	DCM Extract ppm	Total Extracts (ppm)[3] saturates	aromatics	resins	asphaltenes	ROCK EVAL[2] S_1 (mg/g rock)	S_2	S_3	Tmax (°C)	Rmax (%)
1	346/81	72.9	61133	40100	21033	333[4]	2167	10400	8133	36.4	62.5	16.7	477	1.48
2	503/81	50.1	34580	9510	25070	3811	2692	5734	12833	3.3	33.3	10.0	453	1.37
3	85/87	72.2	48093	9110	38983	8517	6864	21780	1822	5.3	81.6	11.7	451	1.33
4	84/87	73.5	37841	24025	13816	42	901	6541	6332	38.2	70.2	15.9	476	1.43
5	1020/82	68.5	20265	6634	13631	2508	3135	2871	5117	4.0	34.5	10.7	481	1.51
6	960/82	68.2	11985[5]	4397	7588	653	1256	2085	3594	3.7	30.3	11.5	505	1.47
6[6]	960/82									3.8	29.6	10.0	467	1.10
6[7]	960/82	70.5								3.4	64.0	6.9	463	1.41

[1]all residues were DCM extracted prior and after pyrolysis;

[2]Rock Eval data from pyrolysis residues extracted with water and DCM;

[3]obtained from combined DCM extracts of water phase and pyrolysis residues;

[4]low absolute weight, accuracy questionable;

[5]doublicate sample yielded 11415ppm;

[6]anhydrous pyrolysis 330°C/72hrs; sample extracted prior, but not after pyrolysis; Rock Eval data on unextracted pyrolysis residue;

[7]Sample mixed with paraffinic crude, pyrolysed, then extracted and analyzed by Rock Eval

ACKNOWLEDGMENTS

We wish to acknowledge the excellent technical assistance of Sneh Achal and Kai Flexhaugh, and the comments of Lloyd Snowdon on an earlier version of this manuscript.

REFERENCES

Cameron, A.R., Kalkreuth, W.D., and Koukouzas, C.
1984: The petrology of Greek Brown coals. International Journal of Coal Geology, v. 4, p. 173-207.

Dobell, P., Cameron, A., and Kalkreuth, W.
1984: Petrographic examination of low-rank coals from Saskatchewan and British Columbia, Canada, including reflected and fluorescent light microscopy, SEM, and laboratory oxidation procedures. Canadian Journal of Earth Sciences, v. 21, p. 1209-1228.

Durand, B. and Paratte, M.
1983: Oil potential of coals - a geochemical approach. In Petroleum Geochemistry and Exploration of Europe, J. Brooks (ed.); Geological Society Special Publication No. 12, p. 255-265, Blackwell Scientific Publications, Oxford.

Eglinton, T.I., Rowland, S.J., Curtis, C.D., and Douglas, A.G.
1986: Kerogen-mineral reactions at raised temperatures in the presence of water. Organic Geochemistry, v. 10, p. 1041-1052.

Fowler, M.G. and Brooks, P.W.
1987: Organic geochemistry of Western Canada Basin tar sands and heavy oils. 2. Correlation of tar sands using hydrous pyrolysis of asphaltenes. Journal of Energy and Fuels, v. 1, p. 459-467.

Khavari Khorasani, G.
1987: Oil-prone coals of the Walloon Coal Measures, Surat Basin, Australia. In Coal and Coal-bearing Strata: Recent Advances, A.C. Scott (ed.); Geological Society Special Publication No. 32, p. 303-310.

Lewan, M.D.
1985: Evaluation of petroleum generation by hydrous pyrolysis experimentation. Philosophical Transactions of the Royal Society of London, Physical Sciences, v. A315, p. 123-134

Muhamad, A.J.
1986: Hydrous pyrolysis of selected organic-rich rocks. University of Newcastle-upon-Tyne, unpublished M.Sc. thesis.

Mukhopadhyay, P.K. and Gormly, J.R.
1984: Hydrocarbon potential of two types of resinite. Organic Geochemistry, v. 6, p. 439-454.

Nissenbaum, A., Goldberg, M., and Aizenshtat, Z.
1985: Immature condensate from southeastern Mediterranean Coastal Plain, Israel. American Association of Petroleum Geologists, Bulletin, v. 69, p. 946-949.

Powell, T.G. and Snowdon, L.R.
1983: A composite hydrocarbon generation model: Implications for evaluation of basins for oil and gas. Erdöl und Kohle, v. 36, p. 163-170.

Schoell, M., Teschner, M., Wehner, H., Durand, B., and Oudin, J.L.
1983: Maturity related biomarker and stable isotope variations and their application to oil/source rock correlation in the Mahakam Delta, Kalimantan; in Advances in Organic Geochemistry 1981, M. Bjorøy et al., (eds.); J. Wiley & Sons Ltd., Chichester, England, p. 156-163.

Shanmugam, G.
1985: Significance of coniferous rain forests and related organic matter in generating commercial quantities of oil, Gippsland Basin, Australia. American Association of Petroleum Geologists, Bulletin, v. 69, p. 1241-1254.

Snowdon, L.R.
1980: Resinite - a potential petroleum source in the Upper Cretaceous/Tertiary of the Beaufort-Mackenzie Basin. In Facts and Principles of World Oil Occurrence, A.D. Miall (ed.); Canadian Society of Petroleum Geologists, Memoir 6, p. 509-521.

Snowdon, L.R. and Powell, T.G.
1982: Immature oil and condensate-modification of hydrocarbon generation model for terrestrial organic matter. American Association Petroleum Geologists, Bulletin, v. 66, p. 775-788.

Teerman, S.C., Crelling, J.C., and Glass, G.R.
1987: Fluorescence spectral analysis of resinite macerals from coals of the Hanna Formation, Wyoming, U.S.A.. International Journal of Coal Geology, v. 7, p. 315-334.

Teichmüller, M.
1974: Generation of petroleum-like substance in coal seams as seen under the microscope. In Advances in Organic Geochemistry 1973, B. Tissot and F. Bienner (eds.); Editions Technip, Paris, p. 379-408.

Thompson, S., Cooper, B.S., Morely, R.J., and Barnard, P.C.
1985: Oil-generating coals. In Petroleum Geochemistry of the Norwegian Shelf, B.M. Thomas et al. (eds.); Graham and Trotman, London, p. 59-73.

Tissot, B.P. and Welte, D.H.
1984: Petroleum formation and occurrence. Berlin and New York, Springer-Verlag, 699 p.

Winters, J.C., Williams, J.A., and Lewan, M.D.
1983: A laboratory study of petroleum generation by hydrous pyrolysis. In Advances in Organic Geochemistry 1981, M. Bjorøy et al. (eds.); J. Wiley & Sons Ltd., Chichester, England, p. 524-533.

Organic petrology of two coal-bearing sequences from the Middle to Upper Devonian of Melville Island, Arctic Canada

F. Goodarzi, T. Gentzis[1], and A.F. Embry
Institute of Sedimentary and Petroleum Geology, Calgary

Goodarzi, F., Gentzis, T., and Embry, A.F., Organic petrology of two coal-bearing sequences from the Middle to Upper Devonian of Melville Island, Arctic Canada. In Contributions to Canadian Coal Geoscience, Geological Survey of Canada, Paper 89-8, p. 120-130, 1989.

Abstract

The petrology of Devonian coals taken from two sections on Melville Island has been studied. The coals occur in Givetian and Frasnian strata of the Weatherall, Hecla Bay and Beverley Inlet formations. Most of the coals are finely banded and are semi-bright. The dominant lithotype is clarain. Vitrain is less common and fusain and durain are very rare. The vitrinite content is low to moderate, consisting of telo- and desmocollinite, whereas the most conspicuous liptinite maceral is sporinite, megaspores in particular. Cutinite, alginite, resinite, exsudatinite and fluorinite are present in small amounts.

The microlithotype composition of the coals (liptinite-rich clarite, vitrinertoliptite) indicates deposition under water, in bays and swamps of the interfluvial areas near the coastline. The reflectance (0.57-0.79 $R_o$max) and spectral fluorescence of the Devonian coals indicate a rank of high volatile bituminous C-B. The high liptinite and low inertinite content makes the coals appropriate for use in liquefaction and gasification processes.

Résumé

La pétrologie des charbons dévoniens provenant de deux coupes situées dans l'île de Melville, a été étudiée. Les charbons se trouvent dans des strates du Givétien et du Frasnien, dans les formations de Weatherall, Hecla Bay et Beverly Inlet. La plupart des charbons sont finements rubannés et semi-brillants. Le lithotype dominant est le clairain. Le vitrain se rencontre moins fréquemment; le fusain et le durain, très rarement. Le contenu en vitrinite varie de bas à modéré, consistant surtout en télo- et desmocollinite tandis que le macéral de type liptinite le plus en évidence est la sporinite, la mégasporinite en particulier. La cutinite, l'alginite, la résinite, l'exudatinite et la fluorinite se rencontrent en petites quantités.

La composition microlithotype de ces charbons (clarite riche en liptinite, vitrinertoliptite) indique que la sédimentation s'est faite sous l'eau, dans des baies et des marais situés entre des fleuves, près du littoral. Le taux de réflectance (0,57 à 0,79 $R_o$max) et la fluorescence spectrale des charbons dévoniens indiquent un rang bitumineux C et B à teneur élevée en matières volatiles. La haute teneur en liptinite et la basse teneur en inertinite rendent ces charbons appropriés aux procédés de gazéification et de liquéfaction.

INTRODUCTION

Coal occurs in almost all geological provinces in the Canadian Arctic Archipelago, ranging in age from Devonian to Tertiary (Ricketts and Embry, 1984). The oldest coals are found in the Middle to Upper Devonian clastic wedge, principally in the western Arctic Islands. This clastic wedge is up to 5000 m thick and contains marine-shelf, deltaic and fluvial deposits (Ricketts and Embry, op. cit.).

Embry and Klovan (1976) have mentioned the occurrence of thin (0.2-0.5 m) coal seams in the Hecla Bay and Beverley Inlet formations in the western Arctic. In addition, Goodarzi et al. (in press), have described a suite of Upper Devonian coals from the Beverley Inlet Formation in eastern Melville Island.

This study describes the petrology of Middle to Upper Devonian coals taken from two sections on Melville Island described by Embry and Klovan (1976). These are: 1) Cape Terrace section, western Melville; and 2) Weatherall Bay section, northeastern Melville.

Regional geology

Weatherall Formation

The Weatherall Formation consists mainly of coarsening-upward cycles of shale, siltstone and very fine to fine grained sandstone of marine shelf origin. It conformably overlies the Cape de Bray Formation and is conformably overlain by the Hecla Bay Formation (Embry and Klovan, 1976). Although over much of Melville Island the formation

[1]Organic Geochemistry Unit, Drummond Building
The University of Newcastle-upon-Tyne
Newcastle-upon-Tyne, NE1 7RU, U.K.

is devoid of coal, on western Melville the upper 400 m of the formation contain intervals of lower delta plain strata which include a few thin coal seams (max. 20 cm thick).

Good palynological control is available for the Weatherall Formation on Melville Island. The oldest section of the Weatherall Formation is at Weatherall Bay on northeastern Melville Island (Embry and Klovan, 1976). The top of the formation becomes younger to the west, being mid-Givetian in the northeast and Frasnian in the west and south (Embry and Klovan, op. cit.).

There was a wide spectrum of depositional environments ranging from open shelf, prodelta, delta front and marsh deposits. Coal and carbonaceous shale, often associated with point bar deposits of meandering distributaries on a deltaic plain, are most likely overbank, lake and marsh deposits (Embry and Klovan, 1976).

Hecla Bay Formation

The Hecla Bay Formation, defined by Tozer and Thorsteinsson (1964), is a distinctive, widespread stratigraphic unit characterized by fine to medium grained crossbedded sandstone of braided stream origin (Embry and Klovan, 1976). On Melville Island, it overlies the Weatherall Formation and is overlain by the Beverley Inlet Formation.

Palynological control is sparse because shales are not common and rarely exposed. The Hecla Bay is believed to be early-middle Givetian to early Frasnian in age (Embry and Klovan, 1976).

The depositional environment for some intervals in the Hecla Bay Formation is marine shelf to lower delta plain (Goodarzi et al., in press). Thin coal seams (30 cm) occur near the base of the formation in eastern Melville Island, and occur throughout the formation on western Melville Island in the shale-siltstone intervals that are believed to be of interdistributary bay origin. Five seams were noted in one section where the formation is 510 m thick.

The coals in the Hecla Bay Formation are Givetian in age and may range into the earliest Frasnian in western Melville Island.

On eastern Melville Island, two informal members of the Hecla Bay Formation are distinguished: 1) a thin, lower unit of interbedded quartzose sandstone, green siltstone and shale; and 2) a massive quartzose sandstone. Marine to brackish conditions of sedimentation within the lower member of the Hecla Bay are indicated by the occurrence of lingulid brachiopods (Harrison et al., 1985).

Beverley Inlet Formation

The Beverley Inlet Formation is 500 to 600 m thick, overlies the Hecla Bay Formation, and is unconformably overlain by the Parry Islands Formation (Embry and Klovan, 1976). On eastern Melville Island it consists almost exclusively of delta plain strata, within which a few thin coal seams (max. 30 cm) occur. To the west, the formation consists of alternating intervals of marine shelf and lower delta plain strata with associated coals (max. 30 cm). Palynological data indicate that the Beverley Inlet Formation is lower to middle Frasnian.

In summary, Devonian coal seams occur in Givetian, Frasnian and Famennian strata and are most often associated with lower delta plain strata. The coals formed mostly in bays and swamps of the interfluvial areas near the coastline.

Sample localities

The Weatherall Bay section, (Fig. 1; latitude 75°51'N to 75°42'N, longitude 106°18'W to 106°55'W) contains 2697 m (8900 ft) of Devonian strata (Embry and Klovan, 1976).

Samples E-72-10 (85 m) and E-72-12 (106 m) have been taken from this section and the relative stratigraphic position of the samples is shown in Table 1.

Samples E-72-15 (120 m), E-72-16 (33 and 120 m), E-72-19 (123 m), E-72-20 (91 m), E-72-23 (40 m) and E-72-24 (86 m) have been taken from the Cape Terrace section, Figure 2 (latitude 75°48'N to 75°36'N, longitude 116°37'W to 117°15'W), consisting of 2303 m (7600 ft) of Devonian strata (Embry and Klovan, 1976). The formations from which samples were taken are shown in Table I.

Experimental

Samples were crushed to pass 20 mesh (850 microns), mounted in resin epoxy, ground and then polished, according to the procedure outlined by Mackowsky (1982).

Reflectance in oil (noil = 1.518) was determined using a Zeiss MPM II microscope connected to a Zonax microcomputer, following the procedure outlined in the International Handbook of Coal Petrology (ICCP, 1975).

Fifty vitrinite reflectance measurements were taken for most of the nine samples studied (Table 1). Petrographic composition, including maceral group and mineral matter, was determined at 500 points using a Swift (model F) automatic point counter and mechanical stage. Three main maceral groups were identified: vitrinite, liptinite and inertinite. Vitrinite was subdivided into telo- and desmocollinite, and liptinite into micro (tenuispores and crassispores) and megaspores.

Spectral measurements (between 420 and 700 nm) of liptinite macerals were made using the same microscope, equipped with a high-powered mercury vapour lamp (100 Watt). The wavelength of the maximum fluorescence intensity (λmax) and red/green quotient (Q) were recorded under standard conditions (filters: excitation at 365 nm, barrier at 420 nm).

Spectral measurements were taken as quickly as possible using a water objective in order to minimize the alteration or fading effect as described by Van Gijzel (1971, 1975).

Coal samples were photographed using white and blue light.

RESULTS

Megascopic characteristics of the coals

Most of the coals are finely banded and have a semi-bright appearance.

The dominant lithotype of samples E-72-12 (106 m), E-72-19 (123 m), E-72-20 (91 m) and E-72-24 (86 m) is clarain. Vitrain is less common and fusain and durain bands are very rare.

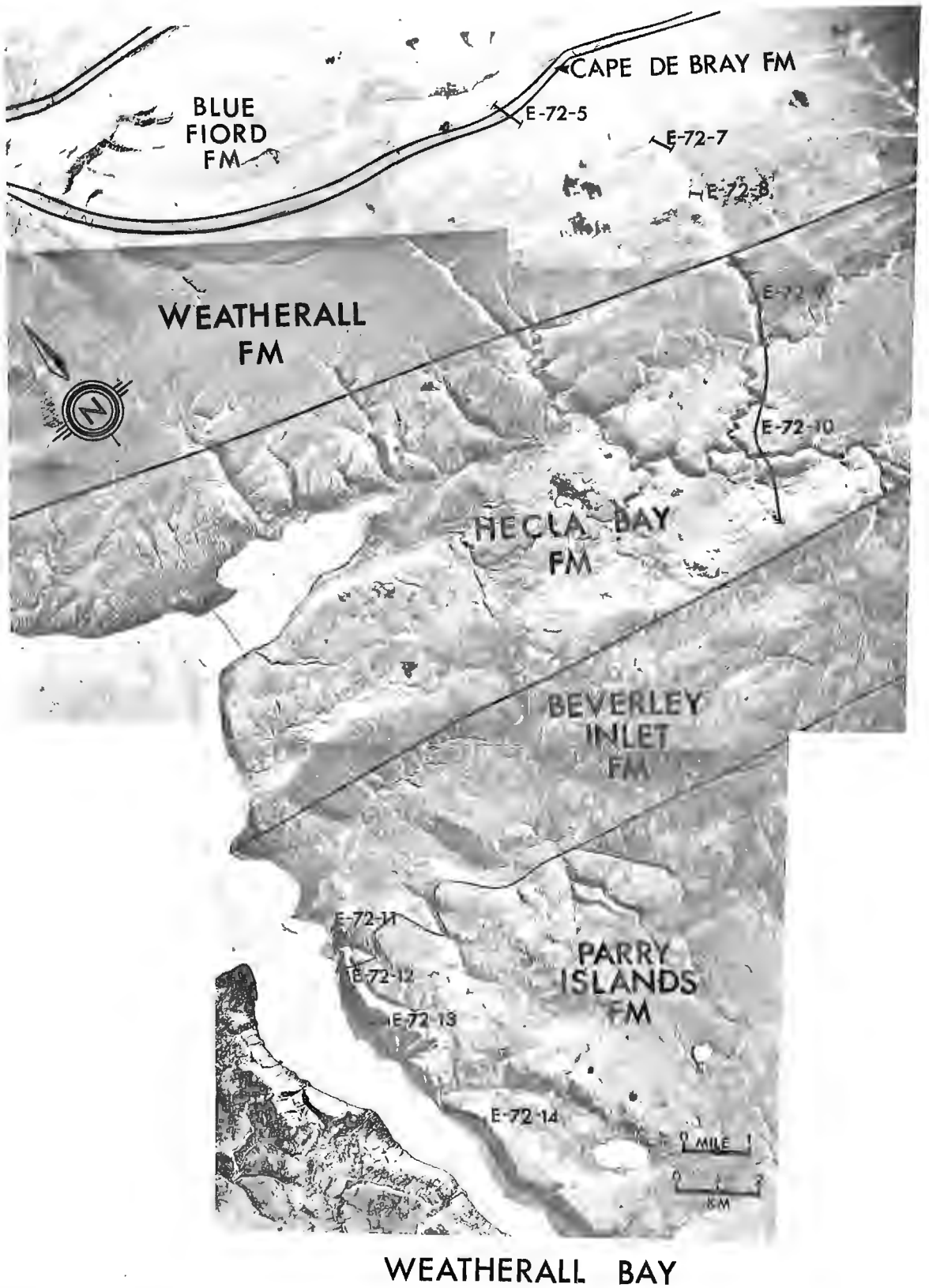

Figure 1. *An aerial photograph of the Weatherall section, northeastern Melville Island, showing section locations.*

Figure 2. An aerial photograph of the Cape Terrace section, western Melville Island, showing section locations.

The roofs of the coal seams are mainly shale with thin siltstone and, less commonly, sandstone. The floors of most of the coal seams are characterized by medium-grey shale with siltstone layers; the latter vary in thickness from 3 to 15 m and no relation between their thickness and the thickness of the overlying coal beds (0.1-0.2 m) was noted.

Petrographic characteristics

Uniform texture, fine microlayering, deficiency in inertinite macerals and high liptinite content are the most conspicuous microscopic characteristics of the above coals.

Vitrinite group

The vitrinite content is, in general, low to moderate ranging from 9 to 72%, averaging about 35% (Table 2). Telocollinite (V_A) (Fig. 3a) occurs as thick layers and predominates over desmocollinite (V_B). The latter occurs as a structureless groundmass in sporinite-rich and cutinite-rich clarite. Corpocollinite is rare and vitrodetrinite is a common constituent of carbargilite (>20% mineral matter; Stach, 1982).

Liptinite group

Liptinite content ranges from 8 to 74%, with distinct variation in the relative proportions of individual macerals (Table 2).

The most conspicuous maceral of the liptinite group is sporinite, particularly of the crassisporinite type. Megaspores (Figs. 3a to 3e) are extremely common, showing ornamentation and a punctate surface. Microspores (Figs. 3b to 3f) are not uncommon. They are well preserved and fluoresce with different intensities.

Occasionally, megaspores show a darker fluorescence rim around the trilete mark, possibly due to weathering or oxidation (Fig. 4a). Cutinite is present in smaller amounts as thin-walled, untoothed tenuicutinite (Figs. 4b and 4c) in cutinite-rich clarites.

Exsudatinite occurs in vein form infilling the rims of the spore tetrad (Fig. 4d). It exhibits a discrete fluorescence intensity, normally stronger than the associated liptinite macerals.

Isolated alginite bodies (Fig. 4e) occur only rarely and in association with sporinite-rich clarites.

Small bodies (<30 microns), which fluoresce weakly to moderately were recorded as liptodetrinite.

Inertinite group

Inertinite macerals do not exceed 4% (Table 2). The macerals of the inertinite group identified in the samples are micrinite, inertodetrinite, fusinite and semifusinite. Fusinite was negligible and observed in isolated fragments, mainly in carbargilite. Inertodetrinite is the common constituent of this group (Fig. 3a) while micrinite is present in the form of cell-infillings associated with phlobaphinitic and/or corpocollinitic structures.

TABLE 1

Sample location, reflectance and statistical parameters

Sample no.	Formation	Matrix	%Ro max.	N[1]	Standard deviation
E-72-10-85[2]	Hecla Bay	coaly	0.64	50	0.02
E-72-12-106	Beverley Inlet	carbonaceous shale	0.57	50	0.03
E-72-15-120	Weatherall	carbonaceous shale	0.76	50	0.02
E-72-16-33	Weatherall	coaly	0.76	50	0.03
E-72-16-120	Weatherall	coaly	0.57	35	0.02
E-72-19-123	Hecla Bay	carbominerite	0.58	50	0.03
E-72-20-91	Beverley Inlet	carbominerite	0.79	25	0.02
E-72-23-40	Beverley Inlet	coaly	0.57	50	0.02
E-72-24-86	Beverley Inlet	coaly	0.68	25	0.03

[1] N = number of measurements
[2] last digits indicate distance from base of section

TABLE 2

Maceral analysis of the samples

a) Maceral Analysis on coals (volume%) under white light

Sample	Vitrinite A	Vitrinite B	Vitrodet.	Inertinite	Liptinite	MM
E-72-10-85	10	28	–	3	46	13
E-72-16-33	16	56	–	–	25	3
E-72-16-120	3	–	20	–	57	20
E-72-23-40	16	–	5	–	74	5
E-72-24-86	17	1	–	3	67	12

b) Analysis of liptinite macerals (volume %) under fluorescent light

Sample	Megaspores	Microspores				Lipto-detri-nite	Matrix bitumi-nite	Other
		Low intensity		Moderate intensity yellow thick-walled	High intensity bright yellow thin-walled			
		orange thick-walled	brown thin-walled					
E-72-10-85	3	22	10	–	5	3	–	3(a)
E-72-16-33	trace	10	13	–	–	2	–	1
E-72-16-120	4	13	8	4	3	1	18	3(b)
E-72-23-40	26	41	4	–	trace	2	–	1
E-72-24-86	65	17	10	5	trace	1	–	1(b)

c) Maceral analysis on carbominerite-carbonaceous shale (volume %) under white light

Sample	Vitrinite A	Vitrinite B	Vitrodet.	Inertinite	Liptinite	MM
E-72-12-106	7	2	–	4	46	41
E-72-15-120	26	2	–	–	8	64
E-72-19-123	25	5	–	1	45	24
E-72-20-91	35	3	–	2	37	23

In E-72-10-85 most spores are smooth-surfaced
In E-72-16-33 'thick' spores are not as thick as in other samples
In E-72-16-120 most microspores are non-ornamented
In E-72-23-40 most spores are ornamented and/or granular textured
In E-72-24-86 most spores are ornamented and/or granular textured
Thick spores are more ornamented than thin

3(a) - cutinite and suberinite
3(b) - resinite and alginite

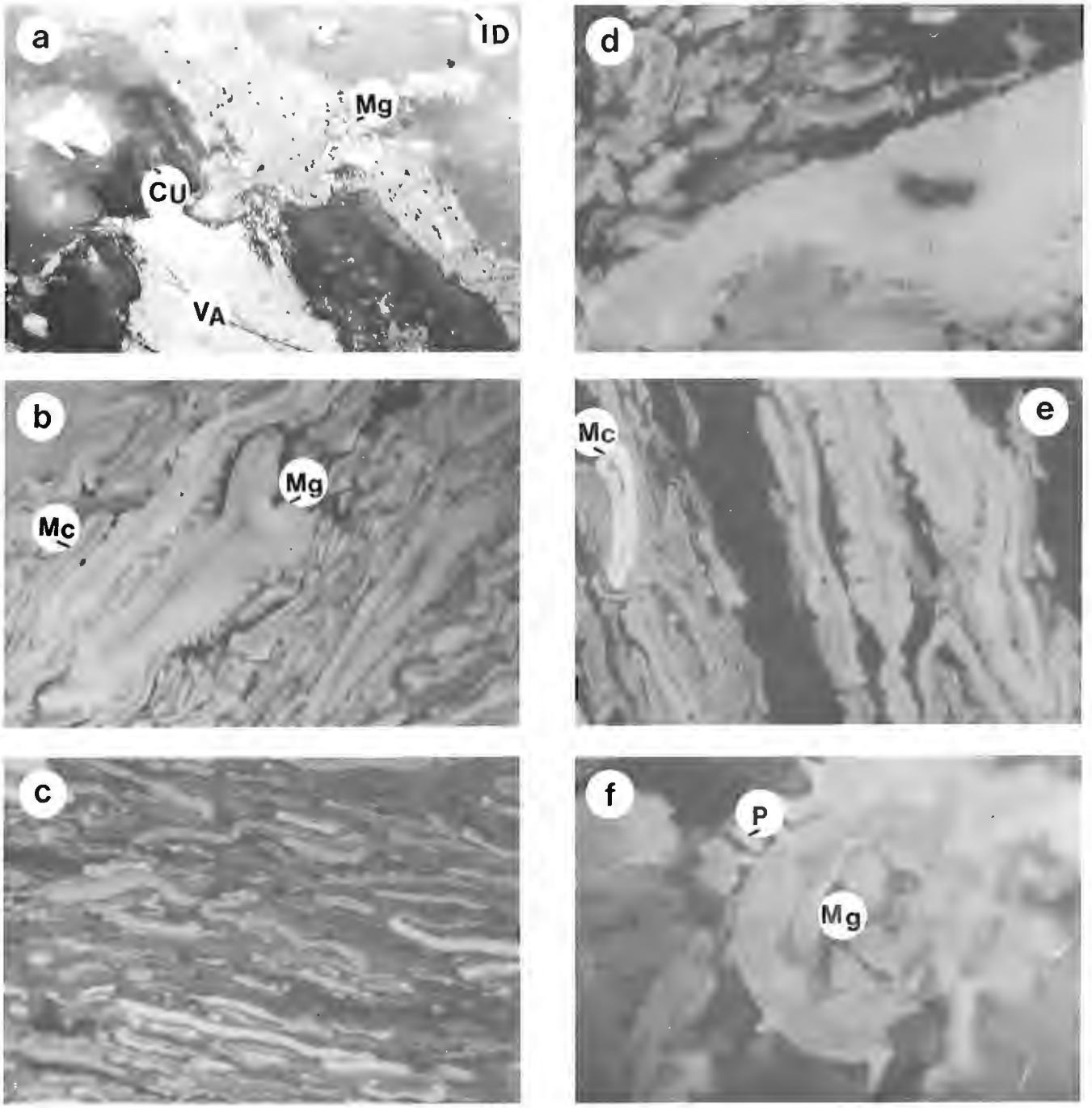

Figure 3. *Macerals of the liptinite group. All photomicrographs in oil immersion, fluorescent blue light, except 3a. Magnification is 500x.*

a) Megaspores (Mg) showing a punctate surface in association with fragments of cutinite (Cu) showing internal reflections. Vitrinite A (telocollinite; V_A) and inertodetrinite (ID) are also present. Reflected white light. Sample E-72-23.

b) A concentration of megaspores (Mg) and microspores (Mc) in a sporoclarite band. Note the ornamentation on the megaspores. Sample E-72-16 (33 m).

c) Similar to 3b; note the distinct microstratification characteristic of cannel coals. Sample E-72-12.

d) Ornamented mega- and microspores. Sample E-72-23 (40 m).

e) Thin-walled microspore (Mc) in association with heavily ornamented megaspores. Note the higher fluorescence intensity of the microspore. Sample E-72-23.

f) A megaspore (Mg) showing characteristic processes (P). Sample E-72-24 (86 m).

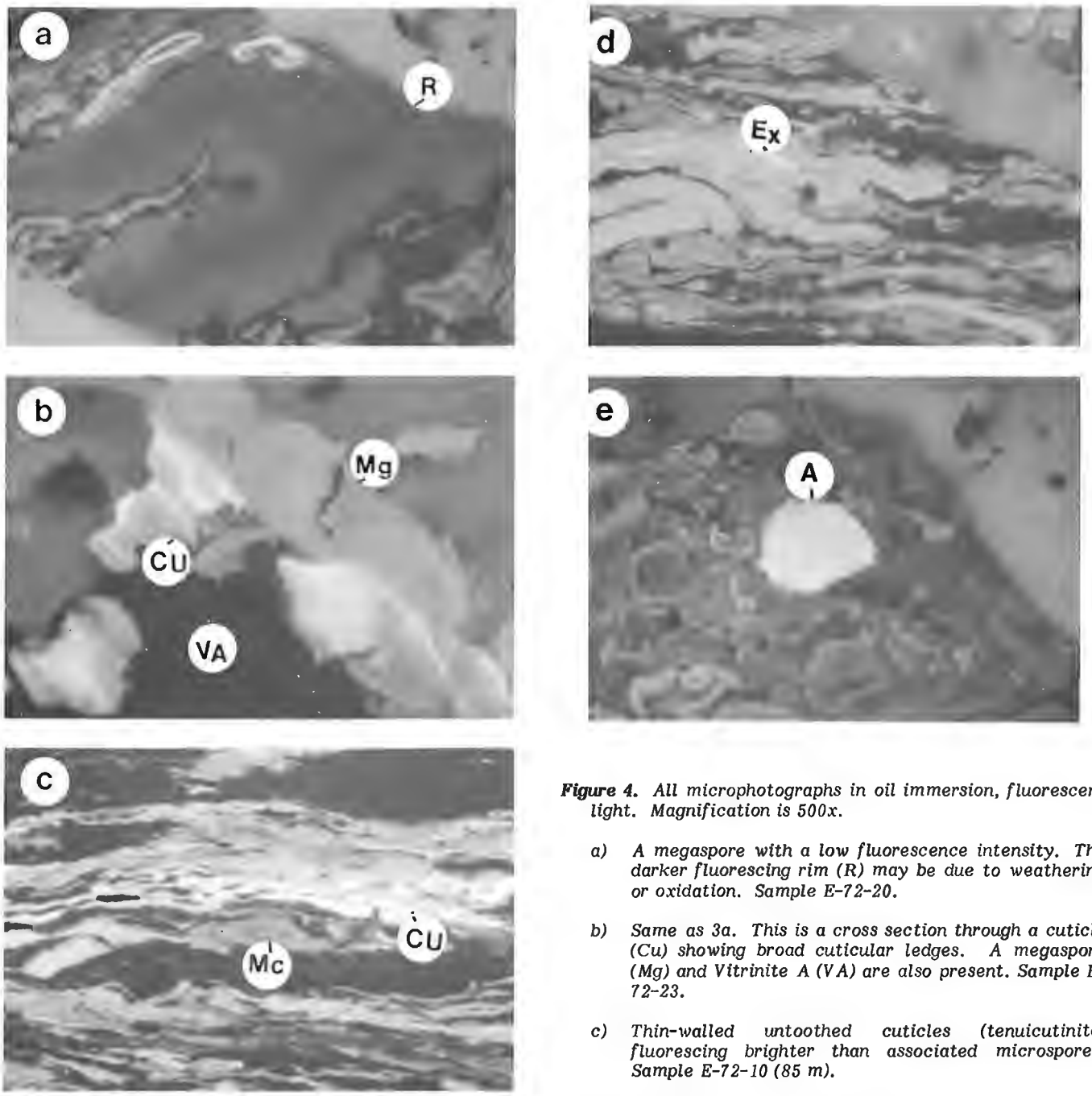

Figure 4. *All microphotographs in oil immersion, fluorescent light. Magnification is 500x.*

a) A megaspore with a low fluorescence intensity. The darker fluorescing rim (R) may be due to weathering or oxidation. Sample E-72-20.

b) Same as 3a. This is a cross section through a cuticle (Cu) showing broad cuticular ledges. A megaspore (Mg) and Vitrinite A (VA) are also present. Sample E-72-23.

c) Thin-walled untoothed cuticles (tenuicutinite) fluorescing brighter than associated microspores. Sample E-72-10 (85 m).

d) Exsudatinite (Ex) within the internal structure of a megaspore. Sample E-72-23.

e) A highly fluorescing algal body (A) cut perpendicular to bedding enclosed by mega- and microspores. Sample E-72-15.

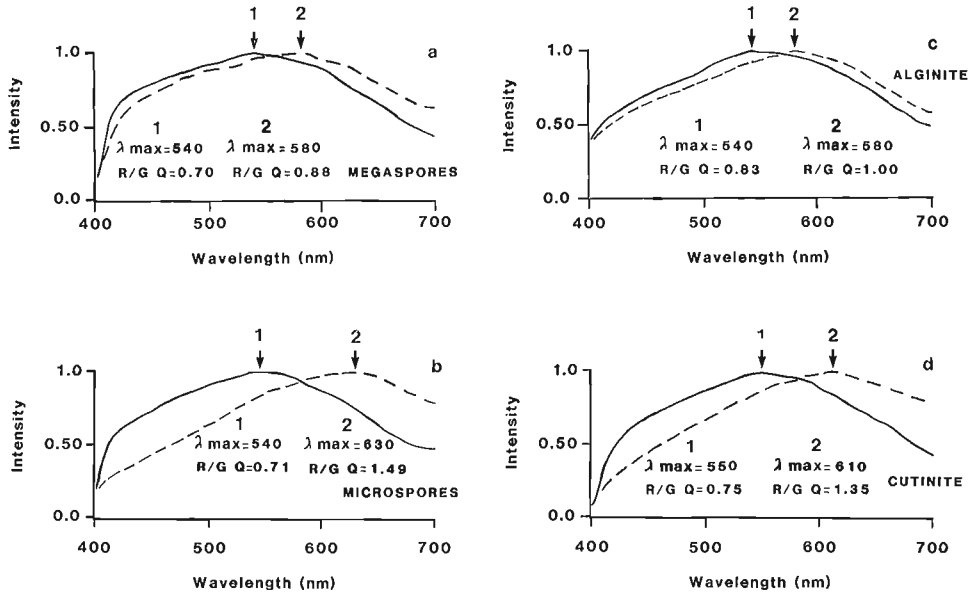

Figure 5. *Spectral fluorescence curves of liptinite macerals.*

a) Megaspores *c) Alginite*

b) Microspores *d) Cutinite*

Mineral matter

Mineral matter varies from 3 to 64%. The common minerals are clays, occurring finely dispersed or infilling cavities. Pyrite and quartz are rare in these coals.

Reflectance

The reflectance of the Devonian coals ranges from 0.57 to 0.79% R_o max, which indicates a coal rank of high volatile bituminous C-B. Due to the high liptinite content of the coals, the true reflectance may be suppressed by as much as 0.2% (Hutton et al., 1980; Price and Barker, 1985; Goodarzi et al., 1987). Nevertheless, reflectance values point to a mature stage of coalification with respect to oil generation. The maceral analysis reveals that a high percentage of macerals could be reactive during technological processes (liquefaction, gasification).

Fluorescence

Only non-weathered samples were used to ensure that no variation in spectral parameters related to weathering or oxidation occurred. Weathering, oxidation and biodegradation of liptinite macerals cause a shift towards the red end of the spectrum and a decrease in fluorescence intensity (Crelling, 1983; Goodarzi, 1986; and Teerman et al., 1987).

The average spectral maximum for megaspores varies between 540 nm (sample E-72-23-40; Fig. 5a) and 580 nm (sample E-72-16-33; Fig. 5a). The corresponding red/green quotients (R/G Q), are 0.70 and 0.88.

Microspores fluoresce with a moderate yellow to orange-brown intensity. The spectral maximum ranges between 540 nm (sample E-72-16-120; Fig. 5b) and 630 nm (sample E-72-20-91; Fig. 5b), with the corresponding R/G Q being 0.71 and 1.49.

Alginite (Botryococcus) fluoresces bright yellow and shows a range in λ max between 540 and 580 nm (R/G Q = 0.83-1.00; Fig. 5c).

Cutinite has a wavelength of maximum intensity between 550 nm (R/G Q = 0.75; Fig. 5d) and 610 nm (R/G Q = 1.35; Fig. 5d). It shows a yellow to light brown fluorescence intensity. Resinite has a narrower average spectral maximum range between 550 and 570 nm (R/G Q = 0.74-0.83; Fig. 6a). It appears as globular bodies displaying a moderate to high yellow intensity.

Fluorinite has a λ max at 540 nm and a quotient of 0.55 (sample E-72-16-120; Fig. 6b).

The spectral fluorescence parameters shown in Table 3 appear to be in good agreement with the reflectance, both pointing to a similar rank level. The study shows that it is not easy to differentiate megaspores from microspores in these samples based only on spectral fluorescence parameters in the range of 540-580 nm.

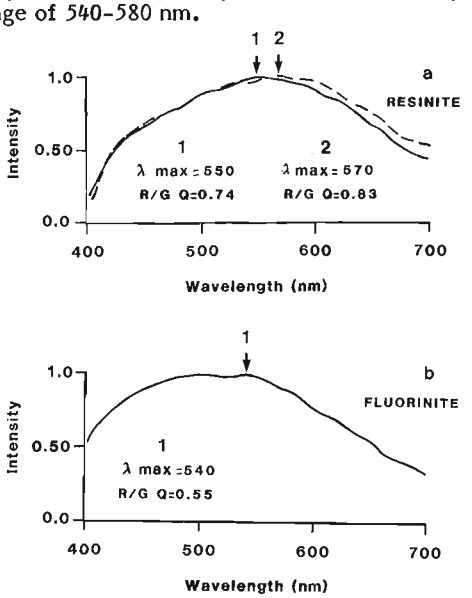

Figure 6. *Spectral fluorescence curves of liptinite macerals.*

a) Resinite *b) Fluorinite*

TABLE 3

Spectral fluorescence parameters of liptinite macerals

Maceral	λ max (nm)	R/G Quotient	Fluorescence colour
Sporinite (megaspores)	540-580	0.70-0.88	moderate-high yellow
Sporinite (microspores)	540-630	0.71-1.49	moderate yellow to orange brown
Alginite	540-580	0.83-1.00	bright yellow
Cutinite	550-610	0.75-1.35	yellow to light brown
Resinite	550-570	0.74-0.83	moderate to high yellow
Fluorinite	540	0.55	bright yellow

DISCUSSION

Devonian coals and carbominerites from Arctic Canada are often rich in liptinite, particularly sporinite (Goodarzi et al., in press). The sporinite content of the coal is as high as 74% (Table 2). Such coals are relatively rare and, to the author's knowledge, have not been described in the literature to any great extent. A coal with such high liptinite and low inertinite (<4.0%) can be of economic importance as feed for gasification and liquefaction processes.

Composition of coal

When the maceral compositions of these coals are plotted on a microlithotype ternary diagram, and on the basis of maceral analysis, the whole coal would be similar to clarite, however all but one falls in the category of clarite with one exception reporting in vitrinertoliptite (Fig. 7).

The dominant components of the microlithotype vitrinertoliptite are macerals of the liptinite group which exceed both the vitrinite and inertinite groups (Stach, 1982). Vitrinertoliptite is a relatively rare microlithotype and may have a history of formation which can vary between those of clarite and durite. Vitrinertoliptites, like the liptinite-rich clarites, are deposited subaquatically (Teichmüller, 1982) in a calm depositional environment. Vitrinertoliptite-rich sediments are somewhat similar to cannel coals and canneloid shales (Moore, 1968) which are also sporinite-rich. The latter contain vitrodetrinite and a variety of other macerals, including sporinite of a uniform size, which indicates the hypautochthonous nature of the macerals. Macerals in vitrinertoliptite-rich sediments are autochthonous. Many of the Devonian coals of this study are liptinite-rich clarites. Liptinite-rich clarite is deposited subaquatically, but contain more liptinite than vitrinite and inertinite. Of the liptinite-rich clarites, the sporinite clarites should be compared with the reed peats and reed brown coals (Teichmüller, 1982). Many of the spores were blown or floated into the area from other environments (Teichmüller, op. cit.). The bituminite and liptodetrinite components of these coals probably formed from algae and other lipid-rich plant remains. Clarites generally suggest formation under water and are particularly common in thin uneconomic seams (Teichmüller, op. cit.).

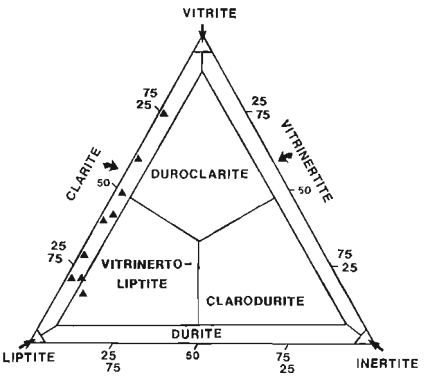

Figure 7. A microlithotype ternary composition diagram (mineral matter free basis) of the samples studied.

Environment of deposition

An environment suitable for the formation of coal is developed gradually and depends on many factors, such as subsidence rate of the basin, type of plant community, rate of sedimentation and tectonic setting of the area (Falini, 1965; Teichmüller and Teichmüller, 1982; Goodarzi and Gentzis, 1987). Any imbalance between the above factors results in drowning or drying of the coal-forming environment, bringing about dilution of organic material (formation of carbominerite) or its disappearance (formation of shale).

In the initial stages of establishment of a coal-forming peat, the rate of input of organic material could be lower than that of the inorganic material (Goodarzi, 1985). The present suite of samples consists mainly of carbominerites and includes five true coals (<20% mineral matter) (Tables 1, 2). Carbominerites are often found in seat earth, partially representing paleosol and/or early stage of coal forming peat (Goodarzi, op. cit.).

The samples are liptinite-rich and show fine micro-layering, which suggests that they were deposited in areas of open water with some input by subaquatic plants. An influence of open reed-type swamps with sedges and herbaceous vegetation is also expected, due to the presence of low to moderate amounts of telo- and desmocollinite.

The low inertinite content further indicates the subaquatic nature of these sediments, because inertinite forms as a result of oxidation/dehydration or charring of the plant materials during peat accumulation (Teichmüller, 1982). In addition, there must have been no alternation of high and low ground water table levels due to temporary drainage of the peat surface.

Environmental interpretations based on megaspore identification are complicated because the habitat and distribution of the Devonian megaspore-bearing flora are unknown (Chi and Hills, 1976). Chi and Hills (op. cit.) observed that the Hecla Bay Formation in another Cape Terrace section, near the section in this study, contained well preserved megaspores. Continental environments usually contain abundant and well preserved megaspores in dark grey, carbonaceous shales and organic-rich siltstones (Chi and Hills, op. cit.). Abundant megaspores are interpreted to represent either continental conditions or an influx of continental sediments into a nearshore-marine environment.

CONCLUSIONS

Devonian coal seams on Melville Island occur in Givetian, Frasnian and Fammenian strata deposited in a lower delta plain environment. The coal seams are very thin (max. 30 cm) and are characterized by a high liptinite and low to moderate vitrinite content.

The coals have been deposited subaquatically in bays in the interfluvial areas near the coastline. Their reflectance values are between 0.57 and 0.79% $R_o$max, which would place them into the mature stage of hydrocarbon generation. There also appears to be good agreement between reflectance and spectral fluorescence parameters.

The coals have potential as feed for liquefaction and gasification processes due to their high liptinite and low inertinite content.

REFERENCES

Chi, B.I. and Hills, L.V.
1976: Biostratigraphy and taxonomy of Devonian megaspores, Arctic Canada. Bulletin of Canadian Petroleum Geology, v. 24, no. 4, p. 640-818.

Crelling, J.C.
1983: Current uses of fluorescence microscopy in coal petrology. Journal of Microscopy, v. 132, p. 251-266.

Embry, A.F. and Klovan, J.E.
1976: The Middle – Upper Devonian clastic wedge of the Franklinian Geosyncline. Bulletin of Canadian Petroleum Geology, v. 24, no. 4, p. 485-639.

Falini, F.
1965: On the formation of coal deposits of lacustrine origin. Geological Society of America Bulletin, v. 76, p. 1317-1346.

Goodarzi, F.
1985: Organic petrology of Hat Creek coal deposit No. 1, British Columbia. International Journal of Coal Geology, v. 5, p. 377-396.

1986: Optical properties of oxidized resinite. Fuel, v. 65, p. 260-265.

Goodarzi, F., Davies, G.R., Nassichuk, W.W. and Snowdon, L.R.
1987: Organic petrology and Rock Eval analysis of Lower Carboniferous Emma Fiord Formation in Sverdrup basin, Canadian Arctic Archipelago. Marine and Petroleum Geology, v. 4, pp. 132-145.

Goodarzi, F. and Gentzis, T.
1987: Depositional setting, determined by organic petrography of the Middle Eocene Hat Creek No. 2 coal deposit, British Columbia, Canada. Bulletin of Canadian Petroleum Geology, v. 35, no. 2, p. 197-211.

Goodarzi, F., Gentzis, T., and Harrison, J.C.
in press: Petrology and depositional environment of Upper Devonian coals from eastern Melville Island, Arctic Canada. Geological Survey of Canada.

Hutton, A.C., Kantsler, A.J., Cook, A.C. and McKirdy, D.
1980: Organic matter in oil shales. Journal of Australian Petroleum Exploration Association, v. 20, pt. 1, p. 44-67.

ICCP (International Committee for Coal Petrology)
1975: International handbook of coal petrology, Supplement to the 2nd edition. Centre Nationale de la Recherche Scientifique, Paris.

Mackowsky, M-Th.
1982: Rank determination by measurement of reflectance on vitrinites. In Stach's Textbook of Coal Petrology, E. Stach et al. (eds.); Gebrüder Borntraeger, Berlin, Stuttgart, p. 319-329.

Moore, L.R.
1968: Cannel coals, bogheads and oil shales. In Coal and coal-bearing strata, D. Murchison and T.S. Westoll (eds.); Oliver and Boyd, Edinburgh and London, p. 18-29.

Price, L.C. and Barker, C.E.
1985: Suppression of vitrinite reflectance in amorphous-rich kerogen – A major unrecognized problem. Journal of Petroleum Geology, v. 8, no. 1, p. 54-85.

Ricketts, B.D. and Embry, A.F.
1984: Summary of geology and resource potential of coal deposits in the Canadian Arctic Archipelago. Bulletin of Canadian Petroleum Geology, v. 32, no. 4, p. 359-371.

Stach, E.
1982: The lithotypes of humic and sapropelic coals. In Stach's Textbook of Coal Petrology, E. Stach et al. (eds.); Gebrüder Borntraeger, Berlin, Stuttgart, p. 171-177.

Teerman, S.C., Crelling, J.C. and Glass, B.G.
1987: Fluorescence spectral analysis of resinite macerals from coals of the Hanna Formation, Wyoming, U.S.A.. International Journal of Coal Geology, v. 7, p. 315-334.

Teichmüller, M.
1982: Origin of the petrographic constituents of coal. In Stach's Textbook of Coal Petrology, E. Stach et al. (eds.); Gebrüder Borntraeger, Berlin, Stuttgart, p. 219-294

Teichmüller, R. and Teichmüller, M.
1982: The geological basis for coal formation. In E. Stach, et al. (eds); Gebrüder Borntraeger, Berlin, Stuttgart, p. 5-82.

Tozer, E.T. and Thorsteinsson, R.
1964: Western Queen Elizabeth Islands, Arctic Archipelago. Geological Survey of Canada, Memoir 332, 242 p.

Van Gijzel, P.
1971: Review of the UV-fluorescnece microphotometry of fresh and fossil exines and exosporia. In Sporopollenin, J.A. Brooks et al. (eds.); Academic Press, London, p. 659-682.

1975: Polychromatic UV-fluorescence microphotometry of fresh and fossil plant substances with special reference to the location and identification of dispersed organic material in rocks. In Petrographie de la matière organique des sédiments, relations avec la paléotempérature et le potentiel pétrolier, B. Alpern (ed.); Centre National de la Recherche Scientifique, Paris, p. 67-91.

The required use of coal density values for calculating average composition of in situ coals

G.G. Smith
Institute of Sedimentary and Petroleum Geology, Calgary

Smith, G.G., The required use of coal density values for calculating average composition of in situ coals. In Contributions to Canadian Coal Geoscience, Geological Survey of Canada, Paper 89-8, p. 131-136, 1989.

Abstract

Coal is a heterogeneous material having composition and properties that can vary within a wide range. The composition of coal is commonly determined according to proportional contribution of constituents to the total weight of the whole coal (proximate analysis), proportional contribution of combustible constituents to the total weight of the products of combustion (ultimate analysis), and proportional contribution of ash constituents to the total weight of residue after combustion (ash analysis). Mathematical averages of results from coal analyses that are expressed on a weight per cent basis must be determined according to relative weight (not relative volume) factors that the analyses represent. Relative weight can be determined from relative volume (e.g. bed thickness) if density of the material is known. In situ bulk density of coal varies as a function of its composition and porosity and can be significantly lower than densities of associated rock units. It can be reliably estimated from information obtained by proximate analysis.

Résumé

Le charbon est un matériel hétérogène possédant une composition et des propriétés qui peuvent varier grandement. La composition du charbon est déterminée communément selon la contribution proportionnelle des constituants par rapport au poids total (analyse immédiate); selon la contribution proportionnelle des constituants combustibles par rapport au poids total des produits de la combustion (analyse élémentaire); selon la contribution proportionnelle des constituants en cendres par rapport au poids total du résidu après combustion (analyse des cendres). Les moyennes mathématiques des résultats des analyses des charbons qui sont exprimées en tant qu'un pourcentage du poids doivent être déterminées selon des facteurs liés au poids relatif (et non selon le volume relatif) que représentent les analyses. Le poids relatif peut être déterminé à partir du volume relatif (par exemple l'épaisseur des couches) si la densité du matériel est connue. La densité apparente in situ du charbon varie en fonction de sa composition et de sa porosité et elle peut être beaucoup plus basse que les densités des unités rocheuses qui lui sont associées. Elle peut être estimée d'une manière fiable à partir de l'information obtenue par analyse immédiate.

INTRODUCTION

The composition and properties of rocks that can be referred to by the generic term "coal" (i.e. rocks comprising mainly plant-derived carbonaceous materials) vary within a wide range. Methods used to characterize and evaluate coal are generally unlike those applied to any other rock-like materials.

A notable attribute of all in situ coals is low bulk density relative to associated rock units. This bulk density can vary within a wide range, depending on composition and porosity of the coal. When averaging analyses of in situ coals that are expressed on a weight per cent basis, values must be proportioned according to relative weights, not relative volumes, that analyzed components contribute to the mix. The weight of any known volume of material can be determined when its bulk density is known.

CHARACTER AND STANDARD ANALYSIS OF COAL

Coal is a heterogeneous material that comprises both organic and inorganic phases. The organic phase comprises a variety of plant tissues that have been progressively altered, both physically and chemically, as a result of diagenesis and catagenesis (i.e. peatification and coalification). Although the relationship between density of the individual organic constituents (i.e. macerals) and increasing coal rank is unclear, the porosity and inherent moisture content of a coal mass decreases during coalification (Sherlock, 1950; Dulhunty and Penrose, 1951). The progressive displacement of empty and water-filled pores by solids during coalification results in a progressive increase in bulk density of the organic phase of coal with increasing rank.

The density of mineral matter in coal is about double that of the organic phase. Variation in the amount of mineral matter in coal of a given rank causes significant variation in the bulk density of the coal.

The composition of coal is commonly determined from the following three distinct types of standard analyses (Fig. 1):

1. **Proximate analysis** is used to determine the general composition of the whole coal, with each constituent reported according to its proportional contribution to the total weight of the whole coal.

2. **Ultimate analysis** is used to determine the composition of the products of combustion that result from burning a coal, with each constituent reported according to its proportional contribution to the total weight of combustibles.

3. **Ash analysis** is used to determine the composition of the residue after burning a coal, with each constituent reported according to its proportional contribution to the total weight of ash.

Whole Coal (Proximate Analysis)	= Products of Combustion (Ultimate Analysis)	+ Residue after combustion (Ash Analysis)
% Moisture	% Carbon	% SiO_2
% Ash	% Hydrogen	% Al_2O_3
% Volatile Matter	% Sulphur	% Fe_2O_3
% Fixed Carbon	% Nitrogen	% P_2O_5
	% Oxygen	% CaO
		% MgO
		% SO_3
		% Others

Figure 1. *Standard analyses used for determining the composition of whole coal and associated combustible and ash components.*

Ply Thickness (tp)	Ash (wt %)	Ply Density (dp)	Relative Ply Weight (wp = tp * dp)
2.0 m	14.0	1.433	2.87
0.5 m	80.0	2.313	1.16
1.0 m	7.5	1.382	1.38
1.5 m	30.0	1.579	2.37
0.5 m	63.0	1.997	1.00
1.5 m	5.0	1.363	2.04
Σtp = 7.0 m			

Figure 2. *Hypothetical mining zone of medium volatile bituminous coal, sampled and tested on a ply-by-ply basis.*

Relative Ply Weight (wp)	Coal Zone	Moisture (wt%)	Ash (wt%)	Volatile Matter (wt%)	Fixed Carbon (wt%)	Heat Value (MJ/kg)
2.87	(2.0 m)	2.0	14.0	22.0	62.0	30.0
1.16	(0.5 m)	2.5	80.0	5.0	12.5	6.0
1.38	(1.0 m)	2.5	7.5	23.0	67.0	32.0
2.37	(1.5 m)	2.0	30.0	19.0	49.0	24.0
1.00	(0.5 m)	3.0	63.0	10.0	24.0	12.0
2.04	(1.5 m)	5.0	5.0	24.0	66.0	31.5
Σwp = 10.82						
Average (by weight)		2.8	26.6	18.9	51.7	25.0
Average (by volume)		2.8	22.8	19.9	54.5	26.3
Difference (%)		(-)	-14.3	+5.3	+5.4	+5.2

Figure 3. *General composition of the "whole coal" as determined by standard proximate analysis of samples representing each ply in the hypothetical mining zone; showing average corresponding composition of the overall zone.*

Relative Weight of Combustibles (wc)	Coal Zone	Carbon	Hydrogen	Sulphur	Nitrogen	Oxygen
2.468	(2.0 m)	90.0	5.0	0.5	1.5	3.0
0.232	(0.5 m)	89.0	5.0	0.5	2.0	3.5
1.276	(1.0 m)	91.0	4.5	0.5	1.5	2.5
1.659	(1.5 m)	88.0	5.0	0.2	1.5	5.3
0.370	(0.5 m)	80.0	5.0	2.0	1.0	12.0
1.938	(1.5 m)	85.0	4.5	1.0	2.0	7.5
Σwc = 7.943						
Average (by weight)		88.0	4.8	0.6	1.6	5.0
Average (by volume)		87.9	4.8	0.6	1.6	5.1

Figure 4. *Composition of the products of combustion (by weight %) as determined by standard ultimate analysis of samples representing each ply in the hypothetical mining zone; showing average corresponding composition of the combustibles for the entire zone.*

Relative Weight of Ash (wa)	Coal Zone	SiO_2	Al_2O_3	Fe_2O_3	P_2O_5	CaO	MgO	SO_3	Others
0.402	(2.0 m)	66.0	23.0	3.0	0.3	1.5	0.5	0.5	5.2
0.928	(0.5 m)	71.0	20.0	2.0	0.1	0.5	1.0	0.5	4.9
0.104	(1.0 m)	54.0	28.5	3.5	1.0	3.5	0.5	2.5	6.5
0.711	(1.5 m)	58.0	29.0	2.0	0.1	3.5	1.0	1.5	4.9
0.630	(0.5 m)	61.0	22.0	6.0	0.5	0.5	2.0	0.5	7.5
0.102	(1.5 m)	50.0	22.0	2.0	1.0	9.0	1.0	8.0	7.0
Σwa = 2.877									
Average (by weight)		63.5	23.5	3.1	0.3	1.8	1.1	1.1	5.6
Average (by volume)		59.1	24.6	2.8	0.5	3.7	0.9	2.6	5.8
Difference (%)		-6.9	+4.7	-9.7	+66.7	+105.6	-18.2	+136.4	+3.6

Figure 5. *Composition of ash (by weight %) as determined by standard ash analysis of samples representing each ply in the hypothetical mining zone; showing average corresponding composition of the ash for the entire zone.*

AVERAGING ANALYTICAL RESULTS

Coal attributes that are determined by standard proximate, ultimate and ash analyses are expressed on a weight per cent basis. Therefore, averaging analytical results from several samples must be according to relative weight of the whole coal, relative weight of the combustible component, or relative weight of the ash that each analysis represents.

For purposes of discussion here, the average composition of a hypothetical mining zone that has been analyzed on a ply-by-ply basis is considered (Figs. 2 to 5). The total weight of ply k (WP_k) is the combined weight of contained combustibles (WC_k) and ash (WA_k):

$$WP_k = WC_k + WA_k$$

The total whole coal weight of ply k (wp_k) relative to that of other plies in the zone is a function of relative ply thickness (tp_k) and ply density (dp_k):

$$wp_k = tp_k * dp_k$$

The relative weight of ash in ply k (wa_k) is the relative weight of the ply (wp_k), times per cent ash (by weight), in the ply ($\%ash_k$):

$$wa_k = wp_k * \%ash_k$$

The relative weight of combustibles in ply k (wc_k) is the relative weight of the ply (wp_k) minus the relative weight of the contained ash (wa_k):

$$wc_k = wp_k - wa_k$$

Figure 2 displays some fundamental attributes of the hypothetical mining zone, including thickness, per cent ash content (by weight), in situ bulk density, and relative weight of each ply.

The general composition (by weight) of each ply, as determined by standard proximate analysis, is shown in Figure 3. The average value (weight %) of a constituent that has been determined by proximate analysis is:

the weight of that constituent in each ply, aggregated over all plies, divided by the aggregate total weight of all plies (WP_{agg}).

$$\overline{PROX} = \sum_{k=1}^{n} [(PROX_k * wp_k)] / WP_{agg}$$

where: $PROX_k$ = value (weight %) of parameter in ply k determined by proximate analysis

wp_k = weight of ply k

Figure 3 shows the difference between results that are averaged by relative volume (i.e. ply thickness). These differences reflect the different in situ bulk densities of the plies. The consequences of feeding coal containing 27% ash to a system designed for a feed containing 23% ash can be severe.

The composition (by weight) of combustibles in each ply, as determined by standard ultimate analysis, is shown in Figure 4. The average value (weight %) of a constituent that has been determined by ultimate analysis is:

the weight of that constituent in each ply, aggregated over all plies, divided by the aggregate weight of combustibles in all plies (WC_{agg}).

$$\overline{ULT} = \sum_{k=1}^{n} [(ULT_k * wc_k)] / WC_{agg}$$

where: ULT_k = value (weight %) of parameter in ply k determined by ultimate analysis

wc_k = weight of combustibles in ply k

Since the composition of the organic phase of coal in a given deposit commonly does not vary within a wide range, average ultimate analysis tends to be similar whether components are averaged by relative weight or by relative volume. Averaging by volume is, however, incorrect.

The composition (by weight) of ash in each ply, as determined by standard ash analysis, is shown in Figure 5. The average value (weight %) of a constituent that has been determined by ash analysis is:

the weight of that constituent in each ply, aggregated over all plies, divided by the aggregate weight of ash in all plies (WA_{agg}).

$$\overline{ASH} = \sum_{k=1}^{n} [(ASH_k * wa_k)] / WA_{agg}$$

where: ASH_k = value (weight %) of parameter in ply k determined by ash analysis

wc_k = weight of ash in ply k

If the average composition of ash in the hypothetical mining zone is determined according to relative ply volumes, significantly different and incorrect averages result (Fig. 5).

IN SITU BULK DENSITY OF COAL

The preceding discussion focuses on the implications of the relative weight of coal and its components when mathematically averaging analytical results. The relative weight of a material can be determined from its volume when the density of the material is known.

In situ bulk density of coal is the ratio of its weight to the volume occupied by its bulk in its in situ natural state. Coal is a porous substance. Its bulk density is a function of both the porosity and "true" densities of its material constituents. In situ bulk density of coal is distinct from "apparent" or "particle" densities, which do not account for total pore volumes in the in situ bulk.

MEASUREMENT OF IN SITU BULK DENSITY

Several standard methods are available for measuring in situ bulk density of rocks, soils and soil-like rock materials, including the following:

1. Measurement method (Lama and Vutukuri, 1978).
2. Buoyancy method (Lama and Vutukuri, op. cit.).
3. Sand-cone method (ASTM D1556-64, 1974).
4. Rubber-balloon method (ASTM D2167-66, 1974).
5. Drive-cylinder method (ASTM D2937-71, 1974).
6. Blast-hole method (CANMET, 1977).

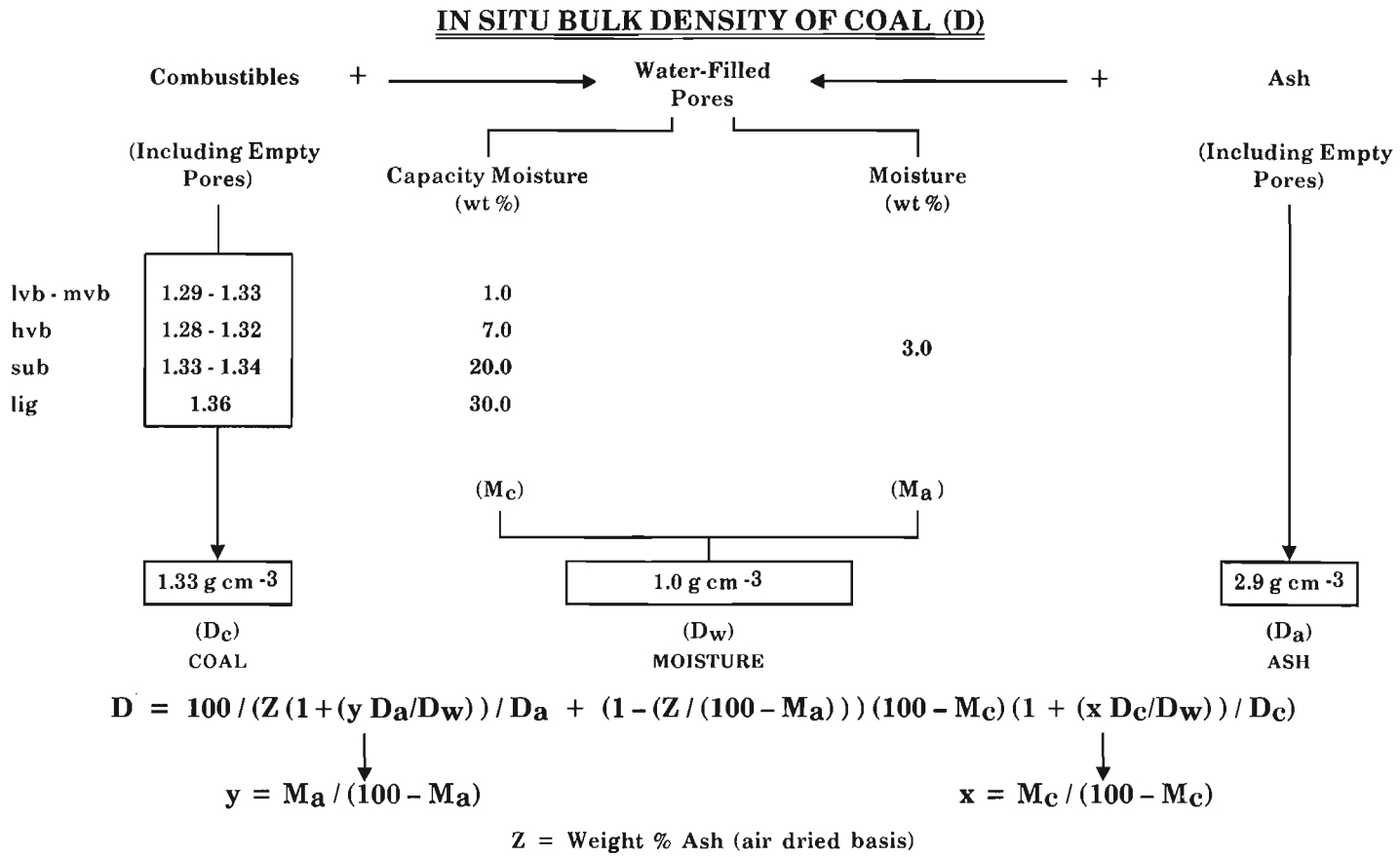

Figure 6. *Basis for the theoretical estimation of in situ bulk density of coal, showing assumed values of related variables.*

Each of these methods is based on extracting and weighing a sample of the material, and determining the volume occupied by the sample in its in situ natural state. Selection of the most appropriate method for particular circumstances depends mainly on the physical nature of the material being tested and/or the type of void that results from sample extraction.

In situ bulk density of coal can vary within a wide range according to composition and porosity of the coal. Measurement of site-specific bulk density values that cover the range of variation can be expensive and time-consuming. These values can be estimated with reasonable accuracy when other coal attributes such as ash and inherent moisture contents have been determined (Smith, in press). These attributes are conventionally determined (proximate analysis) when evaluating a coal deposit.

ESTIMATED IN SITU BULK DENSITY OF COAL AND COAL COMPONENTS

Whole coal can be considered a variable aggregate of combustibles, ash and water. It is reasonable to assume, based on experimental data, that the bulk density of the combustible component (i.e. dry, ash-free component) of all coals, including associated closed pores, is 1.33 g/cm^3 (Mahajan, 1982). [N.B. This assumption is unacceptably low for anthracitic coals, which have a corresponding density of approximately 1.55 g/cm^3]. It is also reasonable to assume on the basis of experimental data that the bulk density of dry ash, including associated closed pores, is 2.9 g/cm^3 (van Krevelen, 1961; Mahajan and Walker, 1978), and that the density of water is 1.0 g/cm^3.

Given these assumed density values and proportionate weights of ash, combustible (i.e. 1 - % ash), and moisture components in the whole coal, the volume required to contain the material constituents of whole coal can be determined and, therefore, overall density (i.e. weight/volume) of material constituents in the whole coal can be calculated (Smith, in press). The only remaining factor required to calculate in situ bulk density is the volume of open empty pores in the bulk.

Capacity moisture content of a coal indicates the total volume of pores in the coal that are capable of containing water. It varies as a function of coal rank. General rank classes of coal (anthracitic coals excluded from discussion) have values that are typically in the following ranges, on a weight per cent ash-free basis:

low and medium volatile bituminous	0.5-4.5%
high volatile bituminous	4.5-3.0%
subbituminous	13.0-30.0%
lignitic	> 30.0%

The in situ ash component of coal is not dry. It is arbitrarily assumed to contain 3% moisture by weight.

In situ bulk density of coal can be reliably estimated when the following factors are either known, or can be assumed with confidence (Smith, in press):

1. general composition of the coal on a weight per cent basis,
2. general rank class of the coal,
3. density of the material constituents.

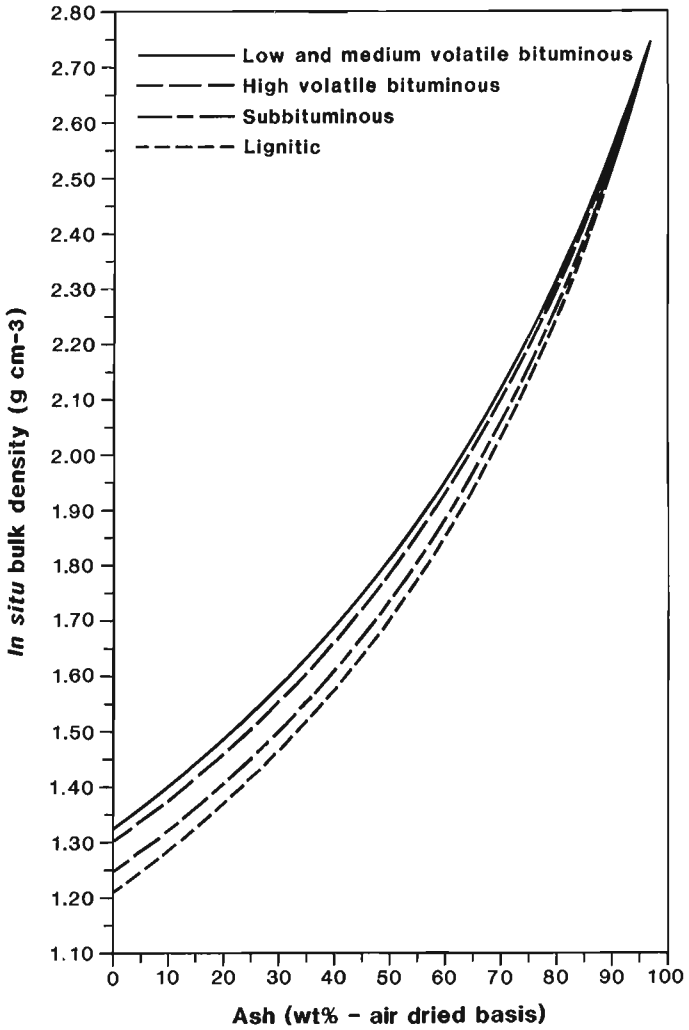

Figure 7. *Estimated in situ bulk density of coal versus weight per cent ash (air dried basis) for four general rank classes of coal.*

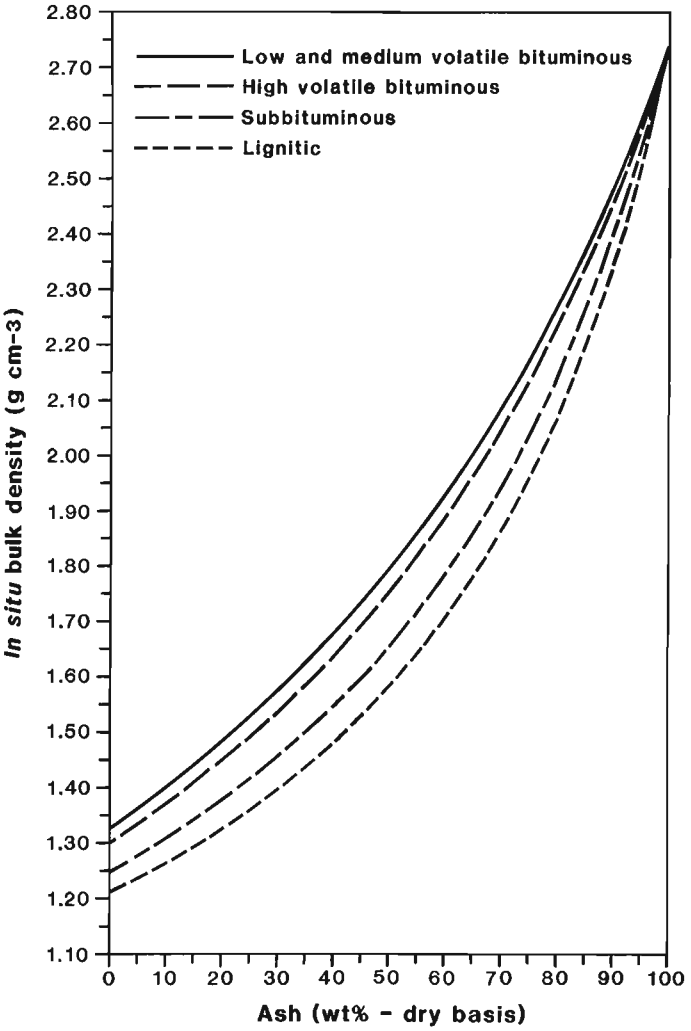

Figure 8. *Estimated in situ bulk density of coal versus weight per cent ash (dry basis) for four general rank classes of coal.*

If assumed values for variables that affect in situ bulk density of coal are set according to Figure 6, then the in situ bulk density of coal (D) can be expressed as a function of the ash content (Z) expressed on a weight per cent, air dried basis, according to the following equations (Smith, in press):

low and medium volatile bituminous: $D = 100/(75.436-0.402Z)$

high volatile bituminous: $D = 100/(76.925-0.417Z)$

subbituminous: $D = 100/(80.150-0.451Z)$

lignitic: $D = 100/(82.634-0.476Z)$

Figures 7 and 8 graphically display the relationship between in situ bulk density of coal and ash content expressed on a weight per cent, air dried (inherent moisture) basis and dry basis, respectively.

CONCLUDING REMARKS

Coal constituents that are determined according to their proportionate contribution to total weight of the whole coal or a component of the whole coal must be mathematically averaged on a relative weight basis and not on a relative volume basis. Failure to correctly combine analytical results can lead to serious errors in evaluating coal deposits and in forecasting coal production expectations. In situ bulk density of coal, which varies within a wide range depending on composition and properties of the coal, is a critical factor for evaluating coal resources. Although there are several means to measure in situ bulk density of coal, it can be reliably estimated from information obtained by proximate analysis.

ACKNOWLEDGEMENTS

The author is grateful for the constructive advice offered by D.W. Lepard and K.E. Mottershead in expressing the concepts expounded on in this paper and earlier presentations on the subject.

REFERENCES

ASTM D1556-64
1974: Standard method of test for density of soil in-place by the sand-cone method. Annual Book of ASTM Standards, ASTM D1556-64, 1974.

ASTM D2167-66
1974: Standard method of test for density of soil in-place by the rubber-balloon method. Annual Book of ASTM Standards, ASTM D2167-66, 1974.

ASTM D2937-71
1974: Standard method of test for density of soil in-place by the drive-cylinder method. Annual Book of ASTM Standards, ASTM D2937-71, 1974.

CANMET
1977: Pit Slope Manual supplement 3-3. Energy, Mines and Resources Canada, CANMET Report 77-27, p. 16.

Dulhunty, J.A. and **Penrose, R.E.**
1951: Some relations between density and rank of coal. Fuel, v. 30, no. 5, p. 109-113.

Lama, R.D. and **Vutukuri, V.S.**
1978: Handbook on Mechanical Properties of Rocks - Testing Techniques and Results - Volume IV. Trans Tech Publications, Clausthal, Germany, p. 322.

Mahajan, O.P.
1982: Coal porosity, In Coal Structure, R.A. Meyers (ed.); Academic Press, Toronto, p. 51-86.

Mahajan, O.P. and Walker, P.L., Jr.
1978: Porosity of coals and coal products. In Analytical Methods for Coal and Coal Products, C. Karr, Jr. (ed.), p. 131.

Sherlock, E.
1950: Studies of some properties of Alberta coals I - Density. Fuel, v. 29, no. 11, p. 245-252.

Smith, G.G.
in press: Theoretical estimation of in situ bulk density of coal. Canadian Mining and Metallurgical Bulletin.

van Krevelen, D.W.
1961: Coal. Elsevier, Amsterdam, 315 p.

The use of automated image analysis to determine conventional coal petrographic parameters - an example from southeastern British Columbia

K.C. Pratt
Institute of Sedimentary and Petroleum Geology, Calgary

Pratt, K.C., The use of automated image analysis to determine conventional coal petrographic parameters - an example from southeastern British Columbia. In Contributions to Canadian Coal Geoscience, Geological Survey of Canada, Paper 89-8, p. 137-145, 1989.

Abstract

The reliable determination of maceral composition of coal by automated image analysis is demonstrated by way of a recently completed automated versus manual comparison. An overview of the automated system is presented followed by a discussion on the accumulation of reflectance histograms used to determine composition of coal samples. The samples used had been studied previously by manual methods and the results of the automated analysis compare favorably. Methods of determining reflectance threshold levels and population characteristics of the inertinite macerals are discussed. The histograms accurately reflect the nature of the sampled surface, provide easy qualitative assessment of sample composition, and offer considerable information in addition to conventional maceral parameters. The histogram represents raw unbiased data which is amenable to any type of treatment for mixtures of distributions. In addition, reduced analysis time and versatility make image analysis a promising petrographic tool.

Résumé

La détermination de la composition macérale du charbon au moyen de l'analyse "par image informatisée" est démontrée à l'aide d'une comparaison entre cette sorte d'analyse et les méthodes manuelles. Une revue complète du système informatisé est ici présentée, suivie par une discussion sur l'accumulation des histogrammes de réflectance employés pour déterminer la composition des échantillons de charbon. Les échantillons utilisés avaient été étudiés auparavant selon des méthodes manuelles et les résultats obtenus par des méthodes informatiques s'avèrent tout aussi utiles. Les méthodes pour déterminer les seuils de réflectance et les caractéristiques des éléments des macéraux de type inertinite sont discutées. Les histogrammes illustrent d'une manière précise la nature de la surface échantillonnée, fournissent aisément une évaluation qualitative de la composition du charbon et ajoutent considérablement aux informations fournies par les paramètres traditionnels. Il s'agit, dans les histogrammes, de données impartiales brutes qui peuvent être adaptées à n'importe quel type de traitement applicable à tout mélange de distributions. De plus, la réduction des délais d'analyse et la versatilité font de l'analyse "par image informatisée" un outil pétrographique prometteur.

INTRODUCTION

The automation of coal petrographic methods has been attempted with good degrees of success by a number of authors. Goodarzi (1987), Riepe and Steller (1984) and Zeiss (1979) have discussed the use of image analysis, while Davis and Vastola (1977), and Davis et al. (1983) have approached the task using automated photometry. For some time the Geological Survey of Canada has been developing automated coal petrographic methods with the goal of achieving high speed yet accurate analysis requiring minimal operator attention. Through the use of a Zeiss IBAS 2 image analysis system grey level histograms are constructed from images of the surface of a polished coal pellet. The interpretation of these histograms provides conventional petrographic parameters, such as maceral composition and random vitrinite reflectance, having a degree of accuracy that compares favorably with manual results. The purpose of this paper is to describe the basic methods of automated image analysis that the GSC presently uses to characterize coals. A comparison of results derived from manual versus automated methods is presented. Some benefits of the automated method over conventional petrography are discussed.

The samples used in the comparison exercise were studied previously by Cameron (1984) and were collected at Sparwood Ridge and Weary Ridge, southeastern British Columbia. All originate from the Mist Mountain Formation of the Jurassic-Cretaceous Kootenay Group. The nomenclature of the group (Gibson, 1979) and the stratigraphic relationship between individual samples are shown in Figure 1. They were selected not only because of the detailed petrographic data available for comparison, but also because samples from this general area contain semifusinite having reflectance values only slightly higher than the associated vitrinite. In Cameron's study, the relationships between distributions of reflectance values of the vitrinite and inertinite maceral groups are examined in detail. As such they offer valuable manually obtained data that could provide insight into the problems of discriminating closely spaced distributions in automatically generated reflectance profiles.

EXPERIMENTAL

Since the actual mounted samples used by Cameron (1984) had been stored for a number of years, they were repolished to ensure that an unoxidized, scratch free surface

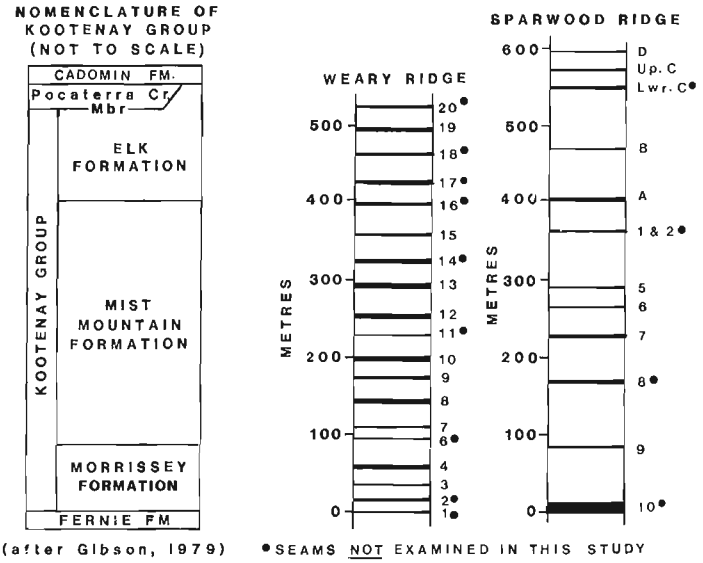

Figure 1. *Stratigraphic relationship of samples studied, modified from Cameron (1984). (•) Seams not examined in this study.*

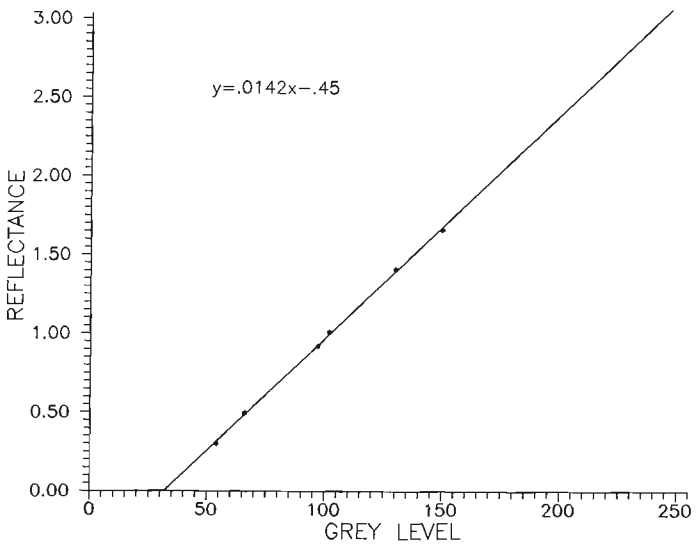

Figure 2. *Linear relationship between grey levels exhibited by glass standards used for conventional photometry (X-axis) and calculated reflectance values (Y-axis).*

was evaluated. The pellets were originally mounted in thermo-setting plastic and polished using conventional methods. The original analyses published by Cameron (1984) were used as manual results. The freshly polished samples were then analysed for random vitrinite reflectance and maceral content using the automated image analysis system. Results from manual and automated methods are shown in Tables 1 and 2. In the course of previous studies several samples had been depleted and, thus, are absent from this study.

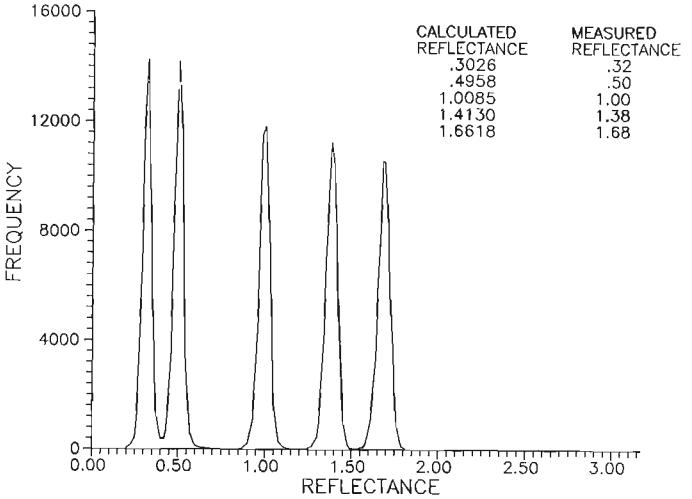

Figure 3. *Whole field measurements of glass standards. Each peak represents mean reflectance of an individual standard, transformed according to relationship in Figure 2.*

OVERVIEW OF THE IMAGE ANALYSIS SYSTEM

The IBAS 2 image analysis system consists of an array processor that manipulates images obtained from a Bausch television camera, which in turn is attached to a Zeiss universal microscope. An automated stage allows scanning of coal pellets by way of a user-defined grid. At each intersection of the grid, an image is input into the array processor in the form of a 512 x 512 element array. Each element (pixel) within this array is evaluated in terms of its density or grey level and is assigned to one of 256 grey levels labelled 0 to 255, 0 representing black and 255 white. Progressively higher values from 0 to 255 represent successively lighter shades of grey. These grey levels can be related to actual reflectance values by way of transformation tables that are developed during standardization of the light source. From each image a histogram is developed representing frequencies of every grey level present after image processing to eliminate unwanted background materials such as epoxy binder or extremely small particles. These frequencies are then added to all those previously collected resulting in a reflectance profile of the sampled surface. It is important to note that this is an additive, as opposed to averaging, process; the histogram produced represents the accumulated total of each frequency for all fields, not the average result per field.

The resulting histogram can then be interpreted by way of a band fitting method in which a cursor is used to define population boundaries for liptinite, vitrinite and inertinite. On the basis of the total frequencies occurring between these boundaries, maceral percentages are calculated. The mode of the vitrinite population is assumed to represent mean random reflectance. A more detailed discussion of the steps involved in accumulating such a reflectance profile follows.

Accumulation of grey level histograms

Standardization of the light source

For any given light source intensity, there exists a linear relationship between the reflectances of a series of glass standards used for calibration of photometer-based

TABLE 1

Summary of composition data from study performed by Cameron (1984) and present study

Composition in per cent						
	Manual Results			Automated Results		
Seam	Vitrinite	Inertinite	Liptinite	Vitrinite	Inertinite	Liptinite
Weary Ridge						
19	92.80	3.80	3.40	90.00	4.20	5.80
15	75.40	22.80	1.80	79.40	17.70	2.90
13	82.40	16.40	1.20	87.60	9.50	2.90
12	83.40	15.80	0.80	85.30	12.90	1.80
10	61.80	37.90	0.30	69.00	28.40	2.60
9	48.80	50.40	0.80	54.00	46.00	0.00
8	54.60	45.40	0.00	59.00	41.00	0.00
7	59.20	40.00	0.80	65.20	34.80	0.00
4	55.40	44.60	0.00	53.60	46.40	0.00
3	64.30	35.70	0.00	64.50	35.50	0.00
Sparwood Ridge						
D	94.40	3.60	2.00	87.00	7.70	5.30
U.C	84.40	11.60	4.00	90.10	9.90	0.00
B	67.40	29.40	3.20	63.80	35.00	1.20
A	71.30	28.60	0.10	79.40	19.30	1.30
5	61.00	38.70	0.30	73.30	25.70	1.00
6	73.00	26.80	0.20	74.40	23.80	1.80
7	52.30	47.40	0.30	66.40	31.70	1.90
9	35.20	64.80	0.00	44.00	56.00	0.00

systems and the grey levels they exhibit on the image analyser. This relationship can provide exact information necessary to scale the class boundaries of the 256 grey levels in the final histogram to meaningful reflectance boundaries. For example, setting the 1.02 reflectance standard to a grey level of 102 dictates that a range of 0 to 3.17 R_o may be measured on the basis of the relationship

$$y = .0142 * x - .45$$

where y = the reflectance in oil corresponding to grey level x.

Accordingly, grey value 32 relates to a reflectance value of 0; anything lower yields negative reflectance values and are, in fact, beyond the lower range of the cameras sensitivity at this light intensity. The grey level 255 yields a reflectance of 3.17, thus giving the range of 0 to 3.17 for a measured grey level interval of 32 to 255. This relationship can be updated periodically to accommodate any changes in illumination. Figure 2 illustrates the relationship between grey levels and reflectances on a series of six standards determined from a set of single point measurements in the centre of the field. Figure 3 shows the resulting histogram if five standards are input as images, processed and the above relationship imposed (the 0.94 R_o standard was eliminated since it would overlap with the 1.02 standard). Histograms such as these are constructed daily to ensure that the individual peaks correspond as closely as possible to the actual reflectance values of the standards.

The nature of a photometer system restricts the user to one light level for any given standard. In image analysis, scaling of grey levels has the advantage of enabling light source intensity to be set at any level depending on the nature of the material being measured. As well, accuracy of reflectance values across the entire measured range is obtained. It is desirable to keep as much of the histogram in the middle of the grey level scale, since experimental data indicate that reflectances obtained are most accurate in this range. A low rank coal may require that light intensity be increased, brightening the huminite macerals and moving them to the middle grey ranges while lowering the upper range of measurable reflectances. This has the effect of decreasing class widths in the histogram. Decreasing the intensity allows brighter materials, (i.e. inertinite in high rank coals) to be included in the measuring range by

TABLE 2

Combined reflectance data from study performed by Cameron (1984) and present study

Random Reflectance in Oil			
Seam	Manual		Automated
	Vitrinite A	Vitrinite B	IBAS
	Weary Ridge		
19	0.96	0.92	0.93
15	1.11	1.07	1.09
13	1.23	1.22	1.18
12	1.26	1.24	1.20
10	1.33	1.31	1.27
9	1.36	1.32	1.27
8	1.37	1.35	1.31
7	1.41	1.39	1.36
4	1.40	1.45	1.44
3	1.41	1.41	1.40
	Sparwood Ridge		
D	0.91	0.87	0.89
U.C	1.06	1.04	1.05
B	1.08	1.05	1.09
A	1.17	1.15	1.10
5	1.28	1.30	1.25
6	1.26	1.25	1.28
7	1.33	1.33	1.28
9	1.38	1.37	1.38

increasing the maximum range, and also the class widths. In effect, changing light source intensity simply alters the slope of the grey level to reflectance relationship, thereby affecting the scaling of the 256 available histogram classes.

Illumination of the field

Due to slight inaccuracies in the centering of both the lamp and the beam path, illumination of the field is rarely perfectly even. As well, since a prism is placed in the beam path to increase contrast, a field of apparently uniform reflectance will exhibit grey values at the top of the image that are somewhat lower than those at the bottom. Shading the image by way of a reference image of such a uniform area corrects these discrepancies to some degree. In Figure 3, the individual peaks of the reflectance standards would not be as sharp, or may in fact be asymmetrical if the image was unevenly illuminated or shading was not performed properly. Daily construction of histograms of the individual standards offers a quick check of these factors, in addition to verifying accuracy of reflectances. Further correction is obtained by utilizing only the pixels within a square of 256 x 256 pixels at the centre of the image.

Stage Movement

After every four fields the focus is automatically checked. The stage controller achieves this by moving the stage vertically a small distance in either direction. If a brighter contrast area is found it is assumed to be the new point of focus. Otherwise it returns to its previous position.

Lateral movement of the sample follows a grid pattern determined at initialization. Stepping distance in the X and Y directions must be carefully chosen since repeated measurements on large particles may bias a histogram. Some 70,000 pixels can contribute values to a histogram from a field dominated by one particle. Particle size is also a factor for similar reasons. Decreasing particle size facilitates closer packing of the coal, allowing sampling of several small particles instead of one large particle in any given field. Since the pellets used in the present study were prepared prior to the use of image analysis, a large stepping distance was used to decrease the possibility of repeated measures on the same particle.

Elimination of background

Epoxy binder is eliminated by the process of discrimination in which grey values below a selected level are set to 0. This level represents the threshold between the grey level of the epoxy and the components of the coal. Care must be taken in the selection of this level since liptinite macerals are often represented by grey levels close to that of the epoxy. Edge effects remaining after the discrimination may be controlled by dilation of the black areas into the coal particles, effectively removing the edges. This also allows a lower discrimination level to be used, thus preserving greater amounts of liptinite. Small areas of epoxy not removed by the lower discrimination level, commonly referred to as 'noise', are eliminated by the subsequent dilation. These two processes used in tandem are effective in dealing with elimination of mineral matter.

Development of measuring program

On the basis of the above processes a measuring program can be developed. After initialization of measuring parameters a loop repeats image input, processing and evaluation operations on fields found at each intersection of the user-defined grid. After the final field, the program terminates the loop and waits for the user to interactively fit maceral population boundaries by a band fitting approach in which the cursor is used to define limits. After each run a standard check indicates if the light source has remained stable, after which the program can be re-initialized and another sample run.

On the samples used for this study, 144 fields were evaluated in a 12 x 12 grid. Reflectance was measured in a range from 0 to 3.03 on the basis of a linear relationship applicable at the time of analysis. A stepping distance of .5 mm was used in both the X and Y directions. Discrimination levels and number of dilations were determined individually for each sample at initialization to account for variations in surface quality due to weathering or mineral matter. These remained fixed throughout the analysis of the sample.

Each sample required approximately 20 to 25 minutes to complete a run. Approximately five minutes were required to analyse any given histogram and to load the next sample. The image analyser can operate unattended during accumulation of histograms. Thus, each sample requires only

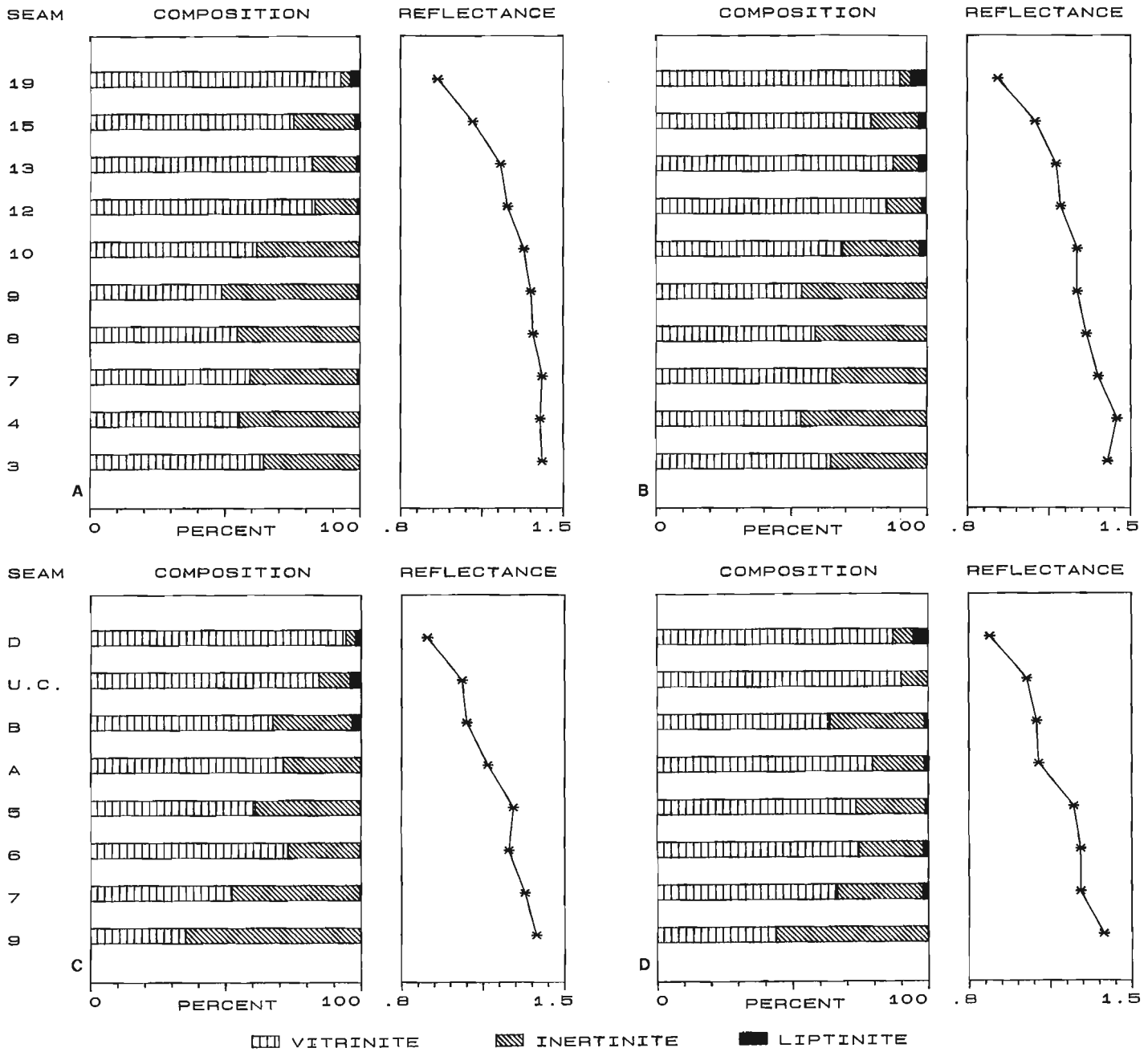

Figure 4. *Graphic representation of data in Tables 1 and 2. a) Weary Ridge, manual data, b) Weary ridge automated results, c) Sparwood ridge manual data, d) Sparwood Ridge automated results. For manual reflectance values vitrinite A was used.*

about five man-minutes for analysis. Run times could be reduced substantially for well polished, well packed pellets of small particle size. In these conditions a 10 x 10 grid with only one dilation per field would suffice, thus reducing processing time. Methods of preparing high quality samples on a large scale are currently being investigated. At the time of writing software is nearing completion that will allow several samples to be loaded and processed at a time. This will allow the image analyser to operate unattended for extended periods, further reducing operator involvement.

RESULTS AND DISCUSSION

Tables 1 and 2 list manual composition and vitrinite reflectance data for the samples analysed, per Cameron (1984). Corresponding results from automated image analysis are also shown. Since the image analysis method of band fitting only allows determination of the three basic maceral groups, Cameron's table has been abbreviated to show only totals for each group. Figure 4 graphically illustrates the composition and reflectance data.

In Figure 4, parts a and c represent the manual data, and parts b and d, the automated results. This illustration shows an excellent agreement between composition and reflectance values for both sets of data and confirms Cameron's observation of increasing rank and inertinite composition with depth. Table 1 indicates a tendency for vitrinite values to be slightly high in automated results. Whereas conventional maceral composition determines percentages of individual points encountered and identified, automated results are derived by interpreting distributions of grey levels obtained from surface areas of particles

encountered. As well, comparisons of conventional maceral determinations using the point counting approach can be difficult. Operator bias and statistical factors contribute to variations in results and it is difficult to determine possible error in the data used for control. Thus, in view of differences in the fundamental methods as well as differences frequently encountered in conventional point counting comparisons, the agreement between automated and manual methods is considered very good and well within limits of variation experienced between human operators.

In Figure 5, several histograms are presented. In each of these the thick solid line represents the natural distribution of reflectance values determined from the surface of a pellet. In Figure 5a, the distribution consists of a sharp peak around which there is little encroachment by other distributions. This, therefore, represents a coal that consists largely of vitrinite. In figures 5b to 5d, the thick line represents distributions measured from coals containing increasing amounts of inertinite (high reflecting). Subsidiary peaks representing low and high reflecting semifusinite distributions are clearly visible to the right of the vitrinite distribution in figures 5c and 5d. The hump to the left of the vitrinite in figures 5b to 5d is an "artifact wedge" (Zeiss, 1979), which is probably the result of the inability of image processing to completely eliminate holes in the inertinite. This can often become quite large in high inertinite coals, causing difficulty in determining liptinite (low reflecting) percentages. In such coals, the presence of the cell lumina causes an increase in edge effects that the discrimination and dilation operations can rarely remove completely. Internal reflections within the lumina cause the grey level within them to increase slightly, causing further difficulty in discrimination. Low reflecting mineral matter may also contribute to an artifact wedge.

In most cases the artifact wedge can be controlled, especially if the coals are well polished and free of mineral matter and weathering effects. A large artifact wedge, or poorly formed vitrinite distribution, is indicative that high mineral matter content or weathered coal may be present. Qualitative assessment of the coal can, therefore, be easily obtained simply by examination of the histogram. It is obvious, for example, that the sample in Figure 5a is vitrinite rich whereas the sample in Figure 5d contains large amounts of inertinite. In either case if there was a very large artifact wedge or the vitrinite distribution did not have the characteristic shape of a normal distribution, poor coal quality would be the likely reason. Methods of quantifying these features are under consideration.

Cameron's study contained a substantial discussion regarding threshold reflectance values between the vitrinite and low reflecting semifusinite populations (Cameron, 1984). In the band fitting approach used to determine maceral composition from reflectance histograms, thresholds are determined between the three maceral groups by observing and marking features in the histogram using a cursor. The threshold between vitrinite and inertinite also represents the threshold between vitrinite and low reflecting semifusinite. However, in examining these and other inertinite-rich western Canadian coals, it has been found that because of overlapping distributions, visually determining these thresholds is not an easy task. In most cases, the left side of the vitrinite distribution strongly resembles that of a normal distribution and the right side is often corrupted by the encroachment of inertinite macerals. As shown above, in coals having high inertinite content, the artifact wedge can become quite large and if liptinites are present, they may be observed as a small hump in the artifact wedge. No method is yet known for deleting precisely the artifact wedge. Although it is suspected to be lognormal in nature, determining its parameters is difficult in view of the overlapping of other normal distributions. To account for these factors a rule of thumb for interpreting histograms of coals having high inertinite content has been developed as follows: The distance between the vitrinite peak and the lower vitrinite boundary is reduced to account for the area within the vitrinite distribution also occupied by the artifact wedge. Taking one-half of this distance and moving slightly more than that above the vitrinite peak determines the approximate upper boundary of the vitrinite population. At this boundary there are often small features in the histogram that indicate the effect of overlapping distributions and illustrate its sensitivity to them. These can assist in determining the upper threshold level. On the basis of such an interpretation, the upper limit is slightly more than one-half the distance from the peak as the lower limit. The lower limit is 2 to 3 standard deviations below the peak (depending on the contribution of the artifact wedge), implying that the upper is in the vicinity of 1.25 to 1.75 standard deviations above. This independently observed "rule of thumb" is similar to the method suggested by Cameron (1984) to determine the boundary between vitrinite A and low reflecting semifusinite. This boundary appeared to be midpoint between the random reflectance of vitrinite A plus one standard deviation, and the random reflectance of low reflecting semifusinite minus one standard deviation.

It is possible to fit theoretical normal distributions to the reflectance histograms that represent populations of several macerals. The method of determining thresholds shown above provides good estimates of the standard deviation of the vitrinite population. The peak most likely represents the mean, unless corruption due to encroachment of the inertinite macerals is extreme. From the mean and the frequency at the mean (i.e. height of the peak) the population size can be determined. These parameters can then be used as estimates to fit the normal distribution. Lotus 1-2-3 provides a convenient means of performing this and for adjustment of parameters to achieve a visual best fit. Since this was not the primary purpose of this study, statistical methods such as least chi squared were not pursued. By subtracting the theoretical distribution from the natural distribution, it was possible to extract the vitrinite population leaving the inertinite population on the right side of the histogram. Following this, similar operations were performed on the low reflecting semifusinite and the high reflecting semifusinite, each being subtracted from the natural distribution in turn. The remaining distribution left after fitting and subtraction of the high reflecting semifusinite was assumed to be fusinite, from which a mean was calculated. The dashed bell curves in Figure 5 are populations fitted in this way. Accumulating the four fitted distributions, a theoretical profile of the combined vitrinite and inertinite components (also shown in Figure 5) can be plotted. This agrees well with natural distributions obtained from image analysis. Also, the size of the artifact component becomes apparent when this is done. Using this method, it was possible to determine mean values for vitrinite and all three inertinite macerals on all samples for comparison with Cameron's data. The results are shown in Table 3 and graphically in Figure 6. There are very good agreements in both the values and trends exhibited by the low reflecting semifusinite. The agreement between high reflecting semifusinite and fusinite is not as good. This is possibly due to several reasons. The higher reflecting material would have higher standard deviations contributing to greater variations in the results. Generally, the two higher reflecting macerals show lower values in automated than in manual analysis. This may be due to relief and scratches being included in the histograms, which could be eliminated by the selection of clean relief free points in manual measurements. Also, Cameron's results include

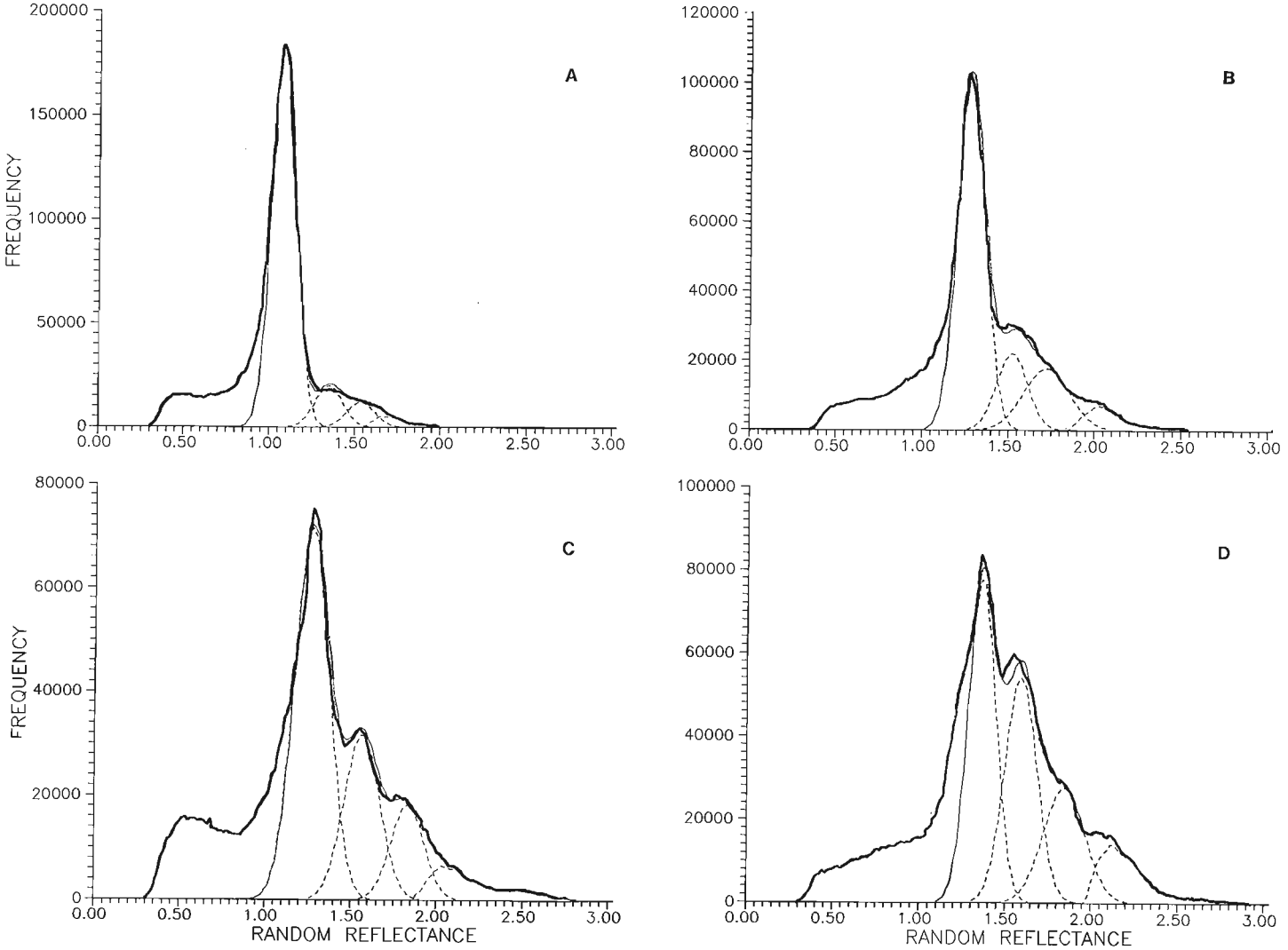

Figure 5. *Typical histograms generated by automated analysis. Thick solid line is measured distribution. Dotted normal curves are fitted distributions of vitrinite, low reflecting semifusinite, high reflecting semifusinite and fusinite (from left to right). Thin solid line represents accumulation of the four theoretical distributions. Inertinite content increases from a through d.*

"other inerts", materials which cannot be classified under the three types determined here. Using this method on the histogram data, it is impossible to eliminate contributions of the other inerts, since they probably originate from a variety of materials. In spite of these negative factors, the increase of reflectance with depth and the relationship between the reflectance levels of the three inertinite macerals agree with Cameron's observations. As well, this confirms Cameron's suggestion that reflectance values for much of the inertinite in these coals is somewhat closer to vitrinite than in coals from other parts of the world (Cameron, 1984, p. 75). It is noteworthy that the collection of Cameron's data took days of tedious effort, whereas these data are readily generated as part of the image analysis process, and in a much shorter time.

Although these methods of histogram interpretation provide good agreement with manual results, there are still problems to be resolved concerning possible contributions of individual inertinite macerals and the artifact wedge. However, it illustrates the versatility of image analysis to produce histograms that accurately reflect the nature of the measured surface. The reflectance histogram provides a picture, or fingerprint, of the coal from which reflectance characteristics of the various macerals may be obtained, in addition to quantitative assessment of maceral content. Data collection time is also reduced substantially.

In its basic form, the histogram represents primary, unbiased data. This factor alone offers an advantage over manual methods that can be subjectively influenced during the data collection. There are numerous methods of interpreting mixtures of distributions. The method shown above has provided encouraging initial results but refinements are needed. At present it can be time consuming, and since several interpretations often produce similar results, subjectivity does become a factor. However, it occurs after, not during, data collection. Computer processing of data may help to standardize error and determine confidence limits by further eliminating subjective involvement. It is clear, however, that the product of automated image analysis is accurate, provides very good maceral and reflectance data, shows the potential of offering more than conventional petrography while providing a good graphical representation of the coal surface, which in turn allows easy and rapid qualitative assessment of the coal. Other possible uses of histograms include quality control of coal blends, determination of reactives and non-reactives, or any other maceral or reflectance related quantitative analysis. Image analysis also offers additional methods such as particle size and shape, texture and porosity analysis (Pratt, 1989). This highly versatile and efficient tool can provide more information in a shorter time and has the potential to enhance significantly the scope of coal petrography in the future.

TABLE 3

Table showing mean values of inertinite distributions in samples studied. Cameron's study reported means obtained manually. In the present study means were determined by fitting of normal distributions as described in the text.

Seam	Cameron's Study			Present Study		
	L.R.S.	H.R.S.	Fus.	L.R.S.	H.R.S.	Fus.
Weary Ridge						
19	1.15	1.44	1.88	N/A	N/A	N/A
15	1.37	1.60	2.19	1.35	1.54	1.86
13	1.42	1.69	2.24	1.44	1.58	1.95
12	1.46	1.76	2.63	1.46	1.63	2.15
10	1.56	1.88	2.31	1.50	1.63	1.99
9	1.58	1.86	2.51	1.58	1.85	2.22
8	1.65	1.82	2.43	1.63	2.00	2.35
7	1.70	1.92	2.51	1.59	1.79	2.13
4	1.68	1.92	2.50	1.64	1.88	2.32
3	1.66	1.94	2.35	1.56	1.85	2.35
Sparwood Ridge						
D	1.15	1.46	2.06	1.02	N/A	N/A
U.C	1.35	1.58	2.20	N/A	N/A	N/A
B	1.24	1.61	2.15	1.34	1.51	2.31
A	1.35	1.65	2.15	1.31	1.51	1.87
5	1.49	1.78	2.14	1.54	1.79	2.15
6	1.57	1.78	2.38	1.51	1.72	2.13
7	1.62	1.89	2.39	1.52	1.72	2.11
9	1.66	1.88	2.38	1.59	1.84	2.24

L.R.S. - Low Reflecting Semifusinite
H.R.S. - High Reflecting Semifusinite
Fus. - Fusinite
N/A - Not analysed due to sparse populations

CONCLUDING REMARKS

This continuing research into automated image analysis is directed to developing reliable, efficient and versatile methods for characterizing coals. To date, it has been demonstrated that results from automated image analysis methods compare favourably with those derived from slower, more tedious, conventional manual coal petrography methods, when appropriate techniques, such as those being developed by GSC, are used.

Large quantities of useful coal maceral and reflectance data can be captured and quickly processed using the automated techniques. Graphical output can provide insight into coal character that might not have been previously evident without detailed manual examination. The ability to easily discriminate subtle variations in coal character might have profound implications in more accurately predicting variations in the technological properties of coals. It is expected that GSC's continuing research into automated image analysis will significantly widen the scope of coal petrography in future. Techniques developed to date already provide significant advantages over conventional manual petrographic methods.

ACKNOWLEDGMENTS

The author wishes to thank A.R. Cameron for critical review of the text, G.G. Smith for helpful advice in preparing the paper, D.J. Smith for assistance in typing the manuscript, and M. Tomica for technical assistance. Lotus 1-2-3 is a registered trademark of Lotus Development Corporation.

REFERENCES

Cameron, A.R.
1984: Comparison of reflectance data for various macerals from coals of the Kootenay group, southeastern British Columbia. Proceedings of the 1984 Symposium on the Geology of Rocky Mountain Coal, North Dakota Geological Society, Bismark, p. 61-75.

Davis, A. and Vastola, F.J.
1976: Developments in automated reflectance microscopy of coal. Journal of Microscopy, v. 109, pt. 1, January 1977, p 3-12.

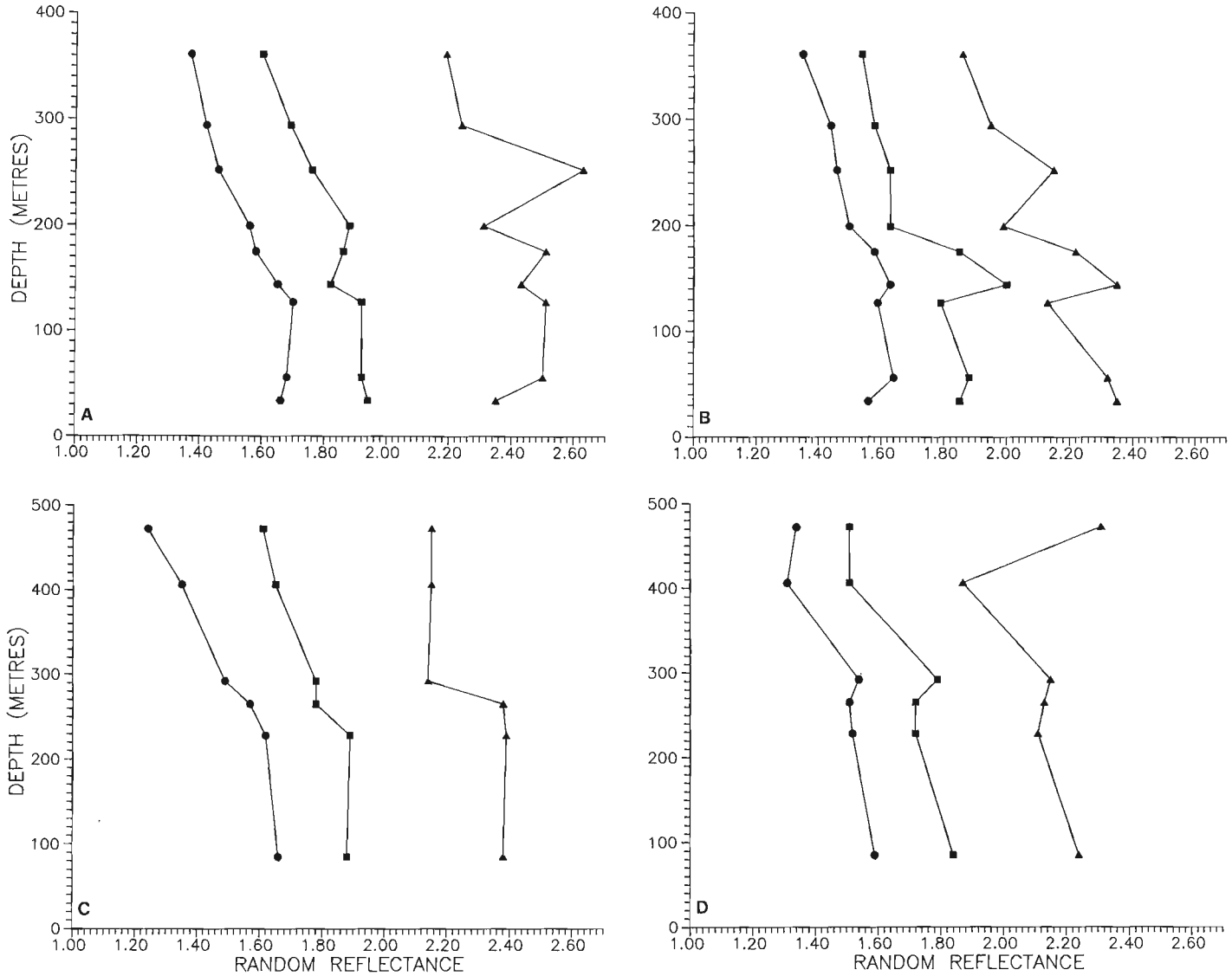

Figure 6. *Graphic representation of data in Table 3. a) Weary Ridge, manual, b) Weary Ridge, automated, c) Sparwood Ridge, manual, d) Sparwood, automated. (●) Low reflecting semifusinite, (■) high reflecting semifusinite, (▲) fusinite. Samples in which one or more macerals were not analysed in Table 3 are excluded.*

Davis, A., Kuehn, K.W., Maylotte, D.H., and St. Peters, R.L.
1983: Mapping of polished coal surfaces by automated reflectance microscopy. Journal of Microscopy, v. 132, part 3, p. 297-302.

Gibson, D.W.
1979: The Morrissey and Mist Mountain formations - newly defined lithostratigraphic units of the Jura-Cretaceous Kootenay Group, Alberta and British Columbia. Bulletin of Canadian Petroleum Geology, v. 27, no. 2, p. 183-208.

Goodarzi, F.
1987: The use of automated image analysis in coal petrology. Canadian Journal of Earth Sciences, v. 24, no. 5, p. 1064-1069.

Pratt, K.C.
1989: Technical Note: Custom programming of image analysis applications for coal petrography. This volume.

Riepe, W. and Steller, M.
1984: Characterization of coal and coal blends by automatic image analysis. Fuel, v. 63, p. 313-318.

Zeiss, H.S.
1979: Automating coal petrography at Bethlehem Steel Corporation. Proceedings of the Ninth International Congress of Stratigraphy and Geology of the Carboniferous, Urbana, v. 4, p. 495-500.

Technical Note: Custom programming of image analysis applications for coal petrography

K.C. Pratt
Institute of Sedimentary and Petroleum Geology, Calgary

Pratt, K.C., Technical Note, Custom programming of image analysis applications for coal petrography. In Contributions to Canadian Coal Geoscience, Geological Survey of Canada, Paper 89-8, p. 146-148, 1989.

INTRODUCTION

The use of automated image analysis to determine conventional coal petrographic parameters has been described by a number of authors (Zeiss, 1979; Riepe and Steller, 1984; Goodarzi, 1987; Pratt, 1989). This new approach provides quick sample analysis as well as other advantages (Pratt, 1989). Future advances in the application of automated image analysis are expected to significantly widen the scope of coal petrography by providing new parameters for the characterization of coal and other organic materials. The ability to program user-defined measuring procedures into routinely used image analysis software adds the flexibility required in the development of analytical research methods. Automated image analysis techniques are being advanced by the Geological Survey of Canada using a Zeiss IBAS 2 system. This note describes this system and the development of one analytical method through customization of image processing software provided with the system.

The image analysis system

Image analysis systems usually deal with images input to a computer from a television camera. In the process of digitization, the image is divided into discrete points and the intensity of light at each point is represented by a grey level value from 0 to 255. These discrete points can be represented as pixels on the system monitor, their grey level being referred to as the 'phase' of the pixel. Using cartesian co-ordinates, a 512 x 512 pixel image has the same appearance as an analog television image. The individual pixels represent elements of an array which is stored in the memory of the computer.

There are two basic approaches used in image processing: a) Multiphase analysis in which pixels are assigned to one of 256 values between 0 and 255 representing a black to white rendering of the image, and b) Binary images in which pixels that are part of a particle or object are assigned a value 255, effectively meaning they are turned on, while those that are part of the background are given a value of 0, and are treated as being off. Given these on or off conditions, binary operations may be applied. Initial input is in the form of a multiphase image which, after some processing, can be converted to a binary image.

Two general types of parameters can be measured from these images: densitometric and geometric. Densitometric parameters use multiphase images to deal with grey level characteristics of an image, such as mean and standard deviation. Geometric parameters include object specific measurements, such as perimeter and area derived from binary images. The former parameters are used for the automated methods of determining conventional petrographic data, i.e. reflectance measurement and maceral composition. The latter have not been used significantly in coal petrography by direct measurement.

A menu allows selection of predefined functions that input, manipulate and measure images, and provide output in a variety of forms. Stage movement can also be achieved, allowing repeated measurement of images at selected points of a user-defined scanning path. Measured data from each image can be accumulated and output in the form of lists or histograms representing distributions of selected parameters collected from the sampled surface.

Most automated methods use a measuring program that consists of a series of functions assembled in a general form as follows: an initial portion of the program allows scaling of images, selection of parameters to be measured, autofocus and scanning stage initialization. This will usually be followed by a loop that performs image input, stage movement, image processing and measurement. After an image is input to memory, the stage is instructed to proceed to the next sampling location based on the pre-defined stage movement scheme. While this movement is under way, some time can be saved by concurrent processing and measuring of the input image. This usually involves discrimination of background material (mostly epoxy embedding media), and erosion or dilation to remove edge effects. Both operations are performed according to parameters input at initialization. At this point densitometric measurements can be made. If geometric parameters are being measured, then it is necessary to convert the processed image to a binary image. This can then be labelled and measured for parameters defined in the initialization phase of the program. The loop continues until scanning of the surface is complete, at which time a flag is set indicating to the program that the loop should be terminated. This is followed by the reporting of the results in the final portion of the program.

Development of a user specified application

Occasionally applications are required that the supplied software cannot accommodate. In these cases, it is possible to design and program user-defined functions and to install them in the menu for use in the same way as any other function. This is done using a software library of FORTRAN subroutines, which perform many image processing and utility functions, allowing the user to input parameters at every call of the function, input identification information for individual particles, format the output for use by other programs on other computers, or measure parameters in a specific fashion as dictated by the application. The following discussion describes one such application.

The analysis of EFR (entrained flow reactor) residues required that geometric and densitometric parameters be measured on individual particles and that each measured particle be assigned a numerical code based on operator description. A tentative classification of such residues suggested the presence of 10 particles types as follows:

1. Thin walled cenosphere - lacy texture.
2. Thin walled cenosphere - empty.
3. Thick walled cenosphere - lacy texture.
4. Thick walled cenosphere - empty.
5. Honeycomb.
6. Solid, angular.
7. Composite >50% full.
8. Composite <50% full.
9. Small fragments.
10. Mineral matter.

Since the method of data collection and output from existing software was not suitable for intended subsequent processing, it was decided that a new function was required which satisfied the above requirements.

The first step in programming any new function is to give careful consideration to how much routine work can be performed by the menu functions already available. Functions such as stage movement, editing of the image, and further image processing utilize already existing menu functions. The amount of programming required for the user-defined portion is therefore kept to a minimum, reducing complexity and facilitating debugging. It was anticipated that two images would be required for the analysis. Both images could be developed using menu operations on input images within the main loop of the program. One would be a multiphase image consisting of the particles in any given field in which the background had been eliminated. This had to be achieved without eliminating voids within the particles since area measurements were to be taken both with and without voids in order to determine porosity. Images also had to be edited using a 'cut and paste' approach to separate particles that were touching, and also to make other minor adjustments to the image. A binary image had to be developed from this multiphase image that represented the particles without voids for measurement of the geometry of the particle as a whole.

In using the subroutine library, COMMON statements allow examination of certain values used by the main program which contain information on the status of the scanning stage. Large amounts of other information regarding system configuration are also available to the programmer in this way. On inspection of the variables, it is possible to determine whether the scan is beginning or ending, or how many images have been evaluated. A means of preserving variables between function calls is provided by way of a configuration file which resides on the system disk. This file contains all the functions in the menu, including any user-developed ones, and codes that determine how each function and its associated variables are to be treated when called. Part of the installation procedure for new functions includes altering this file to accommodate the desired behaviour of the function. Therefore, in addition to allowing integration of new functions into the menu, programming at this level allows better control and monitoring of system and peripheral configurations.

The actual function operates as follows: The user is asked if the current field should be used. If the answer is 'yes' and this is the first field of the scan, then the current level of discrimination between the epoxy binder and the actual particles is obtained and a file is opened having a name input by the user, after which the function proceeds. If the answer is 'no', then the function simply returns to the menu. If the answer is 'yes' and this is not the first field, the function proceeds. Next the user is requested for a particle type, corresponding to the numerical code shown above. The user then places the cursor on the desired particle to measure the densitometry of the particle from the multiphase image. At this point an additional benefit of user-specified coding is exercised. A FORTRAN library subroutine returns an array containing frequencies of every grey level occurring within the particle. The total of these frequencies (i.e. total pixels counted) represents the area including voids. The total of the frequencies occurring above the discrimination level represents the area of the particle without voids. The difference between these represents porosity. Also in a similar fashion, means of the grey levels with and without voids are calculated. This capability is not available from the software as supplied. Next, using the same cursor position, the geometric parameters are measured from the binary image. The data are then output to disk. After this the user may measure other particles in the present image, return to the menu or quit completely. If the user wishes to return to the menu, the file is left open and certain program variables are preserved for the next call. These will remain unaltered unless re-initialized in subsequent function calls. On returning to the menu, the stage moves to the next field and the loop continues. If the next field contains no suitable particles, the user may continue to inspect more fields until a satisfactory one is found. If the 'quit' option is selected then the file is closed so that the user can leave the program with the data preserved.

Program output

The output of this program is a file that can be sent to a PC compatible computer and imported into LOTUS 1-2-3. A portion of a file is shown in Table 1. These data can then be used to determine additional parameters such as porosity %, shape factors and elongation. They can also be plotted directly as shown in Figures 1, 2 and 3. It can be seen in Figure 1 that particles of type 1 are porous. This is expected due to high numbers of devolatization vacuoles in this particle type. Particles of type 6,are not porous and have a high, mean grey value (Figs. 1, 2), and are probably fragments of non-reactive materials, most likely inertinite. In Figure 3, particles of type 1 have a wide variety of areas but are at the top of the graph due to their porosity. Particles of type 9, being small and difficult to identify, are grouped at the lower left. Particles of type 6 are also grouped in the lower left, being smaller, non porous inertinite fragments.

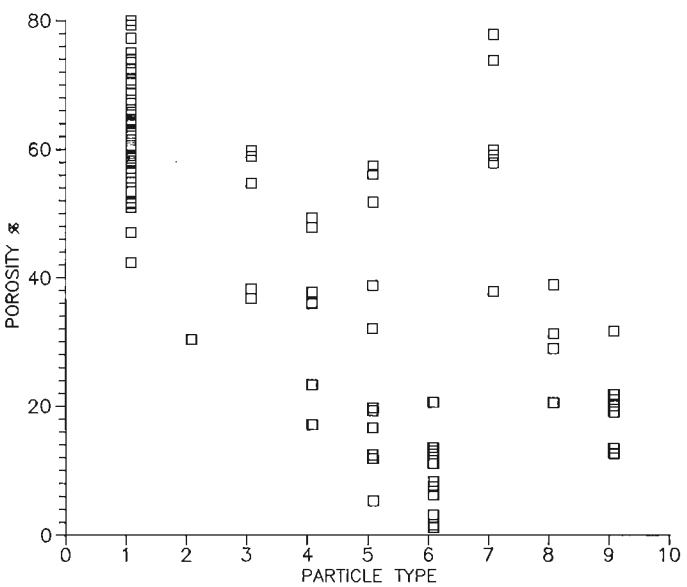

Figure 1. *Particle type versus porosity plotted from data generated.*

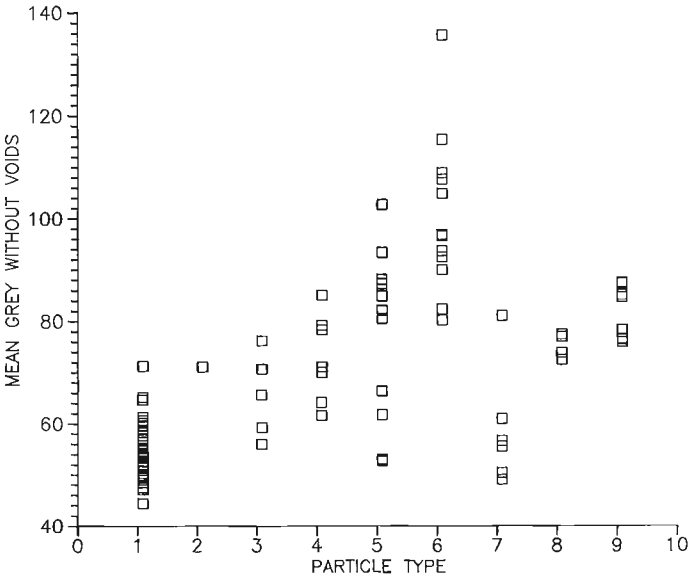

Figure 2. Particle type versus mean grey level without voids plotted from data generated.

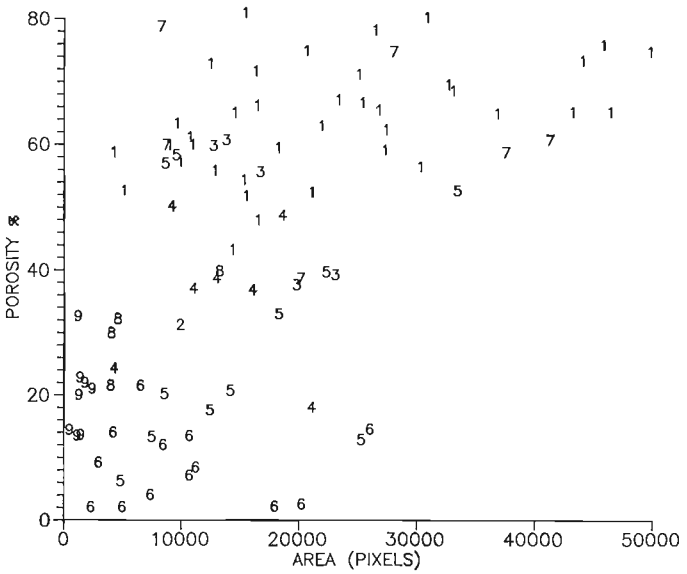

Figure 3. Area versus porosity, plotted with data points labelled by particle type.

TABLE 1

Example output from newly developed function. Circular shape factor, elongation and porosity % are calculated subsequent to program operation

Particle no.	Particle Type	Mean Grey w/o voids	Mean Grey with voids	Void Area	Total Area	Perimeter	Circular Shape Factor	Maximum Diameter	Minimum Diameter	Elongation	Porosity %
1	1	63.21	85.77	10657.00	21167.00	739.27	0.49	237.00	144.34	0.61	50.35
2	6	106.24	107.35	148.00	7316.00	457.83	0.44	178.20	63.60	0.36	2.02
3	1	43.02	65.72	12236.00	15512.00	723.85	0.37	212.98	132.94	0.62	78.88
4	1	58.32	77.93	8045.00	15383.00	566.52	0.60	187.91	123.00	0.65	52.30
5	6	78.82	83.89	3232.00	26005.00	751.71	0.58	226.87	162.60	0.72	12.43
6	5	101.29	108.11	2719.00	25285.00	735.57	0.59	224.86	159.00	0.71	10.75
7	6	95.46	95.48	16.00	17924.00	980.31	0.23	293.40	107.44	0.37	0.09
8	1	57.41	73.68	2596.00	5129.00	311.08	0.67	105.06	72.79	0.69	50.61
9	7	54.15	73.56	5045.00	8717.00	630.37	0.28	223.89	62.77	0.28	57.88
10	5	91.94	93.60	200.00	4783.00	409.55	0.36	158.29	45.68	0.29	4.18

It is important to note that the particle type determination was made on a subjective basis prior to measurement of the particles. No data were available to the operator to guide the selection of type for any given particle. It was felt that this was necessary at the experimental stages to prevent operator influence on the results. From the above discussion it can be seen that this approach provided reasonably good results. In some cases there is overlap between parameters of differing particle type, or data points are too few to be useful. It is clear that some refinements are needed, probably in the form of a computer algorithm that could select particle types purely on the basis of measured data. Additionally, some revision of the particle classification scheme may be necessary.

CONCLUSION

It is outside the scope of this note to discuss applications of these data. However, development of the method illustrates the flexibility offered by programming in a language such as FORTRAN as opposed to being restricted solely to menu operations supplied with the image analyser. This capability also allows user friendly instruction messages, specialized input and output of data depending on the nature of the application, integration of the application into the menu of the image analysis software thereby eliminating the need to program many repetitive tasks, the ability to access primary data within the program, and greater access to system configuration and status information. With continued developments of new applications using these capabilities, image analysis should prove to be a highly versatile research tool in the field of organic petrography.

ACKNOWLEDGMENTS

The author wishes to thank A.R. Cameron for critical review of the text, G.G. Smith for helpful advice in preparing the paper, D.J. Smith for assistance in typing the manuscript, and M. Tomica for technical assistance. Lotus 1-2-3 is a registered trademark of Lotus Development Corporation.

REFERENCES

Goodarzi, F.
1987: The use of automated image analysis in coal petrology. Canadian Journal of Earth Sciences, v. 24, no. 5, p. 1064-1069.

Pratt, K.C.
1989: The use of Automated Image Analysis to determine conventional coal petrographic parameters - an example from southeastern British Columbia. This volume.

Riepe, W. and Steller, M.
1984: Characterization of coal and coal blends by automatic image analysis. Fuel, v. 63, p. 313-318.

Zeiss, H.S.
1979: Automating coal petrography at Bethlehem Steel Corporation. In Proceedings of the Ninth International Congress of Carboniferous strata, Urbana, v. 4, p. 495-500.

Western Canadian Coal Mines - for the record

A. Darragh and J.D. Hughes
Institute of Sedimentary and Petroleum Geology, Calgary

Darragh, A. and Hughes, J.D., Western Canadian coal mines - for the record. In Contributions to Canadian Coal Geoscience, Geological Survey of Canada, Paper 89-8, p. 149-155, 1989.

Abstract

The history of coal mining in Canada dates back to the early part of the 17th Century. It is only since the late 1800s, however, that systematic records of mining operations have been available. These records are kept in provincial and federal government files, which are often difficult to access, particularly for mines which operated prior to 1940.

Recent interest in old mine locations has resulted from concerns over the safety of abandoned mines on existing leases. As a result, the Geological Survey of Canada has commenced an inventory of old mine locations in its files. About 550 such records in Alberta and Saskatchewan have been identified and cross-referenced with provincial records. This report reviews the present status of these records and outlines sources of further information.

Résumé

L'histoire des mines de charbon au Canada date du début du XVII^{e} siècle. Cependant, des archives systématiques ne sont disponibles que depuis la fin du XIX^{e} siècle. Ces documents se trouvent dans les dossiers du gouvernement fédéral et des gouvernements provinciaux. Ces dossiers sont souvent difficiles d'accès, surtout lorsqu'ils concernent les mines qui étaient en opération avant 1940.

Dernièrement, un souci concernant la sécurité de ces mines abandonnées, situées sur des concessions minières encore en vigueur, a suscité de l'intérêt dans les emplacements de ces vieilles mines. Par conséquent, la Commission géologique du Canada a entrepris de faire un inventaire des emplacements des vieilles mines qui peuvent être retracées dans ses dossiers. Environ 550 archives ont été repèrées en Alberta et en Saskatchewan et vérifiées avec les archives provinciales. Le présent rapport fait une révision de l'état présent de ces archives et identifie des sources susceptibles de fournir de plus amples informations.

INTRODUCTION

Although coal mining has been conducted in Canada for more than three hundred years, it is only until relatively recently that systematic records of mine locations and areal extents have been kept. Information from older mines is scattered amongst a variety of sources, and is, therefore, often not available when required. This information may be of critical importance to property owners and to operators of modern surface mines in old mining areas, and may also be incorporated into geological studies of these areas.

This report reviews information available in the files of the Geological Survey of Canada on coal mines in Saskatchewan and Alberta, and discusses other sources of such information in these areas. Maps showing coal mining localities in Saskatchewan are also included.

BACKGROUND

The history of coal mining in Canada dates back to at least the early part of the 17th Century on the Atlantic Coast. Several records from this period referring to coal and coal use are housed in the National Archives in Ottawa. One early reference, dated 1643, was for a shipment of coal by sea from New Brunswick to New England, and another, dated 1672, describes coal resources on Isle Royale, now Cape Breton Island, written by the French Governor and published in Paris (Brown, 1984). These early references indicate that coal was used by the French Military at Fort Louisburg and by early settlers in the Nova Scotia and New Brunswick areas.

On the Pacific Coast of Canada, coal was discovered on Vancouver Island at Squamish near Port McNeill in 1835 (MacGregor et al., 1976). Coal from mines in this region, which started producing in 1849, was used mainly by coastal steamships trading along the West Coast and for local commercial and residential heating.

In the Foothills and Prairie regions of the country, coal was discovered in the late 1700's. The first mining in these regions probably started in Alberta about 1860. Mining in Saskatchewan commenced about ten years later in the 1870's (Irvine et al., 1978).

It is not known how many mines were started, worked out, or closed down between the early 1640's and the early 1880's. These records either did not exist, were lost, or are in archival storage and difficult to retrieve. It is known, however, that since the early 1880's several thousands of coal mines have been opened across Canada, the sites of which are recorded in provincial or federal government files. Saskatchewan and Alberta alone record over 2,200 mine sites (Irvine et al., 1978; ERCB, 1985). In Canada today there are just under 40 individual operating mines, each producing from between 1,000 and 11,000,000 tonnes of coal per year for international and domestic markets. Most of these mines are located in the same general mining areas established by the military and early pioneers one hundred or more years ago.

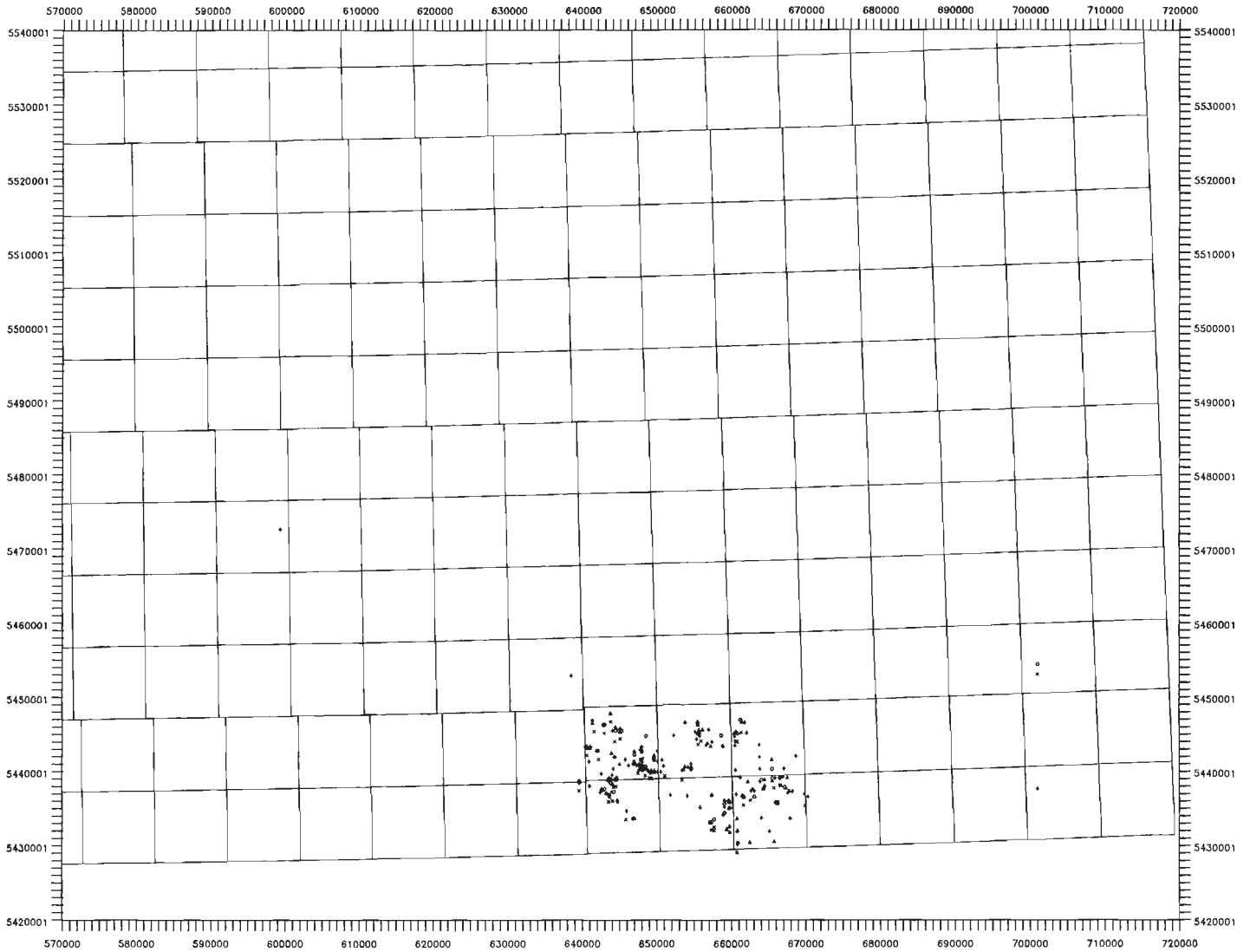

Figure 1. *Weyburn mapsheet (N.T.S. 62E) in the Estevan mining area showing distribution of mines by source of information. Triangles = from files of Saskatchewan Department of Mines and Minerals; Circles = center of area underlain by mines from files of Geological Survey of Canada; x = location of mine entry from files of Geological Survey of Canada; + = from Table 2 in Irvine et al., 1978. Tics along margin are at 1 km intervals. Labels on margin in 6 degree UTM co-ordinates.*

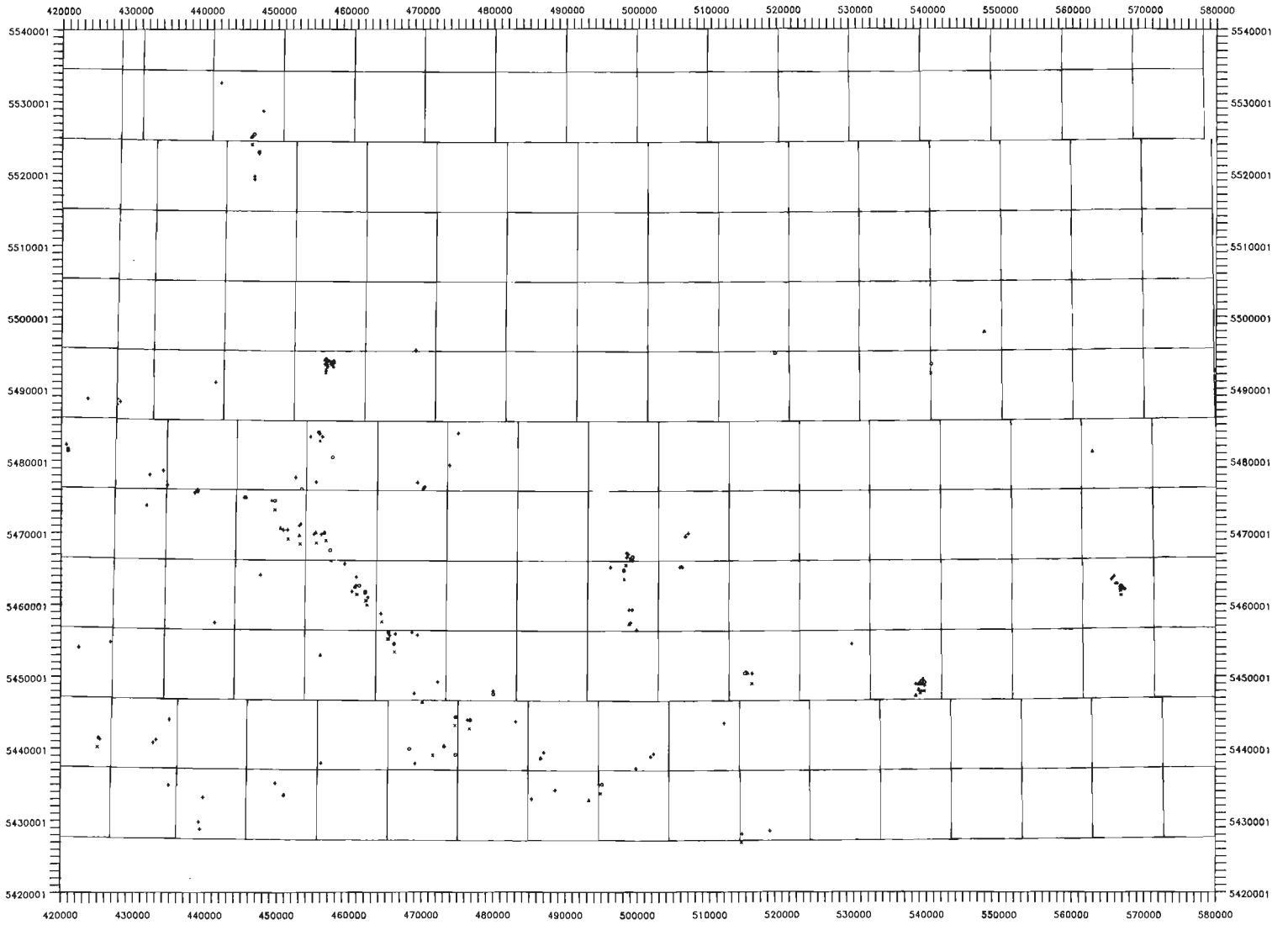

Figure 2. *Willow Bunch Lake mapsheet (N.T.S. 72H) showing distribution of mines by source of information. Triangles = from files of Saskatchewan Department of Mines and Minerals; Circles = center of area underlain by mines from files of Geological Survey of Canada; x = location of mine entry from files of Geological Survey of Canada; + = from Table 2 in Irvine et al., 1978. Tics along margin are at 1 km intervals. Labels on margin in 6 degree UTM co-ordinates.*

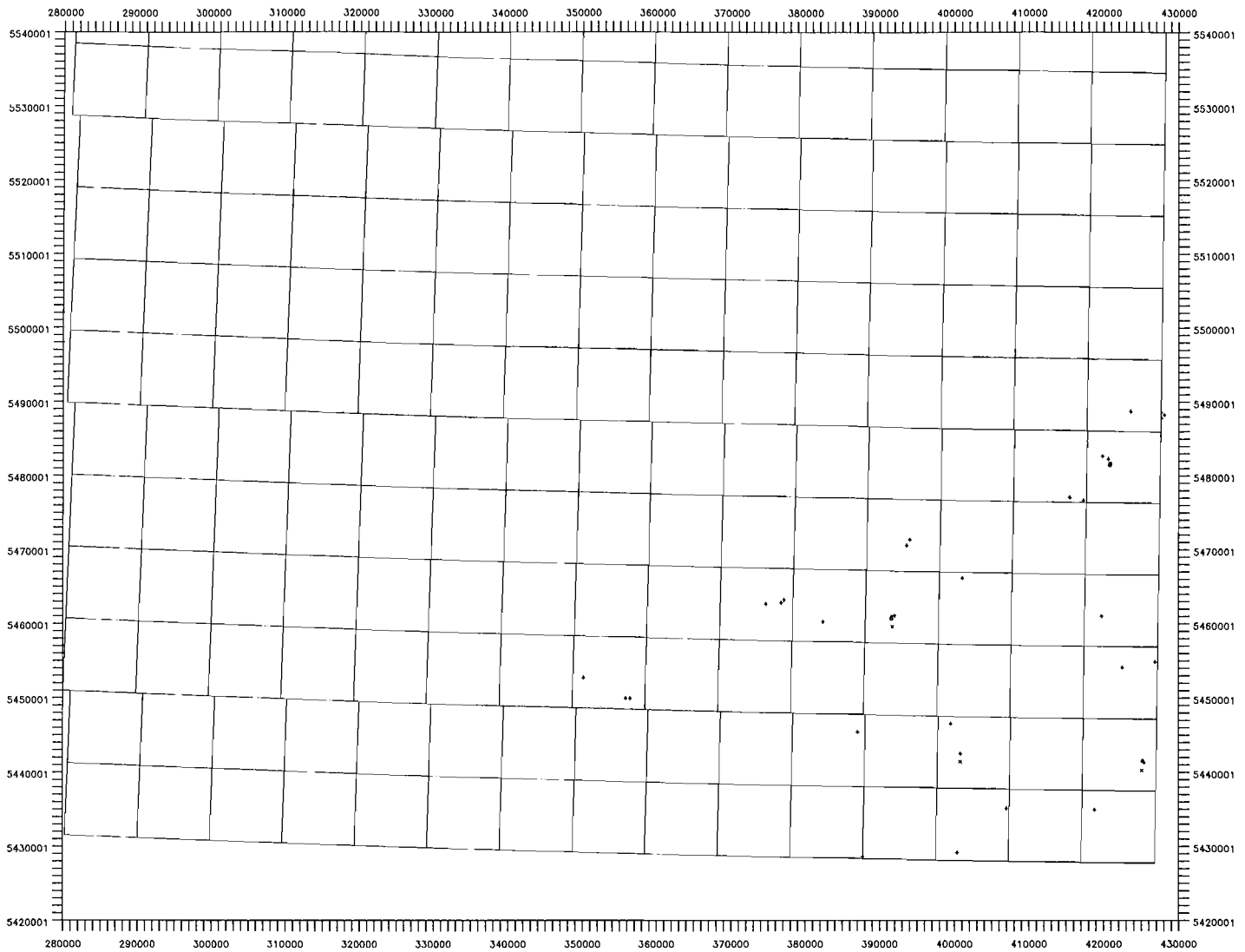

Figure 3. *Wood Mountain mapsheet (N.T.S. 72G) showing distribution of mines by source of information. Triangles = from files of Saskatchewan Department of Mines and Minerals; Circles = center of area underlain by mines from files of Geological Survey of Canada; x = location of mine entry from files of Geological Survey of Canada; + = from Table 2 in Irvine et al., 1978. Tics along margin are at 1 km intervals. Labels on margin in 6 degree UTM co-ordinates.*

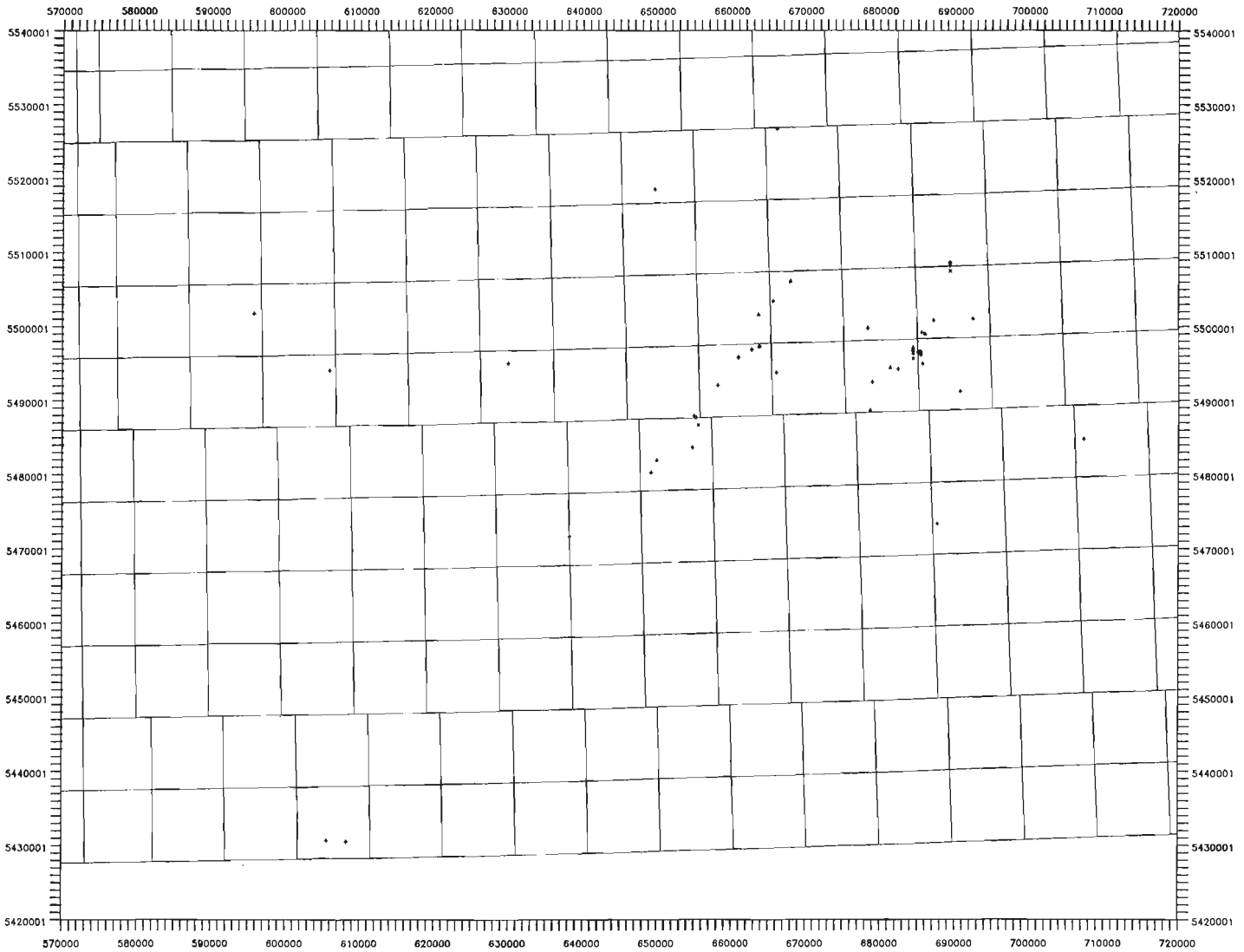

Figure 4. *Cypress Lake mapsheet (N.T.S. 72F) showing distribution of mines by source of information. Triangles = from files of Saskatchewan Department of Mines and Minerals; Circles = center of area underlain by mines from files of Geological Survey of Canada; x = location of mine entry from files of Geological Survey of Canada; + = from Table 2 in Irvine et al., 1978. Tics along margin are at 1 km intervals. Labels on margin in 6 degree UTM co-ordinates.*

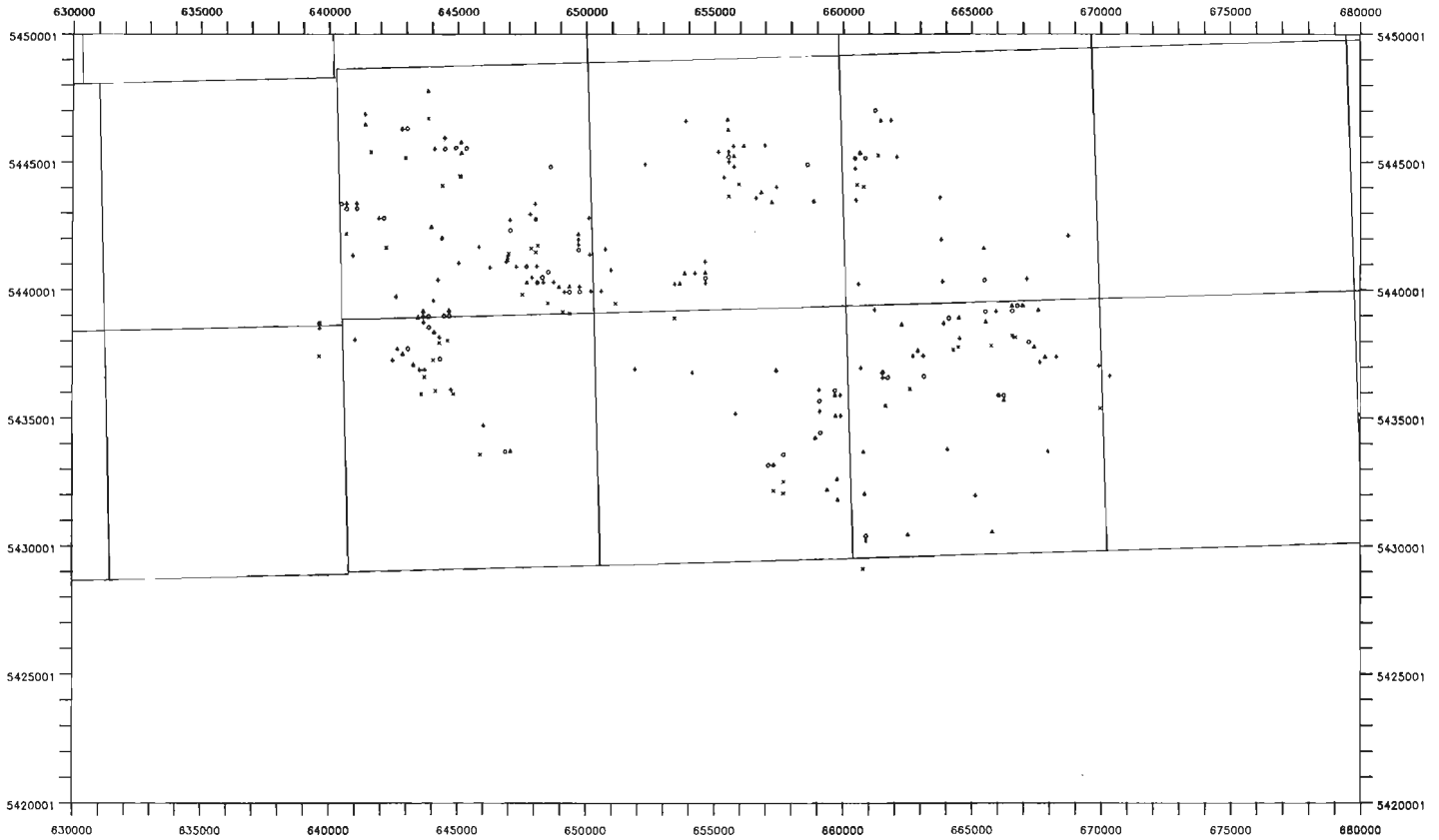

Figure 5. *Expanded scale map of Estevan mining area (N.T.S. 62E) showing distribution of mines by source of information. Triangles = from files of Saskatchewan Department of Mines and Minerals; Circles = center of area underlain by mines from files of Geological Survey of Canada; x = location of mine entry from files of Geological Survey of Canada; + = from Table 2 in Irvine et al., 1978. Tics along margin are at 1 km intervals. Labels on margin in 6 degree UTM co-ordinates.*

The renewed interest today in the location and areal extent of old mine workings results from two major concerns. Prior to World War II, virtually all coal was mined manually from shallow underground seams. These mines may have been simply entries at the coal outcrop or may have extended over areas of tens of hectares. Since World War II, most coal has been extracted from highly mechanized surface mines using large and expensive equipment. In the Prairie regions particularly, these pieces of equipment must at times traverse lands that may contain old mined out areas. Most of these old mines may have collapsed over time and therefore present no cause for concern. Equipment owners do not, however, wish to accelerate this process at the risk of losing or damaging a costly piece of equipment. Further, complete recovery of coal resources in a mine requires knowlege of the boundaries of old mined out areas.

The second main reason for this renewed interest is the possible liability of the current leaseholder for personal and property damage resulting from accidents in old mine workings. This issue is being discussed at all levels and a court case is pending in Saskatchewan concerning a fatality at such an old mine site.

COAL MINE RECORDS IN ALBERTA AND SASKATCHEWAN

As a result of this renewed interest in old mine sites, the Federal Government through the Geological Survey of Canada in Calgary has commenced a search of its records for old mine locations, mainly in Alberta and Saskatchewan. About 550 such records have been identified and cross referenced with records from other sources. These records are mainly in the form of mine plans and notes, some of which are handwritten or hand sketched. They are deteriorating with age and cannot be accessed without incurring damage.

In Alberta, more than 1800 mine localities are already accessible in a computerized form from the Alberta Energy Resources Conservation Board (ERCB, 1985). Records from the 415 mine localities available in Geological Survey of Canada files for Alberta, therefore, have only been cross-referenced against ERCB localities. Most or all of the information available for these localities is resident with the ERCB.

In Saskatchewan, no such computerized inventory of mine localities exists. Information on more than 150 mine localities is available from the Saskatchewan Department of Mines and Minerals in Regina. Geological Survey of Canada files in Calgary contain additional information on 135 localities. A third source of information derived in part from the above and in part from unknown sources, has been published in tabular format in Irvine et al. (1978). Figures 1 through 4 illustrate the locations of mine localities according to source of information for N.T.S. mapsheets 72F, 72G, 72H and 62E, which span the coal-bearing southernmost part of the Province. Figure 5 is an expanded scale map of the Estevan area, where a particularly dense population of old mines occurs. Mine entry locations from GSC files are denoted separately from the underground extents of the workings on these maps.

Tabular information summarizing the locations used to generate the maps in Figures 1 to 5 can be obtained in hardcopy or on diskette from the authors. Textual and other information describing each mine locality in GSC files has also been stored in a computer database, and similarly may be obtained by request from the authors.

CONCLUSIONS

This report is intended to outline the present status of information on old mine localities, primarily in Alberta and Saskatchewan. Individuals requiring further information on specific localities are urged to contact the sources outlined herein.

ACKNOWLEDGMENTS

The authors are grateful to T. LaFrenz, student assistant, who entered and verified information in the computer database, to C.A. Boonstra, of the Geological Survey of Canada, who organized and prepared an initial summary of mine records in GSC files, and to K.N. Nairn, of the Geological Survey of Canada, who provided assistance with co-ordinate conversion and township-range overlays for computer-plotted maps.

REFERENCES

ERCB (Alberta Energy Resources Conservation Board)
1985: Coal Mine Atlas, operating and abandoned coal mines in Canada. Published by Alberta Energy Resources Conservation Board, Calgary, Alberta.

Brown, A.
1984: The development of the coal mining industry in Canada. In Coal in Canada, T.H. Patching (ed.); Canadian Institute of Mining and Metallurgy, Special Volume 31, p. 5-8.

Irvine, J.A., Whitaker, S.H., and Broughton, P.L.
1978: Coal Resources of Southern Saskatchewan: a model for evaluation methodology. Geological Survey of Canada, Economic Geology Report 30, Appendix 1, 156 p.

MacGregor, E.R., Armstrong, W.M., Fyles, J.T., Guelke, C.B., Peel, A.L., Thompson, A.R., and Warren, I.H.
1976: Coal in British Columbia - a technical appraisal. Government of British Columbia, Queen's Printer, Victoria, British Columbia, p.17.

Description of computer methods and computer programs for correspondence analysis and use of the dendograph analysis as means of coal data processing

M. Labonté
Institute of Sedimentary and Petroleum Geology, Calgary

Labonté, M., Description of computer methods and computer programs for correspondence analysis and use of the dendograph as means of coal data processing. In Contributions to Canadian Coal Geoscience, Geological Survey of Canada, Paper 89-8, p. 156-162, 1989.

Abstract

A range of methods that seeks to uncover the structure of datasets derived mostly from instrument measurements is presented. These programs perform multivariate descriptive data analysis. The advent of sophisticated analytical equipment has created the need to process large datasets in geology. Analysis of geological information is often the corroboration of what a geologist suspects from preliminary work. Also the presentation of graphic output is often desirable as it conforms with the spatial analysis often necessary in geology. The evolution of computer technology has permitted the development of a variety of methods, since the advent of personal computers has facilitated the use of statistical software.

Résumé

On présente une série de méthodes capables de révéler la nature de l'information se trouvant dans les ensembles de données obtenues à l'aide d'instruments concus en vue d'effectuer l'analyse de type multivarié de données descriptives. L'introduction de nouveaux instruments analytiques avancés en géologie, crée le besoin de traiter des ensembles de données de grandes dimensions. D'ailleurs, en géologie, l'analyse des données produit souvent des résultats attendus, c'est-à-dire que l'intuition de nature géologique ne sera que prouvée. De plus, la présentation de graphiques est souhaitable, par suite de la nécessité fréquente, en géologie, de compléter une analyse spatiale ou régionale. L'évolution de la technologie informatique permet la mise au point d'une variété de méthodes, et tout spécialement l'arrivée des micro-ordinateurs, sous la forme d'ordinateurs personnels, rend l'utilisation des logiciels de nature statistique plus facile.

INTRODUCTION

In order to analyse data resulting from trace element, ultimate and proximate analyses of coal samples, and data related to various other complex geological problems, a mixture of multivariate methods had to be utilized. The initial methods included: the correspondence analysis and the dendograph. These were followed by derivatives of the dendograph method, namely, correlation analysis, the correlation plot, and the plotting of the triangle of correlations. At a later date, the method of Fuzzy c-MEANS by Bezdek et al. (1984), a kind of cluster analysis, was also utilized. As will be seen, these methods are somewhat interrelated, but from each of these different methods the user derives a particular view of the data under analysis. With these different algorithms, a user is usually capable of achieving a simple synthesis of the data. This approach to information analysis, followed by a limited synthesis, has been successful in geology, and in particular for trace element analysis in coal, where it is sometimes necessary to resolve the classification of both chemical elements or mineralogy, and samples. In other instances, it was found necessary to utilize depth plots to present the information for elemental abundances, because a spatial concept must often be acquired by a geologist when a particular set of data is being analysed.

BASIC DATA PRESENTATION

Presentation and analysis of the basic data

The first step in the analysis of the data, is to present them in a convenient arrangement in which similar variables are listed together. For example, the major elements, the secondary elements and the trace elements of a coal ash analysis, would be distinguished as three groups where the within-group similarities would be greater than the between-group ones. These three groups would allow a convenient discussion of the sampling method and the geological implications. Other situations will demand that two variables be presented in a scattergram (an X-Y plot). A particularly useful program for this has been the graphics part of Lotus 1-2-3 (Campbell, 1986). For logarithmic plots, however, other programs had to be utilized (GRAPHER is an example of such programs; see GRAPHER, Golden Software Inc, 1988). These spreadsheet program/packages are at the lower end of programming capabilities and can be of help if spreadsheet type of number manipulation or simple graphics are needed (c.f. Upstill, 1988).

The descriptive statistics associated with the basic dataset

A version of the program by Jones and Facer (1982) has been modified to include more descriptive statistics such as: maximum and minimum, the geometric mean and the median for each variable found in the dataset. This allows the detection of the presence of log-normality which is usually preponderant in geological data (Ahrens, 1954). The rare earth elements (REE) tend to exhibit a normal (Gaussian) behaviour, whereas a more common element (or what is called a framework element) such as aluminum (Al) will definitely show a log-normal behaviour. An indication which can facilitate these decisions is defined in Reeves and Brooks (1978, p. 375), as follows: "Agreement between the median and the geometric mean suggest lognormality; agreement between the median and the arithmetic mean indicates normality". If one wants to further elucidate the probability distribution law governing the variables being analysed, then the histogram of each variable must be derived as the rule mentioned above only "suggests". The histogram program by Jambu (1978) has been utilized and provides the advantage of giving the samples identification. Thus, a basic understanding of the data is possible even without more elaborate multivariate statistics. Such complex issues as multivariate normality are usually not covered in the realm of basic descriptive statistics, as this is the purpose of normalized descriptive principal components analysis (see Lebart et al., 1984). When the data are definitively lognormal, the program LOGPLOT can be utilized to determine if there is more than one mode present. This program is patterned after the method presented by Tennant and White (1959).

DATA ANALYSIS AND DESCRIPTION

Analysis of the correlation matrix, or more detailed investigations of the data if needed

When the basic data have been presented, and a logarithmic transformation has been performed (or not), we can determine the degree of similarity between the elements being compared by using the Pearson product-moment correlation coefficient (c.f. Labonté and Goodarzi, 1987). This coefficient will indicate if there is a linear relationship between the two random variables being compared. The probability density distribution functions (pdf), of the two sets of values, should be Gaussian in nature because the tables used to compare these correlation coefficients, in order to test them, assume that these are of Gaussian nature only (Lebart, 1975). Press et al. (1986) also warn of the need for the two variables, X and Y, to have a joint distribution not too different from the binormal distribution. Otherwise, the interpretation of the r-statistic (the Pearson product-moment correlation coefficient) will be meaningless. If necessary, the use of transformations like logarithms in order to make these pdf's close to Gaussian is possible. Most trace element data exhibit a mixture of behaviours, so that there exists a need for a somewhat non-parametric multivariate statistical analysis. Use can be made of the Spearman rank correlation coefficient or even of Kendall's tau correlation coefficient (Lebart, 1975) in cases where a mixture of pdf's indicates the need for non-parametric statistics. However, these are also "coefficient of inversion" (Demirmen, 1976) and introduce extra complexities in describing the information contained in a dataset.

It can also be preferable to adopt another view (Rickwood, 1983) and use the concept of distance instead of correlation, because of the difficulties presented above. This role is filled by correspondence analysis. It is however still valuable to use the "empirical" correlation coefficient in order to discover the linear relationships present between any pairs of variables in a dataset without considering the limitations mentioned above (Cailliez and Pages, 1976). We can then proceed to use the scattergrams (X-Y plots), in order to investigate more thoroughly these strong (or at least obvious) relationships. Statistical significance becomes less important some more evident physical relationship known to exist between two variables, so that the effort should proceed further in the direction of a model, such as regression. This happens when we have the correlation matrix and the filtering of the meaningful correlation coefficients is presented. It is then necessary to plot the variables causing the high correlation coefficient values. The facility to do so is provided by the LOTUS package (Campbell, 1986). Since regression is a predictive tool, and factorial methods like correspondence analysis are more descriptive in nature, modelling in this case might involve multiple linear regression, polynomial regression, or even covariance analysis (see Lebart et al., 1979).

The investigative effort might also proceed in the direction of cluster analysis, when one wants to analyse an overdetermined dataset (a dataset that contains more variables than samples) and one is interested in an empirical method for dropping meaningless variables, while leaving enough information in the dataset such that an ensuing cluster analysis could still recover some predetermined groupings of the samples. This approach is purely "empirical", as the variables are retained or dropped as per the notion of their usefulness from a geological point of view. There is often a wealth of intuitive notions related to each geological parameter.

A non-hierarchical method of clustering has been adjoined to the principal component analysis of Lebart et al. (1977), and classifies on the factor co-ordinates output resulting from the latter program. A measure of this classification performance is given by the computation of a kind of cumulative curve enumerating at which percentile values of probability the clusters were formed.

When one considers a more complete multivariate normal analysis, the question of the statistical independence of two given variables can lead to many approaches. Reyment (1971) provided a way to test for the multivariate normality of a given dataset by extending the concept of univariate distribution statistical moments to the multivariate situation. A more useful concept when working with geological datasets is that of partial correlations as presented by Lebart (1975). In this approach, some variables of a multivariate dataset are assumed to be exogenous (independent) and the rest are assumed to be endogenous (dependant on the first group). There is even a principal component analysis based on a correlation matrix partitioned in the manner mentioned above. The dependence of the reflectance of vitrinite on its hydrogen content has been used as a typical case to explore the above considerations. As with most geological datasets, this information is often riddled with missing data-values, or structurally missing values. The concept of structurally missing values in a table of data is explained in Agterberg (1974) in the context of embedded Markov chains (Morrow and Labonté, in press), where the transition matrices have a diagonal made of zero values. As will be discussed later, the above correlation analysis is often helped by the production of a dendograph, (McCammon and Wenninger, 1970; Labonté and Goodarzi, 1984).

The correlation analysis performed by the CORRMAT program (Jones and Facer, 1982) has been modified to provide a file that can be used as an input to the McCammon dendograph program, and this can often help the

interpretation of a geological dataset. One weakness of the dendograph program is that it does not interpret the negative correlation values; this must be accomplished by using the output of the correlation analysis program. A useful output of this program has been the thresholds correlation needed for statistical significance. The ensuing filtering of the meaningful correlation coefficients has proven to be the main tool of correlation analysis.

Presentation of the geological abundance data with depth-plots

The resolution of many geological problems can be helped by the simple graphical presentation of elemental abundances versus depth. Consequently, it became necessary to produce such plots where each variable occupied a small portion of the width in order to achieve a "sandwiched" effect. Thus, one could show a number of elemental abundances in order to demonstrate a trend with depth. When a lithological plot of the section is placed alongside a plot of these abundances, then the sampling process utilized can be seen. This then assumes the nature of a graphics presentation problem because of scale and dimension considerations and the need to emphasize some effects versus others.

Some of the considerations and conclusions that have emerged from this type of analysis are:

1. Size and grouping

There was a need to produce elemental abundance depth-plots of a given size in either the "x" or "y" direction for the variables being plotted. Also, it is desirable to ensure that those chemical elements having affinity with each other are plotted in adjacent positions on depth-plots. Both of these modifications will facilitate the discussion of a geological problem when geochemical data are utilized to establish a point of view.

2. Scaling and numbering

When depth-plots were first produced, the need to post numbers without decimal values became evident. A subroutine first produced by Thayer and Storer (1969) was modified and then adapted to be a part of this program.

3. Plotting abundances upward or downward

The need to satisfy the plotting of the elemental abundances in an upward or a downward fashion was made obvious by the varied sampling methods used in geology. At present, the program can plot downward to any range limits, (that is starting at zero or any positive number), whereas if it is plotting upward, the bottom depth limit must be zero. Missing value codes are allowed (-999.), and will cause the lines (if the joining line option is used) to ignore those values. At present, a column of values cannot start with a missing value code: in other words, the first value must be a valid one.

4. Showing abundances via shading or bars

The need for some shading effects was obvious. The program will allow leftward shading, so as to amplify the effect of abundances. On the other hand, leftward bars indicating amounts, can be plotted alone, where a more localized abundance emphasis is needed.

The preceeding considerations constitute the design aspects of the NLECKIE program.

Use of the dendograph program

The use of the dendograph (McCammon and Wenninger, 1970; Labonté and Goodarzi, 1984) has centered on the ability to resolve geological problems from an input of seemingly complex and multivariate data. This is achieved through a classification of objects for which we have some measurements of different nature. It is an example of a hierarchical classification method and suffers from a lack of fuzzy classification facilities. However, it has been found to be sufficient and has successfully resolved many geological problems, mostly in geochemistry. When conducting a correlation analysis, a dendograph can be used to display the arrangement of the objects, and thus assists significantly in interpreting the correlation matrix. The method is deficient in that it does not offer an interpretation for the negative correlation coefficients in a correlation matrix.

The use of correlation plots or shaded displays of correlation matrices

The concept of plotting a representation of a triangular set of similarity coefficient values, the lower part of a symmetrical similarity matrix, in association with a hierarchical classification was presented by Valentine and Peddicord (1967). Sneath and Sokal (1973) summarily dismissed the representation of a similarity coefficient matrix by plotting a triangle and the use of shading effects as a means of representing graphically the value of each coefficient. They called this kind of plot a 'trellis diagram'. There has been some use of such diagrams in the past, albeit not with shading effects, but with circles, etc. (e.g., see Closs and Nichol, 1975). The classification of objects using the dendograph method offers a way of permutating the correlation values; the concept is explained in Labonté and Goodarzi (1987).

One can extend the presentation of the trellis diagram by using the correlation plot. The correlation coefficient diagram plot is often used in geology. Dissanayake (1984), offered an example in which it was applied to trace elements present in a suite of peat samples. When a suitable permutation of the objects compared is performed, then the correlation plot becomes a method for identifying major relationships or groupings of elements, and thus provides a more detailed presentation of the correlation coefficients than the trellis diagram. Two methods of permutating the classified objects have been utilized here. The first one is the classification afforded by the dendograph, the second one is the first factor axis classification presented by the descriptive principal component analysis of Lebart et al. (1977). A more formal approach to the problem would be to consider the two variables for which one is computing a correlation coefficient, as random vector variables. One can comprehend the nature of correlation coefficients and their comparison more fully by using the method of Escoufier (1973), which provides the proper environment for comparing vector variables. If we then use the structure of a Hilbert space, the correlation diagram becomes a suitable presentation of a set of correlation coefficients, which, when properly permutated, produce a relatively smooth curve, if the successive correlation coefficient values are joined by lines. As an example, the Hilbert space is defined in physics (quantum mechanics), as the space of the eigenstates and eigenfunctions for the Shroedinger equation, or the quantum theory (Coveney, 1988).

Use of the Fuzzy c-MEANS algorithm

The context for using the Fuzzy c-MEANS algorithm was provided by a groundwater analysis reported in Barker et al. (1988). The field of hydrogeology is certainly well endowed with deterministic mathematical/computer methods. The use of statistics is a complement to these methods and can provide some explanations where the deterministic methods are incomplete. In particular, the c-MEANS fuzzy analysis attempts to group the samples in a succession of clusters, where the user provides a range of cluster number values. In this process, a measure of order (entropy) is provided for each cluster value, indicating the optimum clustering situation encountered. The c-MEANS will give membership values from zero (not part of a cluster) to one (definitely a member of this cluster), and the intermediate values are the fuzzy ones. This algorithm is based on mathematical proof provided by Bezdek (1981). When attempting to use this algorithm with a synthetic dataset, where several variables were defined from the end members of a triangle, each is a composition of the end member's content multiplied by different coefficients. This was an attempt to observe the behaviour of this procedure/algorithm when it is used to process a dataset made of variables representing the abundance of a chemical component, as detected by analytical methods or detectors, where a value can contain a mixture of signals as well as noises. Since one end member (meaning one signal) was much higher in magnitude than the others, the Fuzzy c-MEANS assigned clusters made of points on the triangle at the same level, relative to that signal, a behaviour known to exist in triangular contouring packages. Thus, this algorithm can be seen to operate as a contouring algorithm. The difference here is that it was not confused by the dilution of the end members values into several composite variables. Incidentally, descriptive principal components analysis (Lebart et al., 1977) recovered the triangle entirely as its first two factor axes (eigenvectors). Obviously, if one translates this synthetic example into a practical hydrogeology case, one can imagine that principal component analysis should guide the work of the Fuzzy c-MEANS algorithm/method.

The use of descriptive principal components analysis

The use of this program and the attached classification algorithm (Lebart et al., 1977) has given good results in hydrogeology, and also in paleontology. The drawing of printer plans of the factor axes containing both the samples and the variables facilitates the interpretation of the results. This program has successfully resolved a problem of pollen classification in the sense that a complete evolution path is observable on one of the factor plans made by the first two factor axes. Grouping of similar pollen types was observed as well as a "time" line.

Use of correspondence analysis

The version of Lebart et al. (1984) has been installed on a personal computer. This version allows two approaches to the processing of the multivariate datasets. The main difference lies in the computation of the eigenvalues. The in-core approach uses the usual eigenvalue decomposition by the tri-band method. This usually takes care of input matrix sizes of up to 100 variables and a few hundred samples. The out-of-core approach utilizes the stochastic approximation method described in Lebart et al. (1984, p. 151) and computes only the needed eigenvalues.

Since this program does not store the data, or the entire chi-square similarity matrix, in the computer memory, it should be able to resolve much larger input matrix sizes. The correspondence analysis program as it is listed in Lebart et al. (1977) has also been installed on a personal computer and provides an interesting output beyond the plans and printout, namely the scaled and recalculated data sorted by the order on the first factor axis.

The profiles are important for correspondence analysis, because the chi-square distance concept is used to compute the similarity coefficient matrix. It becomes relevant to derive a method to observe the profiles, as the concept of a chi-square distance departs quite significantly from the more familiar correlation coefficient. Another way of defining profiles is to consider them as relative frequencies. Since the distances between the objects on a projection plan produced by correspondence analysis are profile distances, it becomes important to visualize these profiles. Since the plans offered by correspondence analysis are the plans with optimum separating capability [Cailliez and Pages (1976) labelled these plans as "discriminant"], one can use these plans to separate groups of objects, if such groupings are present inherently in the data. Correspondence analysis was utilized for such a purpose, and a simpler program such as the one in Lebart (1975) will suffice. Also this seems to work better with a relatively small dataset. Further, confidence limit circles were drawn on factor plans with plotter graphics, but this is merely a way to represent the masses of the objects being analysed (see Lebart et al., 1984, p. 185). Confidence limit circles are useful, however, to elucidate the over-determination effects. The distributional equivalency property of correspondence analysis is most useful in the process of eliminating highly correlated variables from a multivariate dataset, because the appearance of the factor plans does not change appreciably if only one of a subset of highly correlated variables is left in the total set of data submitted for analysis. This situation is frequently encountered in trace element analysis.

The "Spidergram"

The "spidergram" is a program utilizing the same input files as the "CORRMAT" program, but it produces plots where on the x-axis, the Rare Earth Elements (REE) are disposed by increasing atomic number on the periodic table of elements, and on the y-axis, the abundances of these elements are plotted on a logarithmic scale, after having been normalized with regard to chondrites (Henderson, 1984; Taylor and McClennan, 1985). The program actually seeks variables having the REE chemical symbol names as variable names in the input file variables list.

The Rare Earth Elements were put in the lithophile group of elements by Goldschmidt (see Mason and Moore, 1982). Thus, they exhibit a preference of association with the silicates. This concept for association can then be explored by showing the abundances of these elements in a linear fashion. This concept is applicable not only to the REE, but can be extended to cover more elements as shown by Briqueu et al. (1984), the reasoning being that newly introduced elements are positioned in the suite of the REE, according to their affinity for liquids (hygromagmaphile elements). REE compositions of samples are normalized to chondritic values because the REE abundances in meteors, originating from stars undergoing explosions or supernovas, are used as standards. In this situation, every REE element would be treated in a similar fashion and at such high temperatures, the thermodynamical properties of each of the REE elements are similar (Henderson, 1984). In other words, if one would plot a spidergram or plot the abundances of each

REE of such a meteor, one would obtain a relatively straight line for the abundances. Another point about the REE is their diminishing ionic radius versus increasing atomic number (Muecke and Möller, 1988). The normalization mentioned above will also remove the Oddo-Harkins effect encountered in these elements (Hanson, 1980). The Rare Earth Elements fall into a category of atoms which have a Xenon type of inner shell of electrons and where, with increasing atomic number, the electrons are added into a 4f shell instead of the 6s outside shell. This is known as the main periodicity and the rare earths constitute part of the f period of the Mendeleev table of elements. As electrons filli the 4f shell, the atomic radius (as it is computed by using quantum mechanical methods) diminishes. Consequently, this is known as the "f-shrinkage" (Godovikov and Hariya, 1987). This means that the 5d shell is more or less bypassed except for Gadolinium and Lutecium, which exhibit a secondary periodicity.

The Rare Earths are distinguished by their normal trivalent ionic state, and this is what makes them a particularly homogeneous group of atoms. The REE are usually trapped as ions of the (+3) status in complexes made by other kind of ions, which are then known as ligands. When trapped in solids, the REE will exhibit an "atomic" nature, meaning that their spectra contain very sharp lines (Sinha, 1983). This also means that they are less influenced than other kinds of ions by the adjacency of other ions. Thus, the REE do not participate much in ionic structures other than with their valence electrons (Sinha, 1983, p. 315) This property means that REE can be used as atomic structural probes. The most useful "spidergram" design has been that which was offered by Taylor and McClennan (1985) and it includes the calibration curves such as PAAS (Post Archean Australian Shales) or NASC (North American Shales Composites), allowing the user to judge the abundances of the sample evaluated versus these calibration values. The shales constitute, according to Taylor and McClennan (1985) a natural sampling process capable of providing an average composition of the terrestrial crust, and this proves to be an advantage when it is utilized with certain elements like the REE having an intermediate residency time in the oceans. The abundance signature of these elements in a sedimentary column may thus constitute a proper sampling process of the physical conditions existing in the oceans at a particular geological time. For example, see Liu et al. (1988), where a use is made of the REE element Cerium, to reconstitute paleo-oceanic oxydo-reduction potential conditions. The term "Spidergram" was coined because the Europium anomaly (usually negative in sedimentary rocks or coals), produces a diagram which resembles the legs of a spider.

CONCLUSION

A set of programs performing some aspects of multivariate data analysis are presented. The majority of these programs use a first step in which the data are reduced by computing similarity coefficients. This is probably a left-over from the lack of speed of the early computers that needed to summarize the data first by using a similarity coefficient matrix before proceeding to analyse it. An exception is the c-MEAN or Fuzzy analysis, which must constantly proceed to the original data in order to locate the clusters. As expected, this method is highly computational and requires the resources of a large computer for the usual geological multivariate dataset. Some programs do not perform the classification themselves, but offer optimum discriminating plans of projection such as correspondence analysis. In geology, plotting the abundances by depth, (a mathematical variable), is sometimes sufficient and offers a welcome simplification. In other situations, a permutation of the order of the objects being presented will indicate the subgroups among these objects. This grouping of objects is often a desirable way of understanding the operation of complex classification algorithms/methods, because using these will make some geological effects obvious, which in turn will shed some light upon the real nature of these algorithms/methods. Also, as found in the hydro-geology problem, there is a need for a so-called "bridge" between deterministic methods and the statistical ones. The equilateral triangle of dilution represents a practical but limited insight in these program/methods that provide an experience for further applications.

NOTES

The following are notes pertaining to the use of some programs.

Notes for using the CORDMAT and DENDOGR set of programs

The CORDMAT and DENDOGR programs form a set. CORDMAT is used to perform a correlation analysis as per the Jones and Facer (1982) program CORRMAT, and was modified to accommodate the items listed below. TDENDOGR produces the dendograph plots as per the McCammon and Wenninger (1970) original program, but is slightly modified to allow optional joining lines between the tips of the object lines and the object names. This is to avoid overprinting of these object names if some are highly correlated (similar).

Modifications brought to the CORRMAT program and included in the CORDMAT program

1. Missing values codes. These are set to "-999.00", as opposed to "0.0" in the CORRMAT program.

2. Each record must contain a depth value. (Set to 0.0 if not applicable.) This must be the first numerical value (after the sample identification tag). These depth values do not participate in the computation of the correlations, but the original data values printed in the output file "list" are reordered according to these depth values if these are not all equal to zero.

3. A second flag is introduced in the second input file line. This is to allow a logarithmic transformation of the data. The following codes apply:

   0 ... No input data transformation.
   1 ... The function Log(x) is applied.
   2 ... The function Log(x + 1) is applied.

   The last transformation is used when the input data contain genuine "0" values.

4. A second output file named "cormd" or "corm.d" is produced. This is a temporary file destined to be the input file to the DENDOGR program. This file contains the Pearson product-moment correlation coefficient lower triangular matrix as needed by the DENDOGR program. It is formatted so as to produce a dendograph of suitable dimensions on a plotter, but should be modified by an editor if these dimensions are incorrect.

5. A third file named "oderd" or "oder.d" is produced. This contains the order of the classification of the objects and is destined as an input to the "NLECKIE" program which produces the "depth plots".

Note: the DENDOGR program also produces an output file "list", so the one generated by the CORDMAT program should be printed first as it will be overwritten during the second step. This is due to the "unknown" status present in the "open" statements for the "list" file in both these programs. The "list" file produced by the DENDOGR program informs the user of the within-group and between-group correlations for the classification performed by this program.

Notes for using the NLECKIE program

The NLECKIE program will utilize the following files as input data:

1. An input data file of the same nature as the input data file for CORDMAT. The name of this file is requested by the program upon beginning and must be present in the computer directories. (Path name of 20 characters or less.)

2. An input data file indicating the permutation to be performed on the input data variables before plotting them. The name of the file is "oder.d". This file must be present in the same directory as the NLECKIE program itself.

The NLECKIE program produces an output file called "list" containing information about the data values, etc.

Notes for using the CORAN program

The program by Lebart et al. (1984) has been modified to eliminate the dynamic memory management feature. Otherwise there are no modifications to this program. The name of the input file is requested from the user upon starting the program. The output of the program is contained in a file called "list". A utility program is available to convert a file of the CORDMAT type to that of the CORAN type. The reason for not adapting CORAN to the CORDMAT type is the different nature of the operational requirements of these programs, illustrative variables, etc.

Notes for using the c-MEAN program

The c-MEAN program by Bezdek et al. (1984), along with the ensuing revision, has been implemented. The input data file format reads the usual multivariate dataset and only requires two additional lines at the front end, which contains the parameters.

Notes for using the CORD program

The program named "CORD" produces the correlation diagram. The usual file input is "corm.d", which is the same type of file required by the DENDOGR program. Usually, this "corm.d" file will be reordered by using a program called "REORD", which contains the same classification logic as DENDOGR but not the graphics. The output file of REORD is called "new.d" and if the reordering produced by the dendograph program is the one desired, then this file (new.d) must be sent as input to the CORD program. The result is a smoother correlation line, as shown in Labonté and Goodarzi (1987).

REFERENCES

Agterberg, F.P.
1974: GEOMATHEMATICS: Mathematical background and Geo-Science applications. Elsevier Scientific Publishing Company, Amsterdam, Holland, 596 p.

Ahrens, L.H.
1954: The lognormal distribution of the elements. (A fundamental law of geochemistry and its subsidiary). Geochimica et Cosmochimica Acta, v. 5, p. 49-73

Barker, J.F., Barbash, J.E., and Labonté, M.
1988: Groundwater contamination at a Landfill sited on fractured carbonate and shale. Journal of Contaminant Hydrogeology, v. 3, p. 1-25.

Bezdek, J.C.,
1988: Pattern recognition with fuzzy objective function algorithms. Plenum Press, New York, U.S.A., 256 p.

Bezdek, J.C., Erlich, R., and Full, W.
1984: FCM: Fuzzy c-MEANS clustering algorithm. Computers and Geosciences, v. 10, no. 2-3, p. 191-203. (a correction has been given to the above program by Ms. Vera Pawlowsky on page 660 of v. 11, no. 5 of the same publication).

Briqueu, L., Bougault, H., and Joron, J.L.
1984: Quantification of Nb, Ta, Ti and V anomalies in magmas associated with subduction zones: Petrogenetic implications. Earth and Planetary Sciences Letters, v. 68, p. 297-308.

Cailliez, F. and Pages, J.P.
1976: Introduction à l'analyse des données. SMASH, Paris, France, 616 p.

Campbell, M.
1986: 1-2-3, The complete reference. Osborne McGraw-Hill, Berkeley, U.S.A., 892 p.

Closs, L.G. and Nichol, N.
1975: The role of factor and regression analysis in the interpretation of geochemical reconnaissance data. Canadian Journal of Earth Sciences, v. 12, p. 1316-1330.

Coveney, P.V.
1988: The second law of thermodynamics: entropy, irreversibility and dynamics. Nature, v. 333.

Demirmen, F.
1976: RANK, a FORTRAN IV program for computation of rank correlations. Computers and Geosciences, v. 1, p. 221-229.

Dissanayake, C.C.
1984: Geochemistry of the Muthurajawela peat deposit of Sri-Lanka. Fuel, v. 63, p. 1494-1503.

Escoufier, E.
1973: Le traitement des variables vectorielles. Biometrics, v. 29, p. 751-760.

Godovikov, A.A. and Hariya, Y.
1987: The connection between the properties of elements and compounds: mineralogical-crystallochemical classification of elements. Journal of the Faculty of Science, Hokkaido University, Ser IV., v. 22, no. 2, p. 357-385.

GRAPHER
1988: Reference Manual, and Getting started and Tutorial. Golden Software, Inc., Golden, Colorado, U.S.A.

Hanson, G.N.
1980: Rare earth elements In petrogenetic studies of igneous systems. Annual Review of Earth and Planetary Sciences, v. 8, p. 371-406.

Henderson, P.
1984: Rare Earth Element Geochemistry. Elsevier Publishing Company, Amsterdam, Holland, 510 p.

Jambu, M.
1978: Classification automatique pour l'analyse des données. DUNOD, Paris, France, 2 Volumes, 343 p. and 398 p.

Jones, B.G. and Facer, R.A.
1982: CORRMAT/PROB, A program to create and test a correlation coefficient matrix from data with missing values. Computers and Geosciences, v. 8, p. 191-198.

Labonté, M. and Goodarzi, F.
1985: Use of the dendograph for data processing in fuel science. Fuel, v. 64, p. 1177-1179.

1987: The relationship between dendographs and Pearson product-moment correlation coefficients. In Current Research, Part A, Geological Survey of Canada, Paper 87-1A, p. 353-356.

Lebart, L.
1975: Statistiques et Informatique appliquées. DUNOD, Paris, France, 440 p.

Lebart, L., Morineau, A., and Fénelon, J.P.
1979: Traitement des données statistiques. DUNOD, Paris, France, 513 p.

Lebart, L., Morineau, A., and Tabard, N.
1977: Techniques de la description statistique. DUNOD, Paris, France, 361 p.

Lebart, L., Morineau, A., and Warwick, K.
1984: Multivariate Descriptive Statistical Analysis. John Wiley & Sons, New York, U.S.A., 228 p.

Liu, Y.-G., Miah, M.R.U., and Schmitt, R.A.
1988: Cerium: A geochemical tracer for paleo-oceanic redox conditions. Geochimica et Cosmochimica Acta, v. 52, p. 1361-1371.

Mason, B. and Moore, C.B.
1982: Principles of Geochemistry, Fourth edition. John Wiley & Sons, Publishers, New York, U.S.A., 343 p.

Muecke, G.K., and Möller, P.
1988: The not-so-rare earths. Scientific American, January 1988, v. 258, p. 1.

McCammon, R. and Wenninger, G.
1970: The dendograph. Computer Contribution 48, State Geological Survey, The University of Kansas, Lawrence, 28 p.

Morrow, D.W. and Labonté, M.R.
in press: The Lower Devonian Corridor Member, NWT, Canada: An example of deposition on a tidal flat island complex. In Second International Symposium on the Devonian System, A.F. Embry, J.N. McMillan, D.G. Glass, and D.J. McLaren (eds.); Canadian Society of Petroleum Geologists, Memoir 14.

Press, W.H., Flannery, B.P., Teukolsky, S.A., and Vetterling, W.T.
1986: Numerical recipes: The art of scientific computing. Cambridge University Press, Cambridge, England, 818 p.

Reeves, R.D. and Brooks, R.R.
1978: Trace element analysis of geological materials. John Wiley & Sons, New York, U.S.A. 21 p.

Reyment, R.A.
1971: Multivariate normality in morphometric analysis. International Journal of Mathematical Geology, v. 3, no. 4, 1971, p. 357-368.

Rickwood, P.C.
1983: The use of cluster analysis in diverse geological problems. In The Significance of Trace Elements in Solving Petrogenetic Problems and Controversies, S.S. Augustithis (ed.); Theophrastus Publications S.A., Athens, Greece, 916 p.

Sinha, S.P.
1983: Systematics and the properties of the Lanthanides. D. Reidel Publishing Company, Dordrecht, Holland, 648 p.

Sneath, P.H. and Sokal, R.S.
1973: Numerical taxonomy. W.H. Freeman and Co., San Francisco, U.S.A., 573 p.

Taylor, S.R. and McClennan, S.
1985: The continental crust: its composition and evolution. Blackwell Scientific Publications, Oxford, England, 312 p.

Tennant, C.B. and White, M.I.
1959: Study of the distribution of some geochemical data. Economic Geology, v. 54, p. 1281-1290.

Thayer, R.P. and Storer, R.F.
1969: Scale selection for computer plots. AS 21, Applied Statistics, 18, p. 206-208.

Upstill, C.
1988: The art of scientific programming. Nature, v. 333, p. 613-614.

Valentine, J.W. and Peddicord, R.G.
1967: Evaluation of fossil assemblages by cluster analysis. Journal of Paleontology; v. 41, no. 2, p. 502-507.

Energy, Mines and Resources Canada

Énergie, Mines et Ressources Canada